

Synthesis and testing of Palladium and Platinum phosphine complexes with potential mitochondrial targeting anti-cancer properties

By

Patricia W. Gitari (MSc. Chemistry)

Submitted in fulfilment of the requirements for the degree

PHILOSOPHIAE DOCTOR

In the Faculty of Health Sciences
UNIVERSITY OF PRETORIA
PRETORIA

Supervisor: Professor Connie E. Medlen

Co-supervisor: Professor Simon Lotz

October 2007

Declaration

The work described in this thesis was carried out at the Departments of Pharmacology and Chemistry, University of Pretoria, South Africa from February 2004 to December 2006 under the supervision of Prof Connie Medlen and co-supervision of Prof Simon Lotz. I declare that this thesis is my own, unaided work submitted for the degree of Philosophiae Doctor, and it has not been submitted previously for a degree or examination at this or any other university.

.....

(Patricia W. Gitari)

..... day of, 2007.

Acknowledgements

First and foremost, I would like to thank Almighty God for enabling me to complete this degree. I would also like to thank my supervisor Prof. Constance Medlen for accepting to supervise a chemist who was venturing into a new area of research. I am also grateful to my co-supervisor, Prof. Simon Lotz for his assistance in solving difficult synthetic problems. I would like to extend my gratitude to Dr. Richard Bowen for encouraging me to change disciplines and venture into the world of pharmacology. It is also a pleasure to acknowledge my colleagues in the Department of Pharmacology (Ms M. Nell, Dr G. Joone, Dr D. Cromarty) for their patience and guidance especially in the area of instrumentation and cell culture work.

I would also like to extend my gratitude to Mr Dave Liles for his assistance in x-ray crystallography. I would also like to thank Mr. Patrick Selahle-for carrying out animal studies, Ms Judith Wagener and Dr. J. R. Zeevaart -synthesis of radiolabelled compounds and carrying out *in vivo* experiments. Others are Dr C. Durandt for providing training in flow cytometric techniques and Mr E. Dombodzvuku for editing the final manuscript. The completion of this degree has relied heavily on the assistance I received from the people mentioned above. Hence it confirms the Kikuyu proverb “ kaara kamwe gatiūragaga ndaa” which translates to “ one finger cannot kill a louse”.

Lastly, I would like to thank MINTEK (Pty) for financial assistance that enabled me to study for this degree.

Dedication

To

My dearest mum, Mary Mumbi Gitari (1947-12.10.2007)

My father, A. Gitari Herman

My siblings, nieces and nephews

And lastly,

My dearest daughter Erica Mumbi

Summary

The main theme of this thesis focuses on the preparation of palladium and platinum phosphine complexes that possess the potential to act as anti-cancer agents. The design of the complexes was based on the known compound, $[\text{Au}(\text{dppe})_2]\text{Cl}$ which was shown to have an anti-mitochondrial mode of action on cancer cells. Major problems were experienced in the synthesis of these novel palladium and platinum compounds as the five phosphine ligands required diverse reaction conditions. Instability was the major hindrance as decomposition occurred during purification. This led to the substitution of the counter-ion (Cl^-) with PF_6^- . The complexes prepared in this study were varied in lipophilicity as the gold complex was found to be non-selective due to high lipophilicity. In total, six compounds were prepared, purified and tested for potency against a panel of cancer cell lines as well as normal cells.

The most lipophilic compound, $[\text{Au}(\text{dppe})_2]\text{Cl}$, was non-selective as it exhibited the highest toxicity to both cancerous and normal cells. In general, *in vitro* studies showed that palladium complexes were more toxic than the platinum analogues. These novel compounds were also non-toxic to both resting and stimulated lymphocytes signifying high selectivity for cancer cells. Three compounds, **Pg 3**, **Pg 4a** and **Pg 8** exhibited high toxicity and were hence tested as such on murine cancer cell lines. **Pg 8**, with intermediate lipophilicity, showed toxicity against a larger number of cancer cell lines and this led to further investigations in an attempt to determine its mode of action.

Analysis of the effects of **Pg 8** on the mitochondria showed that it did not depolarise the mitochondrial membrane potential. A seven day analysis showed that while it did not have any effect on the mitochondrial membrane potential, it depolarised the plasma membrane potential from

day 4. In contrast, $[\text{Au}(\text{dppe})_2]\text{Cl}$ depolarised the mitochondrial membrane potential as expected. **Pg 8** was shown to induce apoptosis and necrosis on Jurkat cells after exposure for 48 h. It was also shown to induce cell cycle arrest (after 48 h) as it caused blockade in the S-phase. In contrast, $[\text{Au}(\text{dppe})_2]\text{Cl}$ caused a blockade in the G_0/G_1 phase.

Uptake studies with radiolabelled **Pg 8**, $[\text{}^{103}\text{Pd}(\text{d2pyrpe})_2][\text{PF}_6]_2$, showed that it accumulated significantly in Jurkat cells. Biodistribution studies in Wistar rats demonstrated that it was mostly taken up in the spleen followed by the liver. However, it was excreted faster than $[\text{}^{198}\text{Au}(\text{dppe})_2]\text{Cl}$ as this latter compound accumulated significantly in the lungs followed by the spleen, small intestine and liver. Acute toxicity studies in Balb/c mice showed that **Pg 8** was less toxic than $[\text{Au}(\text{dppe})_2]\text{Cl}$. The latter compound (at 3 and 6 μM) caused a significant reduction of total body weight over a 5-day period. Toxicity was evident as it was also shown to cause elevation of liver enzymes (AST and GGT), contrary to the results obtained from the mice treated with **Pg 8** (at 3, 6, 12 and 15 μM).

Preparation of a patent for the synthesis as well as anti-cancer properties of the novel compound, $[\text{Pd}(\text{d2pyrpe})_2][\text{PF}_6]_2$ (**Pg 8**) is currently in progress.

Table of contents

Declaration	ii
Acknowledgements	iii
Dedication	iv
Summary	v
List of abbreviations.....	xi
List of compounds	xii
Chapter I.....	1
Introduction.....	1
1.1 Cancer	2
1.2 Cancer incidences	2
1.3 Cancer treatment	4
1.4 Limitations of current cancer treatment.....	7
1.5 The need for new anti-cancer drugs	8
1.6 Drug design and targets.....	9
1.7 Metal based drugs	10
1.8 Metal phosphines as anti-tumour agents	16
1.9 Hypothesis	19
1.10 Aim of study	19
1.11 Objectives of the study.....	20
Chapter II.....	22
Phosphines and metal phosphine complexes.....	22
2.1 Phosphine ligands	23
2.2 Pyridylphosphines.....	27
2.3 Metal pyridylphosphines	29
2.4 Metal complexes of diphenylphosphine ligands.....	32
Chapter III.....	34
Preparation and characterisation of Pt and Pd phosphine complexes.....	34
3.1 Synthesis of metal phenylphosphine complexes	35
3.2 Synthesis of metal pyridylphosphine complexes.....	41
3.3 General discussion on the behaviour of the 2, 3 and 4-pyridylphosphine ligands	58
3.4 Structural analysis of compounds 3b, 4e 3f, 1h and 2h	59

Chapter IV	75
Experimental details	75
4.1 General	76
4.2 Synthesis of phenyl phosphine complexes	77
4.3 Preparation of pyridyl phosphine ligands	80
4.4 Preparation of 2-pyridyl phosphine complexes	81
4.5 Preparation of 3-pyridyl phosphine complexes	83
Chapter V	85
Stability, Lipophilicity and Cytotoxicity	85
5.1 Stability	86
5.2 Nuclear Magnetic Resonance Spectroscopy (NMR).....	87
5.3 Evaluation of stability of the test compounds by ³¹ P NMR spectroscopy ...	88
5.4 Materials and methods.....	88
5.5 Results.....	89
5.6 Lipophilicity	96
5.7 Aim of the experiment.....	98
5.8 Materials and methods.....	98
5.9 Results and discussion	99
5.10 Cytotoxicity	101
5.11 Determination of cytotoxicity	102
5.12 Materials and methods.....	102
5.13 General procedure	103
5.14 Statistical analysis	104
5.15 Results and discussion	105
Chapter VI	109
Analysis of mitochondrial function	109
6.1 The Mitochondria	110
6.2 Mitochondria and cancer.....	111
6.3 Mitochondria as cancer drug targets.....	111
6.4 Analysis of mitochondrial membrane potential.....	115
6.5 Objective of this experiment.....	116
6.6 Materials and methods.....	117
6.7 Results and discussion	119
6.8 Plasma membrane Potential.....	124



6.9	Analysis of plasma membrane changes by flow cytometry.....	125
6.10	Materials and methods.....	125
6.11	Results and discussion	127
Chapter VII		134
Apoptosis.....		134
7.1	Introduction	135
7.2	Apoptosis and cancer	139
7.3	Apoptosis and chemotherapy	140
7.4	Detection of apoptosis by flow cytometry.....	142
7.5	Materials and methods.....	143
7.6	Results and discussion	144
Chapter VIII		149
The cell cycle.....		149
8.1	Introduction	150
8.2	Cell cycle and carcinogenesis.....	152
8.3	Cell cycle and chemotherapy	153
8.4	Determination of the effect of Pg 8 and [Au(dppe) ₂]Cl on cell cycle of Jurkat cells.....	155
8.5	Materials and methods.....	155
8.6	Results and discussion	157
Chapter IX		164
Uptake studies.....		164
9.1	Introduction	165
9.2	Preparation of ¹⁰³ Pd labelled [Pd(d2pyrpe) ₂][PF ₆] ₂	166
9.3	Preparation of ¹⁹⁸ Au labelled [Au(dppe) ₂]Cl	167
9.4	Uptake of [¹⁰³ Pd(d2pyrpe) ₂][PF ₆] ₂ and [¹⁹⁸ Au(dppe) ₂]Cl by Jurkat cells ...	168
9.5	Materials and methods.....	168
9.6	Results and discussion	170
9.7	Biodistribution of [¹⁰³ Pd(d2pyrpe) ₂][PF ₆] ₂ and [¹⁹⁸ Au(dppe) ₂]Cl in rats	171
9.8	Results and discussion	173
Chapter X		175
Acute toxicity studies		175
10.1	Introduction	176
10.2	Motivation for the study.....	177

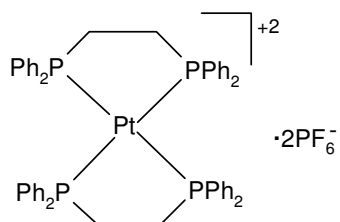


10.3	Aim.....	177
10.4	Materials and Methods:.....	177
10.5	Results and discussion	181
Chapter XI	189
Conclusions	189

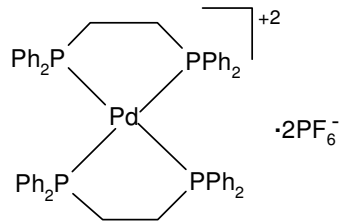
List of abbreviations

ALT	Alanine aminotransferase
AST	Aspartate aminotransferase
ATCC	American Type Culture Collection
CDCl ₃	Deuterated chloroform
D ₂ O	Deuterated H ₂ O
DKFZ	German Cancer Research Center
DMF	Dimethylformamide
DMSO	Dimethylsulphoxide
d ₆ -DMSO	Deuterated dimethylsulphoxide
Dppa	1,2-bis-(diphenylphosphino)acetylene
Dppe	1,2- bis-(diphenylphosphino)ethane
Dppen	1,2-bis-(diphenylphosphino)ethylene
D2pyrpe	1,2-bis-(di-2-pyridylphosphino)ethane
d(pyr)pcp	1,5-bis-(di-2-pyridylphosphino)cyclopentane
ECACC	European Collection of Animal Cell Cultures
GGT	Gamma-glutamyltransferase
Gy	The international system (SI) unit of radiation dose
MS-FAB	Mass Spectrometry Fast Atomic Bombardment
NMR	Nuclear Magnetic Resonance
NRBM	Netherlands Reference Laboratory for Bacterial Meningitis
NSCLC	Non-Small-Cell Lung Cancer
PHA	Phytohaemagglutinin
Pyr	Pyridyl group
THF	Tetrahydrofuran

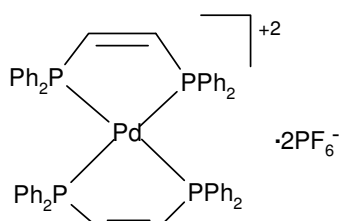
List of compounds



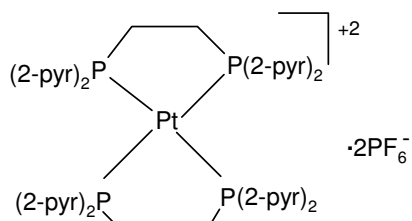
Pg 1



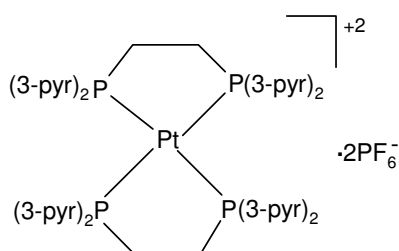
Pg 3



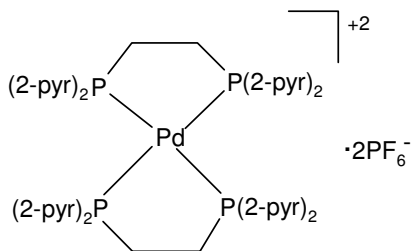
Pg 4a



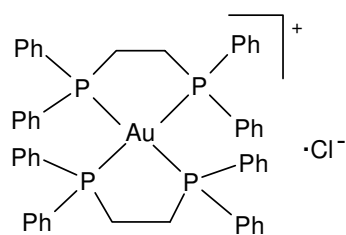
Pg 5



Pg 6

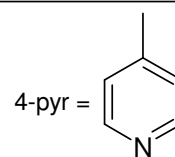
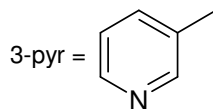
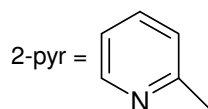
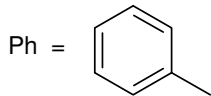


Pg 8



[Au(dppe)₂]Cl

Key



Chapter I

Introduction



1.1 Cancer

Cancer is not a single disease but a broad group characterised by malignant cells that are clearly distinguished from normal cells by uncontrolled growth (Workman, 2001). They are caused by abnormalities in the sequence and expression of critical genes, most notably oncogenes and tumour suppressor genes. The language of cancer is to be found in the resulting deregulation of crucial biochemical pathways that control proliferation, the cell cycle, survival/apoptosis, angiogenesis, invasion and metastasis. Aberrant cellular growth is a primary cause in the development of malignant tumours (Suyama *et al.*, 2002). However, additional events take place, which enable tumour cells to invade tissue barriers and metastasise to distant sites. These events include detachment of cells from the primary tumour, the crossing of tissue boundaries, entrance and exit from the circulatory system, the infiltration of distant organs, and the formation of metastatic implants.

1.2 Cancer incidences

Cancer has troubled humans throughout recorded history. This disease remains a major public health issue at the beginning of the 21st century (Grella *et al.*, 2003). It is the leading cause of death worldwide (www.who.int, 2005). From a total of 58 million deaths worldwide in 2005, it accounts for 7.6 million (or 13%) of all deaths. That is more than the percentage of deaths caused by HIV/AIDS, tuberculosis and malaria put together (McIntyre, 2007). There are currently 25 million people living with cancer.

The main types of cancer leading to overall cancer mortality are: (www.who.int, 2005).

- Lung (1.3 million deaths/year);
- Stomach (almost 1 million deaths/year);
- Liver (662,000 deaths/year);
- Colon (655, 000 deaths/year) and

- Breast (502, 000 deaths/year).

More than 70% of all cancer deaths in 2005 occurred in low and middle income countries. Deaths from cancer in the world are projected to continue rising, with an estimated 9 million people dying from cancer in 2015 and 11.4 million dying in 2030. According to World Cancer Report (World Health Organisation, 2003), this predicted sharp increase will mainly be due to steadily ageing populations in both developed and developing countries. Other factors include current trends in smoking prevalence and the growing adoption of unhealthy lifestyles. However, the report also provides clear evidence that healthy lifestyles and public health action by governments and health practitioners could stem this trend, and prevent as many as one third of cancers worldwide. The report also reveals that cancer has emerged as a major public health problem in developing countries, matching its effect in industrialised nations.

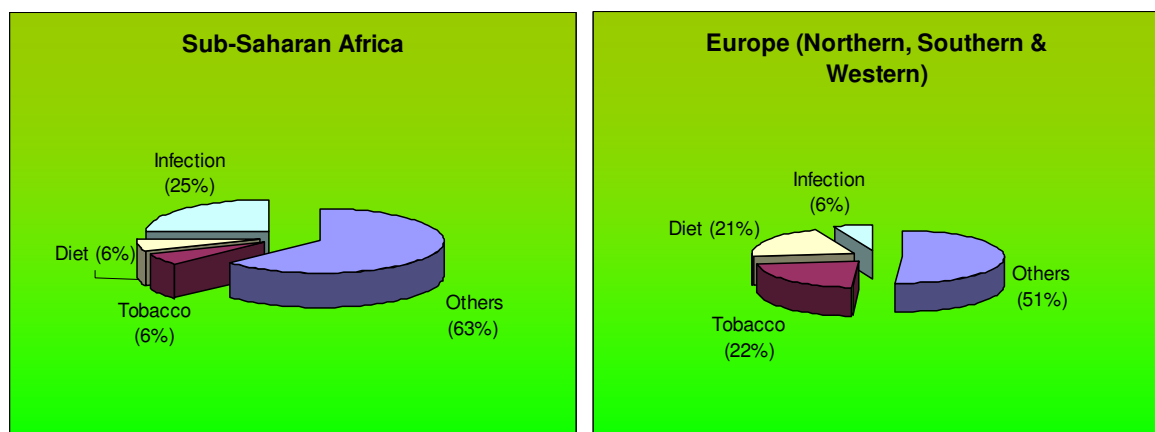


Fig. 1.1: The three main cancer-causing factors in Sub-Saharan Africa and parts of Europe

Tobacco causes cancer at many sites including; lung, throat, mouth, pancreas, bladder, stomach, liver and kidney (Selikoff, 2005). Overweight and obesity are associated with colon, breast, uterus, oesophagus and kidney cancers. One-fifth of cancers worldwide are due to infections (*Fig. 1.1*), mainly from hepatitis viruses (liver), papillomaviruses (cervix), *Helicobacter pylori* (stomach), Schistosomes (bladder), the liver fluke (bile duct) and human immunodeficiency virus (Kaposi's sarcoma and lymphoma).

In South Africa, a total of 29 208 new cancer cases in females and 29 499 new cases in males were reported (The National Cancer Registry, 2003). One in four males and one in five females (adjusted for under-reporting), aged 0-74 years, were at risk of developing cancer. The most common cancers in South Africa are shown in Table 1.1 below.

Table 1.1: The most common cancers in South Africa, in descending order of occurrence

Males	Females	Children (males and females, 0-14 years)
Prostate	Cervix	Leukaemia
Lung	Breast	Kidney
Oesophagus	Colorectal	Brain
Bladder	Oesophagus	Non-Hodgkin's lymphoma
Colorectal	Lung	Bone

1.3 Cancer treatment

Clinically, weapons to fight cancer are surgery, radiotherapy and chemotherapy (Grella *et al.*, 2003).

1.3.1 Surgery

For centuries, surgery alone could offer a cure for cancer (Shiu, 2003). It remains the principal modality of treatment for many of the common cancers seen today. For example, treatment for hepatic colorectal metastases has greatly evolved over the last two decades, such that this rapidly fatal stage IV disease has become treatable by surgery and potentially curable (Morris *et al.*, 2006). In recent years, there have been improvements in clinical and radiologic staging resulting in more rational planning of surgical and adjuvant treatments.

1.3.2 Radiotherapy

Approximately 50% of all cancer patients are treated with radiotherapy, either as primary treatment with curative intent or for palliation of cancer related symptoms (Vink *et al.*, 2007). Likelihood of tumour response after radiotherapy is determined by the total radiation dose required for tumour cell kill and varies between tumour types, ranging from very radiosensitive low grade lymphomas (90% tumour control at 4 Gy) to notoriously radioresistant malignant gliomas (not responsive at clinically achievable doses). For patients treated with radiotherapy, fibrosis, necrosis and severe organ dysfunction may appear months to years after treatment accomplishment (Koukourakis and Danielidis, 2005).

The therapeutic index (TI) defines the ratio of the percentage of tumour control and the percentage of complications associated with a certain therapeutic regimen (Koukourakis and Danielidis, 2005). In radiotherapy, radio-sensitizing agents aim to improve the TI by increasing the tumour control rate, while cytoprotective policies do the same by reducing the complication rate. Cisplatin and carboplatin have a substantial activity in sensitising tumour cells to radiotherapy in head and neck, lung, oesophagus, cervix, bladder and rectum cancer (Desoize and Madoulet, 2002).

1.3.3 Anti-cancer agents

Classical anti-cancer drugs (*Table 1.2*) were grouped as chemotherapy, hormonal therapy and immunotherapy (Espinosa *et al.*, 2003).

Table 1.2: Classical classification of anti-cancer drugs

Chemotherapy	Alkylators
	Antibiotics
	Antimetabolites
	Topoisomerases inhibitors
	Mitosis inhibitors
	Others
Hormonal therapy	Steroids
	Anti-oestrogens
	Anti-androgens
	LH-RH analogs
	Anti-aromatase agents
Immunotherapy	Interferon
	Interleukin 2
	Vaccines

The group “others” has expanded so much and it has been proposed that classification is based on the target (Espinosa *et al.*, 2003). The target may be located in the tumour cell or in other elements that interact with the tumour cells (endothelium, extracellular matrix, immune system, host cells).

The treatment of cancer has traditionally used agents that interfere with the cell division process (Don and Hogg, 2004). More recently, research and novel therapies have targeted the growth signals that drive the proliferation and survival of cancer cells (for example, Herceptin, for the treatment of breast cancer) and the tumour vasculature (for example, antibodies against vascular endothelial growth factor). DNA-interactive drugs in clinical use represent one of the most important drug classes in cancer therapy (Grella *et al.*, 2003). In general, there are three major types of the above mentioned clinically important drugs:

- The intercalators, which insert between the base pairs of the double helix and determine a significant change of DNA conformation being accompanied by unwinding and elongation of the duplex;

- The alkylators, which react covalently with DNA bases and;
- The DNA strand breakers, which generate reactive radicals that produce cleavage of the polynucleotide strands.

Increased cure rates have been achieved in childhood cancer, testicular cancer, leukaemia and lymphoma; and survival improvements have been obtained with adjuvant drug treatment of breast and ovarian cancer (Workman, 2001). However, the goal of routine care or long term management of cancer as a chronic disease remains frustratingly elusive and the development of preventative agents is even more embryonic and challenging.

1.4 Limitations of current cancer treatment

1.4.1 Lack of selectivity

The majority of current cancer drugs are cytotoxic agents that exert their effects on all proliferating cells, both normal and cancerous (Workman, 2001). This is the case even for recently successful drugs such as irinotecan in colorectal cancer, taxanes in breast, ovarian and lung cancer; and carboplatin in ovarian cancer. Since cytotoxic agents have a selectively 'anti-proliferative' action rather than selective 'anti-cancer' properties, the therapeutic window for tumour versus normal tissue is modest at best and toxic side effects are the norm. Exposure of normal tissues that have a high rate of cellular proliferation (such as bone marrow, gastrointestinal epithelial cells and cells of the hair follicles) to these anti-proliferative drugs leads to major toxicities (Mollinedo and Gajate, 2006). Renal and gastrointestinal toxicity has been reduced considerably in the clinic by intravenous hydration and anti-emetics that antagonise the 5-hydroxytryptamine type 3 receptor (Screnci and McKeage, 1999).

1.4.2 Resistance to drugs

Most tumour types are resistant to current chemotherapy or become resistant during treatment (Broxterman *et al.*, 2003). During the past decades, drug resistance research has identified a myriad of ways by which cancer cells can

elude chemotherapy (Nygren and Larsson, 2003). Resistance in the clinic manifests itself as initial lack of meaningful response (refractoriness) to treatment or regrowth of tumour after an initial response (Broxterman *et al.*, 2003). In the latter case, the recurrent tumour is almost invariably more resistant to treatment than it was at first presentation and treatment. Another manifestation of clinical drug resistance is the frequent occurrence of partial responses. Different subpopulations of tumour cells will be invariably present in tumours, where the predominant cell type will determine anti-tumour response, but the most resistant cells may determine the probability of cure.

The other type of resistance is multidrug resistance (MDR) which is usually caused by the presence of membrane-bound glycoprotein pumps in humans, animals and other organisms (Wang *et al.*, 2003). These pumps keep some foreign substances, such as xenobiotics, toxic agents and drugs from being absorbed, and they are usually called multidrug efflux pumps. The pumps are expressed and distributed in various organs and normal tissues, ranging from lung, liver, kidney, gastrointestinal tract to adrenal, gravid uterus and capillary endothelium in the brain. Based on impressive pre-clinical data, most attention in the clinic has been put on strategies for circumvention of Pgp-mediated MDR using, e.g verapamil and cyclosporin A (Nygren and Larsson, 2003).

1.5 The need for new anti-cancer drugs

The clinical application of new anti-neoplastic drugs has been hindered by their low therapeutic index and lack of efficacy in humans (Sanchez *et al.*, 2001). Thus, an approach to improve old and new anti-cancer drugs has been to manipulate their pharmacokinetic properties. Four interrelated factors determine pharmacokinetic behaviour of a drug: absorption, distribution, metabolism and excretion. Problems such as drug-drug interactions, poor efficacy and high toxicity in humans in contrast to action in laboratory animals, or to variation in these problems among subjects within a population, frequently have their origin in drug metabolism issues.

At one time, the treatment of cancer focused on systemic, non-specific, high-dose chemotherapy, whereas now the goal is to find a drug that balances minimal adverse events (AEs) with maximal anti-tumour activity (Abou-Jawde *et al.*, 2003). Initial steps in the development of such cancer treatments have led to the creation of several new anti-cancer agents. Improved systemic drug therapy is particularly important for the treatment of patients with advanced metastatic cancer, for whom surgery and radiation therapy can no longer be curative (Workman, 2001). Advanced technology and an understanding of the genetic changes that transform a normal cell into a cell uncontrolled by the normal feedback mechanism have facilitated the creation of a new generation of targeted treatments and cancer vaccines (Abou-Jawde *et al.*, 2003).

1.6 Drug design and targets

It is important to note that advances in potential anti-cancer therapies have increasingly involved combinations of current cytotoxic agents with new, molecularly targeted agents (Landis-Piwowar *et al.*, 2006). The literature emphasis on combinational chemistry and the screening of millions of compounds tends to obscure the fact that the world of drug-like properties is quite limited, and that most of the information content related to desirable drug-like properties is contained in a relatively small number of compounds (Lipinski, 2000). When evaluating molecular targets for potential combinational therapies, significant drug-development challenges arise, for example, whether to use a single molecularly targeted agent, a molecularly targeted agent combined with a standard chemotherapeutic drug, or a combination of various molecularly targeted agents.

New agents discovered for possible use as anti-cancer therapy include genes, proteins, growth factors and receptors, and those involved in specific pathways, for example, angiogenesis, signal transduction, cell cycle, cell apoptosis, invasion, metastasis, drug resistance and blood flow (Gupta *et al.*, 2002). Many current drugs were discovered by trial and error (Landis-Piwowar *et al.*, 2006). Therefore, the brute force methods such as high-throughput synthesis and screening can be an effective approach when the target information is not known. If the structure of

the target is unknown, a process called ligand-based drug design can be applied in which analysis of known, active ligands is used to find similarity among other, novel ligands that could alter the activity of a target protein.

1.7 Metal based drugs

When one discusses “drugs”, one often thinks only of organic molecules (Tiekink, 2003). This belies the fact that metal complexes too, play an important role in chemotherapy. Against the background that approximately one third of proteins and enzymes require at least one metal ion to function properly, perhaps it is not surprising that metal complexes have a role to play in medicine as well. The interactions of heavy metals such as platinum, gold with N, S-donor atoms have been recognised for their anti-carcinogenic properties with the potential to develop metal-based drugs (Lobana *et al.*, 2000). Metal ions and metal coordination compounds are known to affect cellular processes in a dramatic way (Reedijk, 2003). This metal effect influences not only natural processes, such as cell division and gene expression, but also non-natural processes, such as toxicity, carcinogenicity, and anti-tumour chemistry. However, the mechanisms of action of metal-based drugs are often not well understood (Jakupec *et al.*, 2003).

Medicinal inorganic chemistry is a discipline of growing significance in both therapeutic and diagnostic medicine (Ronconi and Sadler, 2007). Inorganic compounds have been used in medicine for many centuries, but often only in an empirical way with little attempt to design the compounds to be used, and with little or no understanding of the molecular basis of their mechanism of action. Progress in the design of metal-based inorganic drugs has been slow due to problems relating to substitution and hydrolytic equilibria, redox and polymerisation reactions (Berners-Price and Sadler, 1987a).

The interactions of heavy metals such as platinum and gold with N,S donor atoms have been recognised for their anti-cancer properties with the potential to develop metal-based drugs (Amin *et al.*, 2004). The successful use of metal complexes as therapeutic and diagnostic agents depends on the control of their kinetic and

thermodynamic properties through appropriate choice of oxidation state, types and numbers of bound ligands, and coordination geometry (Sadler, 1997). In this way, it is possible to achieve specificity of biological activity and most importantly, to minimise toxic side-effects. However, before rational drug design can be pursued, a detailed knowledge of the mechanism of action is required (Hambley, 1997). Equally, if one is to “design out” toxic side effects, it is important to know what drug/target interactions are responsible for the toxicity.

Broad interest in the pharmacological properties of metal compounds first arose with the pioneering work of Barnett Rosenberg, who in the late 1960s by chance discovered the cytostatic effects of cisplatin and related compounds (Jakupec *et al.*, 2003). It seemed that biological activity (anti-tumour activity) had to be unique among heavy metal compounds (Kuduk-Jaworska *et al.*, 2004). This was seen as a result of the specific kinetic and structural properties of Pt²⁺ centre making possible the specific impact on genomic DNA. It was shown later that in addition to platinum(II) complexes, numerous planar and octahedral platinum complexes as well as compounds of other platinum-group metals exhibited anti-tumour properties. Anti-tumour activity has been reported for a variety of compounds involving metals such as titanium, vanadium, iron, gold, silver, copper, palladium, ruthenium, germanium and tin (Schurig *et al.*, 1989).

1.7.1 Palladium based drugs

The low anti-tumour activity of palladium complexes has been attributed to rapid hydrolysis leading to easy dissociation (in solution) of leaving groups and to the formation of very reactive species unable to reach their pharmacological targets (Akdi *et al.*, 2002). Based on the structural analogy between Pt(II) and Pd(II) complexes, some studies on Pd(II) compounds as suitable drugs have been carried out. However, advances in this area have been scarce probably due to kinetic reasons; it is well known that comparable Pt(II) compounds always react more slowly by a factor of 10⁵ than corresponding Pd(II) complexes.

Relatively few palladium (II) and palladium (IV) complexes have been investigated for their cytotoxic anti-tumour activity (Kuduk-Jaworska *et al.*, 2004). Among them

were complexes with neutral amine ligands such as ethylenediamine, diaminocyclohexane, ammonia, pyridine and pyrimidine derivatives, alkylaminophosphine oxides, mercapto-imidazoles and pyrimidines. The promising anti-proliferative activity was found in Pd-complexes with chelating ligands or alkyl- or aryl-thiosemicarbazones.

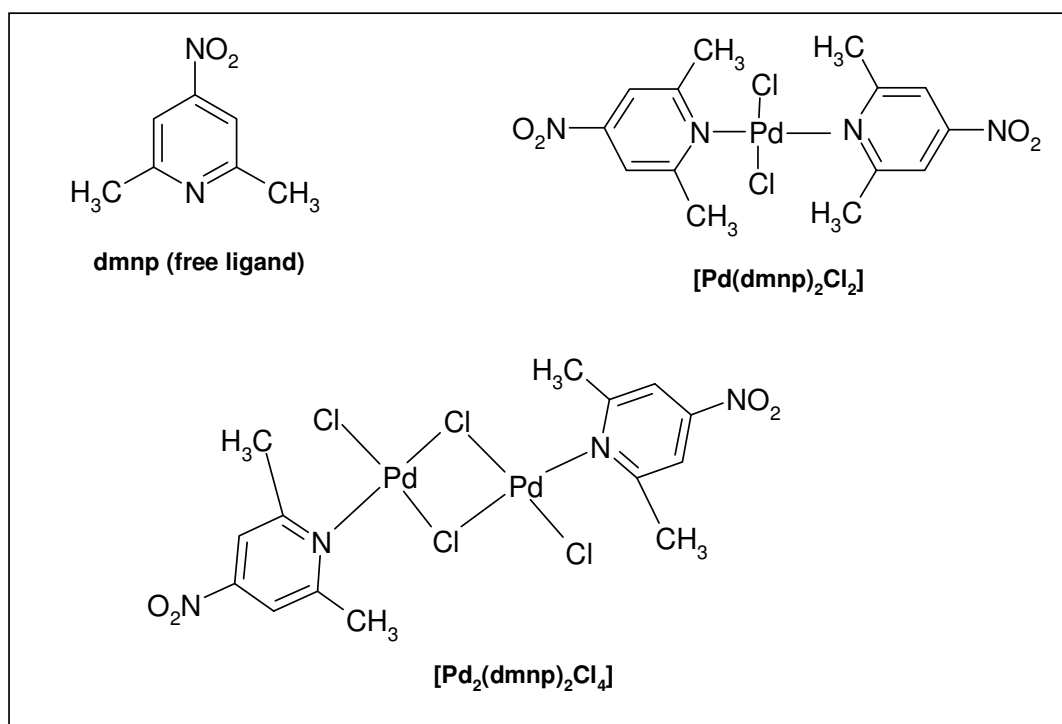


Fig 1.2: Palladium complexes with 2,6-dimethyl-4-nitropyridine that were assayed for *in vitro* cytotoxicity against four human cancer cell lines.

Two kinds of palladium complexes with 2, 6-dimethyl-4-nitropyridine (dmnp) (Fig. 1.2) were prepared and tested for *in vitro* cytotoxicity against four human cancer cell lines: SW707 (adenocarcinoma of the rectum), T47D (breast cancer), HCV (bladder cancer) and A549 (non-small cell lung carcinoma). Free ligand and [Pd₂(dmnp)₂Cl₄] showed moderate activity while [Pd(dmnp)₂Cl₂] was strongly active against all four cell lines (Kuduk-Jaworska *et al.*, 2004). The highest activity was observed against T47D, which is a cell line known to be poorly responsive (rather resistant) to platinum-based drugs. The IC₅₀ (concentration of the compound required to kill 50% of tumour cells) values for the most potent compound ranged from 0.46-8.4 µg/ml.

1.7.2 Platinum based anti-tumour drugs

An important property of platinum coordination compounds is the fact that the Pt-ligand bond has a thermodynamic strength of a typical coordination bond (say 100 KJ/mol or below) which is much weaker than (covalent) C-C and C-N or C-O single and double bonds (which are between 250 and 500 KJ/mol) (Reedijk, 2003). However, the ligand-exchange behaviour of Pt compounds is quite slow, which gives them high kinetic stability and results in ligand exchange reactions of minutes to days, rather than milliseconds to seconds for many other coordination compounds.

Knowledge of the relationship between the ligand structure and cytotoxicity of Pt-based complexes is still limited, even if several rules may be apparent (Alverdi *et al.*, 2004). A number of platinum coordination compounds exhibit anti-viral and anti-tumour activities (Balcarová *et al.*, 1998). Most of the well known anti-cancer complexes have the general formula $\text{cis-[PtX}_2(\text{NHR}_2)_2]$, in which R = organic fragment and X = leaving group, such as chloride or (chelating bis)carboxylate (Reedijk, 2003). Platinum drugs play an important role in the treatment of testis, ovarian and cervical cancer (Screnci and McKeage, 1999). Toxicity to the peripheral nervous system is now the major dose-limiting toxicity for at least some of the platinum drugs currently of clinical interest.

A few platinum drugs currently in clinical use are described below:

a) Cisplatin

The recent history of metal-containing anti-tumour agents began with the unexpected detection of anti-tumour properties of inorganic compound *cis*-diamminedichloroplatinum (II) in 1969 (Kuduk-Jaworska *et al.*, 2004). It was first synthesised in 1844 and named at that time as Peyrone's chloride (Desoize and Madoulet, 2002). Rosenberg, 120 years later, reported its inhibitory activity on *Escherichia coli* division. Its efficacy in human cancer patients was established in 1970's.

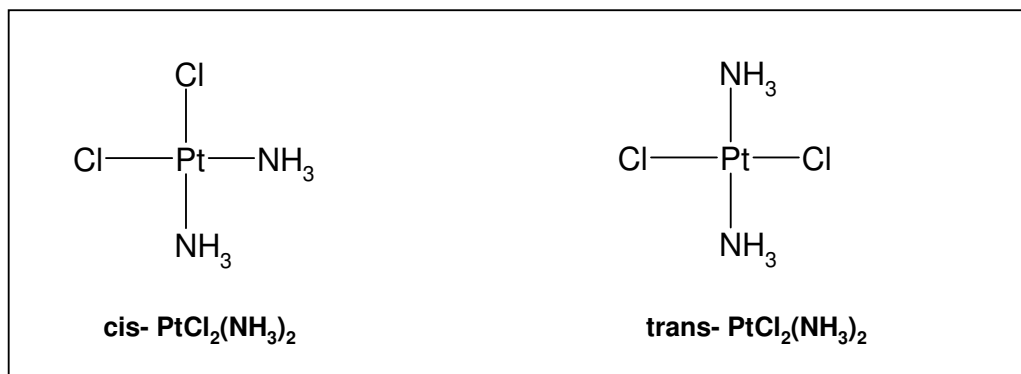


Fig 1.3: Structures of the classical compounds of *cis*-Platin and *trans*-Platin.

The efficacy of platinum agents against cancer could be related to inhibition of DNA synthesis or to saturation of the cellular capacity to repair platinum adducts of DNA (Desoize and Madoulet, 2002). *trans*-Adducts are more easily repaired than *cis*-adducts, for this reason, the *cis* configuration of the diaquo intermediate is 30 times more toxic than the *trans* configuration. Cisplatin is a widely used anti-cancer drug that is highly effective against testicular and ovarian cancers. It is also used alone or in combination with other drugs such as bleomycin, doxorubicin for treatment of tumours of the head and neck, lung, ovarian, cervix and bladder (Daghiri *et al.*, 2004). Its clinical utility has been limited due to the frequent development of drug resistance and severe side effects such as neurotoxicity, nephrotoxicity, ototoxicity, myelosuppression, nausea and vomiting.

Driven by the impressive impact of cisplatin on cancer chemotherapy, great efforts have been made to develop new derivatives with improved pharmacological properties (Jakupec *et al.*, 2003). It has become the prototype of a unique class of anti-neoplastic agents now comprising of numerous derivatives, many of which have been abandoned in pre-clinical or early clinical stages of their development, while a few others have succeeded in becoming established in routine clinical practice. Structure-activity relationships for a class of related compounds confirmed that only those compounds having *cis*-geometry block cell growth.

b) Carboplatin

Carboplatin [(H₃N)₂Pt(CBDC)], (CBDC, 1,1'-cyclobutyldicarboxylato group), a second generation analogue of cisplatin has reduced toxic side effects for the

same efficiency (Abu-Surrah *et al.*, 2003). Briston-Myers Squibb developed this drug, with collaboration of a number of oncologists and academic institutes (Desoize and Madoulet, 2002). After excessive pre-clinical screening, involving a large number of platinum derivatives, carboplatin was selected mainly because of its lower non-haematological toxicity compared with cisplatin. Unfortunately, it exhibits cross-resistance with its parent compound. The dose limiting toxicity is myelosuppression, chiefly thrombocytopenia.

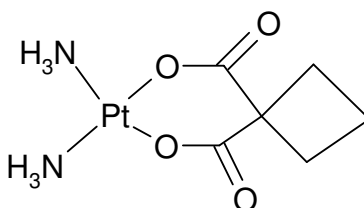


Fig 1.4: Carboplatin

The combination of carboplatin with paclitaxel is of great interest, since toxicity is reduced (Desoize and Madoulet, 2002). This combination is used notably in cancers of the ovary, head and neck, bladder and in non-small-cell lung cancer (NSCLC).

c) Oxaliplatin

Oxaliplatin (*trans*-1,2-diaminocyclohexane platinum(II) oxalate) is a third generation analogue of cisplatin (Abu-Surrah *et al.*, 2003). Oxaliplatin (Eloxatin®, Sanofi-Synthelabo) was first approved in 1998 in France and subsequently in the rest of Europe and more recently (2002) by the Food and Drug Administration in the United States (Galanski *et al.*, 2005).

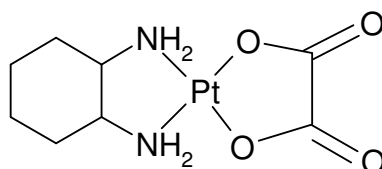


Fig 1.5: Oxaliplatin

This drug gave interesting results in ovarian, breast, head and neck cancer and in non-Hodgkin's lymphoma, malignant melanoma, glioblastoma and NSCLC (Desoize and Madoulet, 2002). It is active against certain tumours which are primarily resistant to cisplatin and carboplatin (Galanski *et al.*, 2005). It is used in clinics in combination with 5-fluorouracil and Leukovorin for the treatment of patients with colorectal cancer, which is the second leading cause of cancer death in developed countries. The toxicity profile of oxaliplatin is favourable, with frequencies for ototoxicity of <1% and for renal toxicity <3%, except for unusual toxicity with regard to peripheral sensory nerves (Kweekel *et al.*, 2005). Sensory neuropathy usually arises during infusion, affects hands, feet and perioral area and is enhanced by cold. These effects appear to be cumulative and generally reverse within 4-6 months after treatment discontinuation.

1.8 Metal phosphines as anti-tumour agents

Currently, platinum complexes with structures different from that of cisplatin are being considered with the idea that they would have a different spectrum of activity and hence not develop cross-resistance to cisplatin (Huq *et al.*, 2004). Somewhat disappointingly, the thousands of compounds estimated to have been prepared and tested have led to few new drugs or fundamental advances (Hambley, 1997). An additional motivation has been the desire to find compounds that do not have the many toxic side effects that cisplatin exhibits.

Progress in the design of metal-phosphine complexes as anti-tumour drugs depends on an understanding of the mechanism of action (Berners-Price and Sadler, 1987a). Phosphorus is an important biological element, but only P(V) compounds are found in biological systems. The relative cytotoxic potencies of phosphines depend on a number of factors, including lipophilicity, redox potential and pK_a . However, there is a paucity of relevant chemical data due to the fact that phosphines are rarely studied under biologically relevant conditions, *i.e.*, in the presence of H_2O and O_2 .

1.8.1 Gold phosphines in medicine

Chemotherapeutic applications of gold(I) complexes for the treatment of rheumatoid arthritis have been studied extensively for more than 60 years (Song *et al.*, 1999). The metal may play an important role in protecting the ligand from oxidation and it has been shown that gold phosphine complexes are much more cytotoxic than the free ligands. Auranofin (*Fig. 1.6*), for instance, has anti-tumour activity, although $P(C_2H_5)_3$ is inactive. This thioglucose derivative of triethylphosphine Au(I) was selected for extensive clinical trials and approved for clinical use in 1985 under the trade name Ridaura.

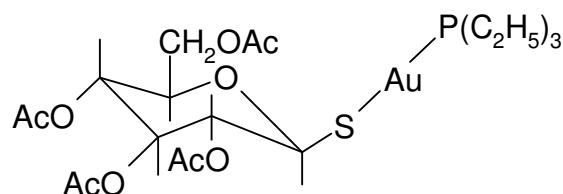


Fig 1.6: Auranofin

This and other linear Au(I) phosphine complexes are potentially cytotoxic to tumour cells in culture (Berners-Price and Sadler, 1996). However, *in vivo*, auranofin exhibits modest anti-tumour activity against only P388 leukaemia in mice, and only when administered intraperitoneally (i.e, the drug comes into direct contact with the tumour cells). Several thiolate-supported gold drugs are commercially used in modern medicine. However, unlike thiols and other sulphur compounds, phosphines are not natural products and are generally difficult to prepare (Song *et al.*, 1999). Therefore, previous clinical tests of anti-cancer gold phosphine complexes have been limited to some simple phosphines that are commercially available. Nevertheless, this pioneering work has shown that the anti-cancer activity of Au(I)-phosphine complexes is critically dependent on the molecular architecture of the phosphine ligands.

1.8.2 Cationic metal complexes as potential anti-tumour agents

The biochemistry of a metal in a certain oxidation state is very much determined by its affinity for various ligands (Ahrlund, 1983). Not only are the absolute strengths of the metal-ligand interactions important, but also the relative affinities between ligands of various properties and types. The *bis*-chelated 1:2 Au(I) diphosphine complex $[\text{Au}(\text{dppe})_2]\text{Cl}$ (Fig. 1.7) (where dppe is $\text{Ph}_2\text{PCH}_2\text{CH}_2\text{PPh}_2$) has been shown to exhibit anti-tumour activity against a range of tumour models in mice (Berners-Price *et al.*, 1999b). Structure-activity relationships have been evaluated for a wide range of diphosphine ligands and their metal complexes.

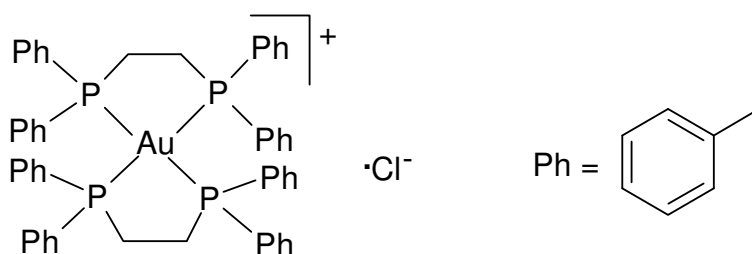


Fig 1.7: $[\text{Au}(\text{dppe})_2]\text{Cl}$

The highest activity for complexes of the type $[\text{Au}(\text{R}_2\text{P}(\text{CH}_2)_n\text{PR}'_2)_2]^+$, is found where $\text{R} = \text{R}' = \text{Ph}$ and $n = 2, 3$ or *cis*- $\text{CH}=\text{CH}$ (Berners-Price *et al.*, 1999b). Phosphorus 31 NMR studies show that in the presence of thiols and blood plasma, these compounds readily undergo ring-closure reactions to form a four-coordinate cation $[\text{Au}(\text{dppe})_2]^+$ (Berners-Price *et al.*, 1992). Salts of this cation exhibit a broad spectrum of anti-tumour activity as do analogous silver(I) and copper(I) diphosphine complexes. Replacement of the phenyl substituents on the phosphine with other groups led to a decrease or loss of anti-tumour activity. Pre-clinical development of $[\text{Au}(\text{dppe})_2]^+$ was abandoned after the identification of severe hepatotoxicity in dogs, attributed to alterations in mitochondrial function (Berners-Price *et al.*, 1999a). $[\text{Au}(\text{dppe})_2]^+$ was extremely lipophilic (containing eight hydrophobic phenyl substituents) and consequently non-selectively targeted mitochondria in all cells.

In recent work, the adopted approach was to modify the diphosphine ligands of metal complexes related to $[\text{Au}(\text{dppe})_2]^+$ in order to vary the hydrophilic character

of the complexes and achieve greater selectivity for tumour cells versus normal cells (Berners-Price *et al.*, 1999a). In order to retain aromatic substituents which seem to be important for anti-tumour activity, Berners-Price and co-workers replaced some or all of them with more hydrophilic pyridyl groups. Their work was stimulated by the observation that the *bis*-chelated Au(I) complex $[\text{Au}(\text{d2pyrpe})_2]\text{Cl}$, [d2pyrpe is 1,2-bis-(di-2-pyridylphosphino)ethane] was found to exhibit activity in mice bearing P388 leukaemia, whereas the corresponding 4-pyridyl complex $[\text{Au}(\text{d4pyrpe})_2]\text{Cl}$ was inactive. They demonstrated that the position of the N-atom in the pyridyl ring finely modulated the lipophilic balance by influencing the structural types that existed for Au(I) and Ag(I) complexes.

Pd analogues of $[\text{Au}(\text{dppe})_2]\text{Cl}$ have previously being prepared and tested for anti-tumour activity (Schurig *et al.*, 1989). These complexes, $[\text{Pd}(\text{dppe})_2]\text{Cl}_2$ and $[\text{Pd}(\text{dppen})_2]\text{Cl}_2$, were tested for cytotoxicity against a tumour cell line composed of murine and human tumour cell lines. The results showed low potency. They were also tested for anti-tumour activity on ip-implanted tumours and both of them showed inactivity and were not well tolerated.

1.9 Hypothesis

Varying the metal and lipophilicity can modify the selectivity and cytotoxic properties of anti-neoplastic drugs containing Platinum Group Metals.

1.10 Aim of study

The aim of the project was to synthesise Pd and Pt analogues of $[\text{Au}(\text{dppe})_2]^+$ that varied in lipophilicity and consequently possessed the ability to exhibit high selectivity and anti-neoplastic activity.

1.11 Objectives of the study

The first objective of this project involved the synthesis of Pd and Pt analogues of $[\text{Au}(\text{dppe})_2]^+$ that varied in alkyl backbones and/or substituents on the phosphorus atom (Fig. 1.8). This was perceived as essential in altering lipophilicity of the complexes. The phenyl complexes contained either an ethane or ethene backbone while the pyridyl ones possessed only the ethane bridge.

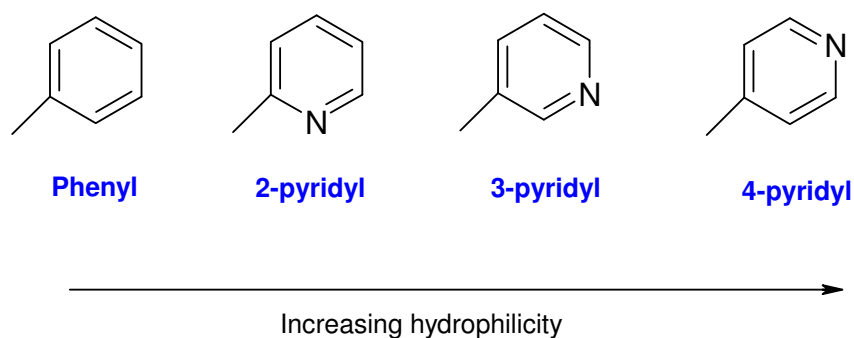


Fig 1.8: Substituents on phosphorus atoms

The complexes synthesised in this project have the general formula shown below (Fig 1.9).

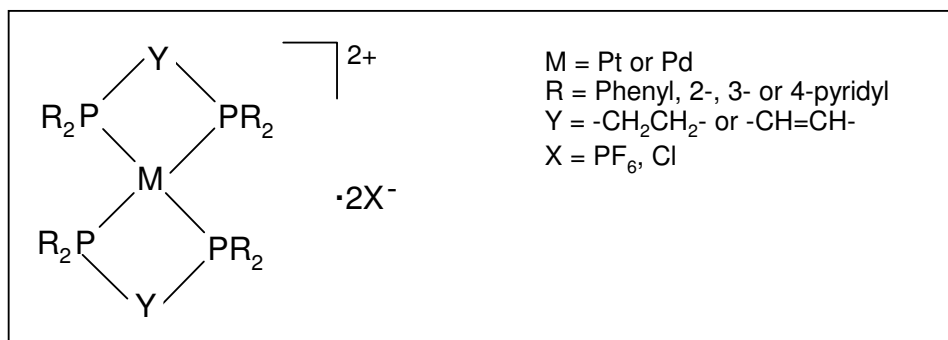


Fig 1.9: General structure of the complexes discussed in this study.

The second aspect of this study dealt with synthesising compounds that were stable enough to reach the target (tumour cells) in the presence of biological fluids. Kinetic lability in the metal-phosphine bonds is of importance so that the phosphine itself is reactive at the target site, as in Au(I), Ag(I) and Cu(I) diphosphine complexes (Berners-Price and Sadler, 1987a). On the other hand, one approach to solving the problem of rapid hydrolysis of palladium complexes is

the identification of novel substances that can be used as binding blocks for palladium anti-tumour drugs (Akdi *et al.*, 2002).

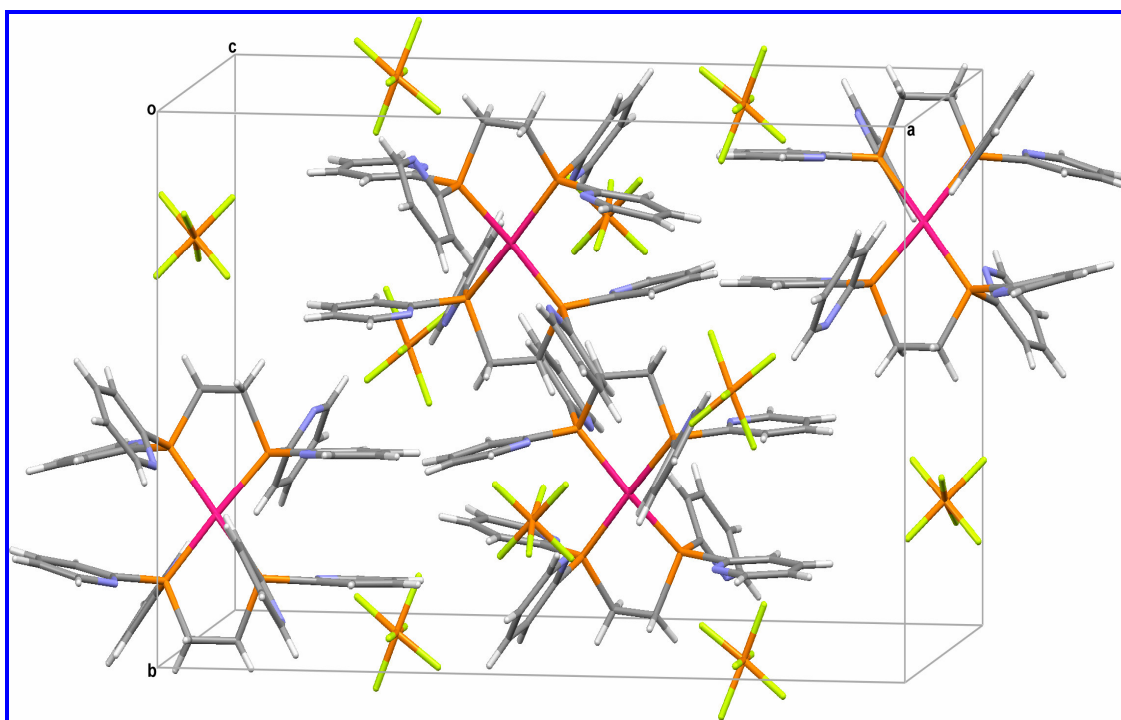
The third objective was to correlate properties of the compounds, i.e. lipophilicity, stability to *in vitro* cytotoxicity and selectivity in both cancerous and normal cells. This was in an attempt to understand the structure-activity relationship that may exist across the range of both Pd and Pt complexes. It has been shown that the different solubility profiles of Au(I) and Ag(I) pyridylphosphine complexes influences their cellular uptake and hence results in differences in anti-tumour selectivity and potency (Berners-Price *et al.*, 1999a).

The anti-neoplastic potency of these complexes against selected cancer cell lines was compared to $[\text{Au}(\text{dppe})_2]\text{Cl}$. No inconsistency was expected in the comparison of compounds with different counterions (PF_6^- vs Cl^-) because studies have shown that activity was found to be independent of the nature of the counterion, I^- or PF_6^- (Tiekink, 2002). The most promising candidate (based on *in vitro* assays) was selected for further investigations with special focus on its anti-mitochondrial activity. This focus was necessary as the study was based on $[\text{Au}(\text{dppe})_2]\text{Cl}$ which has been reported to have an anti-mitochondrial mode of action in tumour cells (Berners-Price *et al.*, 1999a).

Besides anti-mitochondrial action, the modes of cell death (apoptosis vs necrosis) as well as cell cycle effects were investigated. The final objective was to determine the bio-distribution of the radiolabelled lead candidate as well as its maximum tolerated dose *in vivo* (Wistar rats and Balb/c mice, respectively).

Chapter II

Phosphines and metal phosphine complexes



2.1 Phosphine ligands

Organic phosphines (or phosphanes) PR_3 play an important role as ligands in coordination chemistry in general and organometallic chemistry in particular (Vogler and Kunkely, 2002). Phosphines are well known to stabilise transition metals in low oxidation states but their versatility as ligands is also documented by their ability to coordinate to transition metals in higher oxidation states including metals with a d^0 electronic configuration. These ligands provide a lone pair at the phosphorus atom which is used for the formation of an M-PR_3 σ -bond. In the case of d^0 complexes, only this σ -bond exists. However, for the electron-rich d^n metals in low oxidation state, π back bonding becomes important.

2.1.1 Electronic vs Steric effects

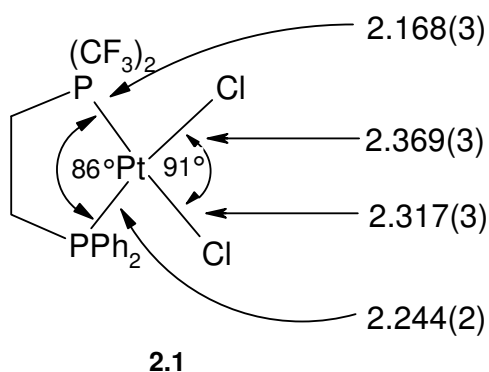
The chemical characteristics of phosphines have continued to be the subject of many theoretical and experimental studies since the pioneering work by Tolman (Tolman, 1977) to define and quantify the steric and electronic properties of these widely used molecules (Fredericks *et al.*, 1994). These two main aspects are involved in the coordination of tertiary phosphine ligands to transition metal atoms (Roodt *et al.*, 2003). The electronic character of the M-P bond is a combined effect of the σ bond formed by donation of the lone pair electron from the P to the M atom and secondly by the ability of the P ligand to accept electron density from the metal by back-donation into a combination of the empty 3d-orbitals and σ^* -orbitals of the P-atom. A second factor influencing the coordination of a ligand is the spatial demand, or steric size, associated with the specific ligand.

Organic substituents on phosphine ligands not only change the electronic properties of the ligands but may also influence their steric requirements (Mingos, 1998). Attempts have been made to quantify these effects for phosphines by measuring the pK_a values of the corresponding values of the subsequent conjugate acids $[\text{HPR}_3]^+$, which provide an estimate of the donor properties of the ligands, and the Tolman cone angle which estimates the steric requirements of the ligands. For example, the dissociation of phosphine ligands in $[\text{Pd}(\text{PR}_3)_4]$ appears to be dominated by steric effects and the dissociation constant K defined below:



It increases in the order $\text{PPh}(\text{Bu}^t)_2 > \text{PCy}_3 > \text{P}(\text{Pr}^i)_3 > \text{PPh}_3 \sim \text{PEt}_3 > \text{PMePh}_2 \sim \text{PMe}_2\text{Ph} \sim \text{PMe}_3$.

In phosphines and cyclopentadienyls, a change of substituent causes a change not only in the steric, but also in the electronic effect of the ligand, because the R group that is varied is directly attached to the donor atom (Crabtree, 2005). For example, going from PPh_3 to PCy_3 causes a change in both factors, and each factor cannot be varied independently. They are both typically cone-shaped, so rotation about the M-L bond should not have major consequences for either steric or electronic effects. More electronegative substituents on P are expected to give a shorter M-P bond because they put more phosphorus s character into the bond (Tolman, 1977). For example, the substituents on the phosphorus atoms of 2.1 are similar in size but very different electronically.



The Pt-P(CF₃)₂ bond is shorter by 0.07 Å compared to the Pt-PPh₂ bond and the corresponding *trans* Pt-Cl bonds differ by 0.05 Å. These effects must be largely electronic. A very similar structure was found for the Pd analogue. In summary, increasing the angles between substituents will decrease the percentage of s character in the phosphorus lone pair (Tolman, 1977). Changing the electronegativity of atoms can also affect bond distances and angles. Thus, electronic and steric effects are intimately related and difficult to separate in any pure way.

2.1.2 Heteroatomic substituents on phosphine ligands

The majority of phosphine ligands PR_3 , carry alkyl and aryl substituents at the phosphorus atom (Vogler and Kunkely, 2002). In a more general sense, R may also be a halogen atom (phosphorus halides, PX_3) or, for example, an OR group [phosphites, $P(OR)_3$]. It has long been recognised that changing substituents on phosphorus ligands can cause marked changes in the behaviour of the free ligands and of their transition metal complexes (Tolman, 1977). The diversity of tertiary phosphines in terms of their Lewis basicity and bulkiness renders them excellent candidates to tune the reactivity of square-planar complexes towards a variety of chemical processes, such as oxidative addition and substitution reactions (Roodt *et al.*, 2003). In general, substituents with better electron-donating capabilities will increase the Lewis basicity of the phosphine, while electron-withdrawing substituents increase the π acceptor ability. The 2-pyridyl group is electron-withdrawing relative to a phenyl substituent, and the weaker σ -basicity of the phosphorus of the $PPh_{3-n}pyr_n$ ligands (versus PPh_3) likely accounts for the relative stabilities (Baird *et al.*, 1995).

2.1.3 Bridging and chelating phosphine ligands

The chelate effect is one of the oldest concepts in coordination chemistry and has been successfully explained largely in terms of the entropy change involved in the chelation process (Minahan *et al.*, 1984). In general terms, the factors that appear to be important include: the nature of the central metal atom, the nature of the ligand donor atoms, the chelate chain length, the rigidity of the chelate backbone, the steric effects of the atoms or groups attached to the donor atoms and the nature of the coordinated anions.

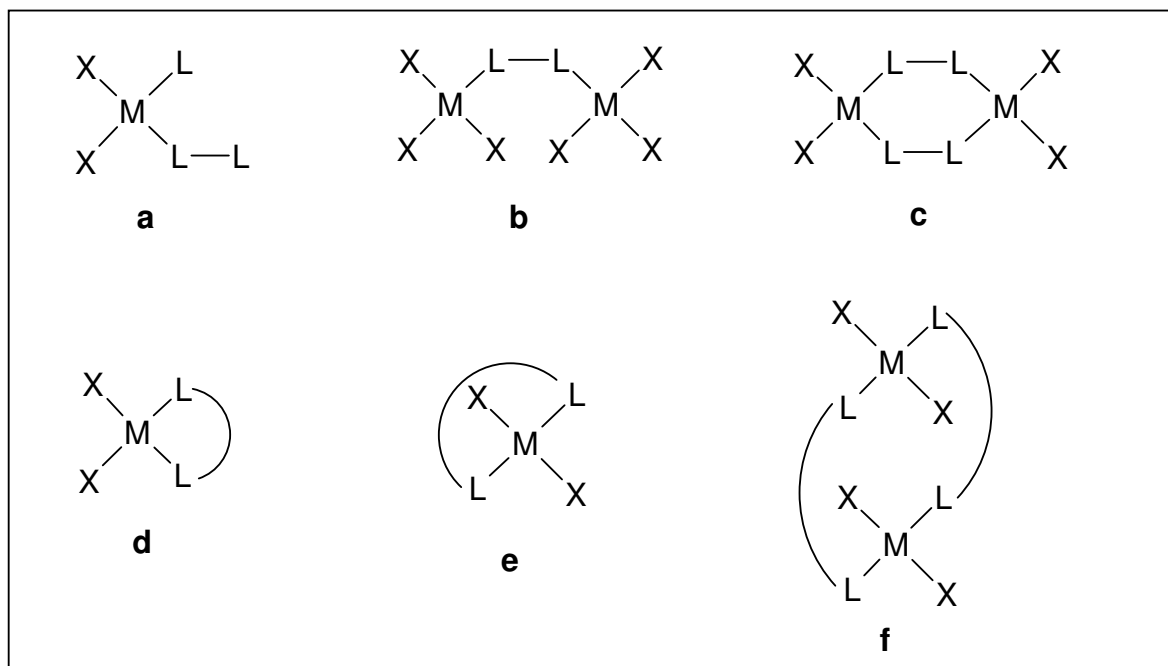
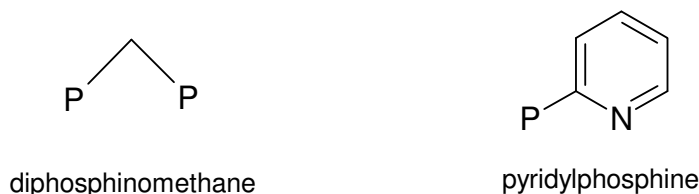


Fig 2.2: Bidentate ligand bonding modes in a square planar complex (Minahan *et al.*, 1984).

The three basic classes of potential phosphine chelate ligands are diphosphines, alkenylphosphines, and ligands with the potential to be cyclometallated (Garrou, 1981). Derivatives of diphosphine itself, H_2PPh_2 , contain two donor atoms linked by a single bond and cannot, on geometrical grounds, undergo chelation (Bell, 1977). As in the case of organic diamines, chelation first appears to be possible when the donor atoms are separated by an ethylene bridge. This is so for the substituted diphosphines, $R_2PCH_2CH_2PR_2$, for example, in diphenylphosphinoethane, where $R = C_6H_5$.

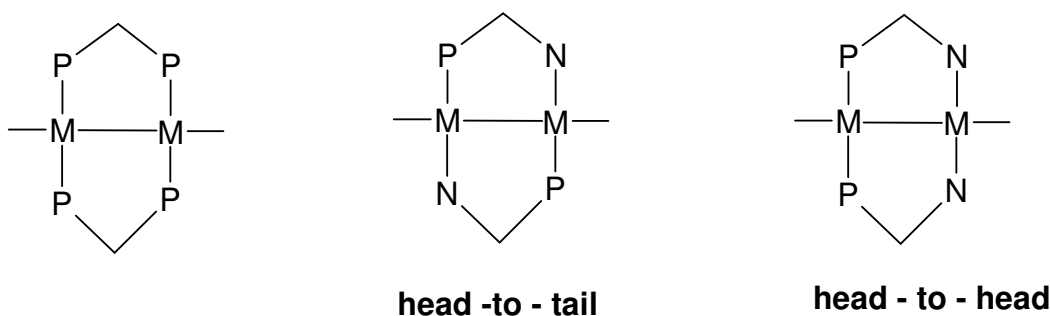
The versatile diphosphine ligands are particularly appropriate for the synthesis of low-valent metal complexes (Effendy *et al.*, 2004). Bis(diphenylphosphino) methane (dppm) and 1,2-bis-(diphenylphosphino)ethane (dppe) are widely used in inorganic chemistry, the former affording binuclear metal complexes in the μ -dppm form, while the latter predominately affords chelating and bridging complexes. Phosphine substitution reactions between $[Ru(\eta^5-C_5H_5)(PPh_3)_2Cl]$ and dppe have shown the latter to act as both bridging and as a chelating ligand with the formation of $[RuCp(dppe)Cl]$ and $[RuCp(Cl)]_2(\mu_2-dppe)_2$ (Moura *et al.*, 1999).

One approach to the synthesis of bimetallic complexes is the use of binucleating ligands that will rather bridge than chelate (Budzelaar *et al.*, 1990). Two of the more popular classes are diphosphinomethanes and 2-pyridylphosphine ligands (2.3).



2.3

Both of these ligands tend to form complexes in which two metal atoms are surrounded by two ligand molecules in a “*trans*” fashion (Budzelaar *et al.*, 1990). Because of the asymmetry of the 2-pyridylphosphine ligand, two types of M_2L_2 complexes may be formed, “head-to-tail” and “head-to-head” (2.4).



2.4

2.2 Pyridylphosphines

The chemistry of heterodifunctional ligands incorporating both “soft” (e.g. P) and “hard” (e.g. N or O) donor atoms continues to attract interest (Jones *et al.*, 1999). Some years ago, Rauchfuss (Jeffrey and Rauchfuss, 1979) introduced the concept of *hemilability* for ligands possessing a combination of soft and hard donor ligands (Espinet and Soslantica, 1999). This term was originally used for phosphine-amine and phosphine ether ligands that ‘would bind well enough to platinum group metals to permit isolation but would readily dissociate the hard end

component, thus generating a vacant coordination site for substrate binding'. A distinguished family of hemilabile ligands is that combining phosphorus and nitrogen atoms. These ligands can display quite different coordination modes compared to P-P or N-N ligands.

Pyridylphosphines are an important class of functionalised phosphines containing both P- and N-donor centres (Durran *et al.*, 2006). Many studies have focused on simple pyridylphosphines most notably Ph₂Ppyr, PhPpyr₂ and Ppyr₃ (pyr = 2-pyridyl). These phosphines have been shown to display various coordination modes, serve as useful building blocks for di- and polynuclear compounds and have catalytic applications. The solubility of these ligands in water increases with increasing number of pyridyl substituents, for example, Ppyr₃ readily dissolves at pH ~3, because the first protonation equilibrium corresponds to a pK_a value of 4.2 at 20 °C (Baird *et al.*, 1995).

Interest in pyridine containing natural products and pharmaceuticals, as well as pyridine building blocks for various applications such as material science and supramolecular chemistry, has resulted in extensive efforts on synthesis methodologies (Trécourt *et al.*, 2000). Lithiation reactions allow many functionalisations either by direct reaction with electrophiles or transmetallation to allow cross-coupling reactions. The first reported preparation of a pyridylphosphine was presented (Davies and Mann, 1944) as part of a study on the optical resolution of tertiary phosphines (Newkome, 1993). Pyridylmagnesium bromide, initially generated via the entrainment process, was treated with phenyl(4-bromophenyl)chlorophosphine to afford (5%) the first pyridylphosphine **a** (Fig. 2.5).

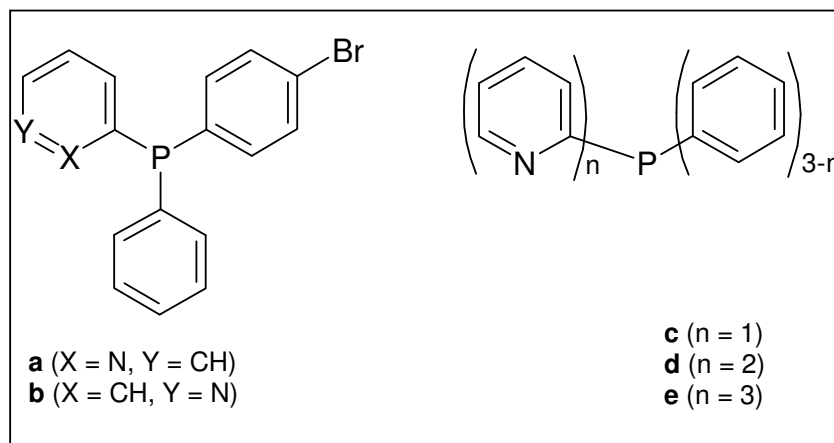


Fig. 2.5: Examples of the first pyridylphosphines

When 3-pyridylmagnesium bromide was reacted similarly, the only known, 3-pyridylphosphine **b** was prepared in poor yield (7%). Tris-2 pyridylphosphine **e** was prepared (13%) from 2-pyridylmagnesium bromide with PCl_3 , whereas in 1948, this procedure was extended to the synthesis of **c** and **d**. Synthetic routes have been improved over the years and compounds **c**, **d** and **e** have been prepared in good yield by straightforward modification of the standard butyllithium metal halogen exchange method (Bowen *et al.*, 1998).

Recent work, using classical synthetic procedures in phosphorus chemistry, has shown that numerous other new pyridylphosphines can be synthesised (Durrant *et al.*, 2006). These include PN-bidentate, mixed OPN-, PNP-, CNP-terdentate, chiral, phosphine oxide, and sulphide based pyridyl modified ligands. Additionally, there are typical *P*-derivatives of pyridylphosphines, which include oxides, sulphides, selenides, methides and methylphosphonium salts (Newkome, 1993).

2.3 Metal pyridylphosphines

Two researchers (Uhlig and Maaser, 1966) initially reported the preparation of Ni(II), Co(II), Zn(II) and Cu(II) complexes of $\text{Ph}_2\text{PCH}_2\text{CH}_2(2\text{-pyr})$ (Newkome, 1993). Throughout the 1970s, a few research groups utilised other simple pyridylphosphines to prepare various uncomplicated metal ion complexes, which were characterised by the application of the traditional techniques, such as infrared, conductivity, molecular weight, magnetic susceptibility, electronic spectra, X-

ray powder diffraction, elemental analyses, as well as studies of their electrochemical properties.

The coordination chemistry of the pyridylphosphines $\text{PPh}_{3-n}\text{pyr}_n$, where $n = 1-3$, has developed noticeably and there have been reports on catalysis using pyridylphosphine complexes (Xie and James, 1991). A few examples are hydroformylation of olefins and water-gas-shift reaction catalysed by Rh species, conversion of methanol to ethanol using Ru species, and conversion of propyne to methylmethacrylate using Pd species. This is due to decades of work on phosphine coordination chemistry that has provided relatively easy synthetic routes to a dazzling array of different complexes (Crabtree, 2005).

One important property of potentially multidentate ligands is that they can stabilise metal ions in a variety of oxidation states and geometries (Espinete and Soullantica, 1999). The π -acceptor character of the phosphorus ligand can stabilise a metal center in a low oxidation state, while the nitrogen σ -donor ability makes the metal more susceptible to oxidative addition reactions. A widely used pyridylphosphine is (diphenyl)(2-pyridyl)phosphine, PPh_2pyr **f** (Fig. 2.6), which as a ligand can adopt three different coordination modes: *P*-monodentate, *P,N*-chelate and *P,N*-bridge (Jones *et al.*, 1999; Zhang and Cheng, 1996).

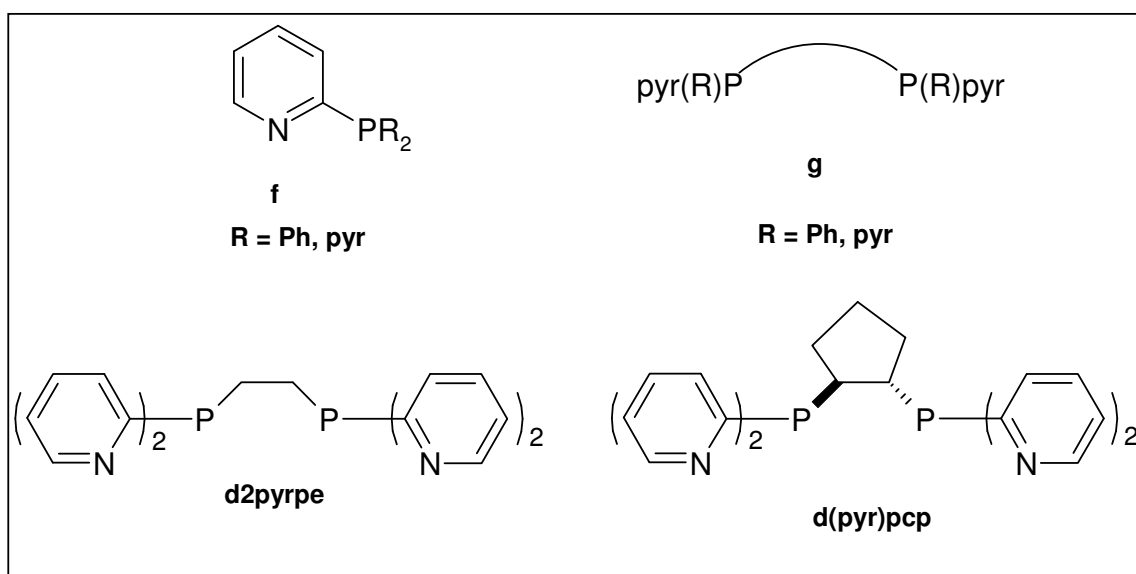


Fig 2.6: Some examples of 2-pyridylphosphine ligands

The formation of complexes where the P-N ligand acts as a chelate depends very much on the stability of the chelate ring formed (Espinete and Soulantica, 1999). In general, four membered rings are strained, whereas seven- or longer membered rings are not often geometrically favoured. Five- and six-membered chelates are expected to have the best and most stable conformation.

Interest in type **g** ligands stems from the idea that protonation of non-coordinated pyridine N atoms on the ligand would be a convenient route to water solubilisation of the corresponding metal complexes, with the ultimate objective being the homogenous catalytic hydrogenation of olefins in aqueous media (Jones *et al.*, 1999). Synthetic and characterisation details of the coordination chemistry of the ligands d(pyr)pcp and d2pyrpe towards a range of Ru(II) and Pt(II) fragments has also been described. [d(pyr)pcp = 1,5-bis-(di-2-pyridylphosphino)-cyclopentane and d2pyrpe = 1,2-bis-(di-2-pyridylphosphino)ethane].

1:2 adducts of Ag(I) and Au(I) with 1,2-bis-(di-n-pyridylphosphino)ethane (dnpyrpe) for n = 2, 3 and 4 have also been synthesised and solution properties determined by multinuclear NMR spectroscopy (Berners-Price *et al.*, 1999b; Berners-Price *et al.*, 1999a). The complexes of d3pyrpe and d4pyrpe are simple monomeric $[M(d3pyrpe)_2]^+$ and $[M(d4pyrpe)_2]^+$ species which have a much higher water solubility than the 2-pyridyl complexes (which crystallise in the solid state as dimeric, $[\{M(d2pyrpe)_2\}_2]^{2+}$, complexes). The 2-pyridylphosphine complexes of Ni(0), Ni(II), monomeric Pt(0), monomeric Pd(II), and dinuclear Pd₂(I) and Pt₂(I) have also been reported (Baird *et al.*, 1995). The d2pyrpe ligand has been shown to exhibit *P,P* bonding at Pt(II) (Jones *et al.*, 1999). Several of its complexes have some solubility in water and are completely soluble in dilute aqueous solution. A comprehensive review on the extensive studies that have been carried out on pyridylphosphines, related ligands, and their metal complexes is available (Espinete and Soulantica, 1999).

2.4 Metal complexes of diphenylphosphine ligands

The ligand bis-(diphenylphosphino)ethane (dppe) is the archetypal bidentate phosphine ligand which has probably been the most extensively used of all bidentate phosphine ligands in organometallic chemistry (Butler *et al.*, 2000). The *bis*-coordinated bis(diphenylphosphino)alkane and –alkene group 8 metal complexes have been synthesised via reaction of suitable group 8 metal precursors with two equivalents of bis-(diphenylphosphino)ethane, -ethene or –propane (Schurig *et al.*, 1989). A range of metal complexes of iron, cobalt, rhodium, iridium, nickel and palladium has been prepared. Complexes of Ag(I), Cu(I) and Au(I) diphenylphosphine have also been reported in the literature (Berners-Price *et al.*, 1988).

Diphosphine bridged-digold complexes $[\{AuCl\}_2(\mu\text{-Ph}_2\text{P(CH}_2)_2\text{PPh}_2)]$ are readily converted into the *bis*-chelated species in the presence of added diphosphine ligand (Berners-Price *et al.*, 1987b). Chelated complexes of the type $[Au(R_2P(CH_2)_nPR'_2)_2]Cl$ ($n = 2$ or 3) form readily when R and R' are phenyl and also with the more rigid ligand *cis*- $\text{Ph}_2\text{PCH=CHPPh}_2$. The interaction between bidentate diphosphines $R_2P(Y)_nPR_2$ ($Y = \text{CH}_2$, $n = 1, 2$ or 3) and silver salts has also attracted a great deal of interest because the resultant complexes have found applications in homogenous catalysis and also as anti-tumour agents (Effendy *et al.*, 2004).

2.4.1 Palladium and Platinum diphenylphosphines

Cationic palladium phosphine complexes have been actively studied due to their role in an enormous number of important synthetic transformations and for the polymerisation of polar and non-polar olefins (Thirupathi *et al.*, 2005). Palladium (II) salts form very stable complexes with tertiary phosphines and arsines (Chow *et al.*, 1974). Among the bidentate group VB chelates coordinated to palladium(II) are: 1,2-bis-(diphenylphosphino)ethane (dppe) and 1,2-bis-(diphenylarsino)ethane, *cis*- and *trans*-1,2-bis-(dimethylarsino)ethylene, *o*-phenylenebis-(dimethylarsine), 1,8-bis-(dimethylarsino)naphthalene, (*o*-diphenylphosphinophenylene)diphenylarsine and *o*-phenylenebis-(diphenylarsine).

The synthesis and characterisation of palladium and platinum complexes of 1,2-bis-(diphenylphosphino)ethane (dppe) and 1,2-bis-(diphenylphosphino)ethene (*cis*-dppen) have previously been described (*Fig. 2.7*) (Westland, 1965; Chow *et al.*, 1974; Oberhauser *et al.*, 1995; Oberhauser *et al.*, 1998,).

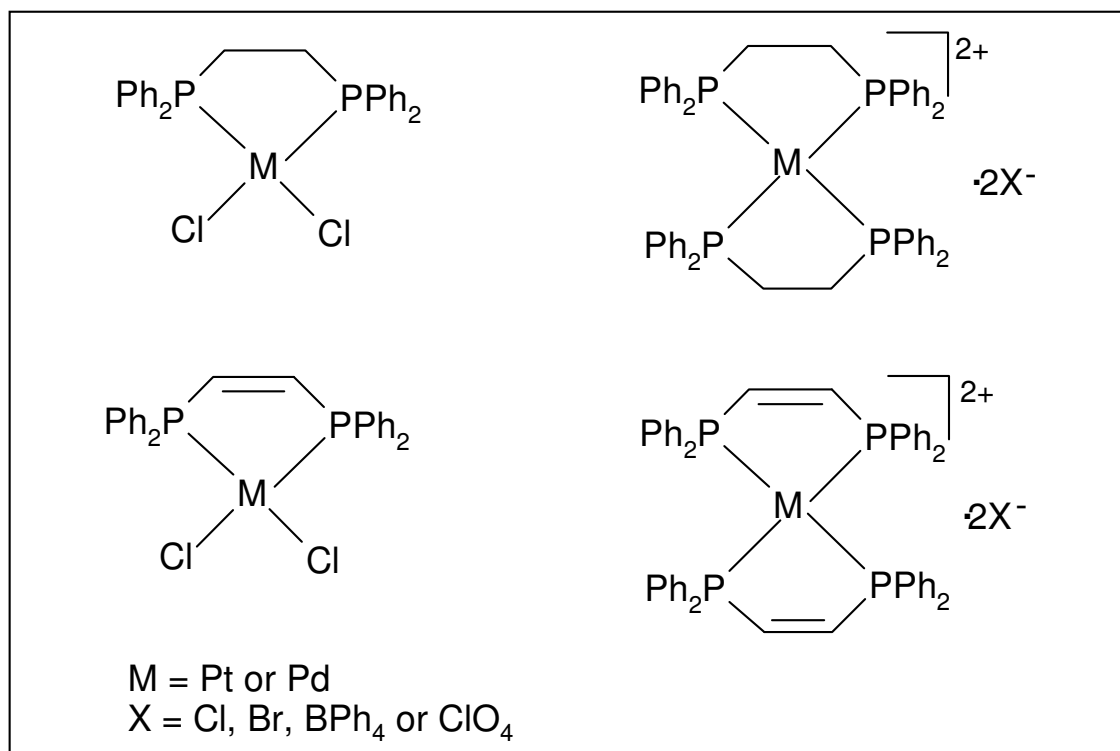
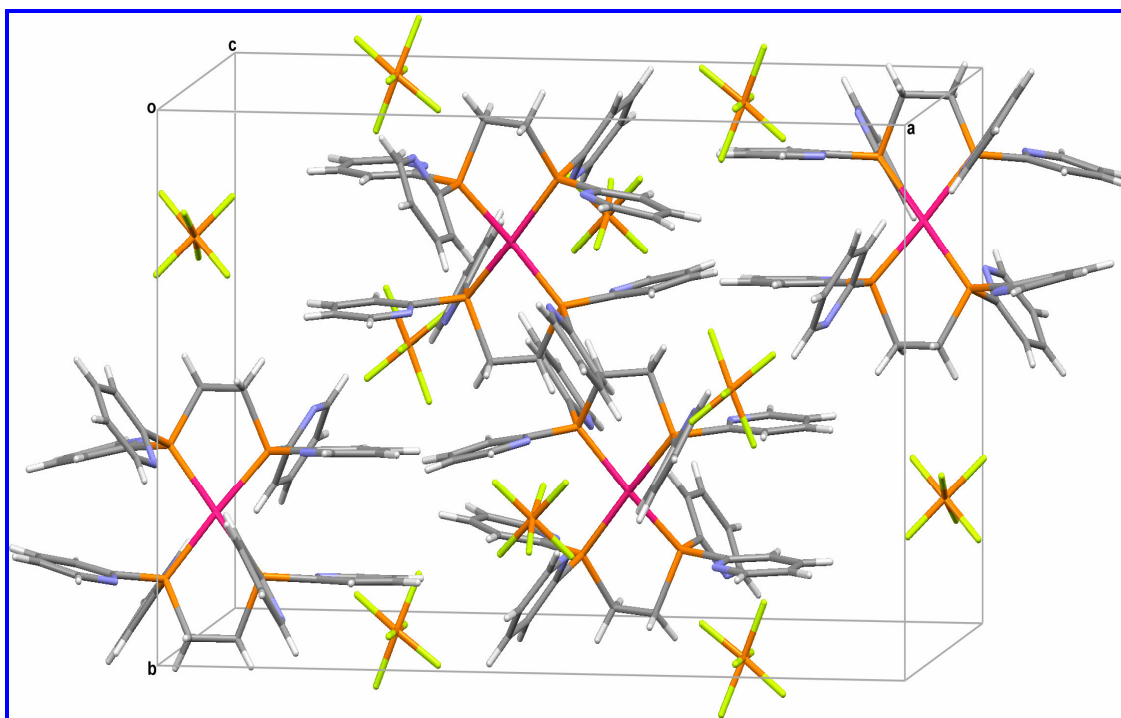


Fig 2.7: Examples of Pd and Pt phenylphosphine complexes

Recent studies have shown that in complexes of diphosphines with unsaturated backbones such as *cis*-dppen or 1, 2-bis-(diphenylphosphino)acetylene (dppa), π bonding, interactions between aliphatic double or triple bonds and the metal-ligand bonds are present (Oberhauser *et al.*, 1998). The unsaturated nature of the chelating diphosphine leads to the enhancement of Pt-to-P π -bonding (Oberhauser *et al.*, 1995). As a consequence, some degree of rehybridisation takes place at the phosphorus and aliphatic carbon atoms. In the case of *cis*-dppen this leads to completely planar structures in [PtCl₂(*cis*-dppen)] and [Pt(*cis*-dppen)₂][BPh₄]₂. Although the influence of π -bonding is less important on the reactivity of most metal phosphine complexes than σ -bonding and steric effects, in the case of dppa, several π - and σ -bonding possibilities occur (Oberhauser *et al.*, 1997a). The metal-phosphorus d π -d π back bonding results in unique bridging properties of dppa.

Chapter III

Preparation and characterisation of Pt and Pd phosphine complexes

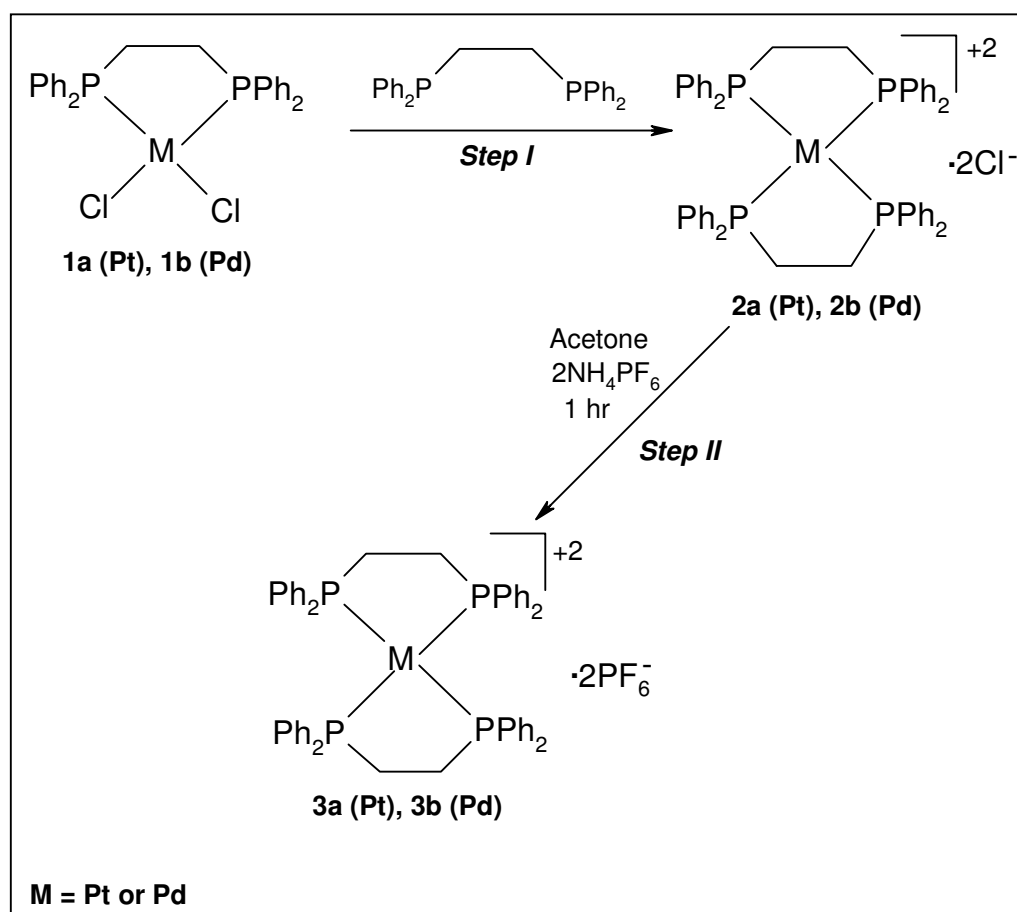


The synthesis of Pt and Pd analogues of $[\text{Au}(\text{dppe})_2]\text{Cl}$ produced compounds that were difficult to purify and manipulate/handle. Due to the fact that stability and purity are essential properties in drug development, the chloride counterion was changed to PF_6^- . The coordination chemistry of cationic Pt and Pd complexes with bis-(diphenylphosphino)ethane or bis-(diphenylphosphino)ethene and bis-(2-, 3- and 4-bipyridylphosphino)ethane ligands were investigated and the results are discussed in this chapter.

3.1 Synthesis of metal phenylphosphine complexes

3.1.1 Preparation of 1,2-bis-(diphenylphosphino)ethane complexes of Platinum and Palladium

Synthesis of the above compounds is summarised below (Scheme 3.1).



Scheme 3.1: Synthetic procedure for the preparation of Pd and Pt complexes with bis(diphenylphosphino)ethane ligands.

The known complexes **1a**, **2a**, **1b** and **2b** were synthesised according to a literature procedure (Westland, 1965) while the substitution of Cl⁻ with PF₆⁻ (*step II*) was carried out by modification of another procedure (Jones *et al.*, 1999). The latter procedure was initially used in the synthesis of a platinum pyridylphosphine complex. The compounds [Pt(dppe)₂][PF₆]₂ (**3a**) and [Pd(dppe)₂][PF₆]₂ (**3b**) were obtained in moderate yields (58 and 48 %, respectively). These complexes were far easier to purify than the corresponding complexes that contained Cl⁻ and stable enough to handle in the solid state as well as in solution. Both complexes were purified from DMF (boiling DMF in the case of the palladium complex) and ether vapour at room temperature. White needle-like crystals were obtained in both cases.

1,2-bis-(diphenylphosphino)ethane- and ethene complexes were insoluble in most NMR solvents and their ¹H NMR spectra showed multiplets in the expected regions (δ 7.2-7.8) due to aromatic protons. Analysis of chelating phosphine complexes is usually accomplished by IR spectroscopy, if dealing with carbonyl complexes, or ³¹P NMR spectroscopy where one observes a deshielding effect upon bonding and thus can easily tell whether a bisphosphine is functioning in a monodentate or bidentate fashion (Garrou, 1981).

Table 3.1: ³¹P{¹H} NMR data of Pt, Pd and Au complexes with 1,2-bis-(diphenylphosphino)ethane

	³¹ P{ ¹ H} NMR	
	δ, ppm	¹ J(¹⁹⁵ Pt- ³¹ P), Hz
dppe	-13.7 (s)	-
PtCl₂(dppe)	43.4 (s), ^b 43.8 (s)	3547, ^b 3600
[Pt(dppe)₂]Cl₂	49.2 (s)	2333
[Pt(dppe)₂][PF₆]₂ (3a)	49.3 (s)	2321
	-143.2 (spt)	712 (PF ₆)
PdCl₂(dppe)	67.5 (s)	-
[Pd(dppe)₂]Cl₂	57.4 (s)	-
[Pd(dppe)₂][PF₆]₂ (6a)	58.1 (s)	-
	-143.3 (spt)	711 (PF ₆)
[Au(dppe)₂]Cl	21.6, ^c 21.9, ^d 18.7	-

^aMeasured in DMSO (δ , ppm). Spectra were run at 298 K.

^bLiterature values in DMSO (Hope *et al.*, 1986)

^cLiterature values in D₂O (Berners-Price and Sadler, 1987b)

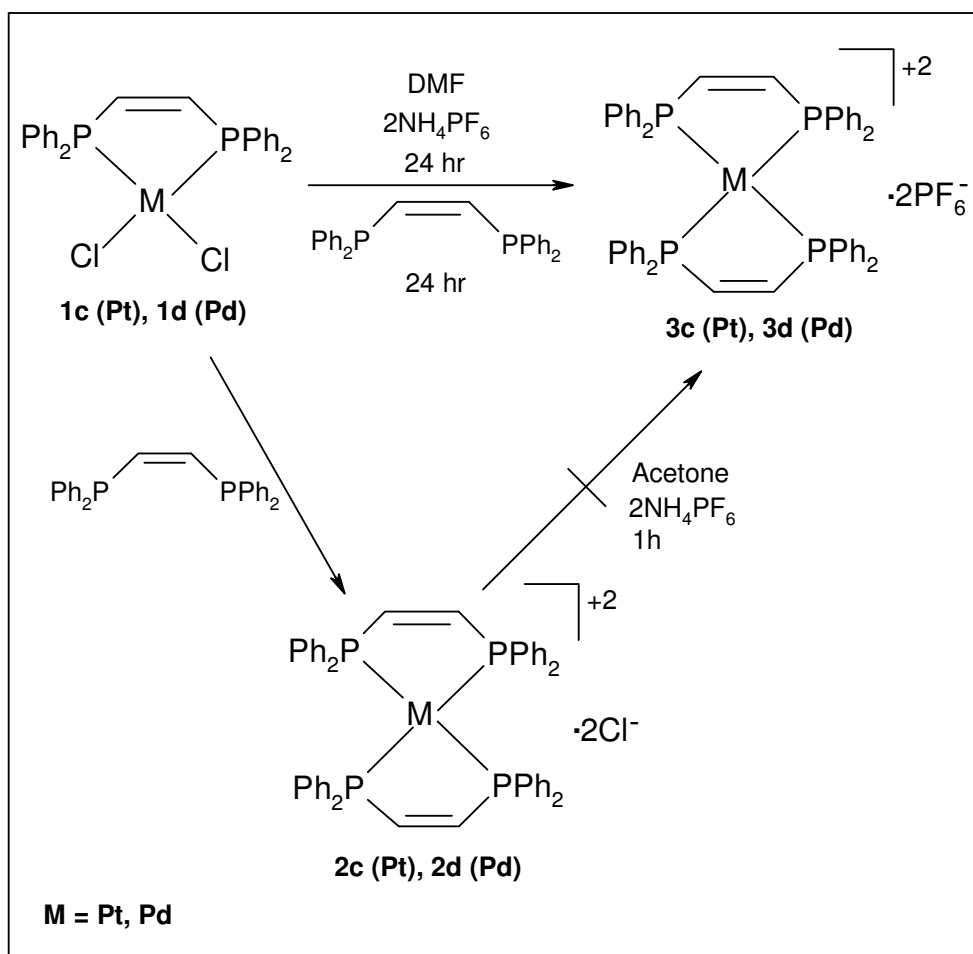
^dLiterature values in CDCl₃ (Berners-Price *et al.*, 1987b)

s = singlet, spt = septet

The ³¹P NMR data presented above (*Table 3.1*) indicates that the free ligand (dppe) is more shielded (-13.7 ppm) than the complexes in both metals. This shift is treated quantitatively as the coordination chemical shift; Δ , defined as $\delta\{\text{P}(\text{coordinated})\} - \delta\{\text{P}(\text{free ligand})\}$ (Gambaro *et al.*, 1989). However, the phosphorus resonances of the complexes behave differently in the formation of *bis*-chelated complexes from *mono*-chelated species. The ³¹P chemical shift of [PtCl₂(dppe)] appears upfield, 43.4 ppm; lit. 43.8 ppm (Hope *et al.*, 1986) with respect to [Pt(dppe)₂]Cl₂ (48.9 ppm) and [Pt(dppe)₂][PF₆]₂ (49.3 ppm). In contrast, ³¹P chemical shift of [PdCl₂(dppe)] (67.5 ppm) appears downfield with respect to [Pd(dppe)₂]Cl₂ (57.4 ppm) and [Pd(dppe)₂][PF₆]₂ (58.1 ppm).

The influence of the non-coordinating anion, PF₆⁻ compared with Cl⁻, is insignificant as demonstrated in the chemical shifts for both platinum and palladium complexes. The observed values of ¹J(¹⁹⁵Pt-³¹P), 2321-3547 Hz, rule out the presence of a system containing a platinum-carbon bond (Banditelli *et al.*, 1982). Ligands with short chelate backbones such as Ph₂P(CH₂)_nPPh₂ (n = 2, 3, 4) form *cis* chelated complexes with both palladium(II) and platinum(II) of general formula [M(L~L)₂]MX₄ or [M(L~L)X₂] (Minahan *et al.*, 1984). In these cases, the length of the chelate backbone prevents the formation of the *trans* chelate since it is not sufficient to span the *trans* positions in a square planar complex.

3.1.2 Preparation of *cis*-1,2-bis-(diphenylphosphino)ethene complexes of Platinum and Palladium



Scheme 3.2: Synthetic procedure for the preparation of Pd and Pt complexes with *cis*-bis(diphenylphosphino)ethene ligands.

Compounds **1c** and **1d** were prepared according to the literature procedures of Hope and Chow (Hope *et al.*, 1986 and Chow *et al.*, 1974), respectively. While the preparation of the palladium compound (**1d**) was straightforward, the platinum analogue (**1c**) was less soluble and had to be dissolved in boiling DMF. If this step is omitted, the products have an oligomeric $[\text{Pt}(\text{Ph}_2\text{PCHCHPPH}_2)\text{X}_2]_n$ composition which are much less soluble in organic solvents (Hope *et al.*, 1986). The amount of the oligomeric product obtained strongly depends on the stirring time (Oberhauser *et al.*, 1995). Independent of the stoichiometry used for $[\text{PtCl}_4]^{2-} : \text{cis-dppen} = 1:1$ or $1:2$, a species of the type $[\text{Pt}(\text{cis-dppen})_2]^{2+}$ is formed. Compounds **2c** and **2d** were prepared according to Oberhauser *et al.*, 1995.

Preparation of *cis*-dppen compounds using a similar route to that of the dppe complexes (*Scheme 3.1*) led to extremely poor yields in the case of **3c** [Pt(*cis*-dppen)₂][PF₆]₂. In the synthesis of the palladium complex, ³¹P{¹H} NMR spectrum displayed a mixture of minor peaks of **1d** [PdCl₂(*cis*-dppen)] at 74.4 ppm and **3d** [Pd(*cis*-dppen)₂][PF₆]₂ at 64.6 ppm; and unidentified major peak at 18.0 ppm. The structural and reactivity differences between [MCl₂(dppe)] and [MCl₂(*cis*-dppen)] (M = Pd, Pt) complexes have been widely addressed in the literature (Devic *et al.*, 2004). The authors assigned the special properties of the *cis*-dppen ligand when compared with the saturated dppe counterpart to an enhancement of the M-to-P π bonding interaction, due to the unsaturated nature of the aliphatic backbone in the dppen.

An alternative synthetic route for the synthesis of both the palladium and platinum complexes was devised by modification of a literature procedure (*Scheme 3.2*) (Oberhauser *et al.*, 1995). In the syntheses of related complexes, the authors emphasised that the removal of the chloride from [MCl₂(*cis*-dppen)] (M = Pd, Pt) was important for the completion of the reactions. This was achieved by either substitution of the coordinated chlorides by other ligands and simultaneous replacement of the resulting anionic chlorides with BPh₄⁻ or by precipitating AgCl with a silver salt leading to a cationic intermediate. In our case, the platinum compound [Pt(dppen)₂][PF₆]₂ was still obtained in poor yields (19%) while the palladium compound [Pd(dppen)₂][PF₆]₂ was ultimately obtained in moderate yield (51%).

Other research groups have reported partial loss of chloro ligands or complete failure to abstract coordinated Cl with thallium triflate despite prolonged treatment with an excess of the salt (Devic *et al.*, 2004). Reaction of PdCl₂(dppen) with an excess of thallium triflate in CH₂Cl₂ afforded a complex salt, formulated as [PdCl(dppen)]₂(OTf)₂, indicating a partial dechlorination.

Table 3.2: $^{31}\text{P}\{^1\text{H}\}$ NMR data of Pt and Pd complexes with 1,2-bis-(diphenylphosphino)ethene

	$^{31}\text{P}\{^1\text{H}\}$ NMR	
	δ , ppm	$^1J(^{195}\text{Pt}-^{31}\text{P})$, Hz
dppen	-23.3 (s)	-
$^{\text{b}}\text{PtCl}_2(\text{dppen})$	50.1(t)	3623
$[\text{Pt}(\text{dppen})_2]\text{Cl}_2$	59.6 (t)	2355
$[\text{Pt}(\text{dppen})_2][\text{PF}_6]_2$ (3b)	60.2 (t)	2350
	-143.3 (spt)	711
$^{\text{b}}[\text{Pt}(\text{dppen})_2][\text{BPh}_4]_2$	60.9 (s)	2334
$\text{PdCl}_2(\text{dppen})$	74.4, $^{\text{b}}71.3$ (s)	-
$[\text{Pd}(\text{dppen})_2]\text{Cl}_2$	64.4 (s)	-
$[\text{Pd}(\text{dppen})_2][\text{PF}_6]_2$ (6b)	64.3 (s)	-
	-143.3 (spt)	711 Hz
$^{\text{b}}[\text{Pd}(\text{dppen})_2][\text{BPh}_4]_2$	66.2 (s)	-

^aMeasured in DMSO (δ , ppm). Spectra were run at 298 K.

^bLiterature values (Hope *et al.*, 1986, Oberhauser *et al.*, 1995). The solvents used by the authors were DMF (for Pd-complexes) and CH_2Cl_2 or DMSO (for Pt-complexes).

s = singlet, t = triplet, spt = septet

$^{31}\text{P}\{^1\text{H}\}$ NMR data presented above (Table 3.2) shows a similar trend to that observed in dppe complexes (platinum complexes show a downfield shift in the formation of the *bis*-chelated complex from *mono*-chelated species while palladium complexes display the opposite behaviour). The rigidity of *cis*-dppen has been thought to be responsible for anomalous ^{31}P NMR chemical shifts in a series of comparable compounds (Oberhauser *et al.*, 1995). From this it is clear, that there are a number of effects which distinguish *cis*-dppen from its saturated analog dppe.

Similarly to reported data (Oberhauser *et al.*, 1995), $^1J(\text{Pt},\text{P})$ values of the *mono*- and *bis*-chelated platinum *cis*-dppen complexes (3623 Hz and 2350 Hz, respectively) are very close to the corresponding complexes containing dppe (3600 and 2321 Hz). It seems likely that these $^1J(\text{Pt},\text{P})$ parameters are completely dominated by the difference of the *trans* influences of chloride and a phosphine,

respectively (Oberhauser *et al.*, 1995). Additionally, the variation of these coupling constants, although the range is very small, tends to confirm that the strength of the Pt-Cl bonds within this series increases from [PtCl₂(dppe)] to [PtCl₂(dppen)], as a consequence of a stronger σ -bonding effect (Devic *et al.*, 2004).

It is worth noting that the solution ³¹P NMR spectrum of the [Au(dppen)₂]⁺ (CDCl₃) consists of a single resonance at δ 23.2, similar to that found for the chloride salt, together with a multiplet of the PF₆⁻ anion [δ (PF₆) -143.6, J (P-F) = 714 Hz] (Berners-Price *et al.*, 1992).

3.2 Synthesis of metal pyridylphosphine complexes

The ligands shown below (Fig.3.1) were synthesised according to the literature procedures (Bowen *et al.*, 1998) and complexed to either palladium or platinum.

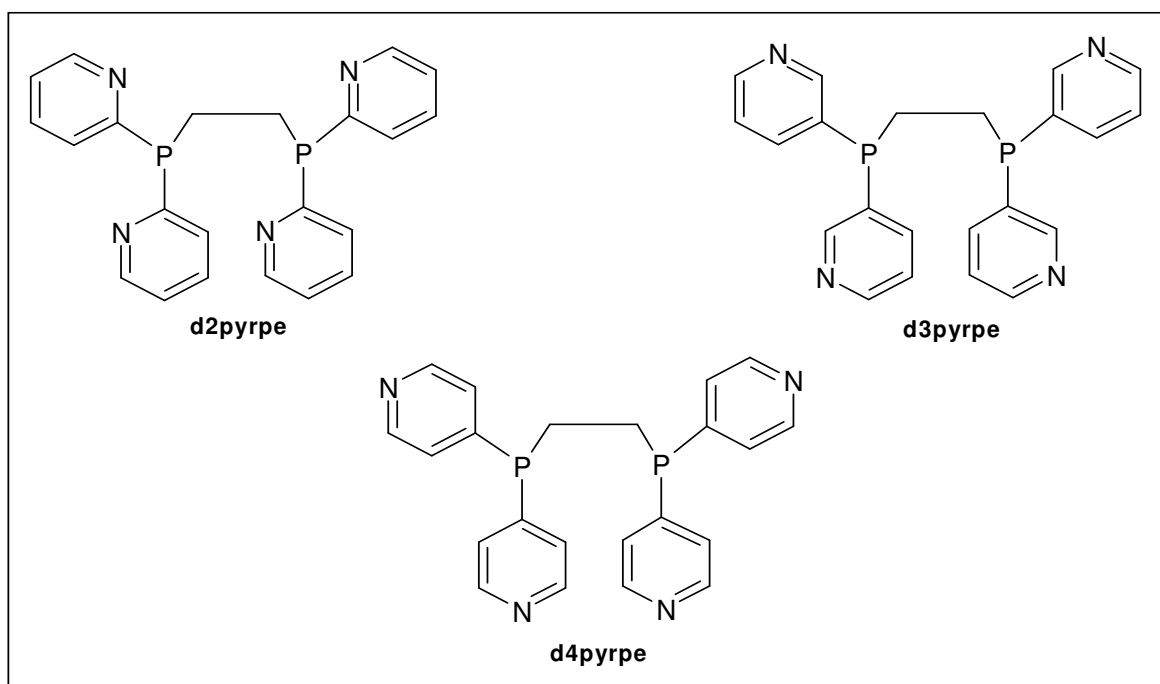


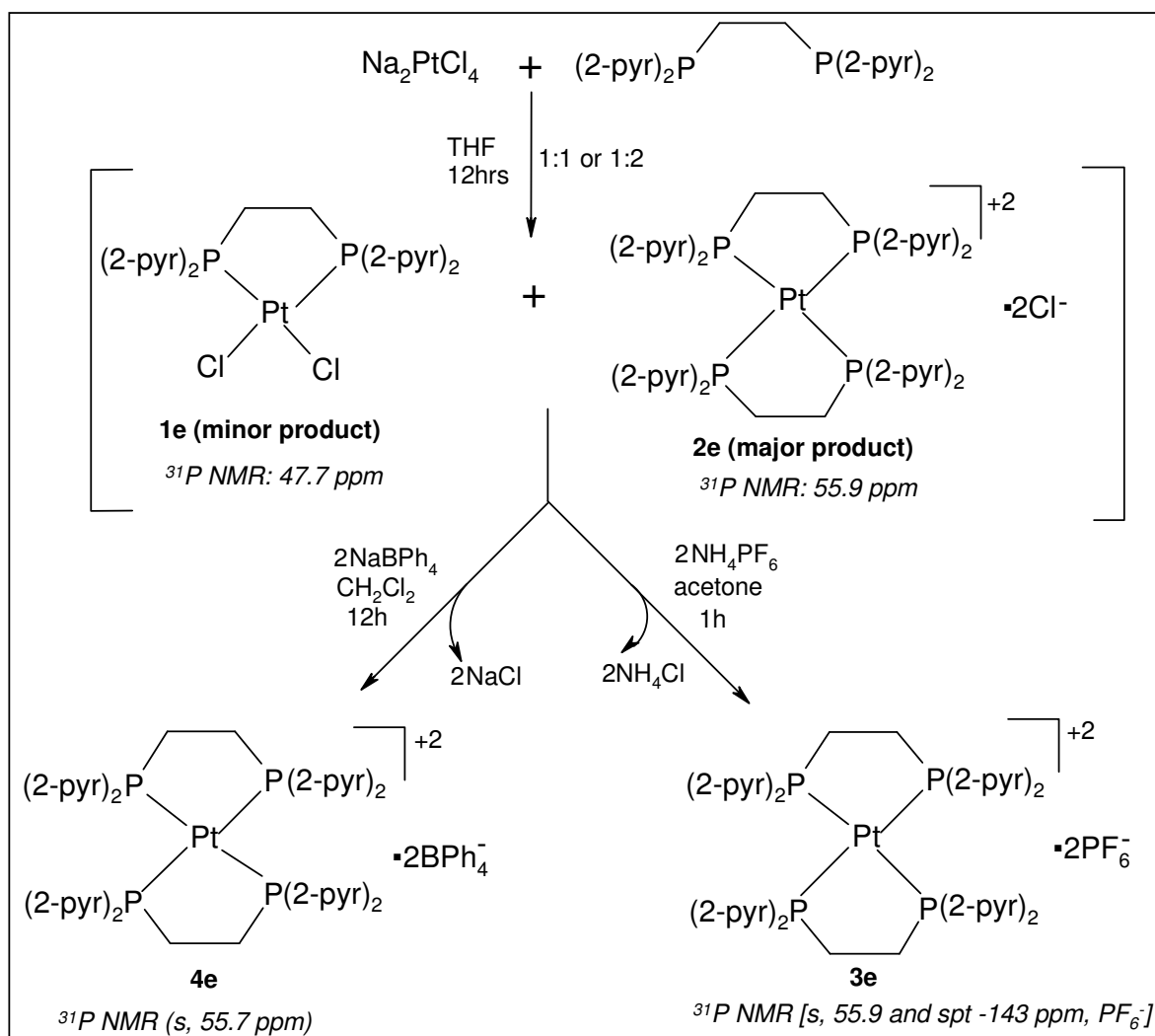
Fig. 3.1: 1,2-bis-(dipyridylphosphino)ethane ligands that have been used to prepare the palladium and platinum complexes discussed in this project. d2pyrpe, d3pyrpe d4pyrpe are 1,2-bis-(di-2-pyridylphosphino)ethane, 1,2-bis-(di-3-pyridylphosphino)ethane and 1,2-bis-(di-4-pyridylphosphino)ethane, respectively.

Synthetic routes differed among the three ligands (2-, 3- and 4-pyridyl) as well as between the two metals (M = Pt, Pd). In the preparation of the complexes,

mixtures of compounds were obtained and identified by ^{31}P NMR on the basis of the known patterns in chemical shifts as well as coupling constants.

3.2.1 Preparation of 1,2-bis-(di-2-pyridylphosphino)ethane platinum(II) complexes

Synthesis of these complexes is summarised below (Scheme 3.3).



Scheme 3.3: Synthesis of 1,2-bis(di-2-pyridylphosphino)ethane platinum(II) complexes. $^{31}\text{P}\{^1\text{H}\}$ NMR chemical shifts (ppm) are indicated in italics.

Reaction of $\text{Na}_2[\text{PtCl}_4]$ and 1,2-bis-(di-2-pyridylphosphino)ethane (d2pyrpe) yielded a yellow mixture (insoluble in THF) of the *mono*-chelated (**1e**) and *bis*-chelated (**2e**) compounds irrespective of stoichiometry. Attempts to separate the mixture by various methods proved to be unsuccessful and only decomposition

products were obtained. It is worth noting that synthesis of the two compounds **1e** and **2e** has been attempted previously and reported in the literature (Jones *et al.*, 1999) whereby [PtCl₂(cod)] was used as a starting material. X-ray quality crystals of compound **1e** co-crystallised with a solvent molecule in the lattice (CH₂Cl₂) were recorded, but satisfactory elemental analysis of compound **2e** could not be obtained.

The ³¹P{¹H} NMR spectrum (DMSO) of the mixture exhibited two phosphorus signals. One at $\delta = 47.7$ ppm, [lit: $\delta = 47.1$ ppm in CDCl₃ (Jones *et al.*, 1999)] and $\delta = 55.1$ ppm indicating the presence of two species. These singlets were characterised by corresponding pairs of ¹⁹⁵Pt satellites (*sat*) [¹J_{Pt} = 3480 (lit. 3481 Hz)], and 2470 Hz, respectively. Complex **1e** with ¹J_{Pt} = 3480 Hz is consistent with equivalent, mutually *cis* P atoms in a square planar arrangement; complexes of the type *cis*-Pt(halide)₂(pyridylphosphine)₂ invariably have J(PtP) values in the range ~3500-3900 Hz (Xie and James, 1991).

The problems encountered in the synthesis of **2e**, i.e instability and difficulty in purification, posed problems for its proposed application. Possibilities of decomposition taking place before reaching the target site in the investigation for potential anti-tumour activity were imminent. Circumvention of these problems was achieved by replacement of the counterion (Cl⁻) with BPh₄⁻ or PF₆⁻. **3e** was prepared according to a literature procedure (Jones *et al.*, 1999) and obtained in good yield (65%) while **4e** was prepared via metathesis of the crude mixture (**1e** and **2e**) with NaBPh₄. Colourless crystals of **4e** suitable for study by X-ray diffraction were obtained from dichloromethane/ether at -20 °C.

3.2.2 Preparation of 1,2-bis-(di-2-pyridylphosphino)ethane palladium(II) complexes

As previously observed in the preparation of the Pt compound, a mixture of the *mono*-[PdCl₂(d2pyrpe)] (**1f**) and *bis*-chelated compound [Pd(d2pyrpe)₂]Cl₂ (**2f**) was obtained irrespective of stoichiometry used, d2pyrpe:(Na₂[PdCl₄]). The ³¹P{¹H} NMR spectrum of the mixture showed two singlets (70.4 and 64.0 ppm in DMSO)

and (69.9 and 62.5 ppm in CDCl_3) for the respective compounds. In order to distinguish the representative peaks in ^1H and ^{31}P NMR spectra, $[\text{PdCl}_2(\text{d2pyrpe})]$ was prepared from either PdCl_2 or $[\text{PdCl}_2(\text{NCCH}_3)_2]$. A brown solid was obtained from the reaction of PdCl_2 with d2pyrpe (1:1). Interestingly, a portion of this compound was soluble in DMSO while the other fraction dissolved in CDCl_3 . The $^{31}\text{P}\{^1\text{H}\}$ spectrum of the former sample showed the presence of only $[\text{PdCl}_2(\text{d2pyrpe})]$ (s, $\delta = 70.4$ ppm) while the latter sample exhibited a singlet ($\delta = 62.5$ ppm) that signified the presence of the *bis*-chelated compound, $[\text{Pd}(\text{d2pyrpe})_2]\text{Cl}_2$. Attempts to purify the mixture from DMF/ether were not successful.

In the other reaction, PdCl_2 was refluxed in acetonitrile to form the yellow intermediate, $[\text{PdCl}_2(\text{NCCH}_3)_2]$, (Mohlala *et al.*, 2005) which was subsequently reacted with the ligand, d2pyrpe (1 eq.). The orange product was insoluble in numerous solvents (acetonitrile, acetone, methanol, ether, dichloromethane) and only soluble in DMF. It is worth noting that only $[\text{PdCl}_2(\text{d2pyrpe})]$, was formed whether 1:1 or 1:2 ratio of $[\text{PdCl}_2(\text{NCCH}_3)_2]:\text{dpyrpe}$ was utilised. The observed singlet in $^{31}\text{P}\{^1\text{H}\}$ NMR spectra at 70.4 ppm in DMSO (69.9 ppm in CDCl_3) as well as MS-FAB spectrometry ($\text{M}^+ - \text{Cl} = 543$), assisted in distinguishing between the *mono*- and *bis*-chelated compounds in the previously obtained mixtures. Reaction of this *mono*-chelated compound with a second equivalent of d2pyrpe , did not lead to the formation $[\text{Pd}(\text{d2pyrpe})_2]\text{Cl}_2$.

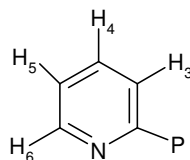
As observed earlier in the preparation of *cis*-dppen complexes $[\text{MCl}_2(\text{cis-dppen})]$ ($\text{M} = \text{Pd}, \text{Pt}$), the removal of the chloro ligands from $[\text{PdCl}_2(\text{d2pyrpe})]$ seemed to be crucial for the completion of the reactions. Further attempts to obtain the desired compound were pursued by substituting the chloro ligands with CF_3SO_3^- by using silver triflate (AgOTf ; $\text{OTf} = \text{CF}_3\text{SO}_3^-$). Trifluoromethanesulphonate is a readily available (counter) anion in the presence of stronger coordinating ligands (Kim *et al.*, 2002). It has been known as a weak base and hence a good leaving group, and is useful in generating new species that cannot be approached by direct synthetic methods. Numerous palladium or platinum complexes such as $[\text{M}(\text{P-P})(\text{OTf})_2]$, have been used within the past decade as building blocks for the

formation of supramolecular assemblies, upon triflate displacement and subsequent complexation with bridging pyridine ligands (Devic *et al.*, 2004).

Replacement of the chloro ligands with the weakly coordinating triflate anions (with concomitant precipitation of AgCl) was attempted by reacting [PdCl₂(d2pyrpe)] with AgO₃SCF₃. However, an intractable compound was obtained as it also precipitated out of the reaction solvent (CH₂Cl₂). There was an insignificant change in ³¹P{¹H} NMR parameter (δ 71.1 vs 70.4 ppm). Addition of a second equivalent of d2pyrpe to the deep yellow mixture led to the formation of brick red/dark orange mixture that had traces of a yellow residue. Replacement of the triflate ions with a second equivalent of d2pyrpe was expected to lead to a cationic intermediate with triflate counter ions (Oberhauser *et al.*, 1995).

Insolubility of these mixtures in deuterated solvents resulted in poorly resolved NMR spectra and these synthetic routes were not pursued further. Solubility problems have been encountered by others in the preparation of Pd complexes containing triflate (Zhuravel and Glueck, 1999). It is worth noting that many side reactions leading to formation of decomposition products (and consequently lower yields of intended compound) occurred when following these long synthetic routes that involved many handling and isolation steps.

[Pd(d2pyrpe)₂][PF₆]₂ (**3f**) was finally prepared in the same manner (*Scheme 3.3*) as the Pt analogue by using the precursor (Na₂[PdCl₄]) and an impure sample of [Pd(d2pyrpe)₂]Cl₂. Colourless crystals of **3f** suitable for single X-ray diffraction studies were obtained from DMF/ether. ¹H and/or ³¹P{¹H} NMR data of the identifiable products in the preparation of both platinum and palladium complexes are presented below (*Table 3.3*).



Labelling of protons for 2-pyridylphosphine ligands (Baird *et al.*, 1995).

Table 3.3: ^1H and $^{31}\text{P}\{^1\text{H}\}$ NMR data of 1,2-bis-(di-2-pyridylphosphino)ethane and its Pt and Pd complexes

Compound	Solvent	Pyridyls ^1H data (δ)					^{31}P data		
		H ₃	H ₄	H ₅	H ₆	CH ₂ ^a	δ	$^1J_{\text{PtP}}$ or $^1J_{\text{PF}}$ (Hz)	
^b d2pyrpe	CDCl ₃	7.43	7.53	7.12	8.63	2.53 (8.28)	-6.0	-	
^c 1e and 2e	DMSO	^d 7.78	^d 7.78	7.45	8.42	2.84	47.7 & 55.1	3480 & 2470	
^e [Pt(d2pyrpe) ₂][BPh ₄] ₂	DMSO	6.88	7.00	6.64	7.61	2.00 (19.38)	55.7	2460	
[Pt(d2pyrpe) ₂][PF ₆] ₂	DMSO	6.93	7.00	6.67	7.64	2.06 (19.38)	^f 55.9 & -143	^f 2459 & 711	
^g 1f and 2f	DMSO	8.00 & ^d 7.74	8.12 & ^d 7.74	7.61 & 7.43	8.77 & 8.42	2.89	70.4 & 64.0	-	
[PdCl ₂ (d2pyrpe)]	DMSO	7.99	8.11	7.61	8.76	2.93 (21.35)	70.4	-	
[PdCl ₂ (d2pyrpe)]	CDCl ₃	7.74	8.42	7.35	8.64	3.06 (20.67)	69.9	-	
[Pd(d2pyrpe) ₂]Cl ₂	CDCl ₃	^d 7.53	7.93	^d 7.53	8.33	3.01	62.5 (^h 64.0)	-	
[Pd(d2pyrpe) ₂][PF ₆] ₂	DMSO	7.67	7.74	7.46	8.42	2.85	64.0 & -143	711 (spt, [PF ₆] ⁻)	

Spectra were run at 298 K. All the pyridyl protons appeared as multiplets and phosphorus occurred as singlets (except for PF₆⁻). The ligand data was in agreement with that reported in the literature (Baird *et al.*, 1995, Bowen *et al.*, 1998).^aBroad singlet or quasi-triplet ($J = [^2J(^{31}\text{P}-^1\text{H}) + ^3J(^{31}\text{P}-^1\text{H})]$ (Hz) in parentheses where resolved (Berners-Price *et al.*, 1999b) and broad doublet (only in Pd complexes). ^bProton numbering scheme is based on lit. (Berners-Price *et al.*, 1999b) and their values are in close agreement (solvent was CD₃OD). ^c1e and 2e are [PtCl₂(d2pyrpe)] and [Pt(d2pyrpe)₂]Cl₂, respectively. ^dOverlap of the signals. ^ePhenyl protons (multiplets) of BPh₄⁻ at $\delta = 5.97$ (8H), 6.10 (16H) and 6.35 (16H). ^fSinglet and septet (spt, $^1J_{\text{PF}}$), respectively, Lit. values = δ 54.4 (2477 Hz) and -144 (712 Hz) in CD₃OD (Jones *et al.*, 1999). ^g1f and 2f are [PdCl₂(d2pyrpe)] and [Pd(d2pyrpe)₂]Cl₂, respectively which were obtained as a mixture. ^hChemical shift in DMSO.

The proton data showed above (*Table 3.3*) shows pyridyl protons occurring as multiplets in the expected aromatic region. The ^1H NMR chemical shift differences between the free ligand (δ 7.43-8.63) and the coordinated complexes (δ 6.64-8.77) were not significant. ^1H NMR signal for the H_6 protons always gives the most downfield signal (Baird *et al.*, 1995). More generally, the relative positions of H_3 - H_5 for 2-pyridyl protons are found to vary with the solvent, and the nature of the complex.

The ethane protons (bridging CH_2) were also found in the expected regions (δ 2.00-3.06, depending on the solvent used) but coupling constants differed between the free ligand (8.28 Hz) and the complexes (19.38-21.35 Hz). The ligand (δ = 2.53) appeared as a quasi-triplet (8.28 Hz), lit. (δ 2.44 and 8.7 Hz in CD_3OD) (Berners-Price *et al.*, 1998). The ^1H NMR data is similar to that observed in Ag(1) complexes which is consistent with the formation of simple monomeric species. For bidentate phosphines with $(\text{CH}_2)_2$ backbones (e.g. dppe), the CH_2 protons constitute the AA' part of an $\text{A}_2\text{XX}'\text{A}_2'$ spin system as a result of unequal ^{31}P - ^1H spin-spin coupling to the two P atoms and give rise to a quasi triplet in which the separation of the outer two peaks corresponds to $|^2J(^{31}\text{P}-^1\text{H}) + ^3J(^{31}\text{P}-^1\text{H})|$ (Berners-Price *et al.*, 1998).

The major difference is that while the Pt complexes $[\text{Pt}(\text{d}2\text{pyrpe})_2][\text{BPh}_4]_2$ and $[\text{Pt}(\text{d}2\text{pyrpe})_2][\text{PF}_6]_2$ gave rise to quasi triplets (19.38 Hz), the *bis*-chelated Pd complexes, $[\text{Pd}(\text{d}2\text{pyrpe})_2]\text{Cl}_2$ and $[\text{Pd}(\text{d}2\text{pyrpe})_2][\text{PF}_6]_2$ displayed broad singlets (*Table 3.3*). In contrast, Pd *mono*-chelated species, $[\text{PdCl}_2(\text{d}2\text{pyrpe})]$ exhibited a quasi-doublet (20.67 and 21.35 Hz in DMSO and CDCl_3 , respectively). This difference in the splitting is ascribed to spin-spin coupling ($^1J_{\text{PtP}}$) which results in unequal ^{31}P - ^1H spin-spin coupling ($J_{\text{P-CH}_2}$) while Pd does not induce any coupling. In *bis*-chelated gold(I) diphosphine complexes, the broadening of the $(\text{CH}_2)_2$ resonance gave an unresolved multiplet (Berners-Price *et al.*, 1998).

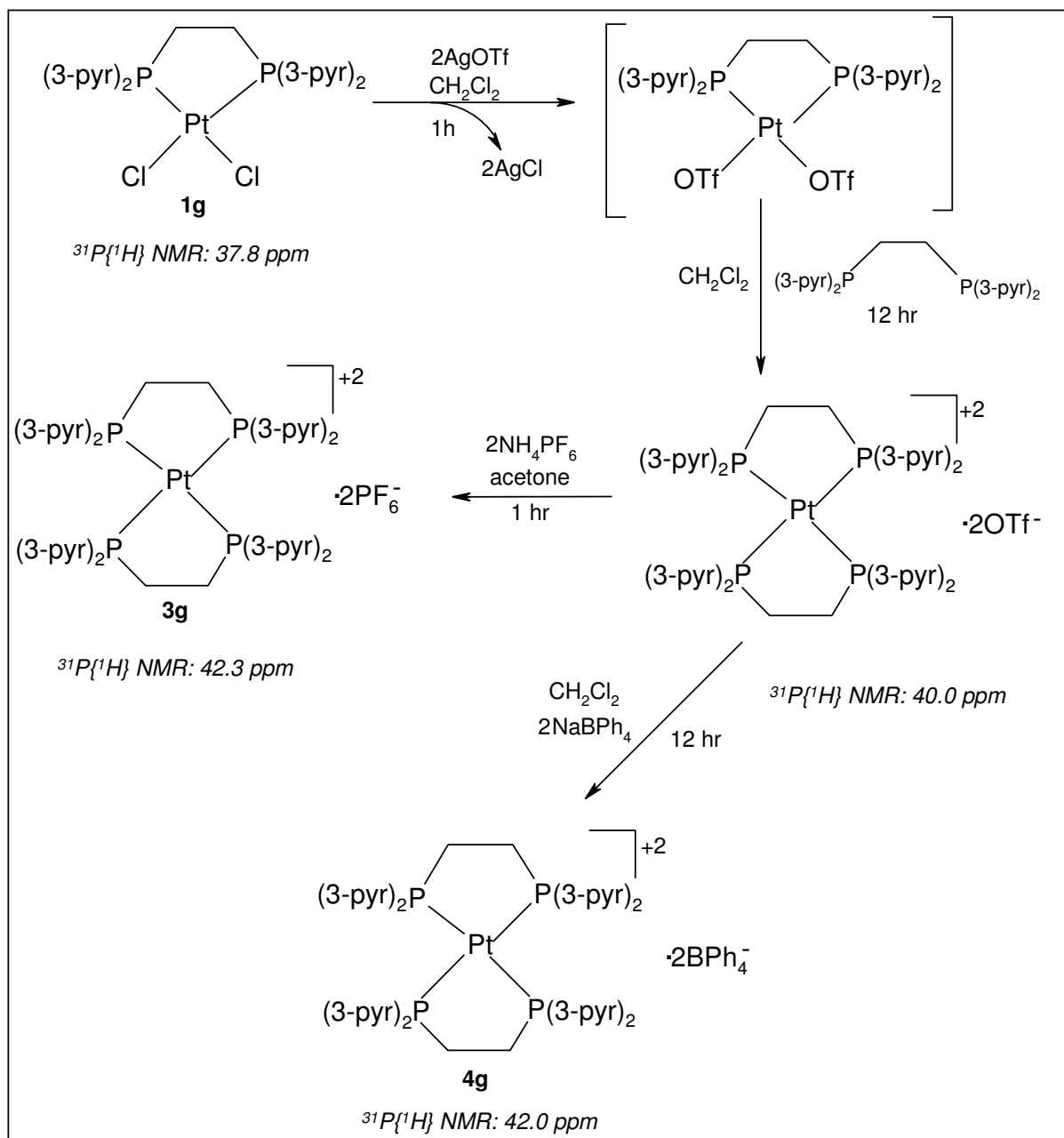
The singlet ^{31}P NMR chemical shifts for all the complexes fall in the downfield region, consistent with the reported, relative to deshielding of P nuclei in five-membered chelate rings (Jones *et al.*, 1999). As previously observed in dppe and dppen complexes, formation of the Pt *bis*-chelated complexes from the mono-

chelated species resulted in a ^{31}P downfield chemical shift (δ 47.7 to 55.9) while the reverse (shift to highfield region) occurred in the palladium complexes (δ 70.4 to 64.0). The magnitude of $^1J(\text{Pt}, \text{P})$ for the *mono*- and *bis*-chelated species were in the ranges previously observed in dppe and dppen complexes (3480 and \sim 2500 Hz, respectively).

3.2.3. Preparation of 1,2-bis-(di-3-pyridylphosphino)ethane platinum(II) complexes

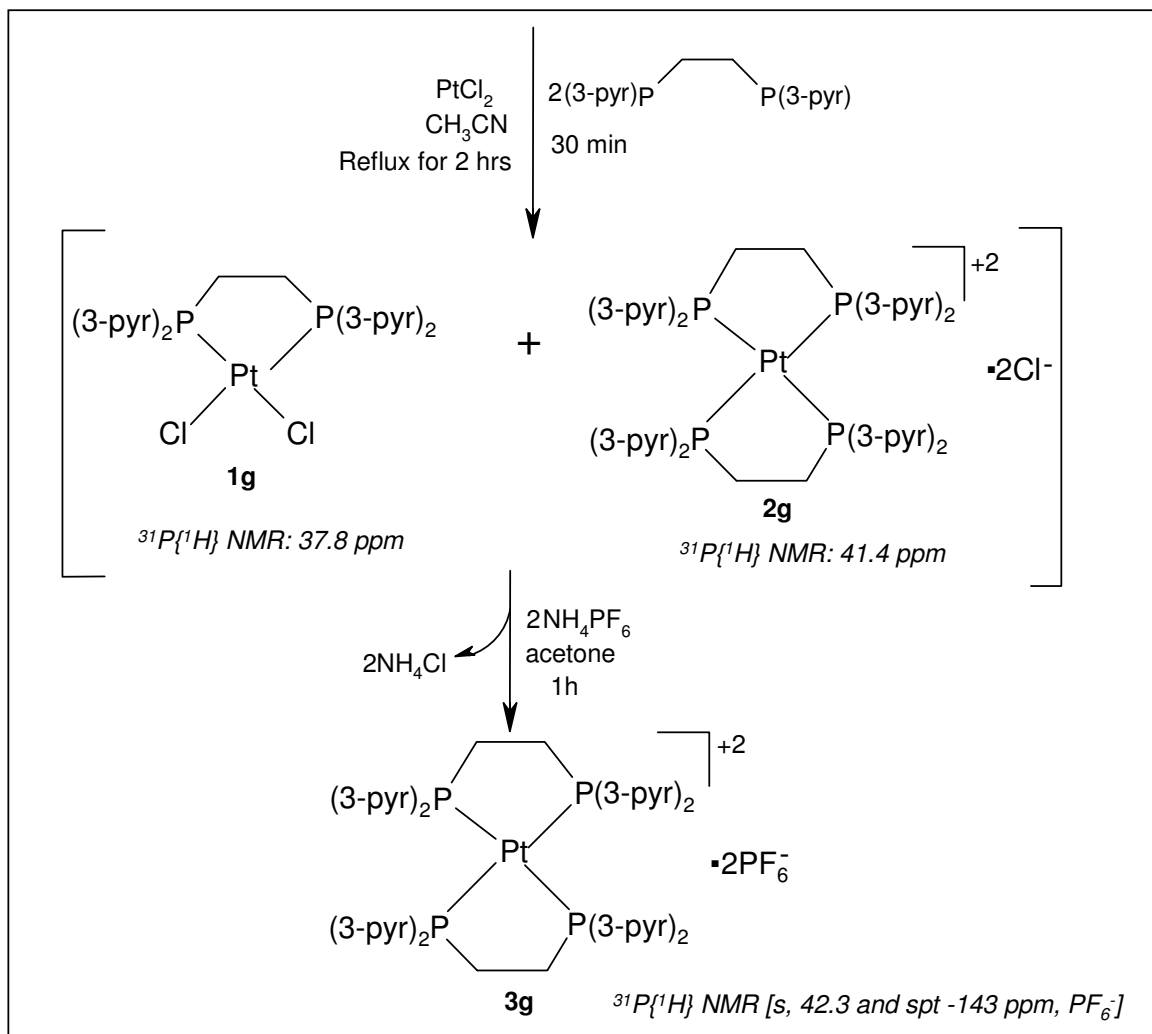
Attempts to prepare $[\text{Pt}(\text{d3pyrpe})_2][\text{PF}_6]_2$ using Scheme 3.3 were not successful. Unlike the 2-pyridyl complex, equal amounts of $\text{Na}_2[\text{PtCl}_4]$ and d3pyrpe stirred (in THF) at room temperature for 12 hours yielded only the mono-chelated complex $[\text{PtCl}_2(\text{d3pyrpe})]$, **1g**. The $^{31}\text{P}\{^1\text{H}\}$ NMR spectrum of this compound revealed a singlet at 37.8 ppm [$^1J_{\text{P-Pt}} = 3582$ Hz]. Reaction of **1g** with a second equivalent of the ligand failed to give the expected *bis*-chelated compound even at elevated temperature (50 °C). This idea was derived from a similar procedure that was successfully used in the preparation of $[\text{Ni}(\text{d2pyrpe})_2]$ from $[\text{Ni}(\text{cod})_2]$ and d2pyrpe (1:2 ratio, respectively) (Baird *et al.*, 1995). The above complex required heat (50 °C) for its formation, but once formed, the chelate was significantly more stable in air and in solution than the tetrakis(monodentate ligand) species, $[\text{Ni}(\text{Ppyr}_3)_4]$.

Preparation of d3pyrpe complexes of Pt is shown below (Scheme 3.4). Unfortunately, this method was time consuming, labour intensive and it also led to extremely low yields. Isolation of $[\text{Pt}(\text{OTf})_2(\text{d3pyrpe})]$ prepared from $[\text{PtCl}_2(\text{d3pyrpe})]$ was attempted and the $^{31}\text{P}\{^1\text{H}\}$ NMR spectrum showed no difference in the chemical shift and coupling constant $^1J_{(\text{PtP})}$ (δ 37.8 and 3582 Hz). Isolation was henceforth omitted and the solution containing the intermediate $[\text{Pt}(\text{d3pyrpe})_2][\text{OTf}]_2$ was prepared *in situ* by adding excess d3pyrpe. Both of these compounds were unstable in air, extremely insoluble in numerous solvents and purification processes were unsuccessful. Satisfactory ^1H NMR spectra were not obtained while the $^{31}\text{P}\{^1\text{H}\}$ NMR spectrum revealed a singlet [δ 40.0 ppm, $^1J_{\text{PtP}} = 2382$ Hz] for the proposed *bis*-chelated complex, $[\text{Pt}(\text{d3pyrpe})_2][\text{OTf}]_2$.



Scheme 3.4: Initial synthetic route for the preparation of Pt 3-pyridyl complexes.

Preparation of **4g** was carried out in a similar manner as the 2-pyridyl analogue and a pure product was obtained from $\text{CH}_2\text{Cl}_2/\text{ether}$.



Scheme 3.5: Synthesis of 1,2-bis(di-3-pyridylphosphino)ethane platinum(II) complexes.

Illustrated above (*Scheme 3.5*) is a less laborious procedure that utilised fewer steps in the synthesis of **3g**. This method modified from the literature (Jones *et al.*, 2005) involved refluxing PtCl_2 in acetonitrile followed by the addition of ligand (2 eq.) to the hot grey solution. ^1H and $^{31}\text{P}\{^1\text{H}\}$ NMR spectrum of the yellow solid showed the formation of both $[\text{PtCl}_2(\text{d}3\text{pyrpe})]$ and $[\text{Pt}(\text{d}3\text{pyrpe})_2]\text{Cl}_2$ with $^{31}\text{P}\{^1\text{H}\}$ NMR chemical shifts and coupling constants $^1J_{(\text{PtP})}$ of (δ 37.8, 3583 Hz) and (δ 41.4 and 2352 Hz), respectively. Separation of the two complexes was not possible as decomposition took place and hence conversion to the PF_6^- salt was carried out immediately. In addition to $[\text{Pt}(\text{d}3\text{pyrpe})_2][\text{PF}_6]_2$, both ^1H and $^{31}\text{P}\{^1\text{H}\}$ NMR spectra showed the presence of small amounts of $[\text{PtCl}_2(\text{d}3\text{pyrpe})]$ as well as decomposition products. The mixture was triturated with various solvents (CH_2Cl_2 , THF) but there was no change in the spectra.

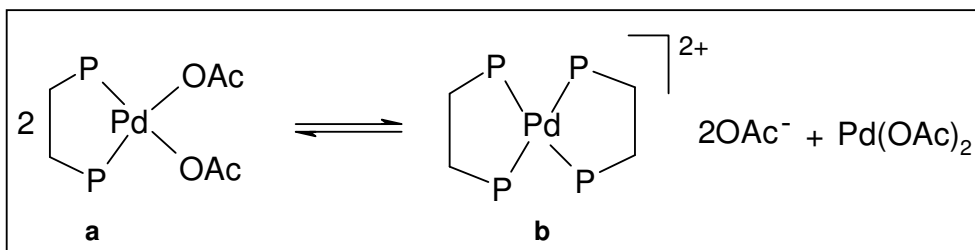
3.2.4 Preparation of 1,2-bis-(di-3-pyridylphosphino)ethane palladium (II) complexes.

Reaction of $\text{Na}_2[\text{PdCl}_4]$ and d3pyrpe resulted in the formation of $[\text{PdCl}_2(\text{d3pyrpe})]$ (**1h**) irrespective of stoichiometry used (1 or 2) although there was unreacted ligand left over even after 12 h. The presence of the complex was confirmed by $^{31}\text{P}\{^1\text{H}\}$ NMR spectra (δ -value of 56.0 ppm in CDCl_3 and 61.0 ppm in DMSO). The same complex was also formed from PdCl_2 or $[\text{PdCl}_2(\text{NCCH}_3)_2]$ although the former reagent produced a mixture which contained small traces of $[\text{Pd}(\text{d3pyrpe})_2]\text{Cl}_2$ (**2h**), $^{31}\text{P}\{^1\text{H}\}$ NMR (DMSO): 48.0 ppm. As previously observed in the synthesis of the Pt analogue, preparation of $[\text{Pd}(\text{d3pyrpe})_2]\text{Cl}_2$ by direct addition of d3pyrpe to $[\text{PdCl}_2(\text{d3pyrpe})]$ led to excessive decomposition. Abstraction of the coordinated chlorides with silver triflate was attempted (*Scheme 3.4*) and as before, solubility problems resulted in failure to isolate pure complexes. The triflate intermediates were insoluble in a number of solvents (CH_2Cl_2 , THF, acetone) and hence could not be separated from AgCl . Satisfactory ^1H NMR spectra were not obtained but $^{31}\text{P}\{^1\text{H}\}$ NMR spectrum showed two singlets (δ 61.1 & 50.1 in DMSO), the latter (highfield) peak was assigned to a *bis*-chelated compound.

Preparation of the PF_6^- compound was attempted by reaction of the above mixture with NH_4PF_6 (2 eq.). $^{31}\text{P}\{^1\text{H}\}$ NMR spectrum of the product showed no changes and notably, no phosphorus resonance attributable to PF_6^- . As seen earlier in the synthesis of $[\text{Pd}(\text{dppen})_2][\text{PF}_6]_2$ (**3d**), removal of the chloride from $[\text{PdCl}_2(\text{dppen})]$ was important for the completion of the reactions. Similar attempts to achieve this by first reacting $[\text{PdCl}_2(\text{d3pyrpe})]$ with NH_4PF_6 (2 eq.) followed by addition of d3pyrpe produced the previously obtained mixture. This mixture was purified from DMF/ether over several days and crystal structure showed co-crystallisation of the *mono*- and *bis*-chelated diphosphine complexes (discussed in section 3.3). This confirmed that abstraction of the chlorides was not successful and that the expected intermediates may not have been obtained.

It has been shown that the reaction of $\text{Pd}(\text{OAc})_2$ with dppe in methanol yielded the *bis*-chelated complex $[\text{Pd}(\text{dppe})_2](\text{OAc})_2$ as a kinetic product, which slowly

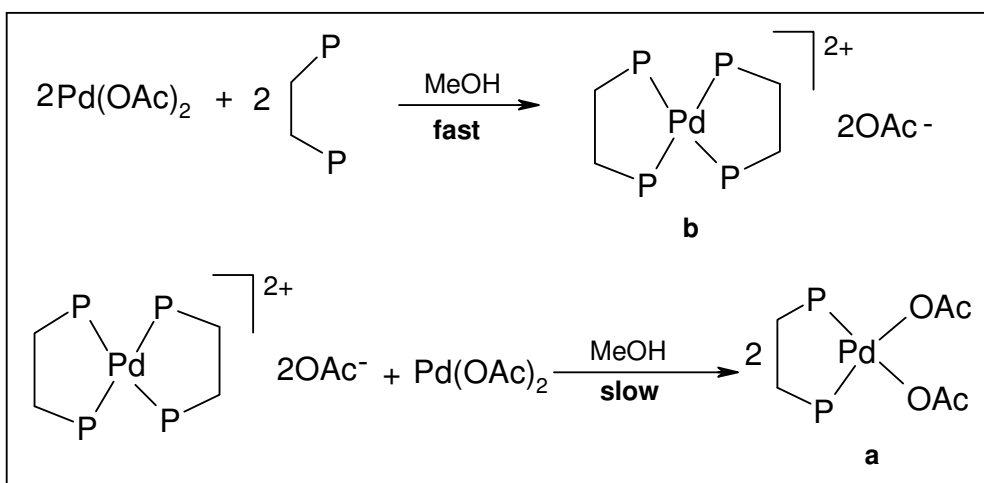
converted to the thermodynamic *mono*-chelate [Pd(OAc)₂(dppe)] (Bianchini *et al.*, 2003). This was concluded from investigations of alternating copolymerisation of carbon monoxide and ethene in MeOH by using Pd(OAc)₂ (as catalyst precursor) modified with chelating diphosphines (e.g dppe).



Scheme 3.7

Their interpretation of experimental evidence was that the *mono*-substituted *bis*phosphine complex in MeOH ($\epsilon = 32.6$) undergoes a fast auto-ionisation process to give the bischelate and free acetate ions (Scheme 3.7). The mechanism of formation of **a** was also proposed in CH₂Cl₂ but the rate was too fast to allow for kinetic studies (Bianchini *et al.*, 2003). The faster kinetics in CH₂Cl₂ may be due to the fact that Pd(OAc)₂ exists mainly as a linear dimer in dilute solutions of halogenated solvents such as those used in this study.

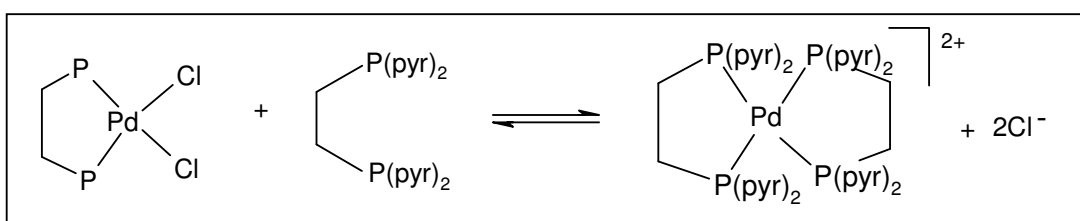
In late 2002, a publication (Marson *et al.*, 2002) showed unambiguously that the *bis*-chelated complex (**b**) was the kinetic product of the stoichiometric reaction between Pd(OAc)₂ and dppe in methanol (Scheme 3.8).



Scheme 3.8

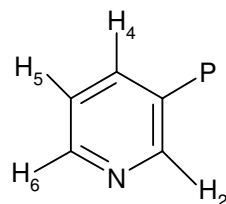
On standing in this solvent at room temperature, it slowly converted into the thermodynamic product (*mono*-chelated phosphine, **a**). Furthermore, they showed that **a** and **b** (in contrast to Bianchini's conclusion) were not involved in autoionisation equilibrium (*Scheme 3.7*), otherwise the conversion of **b** into **a** would not have proceeded to completeness.

From the experiments executed in our laboratories and results obtained by Marson and co-workers, it is clear that the chloro ligands were only partially removed during the reaction with silver triflate. Furthermore, equilibrium existed between the neutral complex with one bisphosphine ligand and the cationic complex ion with two bisphosphine ligands; and the charge was balanced by chloride ions (*Scheme 3.9*). The mixture was confirmed by the ^{31}P NMR spectrum.



Scheme 3.9

Phosphine binding is reversible and so initial errors in binding mode can be corrected and the thermodynamic chelate product can be formed in the end (Crabtree, 2005).



Labelling of protons for 3-pyridylphosphine ligands.

Table 3.4: ^1H and $^{31}\text{P}\{^1\text{H}\}$ NMR data of 1,2-bis-(di-3-pyridylphosphino)ethane and its Pt and Pd complexes

Compound	Solvent	Pyridyls ^1H data (δ)					^{31}P data		
		H ₂	H ₄	H ₅	H ₆	CH ₂ ^a	δ	$^1J_{\text{PtP}}$ or $^1J_{\text{PdP}}$ (Hz)	
^b d3pyrpe	DMSO	8.54	7.74	7.35	8.54	2.25 (10.06)	-20.8	-	
[PtCl ₂ (d3pyrpe)]	DMSO	9.03	8.27(19.83)	7.60	8.78	2.90 (20.1)	37.8	3583	
^c 1g and 2g	DMSO	9.03 & 8.69	8.27 & 7.85	7.61 & 7.41	8.79 & 8.69	2.89	37.8 & 41.4	3583 & 2352	
^d [Pt(d3pyrpe) ₂][BPh ₄] ₂	DMSO	7.89	6.97	6.60	7.89	^e 2.65	42.0	2332	
^f [Pt(d3pyrpe) ₂][PF ₆] ₂	DMSO	7.80	7.42	^g 7.08 (102.18)	7.54	2.95	^h 42.3 & -143	2332 & 711	
[PdCl ₂ (d3pyrpe)]	DMSO	9.03	8.31	7.59	8.81	3.04 (24.3)	61.0		
[PdCl ₂ (d3pyrpe)]	CDCl ₃	ⁱ 8.82 (18.6)	8.47	^j 7.47 (12.2)	ⁱ 8.82 (18.6)	2.70 (23.5)	56.0		
^k 1h & 2h	DMSO	9.05 & 8.62	8.30	7.60 & 7.34	8.80	3.06 & 2.99	61.0 & 49.8		

Spectra were run at 298 K. All the pyridyl protons appeared as multiplets and phosphorus occurred as singlets (except for PF₆⁻). The ligand data was in agreement with that reported in the literature (Bowen *et al.*, 1998). ^aBroad singlet or quasi-triplet ($J = [^2J(^{31}\text{P}-^1\text{H}) + ^3J(^{31}\text{P}-^1\text{H})]$) (Hz) in parentheses where resolved (Berners-Price *et al.*, 1999b) and broad doublet (only in Pd complexes). ^bProton numbering scheme is based on lit. (Berners-Price *et al.*, 1999b) and their values are in close agreement (solvent is CDCl₃). ^c1g and 2g are [PtCl₂(d3pyrpe)] and [Pt(d3pyrpe)₂]Cl₂, respectively. ^dPhenyl protons (multiplets) of BPh₄⁻ at $\delta = 5.97$ (8H), 6.10 (16H) and 6.35 (16H). ^eTentative assignment due to overlap with solvent peak. ^fTentative assignment due to the presence of [PtCl₂(d3pyrpe)] that caused overlaps. ^gSharp triplet with a resolved large coupling constant (also present in 1h and 2h). ^hSinglet and septet (spt, $^1J_{\text{PdP}}$), respectively. ⁱquasi-triplet. ^jquasi-doublet. ^k1h and 2h are [PdCl₂(d3pyrpe)] and [Pd(d3pyrpe)₂]Cl₂, respectively which were obtained as a mixture. ^lTentative assignment due to overlap of peaks and the ratio that exists in the mixture 5d:6d = 2:1.

NMR data for the 3-pyridyl complexes exhibited a similar trend to that found in the 2-pyridyl analogues. The chemical shift position of the ethane protons of the ligand did not differ greatly to those found in the complexes. However, coupling constants (J_{PH}) of the ligand were half the magnitude (~ 10 Hz) of those found in the complexes (~ 20 Hz). As observed in the d2pyrpe complexes, Pt complexes of d3pyrpe showed a ^{31}P resonance at highfield, i.e., δ 37.6 for $[\text{PtCl}_2(\text{d3pyrpe})]$ while Pd analogues resonated downfield, i.e., δ 61.0 for $[\text{PdCl}_2(\text{d3pyrpe})]$. It has been noted that for the same coordination number, molecular geometry, oxidation state, and phosphine, one generally observes a highfield shift of the ^{31}P resonance as one descends in a given group (Garrou, 1981).

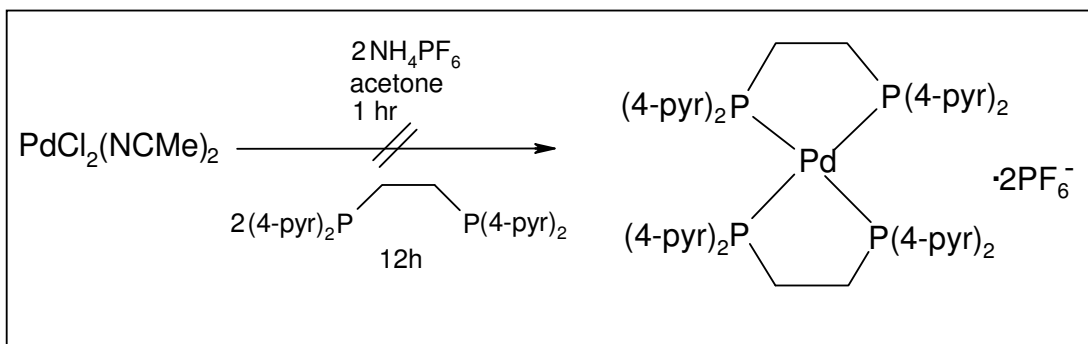
In general, NMR data of the *mono*-chelated Cl^- complexes showed that although the chemical shift of the 3-pyridyl compound appeared in highfield region as compared to the 2-pyridyl analogue (37.6 vs. 47.7 ppm), their Pt-P coupling constants were in the same range (3583 vs 3480 Hz), respectively. The electronegativity of substituents on phosphorus and the angles between them are the two most important variables determining ^{31}P NMR chemical shifts (Tolman, 1977). In chelating diphosphines, the coordination chemical shift Δ , ($\Delta = \delta_{\text{complex}} - \delta_{\text{free ligand}}$) depends on the ring size. Large downfield shifts are general for five membered chelate rings. Metal-phosphorus coupling constants depend on both electronic and steric factors, and in chelates, they depend on structural constraints.

3.2.5 Preparation of 1,2-bis-(di-4-pyridylphosphino)ethane platinum(II) complexes

Reaction of d4pyrpe and Na₂[PtCl₄] (1:1 or 1:2, respectively) produced a compound with a ³¹P singlet at 39.6 ppm with no indication of Pt-P coupling (¹J_{PtP}) as well as the peak at 28.9 ppm (decomposition products). Na₂[PtCl₄] was replaced with PtCl₂ (similar to the preparation of the 3-pyridyl analogue-*Scheme 3.5*) and the formation of [Pt(d4pyrpe)₂]Cl₂ was confirmed by ³¹P{¹H} NMR (δ at 42.9 ppm and Pt-P coupling of 2501 Hz). Despite obtaining a compound with significantly fewer decomposition products, plenty of unreacted ligand (δ at -15.4 ppm) remained in the mixture even with longer reaction time; this was in contrast to what was observed in the preparation of the 3-pyridyl compound. [Pt(d4pyrpe)₂][PF₆]₂ was not obtained in sufficient quantities to obtain a satisfactory ¹H NMR spectrum. However, a singlet at 45.2 ppm (with no Pt-P coupling) was observed in ³¹P{¹H} NMR (P-F coupling was observed). Attempts to optimise the yields were not pursued further as the compound was obtained in very low yields as a pale yellow fine powder at all times, similar to [Pt(dppen)₂][PF₆]₂.

3.2.6 Preparation of 1,2-bis-(di-4-pyridylphosphino)ethane palladium (II) complex.

Reaction of d4pyrpe and Na₂[PdCl₄] (1:1) produced a compound that was poorly soluble in NMR solvents although a ³¹P chemical shift of 60.0 ppm (CDCl₃) was observed. This was presumed to be [Pd(d4pyrpe)₂]Cl₂ although purification attempts led to its decomposition. Preparation of [Pd(d4pyrpe)₂][PF₆]₂ was attempted by reacting [PdCl₂(NCCH₃)₂] with NH₄PF₆ (2 eq.) followed by addition of 1,2-bis-(di-4-pyridylphosphino)ethane (d4pyrpe) (*Scheme 3.8*). As seen in the preparation of the Pt analogue, ³¹P{¹H} NMR spectra showed presence of large amounts of unreacted ligand even after 12hrs and plenty of decomposition products (δ 28.9).



Scheme 3.10: Synthetic route for the attempted preparation of $[\text{Pd}(\text{d4pyrpe})_2][\text{PF}_6]_2$

$^{31}\text{P}\{^1\text{H}\}$ NMR analysis of the crude compound showed the presence of a singlet (δ 65.9) and the characteristic septet of $[\text{PF}_6]^-$. However, after purification with DMF/ether, the pale yellow solid with a ^{31}P chemical shift at 66.3 ppm did not contain the septet, signifying that the product had not been obtained initially. The $^{31}\text{P}\{^1\text{H}\}$ NMR data implies only P-coordination to the metal centre as indicated by the downfield shifts (Durrant *et al.*, 2006). ^1H NMR spectrum showed presence of quasi-doublet of the bridging CH_2 (δ 3.01, PH coupling = 24.9 Hz), aromatic protons (δ , m, 7.87 and 8.80).

Reactions of d4pyrpe with both Pt and Pd yielded complex mixtures of products which were identified by ^{31}P NMR on the basis of known trends in chemical shifts. Due to problems of solubility, decomposition, extremely low yields, failure to abstract the chloride etc., preparation of the desired compounds was not pursued further. One research group showed that 2-pyridyl complexes (2-metallated pyridines) reacted with organic halides about one order of magnitude faster than their 4-pyridyl analogues (Canovese *et al.*, 1996). They also showed that replacement of palladium with platinum in structurally related complexes brought about a three fold increase in reactivity and also one to two unity increase in the $\text{p}K_a$ values, indicating a better electron donating ability of the platinum centre.

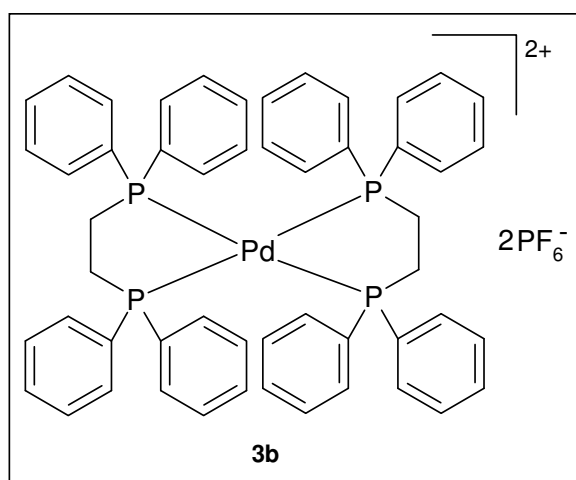
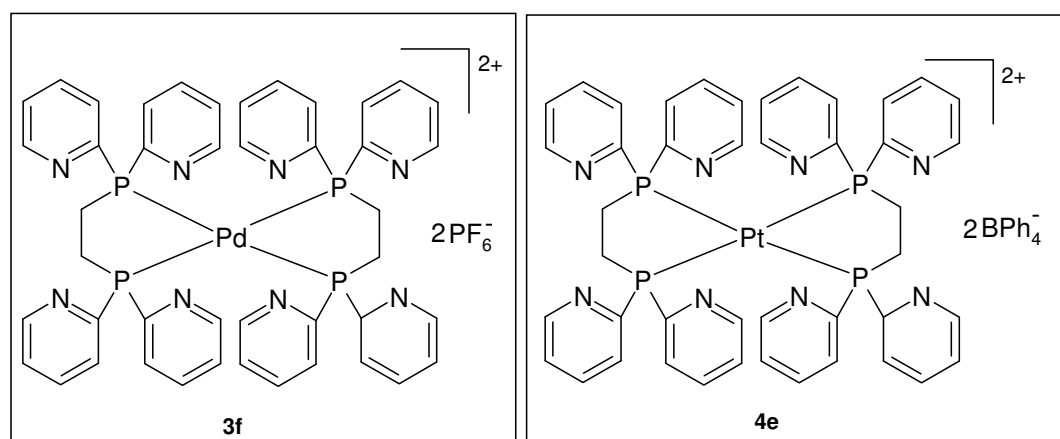
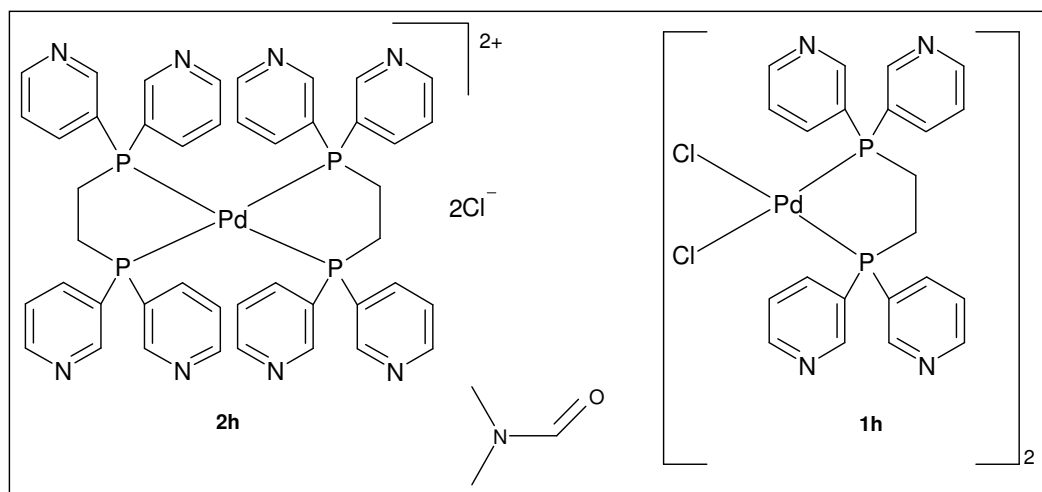
3.3 General discussion on the behaviour of the 2, 3 and 4-pyridylphosphine ligands

^{31}P NMR spectroscopy is a valuable probe to study electronic and structural features of complexes with phosphine ligands. $^{31}\text{P}\{^1\text{H}\}$ NMR spectroscopy studies carried out on Ag complexes of 1,2-bis-(di-*n*-pyridylphosphino)ethane for $n = 2, 3$ or 4 showed that d3pyrpe and d4pyrpe complexes existed in solution as monomeric *bis*-chelated $[\text{Ag}(\text{d3pyrpe})_2]^+$ and $[\text{Ag}(\text{d4pyrpe})_2]^+$, whereas the d2pyrpe complex formed equilibrium mixtures of the monomeric $[\text{Ag}(\text{d2pyrpe})_2]^+$, dimeric $[\{\text{Ag}(\text{d2pyrpe})_2\}_2]^{2+}$ and trimeric $[\{\text{Ag}(\text{d2pyrpe})_2\}_3]^{3+}$ (Berners-Price *et al.*, 1998). A similar trend was observed in Au complexes (Berners-Price *et al.*, 1999b). The d2pyrpe ligands coordinated in both bridging and chelated modes with the relative percentages of the species present are dependent on the temperature and solvent, making the ^{31}P NMR solution spectra for the 2-pyridyl considerably more complex.

The authors concluded from their results that the position of the pyridine nitrogen in the ring had a significant effect on this chemistry (Berners-Price *et al.*, 1998). The 2-pyridyl complex had limited solubility in water while the increased hydrophilic character of the monomeric 3-pyridyl and 4-pyridyl complexes was as a consequence of the more exposed N atoms. In our preparations, the different reactivity of the three ligands (2-, 3- and 4-pyridyl) towards the metals (Pd and Pt) confirmed the theory stated above. It is notable that reports of the preparation, reactions and catalytic properties of pyridylphosphines and their metal complexes have been confined, almost exclusively, to those with 2-pyridyl substituents (Bowen *et al.*, 1998).

3.4 Structural analysis of compounds 3b, 4e 3f, 1h and 2h

In this section, the structures of each of the 4 compounds are discussed. The structures were determined in order to make a comparison with similar Pt and Pd complexes from the literature.



3.4.1 Crystal structures of (1h, 2h), 3f, 4e and 3b

Table 3.5 summarises crystal data for compounds **1h**, **2h**, **3f**, **4e** and **3b**. Comprehensive crystallographic data is available on CD-ROM on request.

Table 3.5: X-ray data collection and structure refinements

	1h and 2h	3f	4e	3b
Formula	2(C ₂₂ H ₂₀ Cl ₂ N ₄ P ₂ Pd))+ C ₄₄ H ₄₀ Cl ₂ N ₈ P ₄ Pd + C ₃ H ₇ NO	C ₄₄ H ₄₀ F ₁₂ N ₈ P ₆ Pd	C ₉₂ H ₈₀ B ₂ N ₈ P ₄ Pt	C ₅₂ H ₄₈ F ₁₂ P ₆ Pd
FW	1159.40 + 982.08 + 73.09	1201.66	1638.23	1193.12
T (K)	293(2)	293(2)	173(2)	293(2)
λ, Å	0.7107	0.7107	0.7107	0.7107
Crystal size/mm³	0.28 x 0.12 x 0.10	0.44 x 0.24 x 0.18	0.28 x 0.14 x 0.14	0.36 x 0.28 x 0.20
Crystal system	Monoclinic	Orthorhombic	Triclinic	Monoclinic
Space group	<i>P2₁/n</i>	<i>Pnna</i>	<i>P-1</i>	<i>P2₁/n</i>
a, Å	9.2654(7)	23.436(2)	15.0836(3)	11.0285(9)
b, Å	24.3917(19)	14.488(1)	16.5635(3)	16.4251(14)
c, Å	21.7761(16)	14.683(1)	18.2187(4)	14.0426(12)
α,	90,	90,	77.412(1),	90,
β,	97.8240(10),	90,	72.435(1),	96.2830(10),
γ (°)	90	90	65.290(1)	90
V, Å³	4875.6(6)	4985.5(8)	3919.94(14)	2528.5(4)
Z	2	4	2	2
ρ Mg/m³	1.508	1.600	1.388	1.567
2θ, range, deg				2.23 to 26.46
Index ranges	-11<=h<=4 -30<=k<=30 -21<=l<=25	-28<=h<=26 -6<=k<=18 -18<=l<=17	-19<=h<=19 -21<=k<=21 -24<=l<=24	-13<=h<=13 -17<=k<=19 -17<=l<=7
R indices (all data)	R1 = 0.0524 wR2 = 0.1190	R1 = 0.0448 wR2 = 0.1111	R1 = 0.0374 wR2 = 0.0631	R1 = 0.0466 wR2 = 0.1056

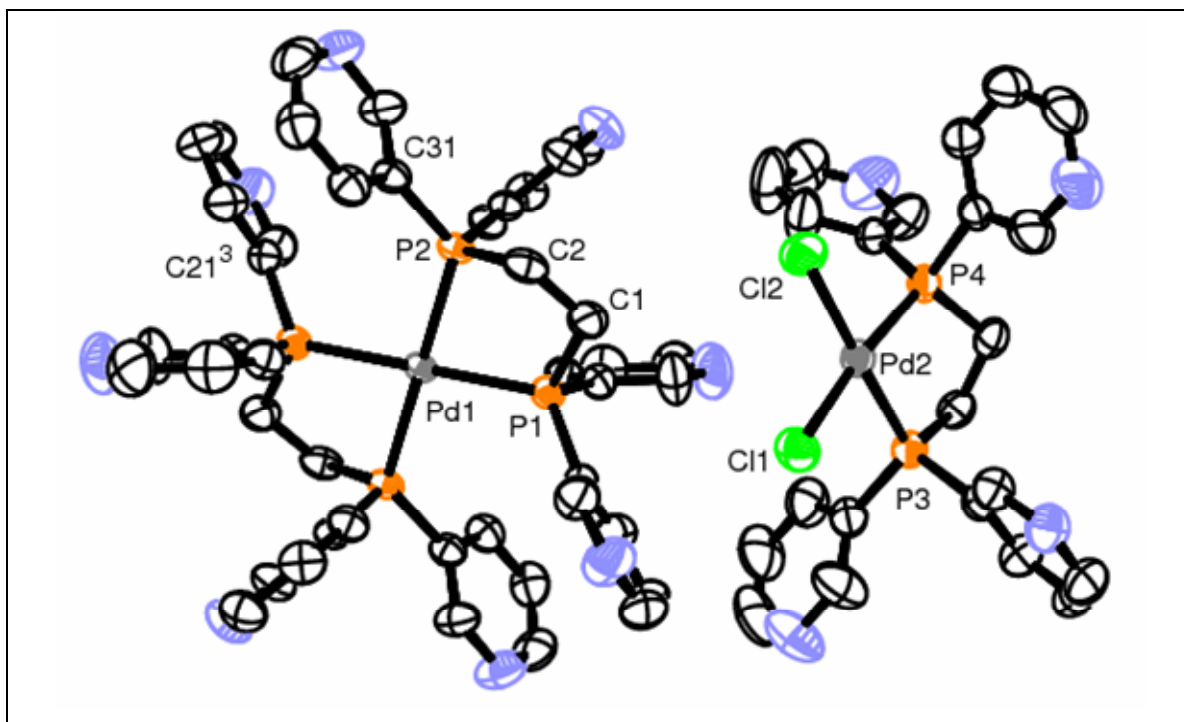


Figure 3.4: ORTEP representation of bis-(1,2-bis-(bis(3-pyridyl)phosphino)ethane-P-P')-palladium(II) dichloride (**6d**) and Bis[dichloro(1,2-bis(bis(3-pyridyl)phosphino)ethane-P-P')-palladium(II)] (**5d**). The hydrogen atoms, the solvate and the Cl counter ions are left out for clarity.

Compounds **1h** and **2h** co-crystallise in the monoclinic space group $P2_1/n$, $Z = 2$ with half a molecule of **1h**, one molecule of **2h**, a Cl counter ion and one ion of N,N-dimethylformamide solvate. The atom numbering scheme used in the corresponding tables and discussion are illustrated in Figure 3.4 and the unit cell is shown in Figure 3.5.

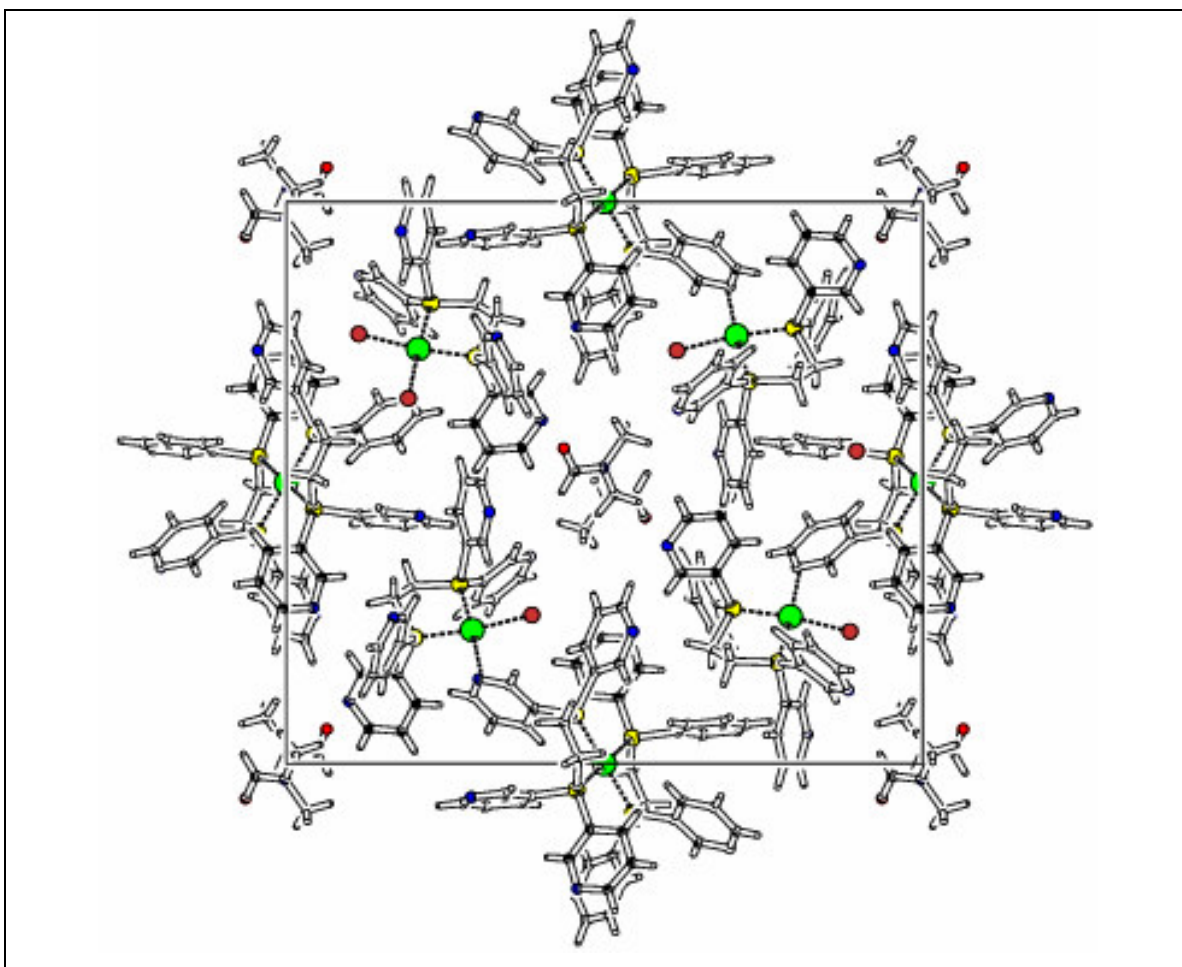


Fig 3.5: A view of the unit cell of **1h** and **2h** as viewed down the crystallographic *a* axis showing the dimethylformamide molecule surrounded by **1h** and **2h**.

In **1h** and **2h**, the crystals are arranged such that the plane containing the atoms Pd1, P1, P1', P2 and P2' in **1h** and that containing Pd2, P3, P4, Cl1 and Cl2 are at an angle of $56.67(3)^\circ$; such that the two are linked by weak C-H...Cl intermolecular interactions forming parallel layers of both molecules that run in the crystallographic *a* direction. The Cl counter ions then link **1h** and **2h** and all three molecules surround the dimethylformamide solvate. This solvate also forms C-H...O hydrogen bonded dimers that run parallel to *a* axis and is connected to the **2h** through another C-H...O interaction (see packing diagram in Figure 3.5).

Figure 3.6 shows the molecular structure of compound **3f** together with the atom numbering scheme as used in this discussion.

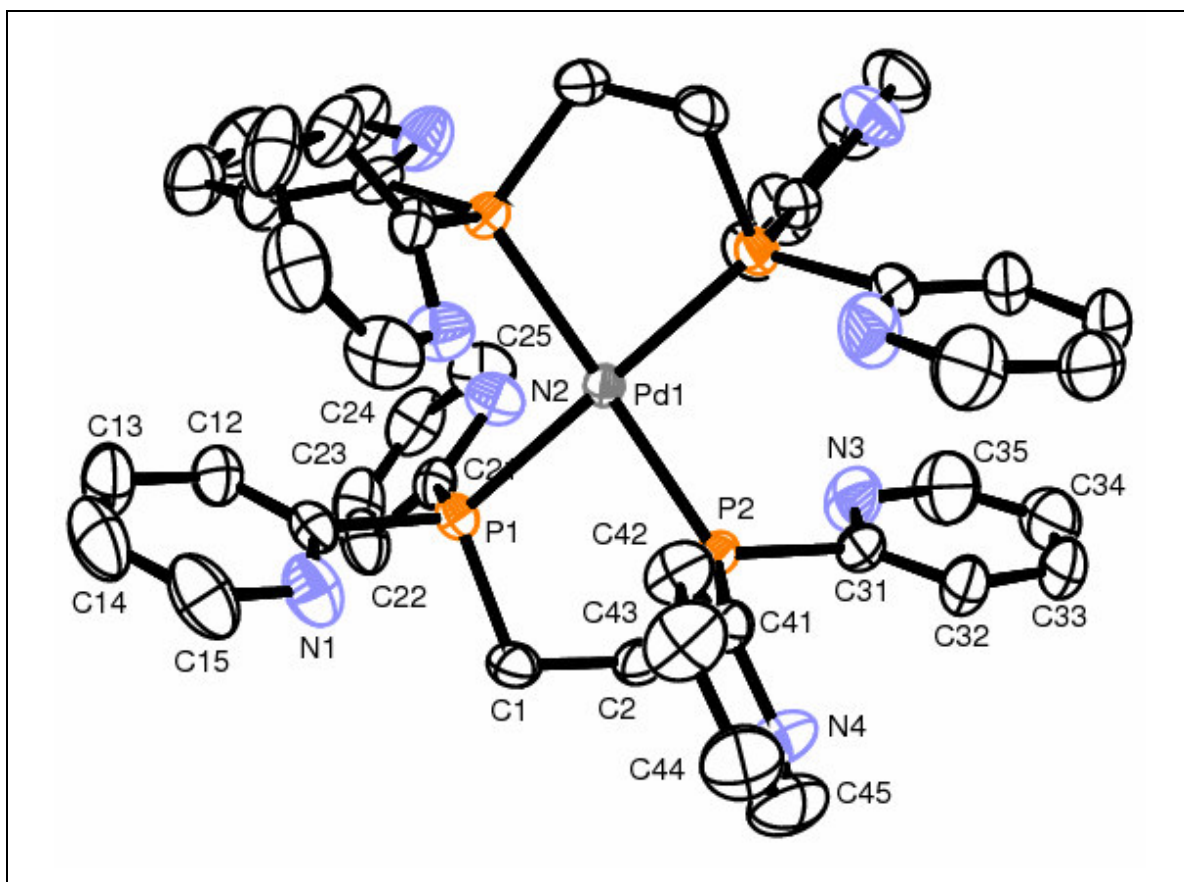


Figure 3.6: ORTEP diagram of bis{1,2-bis(bis(2-pyridyl)phosphino)ethane-P-P'}-palladium(II).bis(hexafluorophosphate) **3f**. Hydrogen atoms and the two ions of PF₆ have been omitted for purposes of clarity. Ellipsoid probability is at 50%.

Compound **3f** crystallises in the non-centrosymmetric space group *Pnna* with half a molecule of the palladium complex and two ions of PF₆ in the asymmetric unit. The two PF₆ molecules are disordered. One has only the equilateral fluoride atoms disordered in a general position while the second has both axial and equilateral fluoride atoms disordered also in a general position but resulting in distorted octahedral geometry. Connection of molecules in the crystal is mainly through C-H...F intermolecular interactions.

Packing in the crystal is such that the solvate molecules are sitting in the voids between the palladium complex molecules with the less disordered ions of PF_6 being on the same axis as Pd atoms while the more disordered PF_6 molecule is positioned between the Pd complexes (*Fig. 3.7*). In compound **3f**, the conformations of the ligands are such that the pyridyl rings get positioned more above and below the coordination plane. Two pyridyl nitrogens, one on each side of the coordination plane are just over 3\AA from the Pd (Liles, 2006).

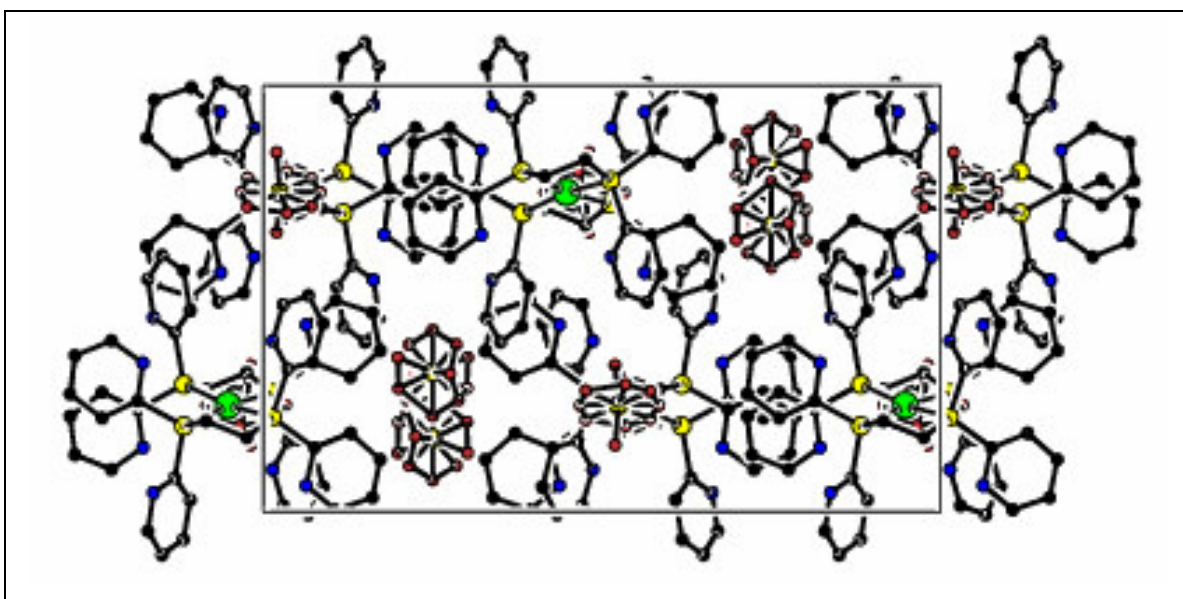


Figure 3.7: Packing diagram of compound **3f** showing the solvate molecules of PF_6 as viewed down the crystallographic *b* axis.

The molecular structure of **4e** is given in Figure 3.8 along with atom numbering scheme as used in this discussion.

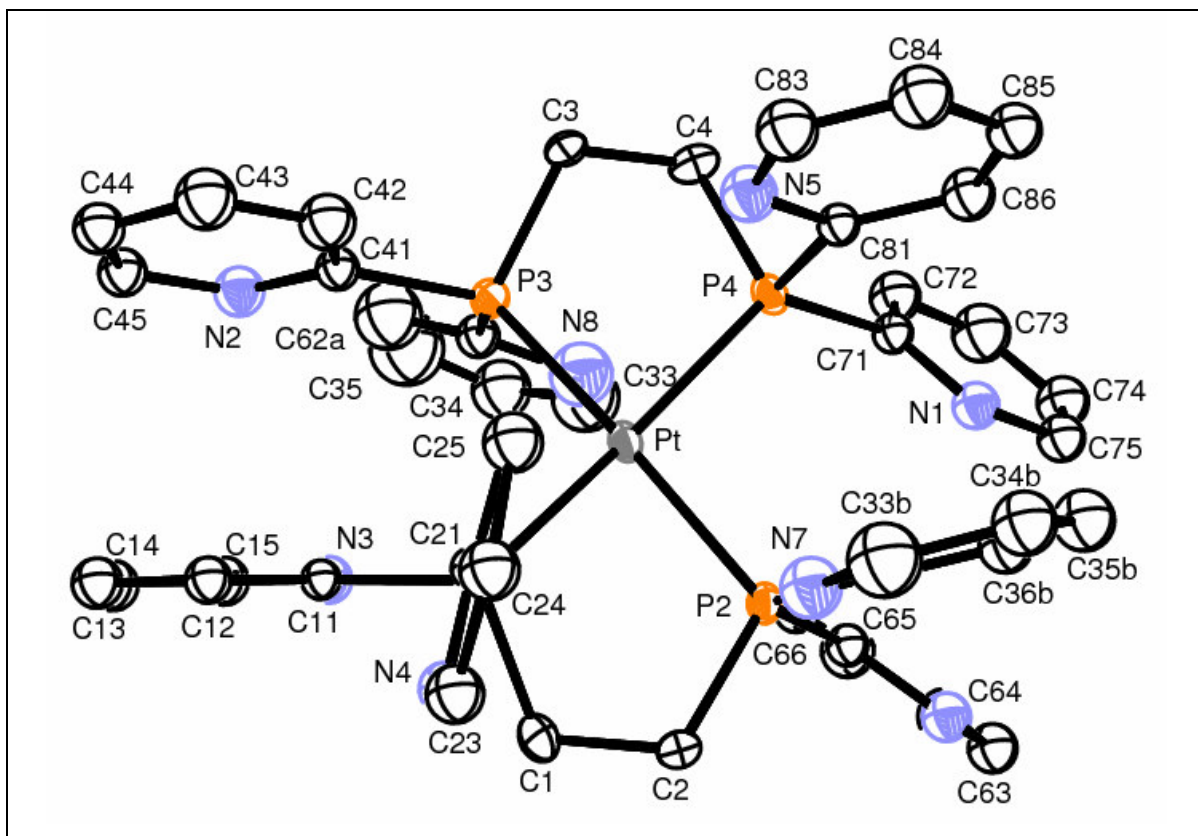


Figure 3.8: ORTEP diagram of bis{1,2-bis(bis(2-pyridyl)phosphino)ethane-P-P'}-platinum(II).bis(tetraphenylborate) **4e**. All hydrogen atoms and the two tetraphenylborate ions have been omitted for clarity purposes. Ellipsoid probabilities are given at 50%.

Compound **4e** crystallises in the centrosymmetric space group $P\bar{1}$ with one molecule of the platinum complex and two ions of tetraphenylborate. The pyridyl rings containing N7 and N8 are disordered in general positions. The orientation of the pyridyl groups seem to be affected by weak intra-molecular interactions, for example C62a-N2.

Figure 3.9 below shows the molecular structure of compound **3b** together with the atom numbering scheme as used in this discussion.

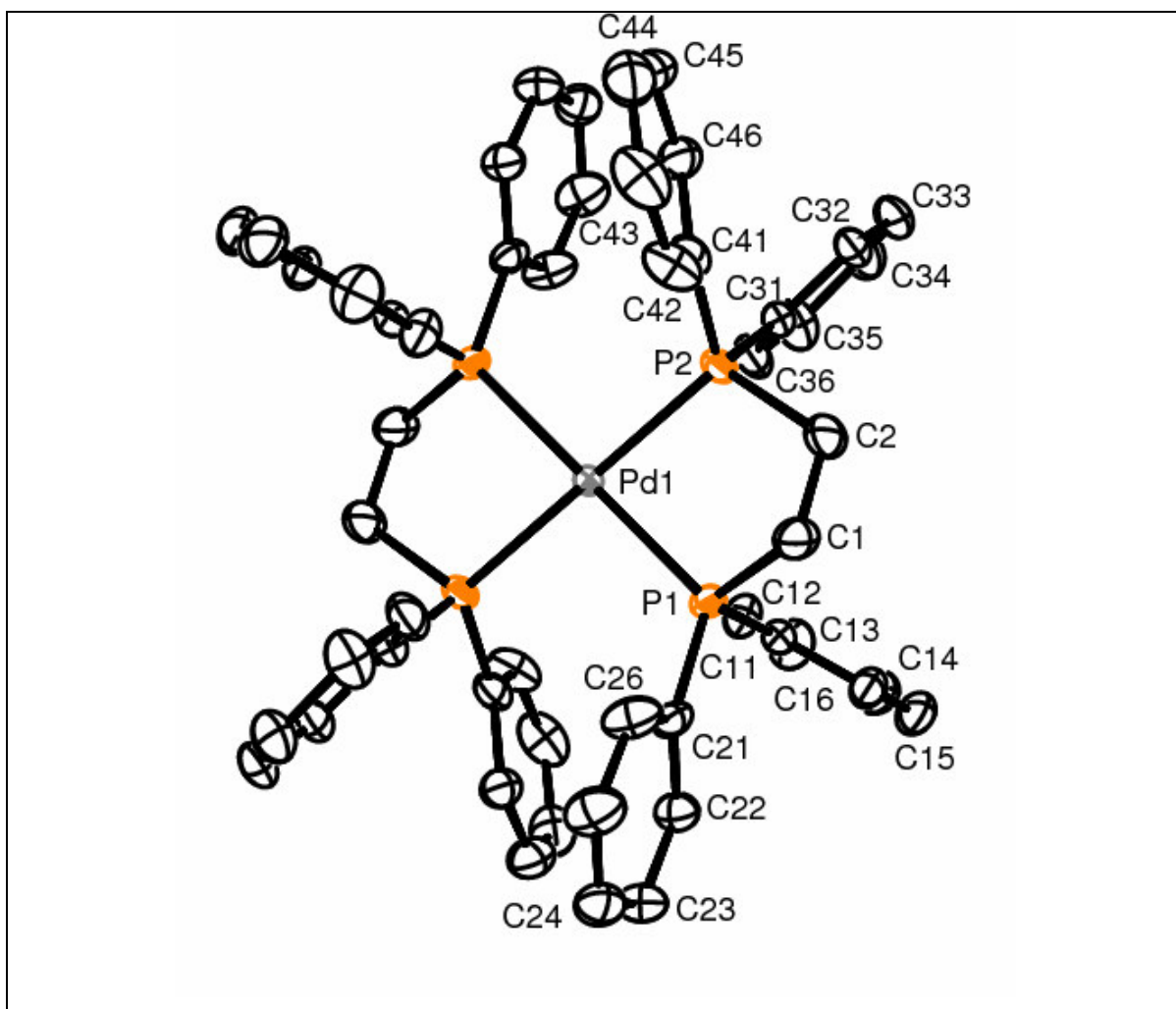


Figure 3.9: ORTEP diagram for bis{1,2-bis(diphenylphosphino)ethane-P-P'}-palladium(II).bis(hexafluorophosphate) **3b**. Hydrogen atoms and the two ions of PF_6^- have been left out for the purposes of clarity. Ellipsoid probability is at 30%.

Compound **3b** crystallises in the centrosymmetric space group $P2_1/n$ with half a molecule of the palladium complex and one ion of phosphorus hexafluoride in the asymmetric unit. The other half of the palladium complex is generated by a glide plane. The phosphorus hexafluoride ion is disordered in the general position.

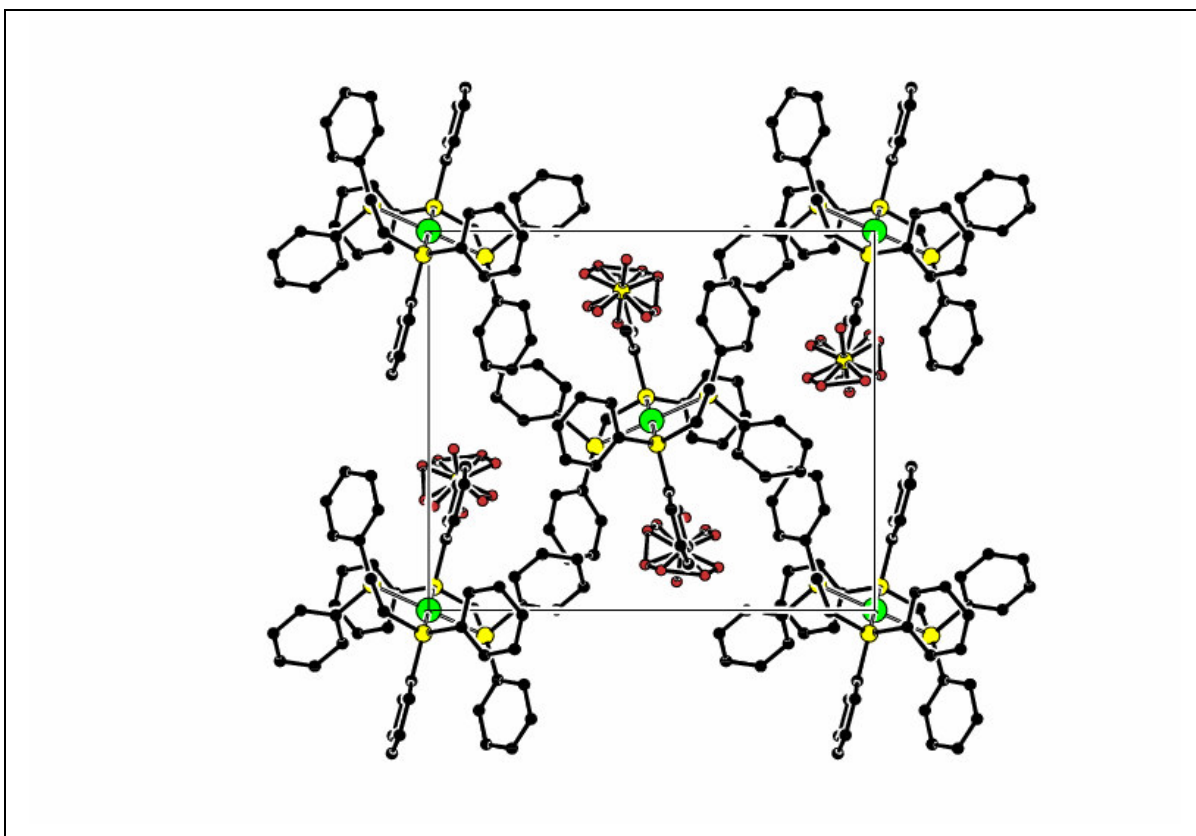
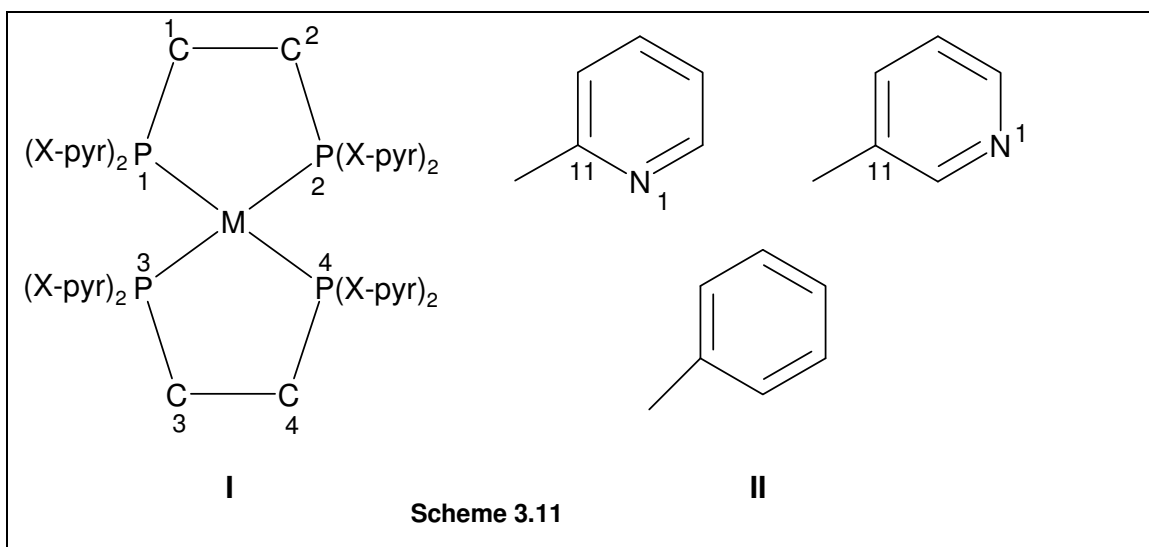


Figure 3.10: Packing diagram for compound **3b**. Hydrogen atoms are left out for clarity.

In the unit cell, the palladium atoms are sitting in special positions (*Fig. 3.10*). The crystal is stabilised through C-H...F interactions between the phenyl rings of the palladium complex and the fluorine atoms of the PF₆ anion.

3.4.2 Molecular structures of (1h, 2h), 3f, 4e and 3b



The structural diagram and general atom-numbering scheme for the four metal complexes is given above (*Scheme 3.11*). Each of the four compounds is distinctly different with respect to the metal and the position of the nitrogen atom on the pyridyl ring. X = position of nitrogen atom on the pyridyl ring (2 or 3), M = Metal (Pt or Pd). For each of the metal pyridyl complexes (**1h** and **2h**, **3f** and **4e**), there are eight pyridyl rings (**II**) each attached to the phosphorus atoms through C11 (as shown in the scheme) or C21, C31, C41, C51, C61, C71 and C81. All compounds were crystallised from a variety of solvents in accordance with their solubilities.

Important bond distances and angles of **1h** and **2h**, **3f**, **4e** and **3b** are tabulated below (*Table 3.7*).

Table 3.7: Selected bond distances (Å) and angles (deg) for **1h** and **2h**, **3f**, **4e** and **3b** with estimated standard deviations in parentheses

	1h	2h	3f	4e	3b
M-P1	-	2.3434(9)	2.3331(6)	2.2825(6)	2.3412(8)
M-P2	-	2.3283(8)	2.2999(6)	2.3161(6)	2.3562(8)
M-P3	2.231(1)	-	-	2.3038(6)	Same M-P1
M-P4	2.232(1)	-	-	2.3215(6)	Same M-P2
P1-C1	-	1.845(4)	1.829(3)	1.815(2)	1.829(1)
P2-C2	-	1.816(3)	1.828(3)	1.845(2)	1.854(4)
P3-C3	1.826(4)	-	-	1.829(2)	-
P4-C4	1.825(4)	-	-	1.829(3)	-
P1-C11	-	1.803(4)	1.822(3)	1.820(2)	1.809(3)
P1-C21	-	1.813(4)	1.820(3)	1.827(2)	1.804(3)
P2-C31	-	1.806(4)	1.822(3)	1.827(7)	1.804(4)
P2-C41	-	1.809(3)	1.821(3)	1.819(2)	1.809(4)
C1-C2	-	1.526(5)	1.516(4)	1.523(3)	1.461(5)
C3-C4	1.538(6)	-	1.516(4)	1.519(4)	1.461(5)
P-F (<i>ave</i>)	-	-	1.517	-	1.561
P1-M-P2		81.59(3)	83.10(2)	83.13(2)	82.94(3)
P3-M-P4	86.47(4)	-	-	83.74(2)	82.94(3)
P1#1-M-P2	-	98.41(3)	98.02(3)	97.26(2)	97.06(3)
P1-M-P1#1		180.00(4)	171.62(2)	170.87(2)	180.0
P1-M-P2#1			97.01(3)	97.22(2)	97.06(3)
Cl1-Pd-Cl1	94.22(2)	-	-	-	-
P3-Pd2- Cl1/Cl2	88.98(4) /90.41(4)	-	-	-	-
C1-P1-M	-	108.80(1)	109.37(9)	107.05(8)	105.92(1)
C2-P2-M	-	103.87(1)	107.82(9)	109.50(8)	108.07(1)
C3-P3-M	108.52(1)	-	-	-	-
C4-P4-M	107.71(1)	-	-	-	-
M-P1-C11		111.01(1)	123.49(9)	120.99(8)	110.63(1)
M-P1-C21		122.08(1)	104.04(9)	108.03(7)	121.24(1)
M-P2-C31		125.04(1)	118.91(1)	114.0(2)	114.66(1)
M-P2-C41		108.32(1)	112.18(9)	112.70(9)	117.16(1)
C11-P1-C21	-	104.72(1)	108.43(1)	109.80(1)	106.91(1)
C31-P2-C41	-	105.83(1)	108.61(1)	113.2(3)	106.92(1)

The molecular geometry of the four compounds (**1h** and **2h**, **3f**, **4e** and **3b**) is similar in that all show a distorted square planar arrangement of the phosphorus atoms around the central metal atom. The deviation from the mean square plane through the five atoms ranges from 81.59 to 83.13° and is as a consequence of the endocyclic P1-M-P2 angle being constrained between 81-84° (Oberhauser *et al.*, 1995). These angles seem to be similar for all the compounds and compare well with those of dppe containing Pd(II) and Pt(II) complexes from the literature with 81.65(8)° in [Pd(dppe)₂]Cl₂ (Oberhauser *et al.*, 1997b), 82.66(4)° in [Pd(dppe)₂][PO₂(OPh)₂]₂ (Stockland *et al.*, 2004), 82.09(5) in [Pt(dppe)₂]₂·2CDCl₃ (Ferguson *et al.*, 1993) and 81.88(3)° in [Pd(dppe)₂][CB₁₁H₁₁Cl]₂·3CH₂Cl₂ (Lassahn *et al.*, 2003). The latter group also found that the phenyl rings of the opposing dppe ligands in [Pd(dppe)₂]²⁺ cations were too far apart for a meaningful π - π interaction, which was different from the situation in the [Ni(dppe)₂]²⁺.

The corresponding exocyclic angles between the phosphorus atoms not chelating are therefore open slightly more than 90°. The bridging carbon atoms lie on either sides of the coordination plane of metal atoms with torsion angles about the C-C bond being -40.66 (**4e** Pt 8.11), -40.26 (**3b** Pd 0.01), 49.62 (**3f** Pd 8.38), -37.70 (**1h** Pd 0.01) and 48.50 (**2h** Pd 0.01). There is a marked deviation from sp³-hybridisation around the phosphorus atom for all the four complexes since most of the angles are not very close to 109.5°. The M-P-C(aryl) angles differ significantly and range from 108.32(1)-125.04(1) in **2h**, 108.03(7)-120.99(8) in **4e**, 104.04(9)-123.49(9) in **3f** and 110.63(1)-121.24(1)° in **3b**. This represents the electronically most favoured sites resulting from the crowded square planar geometry of the complex and the puckered chelate ring.

Changing the *mono*-chelate system as in **1h** to a *bis*-chelate system like in **2h**, **3f**, **4e** and **3b** leads to a structural change in which the C-C bond distance between the bridging carbons is slightly shortened by about 0.01 Å. However, the C-C “backbone” distances found in **1h**, **2h**, **3f** and **4e** [1.538 (6), 1.526 (5), 1.516 (4) and 1.523(3) Å] are comparable to those found in the free (d2pyrpe) and coordinated ligand, [PtCl₂(d2pyrpe)₂], 1.527 and 1.531 Å, respectively (which are essentially identical) (Jones *et al.*, 1999). There is a significant variation in P-CH₂ bond lengths in three of the four structures with 1.816(3) and 1.845(4) in **2h**;

1.815(2) and 1.845(2) in **4e**; and 1.829(4) and 1.854(4) Å in **3b**. The same effect is not observed in **1h** [P-CH₂ bond lengths of 1.825(4) and 1.826(4)] and **3f** [P-CH₂ bond lengths of 1.828(3) and 1.829(3)].

3b has average P-C(CH₂) and C-C bond lengths of 1.842(4) and 1.461(5) Å while distances of 1.829(3) and 1.521(7) Å are found in free dppe, respectively (Zhuravel and Glueck, 1999). The difference observed between free dppe and **3b** may indicate that the chelating dppe is sterically constrained. This difference in turn affects the C1-C2 bond length in **3b** [1.461(5) Å]. As expected, the average P-C(sp³) bond lengths of 1.8305(3) in **2h** and 1.8415 (4) Å in **3b** Å are longer than the corresponding P-C(sp²) bond lengths of 1.8078(4) and 1.8065(3) Å, respectively. However, significant differences between P-C(sp³) bond lengths and P-C(sp²) are not observed in **1h**, 1.8255(4) vs 1.8123(4); 1.8285(3) vs 1.8233(3) in **4e**; and 1.8300(2) vs 1.8213(3) Å in **3f**. The free ligand (d2pyrpe) of the two latter complexes exhibits significantly longer P-C(CH₂) and P-C(sp²) bond lengths of 1.842 and 1.848 Å, respectively (Jones *et al.*, 1999).

Another observation is that the P-C_(sp²) bond lengths of **1h** [1.8123(4)], **2h** [1.8078(4)] and **3b** [1.8065(3)Å] are noticeably shorter than those found in the complexes coordinated to 2-pyridyl ligands [**4e** = 1.8233(3) and **3f** = 1.8213(3) Å]. The latter complexes have similar values to those observed in [PtCl₂(d2pyrpe)] (1.820 Å) (Jones *et al.*, 1999). In contrast to **3b**, longer average P-C(Ph) bond lengths (1.827 Å) are reported for dppe complexes (Jones *et al.*, 1999).

Most of the remaining bond distances and angles are comparable to those of corresponding complexes from the literature supporting the notion that replacing palladium with platinum causes a very small and barely significant change in M-P distances (Engelhardt *et al.*, 1984). An example is the analogous platinum complex of [Pd(dppe)₂]²⁺, bis[1,2-bis-(diphenylphosphino)ethane]platinum(II) iodide which has Pt-P distance of 2.3310(13) Å (Ferguson *et al.*, 1993) which is not dissimilar to that found in **3b** [Pd-P = 2.3412(8) Å]. In general, the M-P distances for **2h**, **4e**, **3f** and **3b** (2.2825 – 2.3434 Å) are within the range for square-planar d⁸ complexes of palladium and platinum, for compounds with two phosphines *trans* to each other (Engelhardt *et al.*, 1984). While the *trans*-effect of

replacing phosphorus by chlorine in the coordination sphere (as in **1h** and **2h**) is very pronounced, causing a contraction in the metal-phosphorus bond of 0.1 Å (average length of 2.232(1) vs 2.3359(8) Å, respectively), the effect of this upon the two different metal atom systems does not differ significantly in respect of M-P bond lengths (Engelhardt *et al.*, 1984).

This phenomenon is also observed in **4e** where the average Pt-P bond length (2.316 Å) is significantly longer than that determined for [PtCl₂(d2pyrpe)]·CH₂Cl₂ (2.210 Å) while the P-Pt-P angle is significantly smaller (83.44 vs 86.17°) (Jones *et al.*, 1999). This can be attributed to a competitive π-interaction of two *trans* P-atoms in square planar geometry and a greater congestion of atoms caused by the pyridyl substituents of two chelating rings compared to one. A value of 86° for P-Pt-P angles is consistent with values found in structures of other Pt-bidentate phosphine complexes with five membered chelate rings (Miedaner *et al.*, 1993). The two chelate rings in **4e** differ with one having shorter Pt-P distances compared to the other chelate ring [2.2993(6) vs 2.3127(6) Å]. This is also reflected in the bite angles of the chelate rings [C11-P1-C21 = 109.80(1) and C31-P2-C41 = 113.2(3)°].

Table 3.7 below shows analytical data, melting points and % yields of all the pure compounds.

Table 3.7: Analytical data and melting points of the complexes that were obtained as pure compounds

Compound & Formula	^a Elemental analysis			m.p (°C)	% yield
	C	N	H		
[Pt(dppe) ₂][PF ₆] ₂ (C ₅₂ H ₄₈ P ₆ F ₁₂ Pt) (FW: 1281.8)	48.72 (48.01)		3.77 (3.49)	190-192	58
[Pd(dppe) ₂][PF ₆] ₂ (C ₅₂ H ₄₈ P ₆ F ₁₂ Pd) (FW: 1193.12)	52.35 (52.09)	(0.12)	4.06 (4.05)	214-216 (dec.)	48
[Pd(dppen) ₂][PF ₆] ₂ (C ₅₂ H ₄₄ P ₆ F ₁₂ Pd) (FW:1189.16)	52.52 (53.37)	(1.57)	3.73 (4.48)	210-212 (dec.)	51
[Pt(d2pyrpe) ₂][PF ₆] ₂ (C ₄₄ H ₄₀ N ₈ P ₆ F ₁₂ Pt) (FW:1289.76)	40.98 (39.32)	8.69 (8.45)	3.13 (2.54)	170-172 (dec.)	65
[Pd(d2pyrpe) ₂][PF ₆] ₂ (C ₄₄ H ₄₀ N ₈ P ₆ F ₁₂ Pd) (FW: 1201.66)	44.00 (44.26)	9.33 (9.32)	3.36 (3.31)	208-210 (dec.)	37
^b [Pt(d3pyrpe) ₂][PF ₆] ₂ (C ₄₄ H ₄₀ N ₈ P ₆ F ₁₂ Pt) (FW: FW:1289.76)	40.98 (42.46)	8.69 (10.46)	3.13 (4.24)	176-178 (dec.)	45
[Pt(d2pyrpe) ₂][BPh ₄] ₂ (C ₉₂ H ₈₀ N ₈ P ₄ B ₂ Pt) (FW: 1638.23)	67.45 (67.69)	6.84 (6.83)	4.92 (4.96)	>230	50
^c [Pt(d3pyrpe) ₂][BPh ₄] ₂ (C ₉₂ H ₈₀ N ₈ P ₄ B ₂ Pt) (FW: 1638.23)	67.45 (62.54)	6.84 (6.27)	4.92 (5.35)	140-145 (dec.)	40

^aCalculated and found (in parentheses) data in %. All the compounds except the last two were recrystallised from DMF/ether. All the phenyl complexes and [Pt(d3pyrpe)₂][PF₆]₂ had DMF coordinated to them leading to great differences between the expected and obtained values (%). ^b[Pt(d3pyrpe)₂][PF₆]₂·4DMF (C₅₆H₆₈N₁₂O₄P₆F₁₂Pt) - calc. C, 42.51; N, 10.62; H, 4.33 % and ^c[Pt(d3pyrpe)₂][BPh₄]₂·2CH₂Cl₂ (C₉₄H₈₄N₈P₄B₂Cl₄Pt, 1808.17) - calc. C, 62.44; N, 6.20; H, 4.68 % which correspond closely to the obtained values shown in the table.

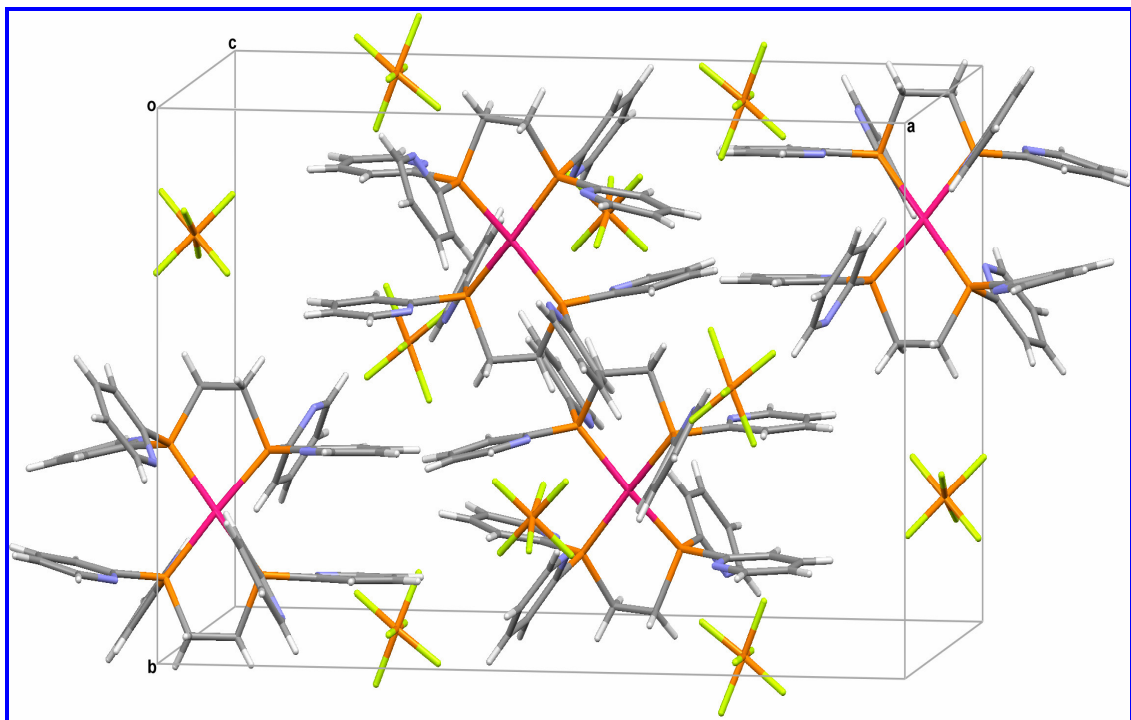
The colour of all the PF₆ complexes that were successfully synthesised ranged from yellow to white, were air-stable, and soluble in polar solvents such as acetonitrile, dimethylsulphoxide and dimethylformamide. They were partially soluble in chlorinated solvents such as CH₂Cl₂ and CHCl₃ and insoluble in ether, hexane, water and tetrahydrofuran. This low solubility has been shown in similar complexes containing PF₆⁻ as the counterion (Tanase *et al.*, 1993). It is also worth noting that complexes that required long synthetic routes as well as those that were obtained in poor yields were not investigated for biological activity. This was due to the fact that short and simple synthetic routes that produce higher yields are ideal in the production of pharmaceutical products. Additionally, some of them could not be characterised conclusively due to poor yields coupled by solubility problems.

Finally, six complexes were used in biological assays that are described in the Pharmacology Sections (Chapter 5-10). ¹These are [Pt(dppe)₂][PF₆]₂ (**Pg 1**), [Pd(dppe)₂][PF₆]₂ (**Pg 3**), [Pd(*cis*-dppen)₂][PF₆]₂ (**Pg 4a**), [Pt(d2pyrpe)₂][PF₆]₂ (**Pg 5**), [Pt(d3pyrpe)₂][PF₆]₂ (**Pg 6**), [Pd(d2pyrpe)₂][PF₆]₂ (**Pg 8**), and [Au(dppe)₂]Cl (used as a standard in all investigations). The compounds used in biological assays were purified by washing with diethyl ether (as described in Chapter 4) and not purified from DMF. This is due to the fact that DMF coordinated to the complexes (as seen in X-ray structure) and also demonstrated from elemental analyses.

¹ The naming scheme depicted for the test compounds is different from the ones shown in the synthetic routes.

Chapter IV

Experimental details



4.1 General

All manipulations (unless stated otherwise) were carried out under an argon atmosphere, using standard Schlenk techniques. Solvents were distilled from sodium/benzophenone ketyl and degassed.

4.1.1 NMR spectroscopy

NMR spectra were recorded in DMSO and CDCl_3 at 298 K using the following Bruker instruments; AVANCE 300 and ARX 300 (^1H , 300.1 MHz; ^{13}C , 75.5 MHz; ^{31}P , 121.5 MHz) and referenced internally to residual solvent resonances (data in δ) in the case of ^1H and ^{13}C NMR spectra. The ^{31}P NMR spectra were referenced externally to 85% H_3PO_4 . All NMR spectra other than ^1H were proton decoupled. First order analysis was used to assign the spectra. Recording of ^{13}C NMR spectra proved to be problematic due to solubility problems (as discussed in 3.1.1) and hence only the complexes with distinguishable chemical shifts are reported below.

4.1.2 Melting points

Melting points were recorded in unsealed capillaries and are uncorrected.

4.1.3 Elemental analysis

Elemental analysis (empirical formulae shown) was determined by the Institute for Soil, Climate and Water, Pretoria.

4.1.4 MS-FAB

Fast atomic bombardment mass spectra were recorded with a VG70SEQ by micromass.

4.1.5 X-ray crystallography

Intensity data, for the crystal structure **4e** was collected on a Bruker SMART 1K CCD area detector diffractometer with graphite monochromated Mo K_{α} radiation (50kV, 30mA) at 173 K. The collection method involved ω -scans of width 0.3°. Data reduction was carried out using the program *SAINT* (Bruker, 1999a) and the absorption corrections were made using the program *SADABS* (Sheldrick, 1996). The crystal structure was solved by direct methods using *SHELXTL* (Bruker, 1999b). Hydrogen atoms were located in the difference map then positioned geometrically and allowed to ride on their respective parent atoms. Diagram and publication material were generated using *SHELXTL* (Bruker, 1999b) and *PLATON* (Spek, 2003).

Intensity data, for the crystal structures (**3f**, **1h** and **2h**, **3b**) were collected on a Bruker SMART 1K CCD area detector diffractometer with graphite monochromated Mo K_{α} radiation (50kV, 30mA) at 298 K.

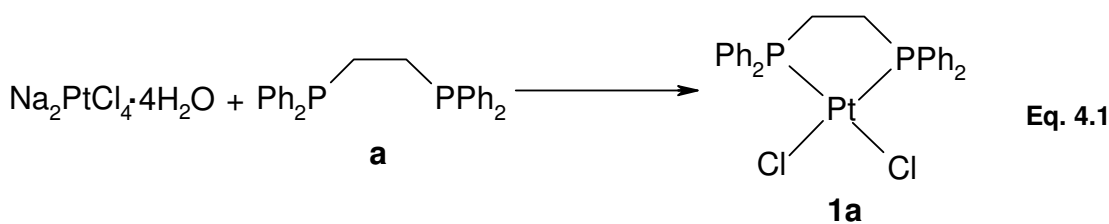
4.2 Synthesis of phenyl phosphine complexes

4.2.1 Synthesis of $[Au(dppe)_2]Cl$

This compound was prepared by modification of a literature procedure (Berners-Price and Sadler, 1986). 1,2-bis-(diphenylphosphine)ethane (0.56 g, 1.406 mmol) in THF (10 ml) was added dropwise to a stirring solution of $ClAuSMe_2$ (0.185 g, 0.713 mmol) at 0 °C. The mixture was stirred for 15 mins then allowed to warm to room temperature to give a white solid. The solvent was removed *in vacuo*. Yield: 87% (0.62 g). $^{31}P\{^1H\}$ NMR, (DMSO, δ , ppm): 21.7; lit. 21.9 (Berners-Price and Sadler, 1987b). MS-FAB, m/z 993 ($M^+ - H$).

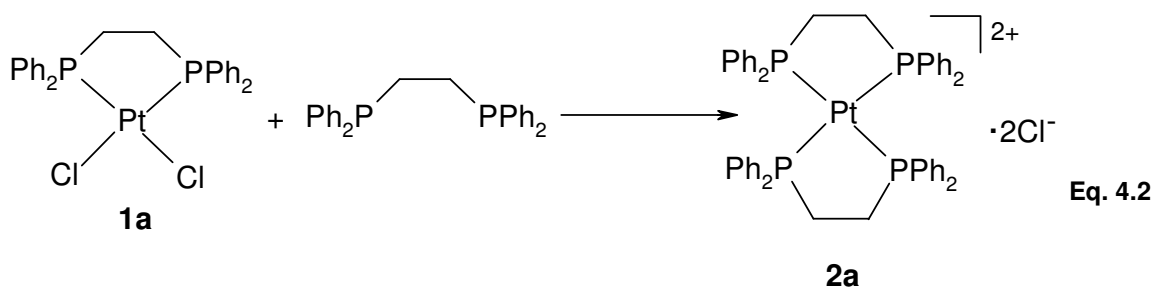
4.2.2 Synthesis of $[PtCl_2(dppe)]$ (**1a**)

The compound was synthesised according to a literature procedure (Westland, 1965) (*Eq. 4.1*). A fine white compound was obtained. Yield: 300 mg (35 %). $^{31}P\{^1H\}$ NMR (DMSO, δ , ppm): 43.4 ($J_{PtP} = 3547$ Hz).



4.2.3 Synthesis of $[\text{Pt}(\text{dppe})_2]\text{Cl}_2$ (**2a**)

Compound **1a** was treated with 1,2-bis-(diphenylphosphine)ethane (dppe) to yield **2a** according to equation 4.2 (Westland, 1965). It was isolated in good yield (320 mg, 83 %). $^{31}\text{P}\{^1\text{H}\}$ NMR (DMSO, δ , ppm): 48.9, ($J_{\text{PtP}} = 2331$ Hz).



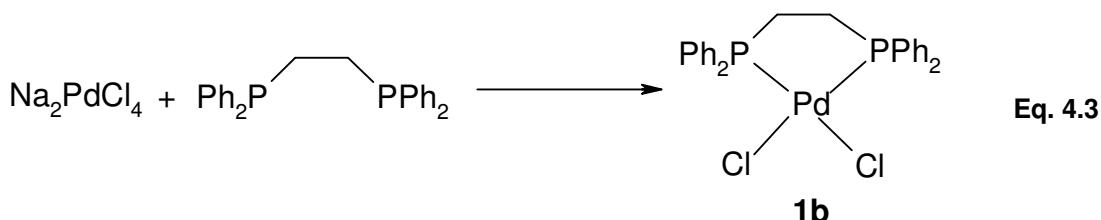
4.2.4 Synthesis of $[\text{Pt}(\text{dppe})_2][\text{PF}_6]_2$ (**3a**)

3a was prepared according to a literature procedure (Jones *et al.*, 1999). NH_4PF_6 (0.03 g, 0.184 mmol) was added to a stirred solution of $[\text{Pt}(\text{dppe})_2]\text{Cl}_2$ (0.10 g, 0.094 mmol) in acetone (25 ml). The white mixture was stirred for 45 min and the resultant mixture filtered through celite 545, which was subsequently washed with acetone (3 x 5 ml). The combined colourless filtrate was reduced to ~3ml to yield a white precipitate and ether (15 ml) was added to facilitate more precipitation. The white compound was isolated by filtration, washed with ether (3 x 5ml) and dried *in vacuo*.

Yield: 70 mg (58 %). $^{31}\text{P}\{^1\text{H}\}$ NMR (DMSO, δ , ppm): 49.3 ($^1J_{\text{PtP}} = 2323$ Hz), -143 (spt, $^1J_{\text{PF}} = 712$ Hz, PF_6^-). ^{13}C NMR (DMSO): δ 29.4 (s, bridging CH_2), 125.3 (*lps*-C), 129.4 (s, *m*-Ph), 133.3 (s, *p*-Ph), 134.0 (s, *o*-Ph). MS-FAB; m/z 991 ($\text{M}^+ - 2\text{PF}_6$). Anal. Calcd for $\text{C}_{52}\text{H}_{48}\text{P}_6\text{F}_{12}\text{Pt}$ (1281.8): C, 48.72; H, 3.77; found: C, 48.01; H, 3.49; N (DMF), 0.28 %.

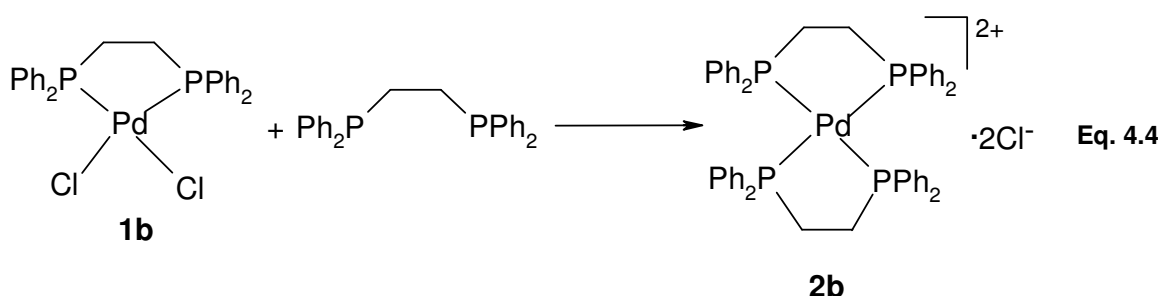
4.2.5 Synthesis of $[PdCl_2(dppe)]$ (**1b**)

This pale yellow compound was synthesised according to a literature procedure (Westland, 1965) (Eq. 4.3). Yield 480 mg (61 %). $^{31}P\{^1H\}$ NMR (DMSO, δ , ppm): 67.5 (s).



4.2.6 Synthesis of $[Pd(dppe)_2]Cl_2$ (**2b**)

1b was treated with 1,2-bis-(diphenylphosphine)ethane (dppe) to yield **2b** according to equation 4.4. Yield: 1.19 g (37 %). $^{31}P\{^1H\}$ NMR (DMSO, δ , ppm): 57.4 (s).



4.2.7 Synthesis of $[Pd(dppe)_2][PF_6]_2$ (**3b**)

3b was prepared following the same procedure used for **3a**. A mixture of NH_4PF_6 (0.29 g, 1.779 mmol) and **2b** (0.88 g, 0.903 mmol) in acetone were stirred for 1 hr. A white compound was obtained after work up as described above (4.2.4).

Yield: 520 mg (48 %). $^{31}P\{^1H\}$ NMR (DMSO, δ , ppm): 58.1 (s), -143.3 (spt, $^1J_{PF} = 711$ Hz, PF_6^-). MS-FAB; m/z 902 ($M^+ - 2PF_6$). Anal. Calcd for $C_{52}H_{48}P_6F_{12}Pd$ (1193.2): C, 52.35; H, 4.06; found: C, 52.09; H, 4.05; N (DMF), 0.12 %.

4.2.8 Synthesis of $[Pt(dppen)_2][PF_6]_2$ (**3c**)

This compound was prepared in the same manner as **3a**. Reaction of $[Pt(dppen)_2]Cl_2$ (0.10 g, 0.094 mmol) and NH_4PF_6 (0.03 g, 0.189 mmol) in acetone (25 ml) yielded a white compound. Yield: 30 mg (25 %). $^{31}P\{^1H\}$ NMR (DMSO, δ , ppm): 60.2 ($^1J_{PtP} = 2350$ Hz), -143 (spt, $^1J_{PF} = 711$ Hz, PF_6). MS-FAB; m/z 989 ($M^+ - 2PF_6$), (FW = 1277).

Alternative route, NH_4PF_6 (0.18 g, 1.310 mmol) was added to a stirring solution of $[PtCl_2(dppen)]$ (**1c**) (0.30 g, 0.547 mmol) in DMF for 24h. The precipitated NH_4Cl was filtered and *cis*-dppen (0.021 g, 0.053 mmol) was added to the remaining pale yellow solution. Yield: 13 mg (19 %).

4.2.9 Synthesis of $[Pd(dppen)_2][PF_6]_2$ (**3d**)

A modified procedure (Oberhauser *et al.*, 1995) was used to prepare this compound. $[PdCl_2(dppen)]$ (0.15 g, 0.326 mmol) and NH_4PF_6 (0.11 g, 0.653 mmol) were suspended in DMF. The orange mixture was stirred for 24 h at room temperature. The formed NH_4Cl was filtered off. *cis*-dppen (0.12 g, 0.295 mmol) was added to the remaining yellow solution and stirred for a further 24 h at room temperature. The solution was concentrated *in vacuo* followed by addition of ether to induce precipitation. The white solid was washed with ether (3 x 5 ml) and dried *in vacuo*.

Yield 180 mg (51 %). $^{31}P\{^1H\}$ NMR (DMSO, δ , ppm): 64.3 (s), -143 (spt, $^1J_{PF} = 711$ Hz, PF_6^-). MS-FAB; m/z 899 ($M^+ - 2PF_6$). Anal. Calcd for $C_{52}H_{44}P_6F_{12}Pd$ (1189.1): C, 52.52; H, 3.73; found: C, 53.37; H, 4.48; N (DMF), 1.57 %.

4.3 Preparation of pyridyl phosphine ligands

4.3.1 Preparation of 1,2-bis-(di-2-pyridylphosphino)ethane (*d2pyrpe*)

A literature procedure was followed in the preparation of this ligand (Bowen *et al.*, 1998). The general procedure is shown in equation 4.5.

pyr), 150.8 (s, CN). *Ips*o-C of pyridyl moiety was not observed. MS-FAB; *m/z* 999 ($M^+ - 2PF_6$). Anal. Calcd for $C_{44}H_{40}N_8P_6F_{12}Pt$ (1289.8): C, 40.98; N, 8.69; H, 3.13; found: C, 39.32; N, 8.45; H, 2.54 %.

4.4.3 Preparation of the $[Pt(d2pyrpe)_2][BPh_4]_2$ (**4e**)

$NaBPh_4$ (0.19 g, 0.560 mmol) was added to a stirred solution of impure $[Pt(d2pyrpe)_2]Cl_2$ (0.30 g, ~0.280 mmol) in CH_2Cl_2 . The mixture was stirred for 12 hrs at room temperature. The formed NaCl was filtered off and the clear yellow solution was removed *in vacuo* to yield a yellow solid. Colourless crystals of **4e** were obtained (at $-5^\circ C$) by dissolving the crude compound in excess dichloromethane and layering with ether.

Yield: 250 mg, (50 %). $^{31}P\{^1H\}$ NMR (DMSO, δ , ppm): 55.7 ($^1J_{PtP} = 2460$ Hz). ^{13}C NMR (DMSO): δ 26.8 (s, bridging CH_2), 121.5 (s, BPh), 125.3 (s, BPh), 126.4 (s, BPh), 130.4 (s, *p*-pyr), 135.5 (s, *o*-pyr), 136.9 (s, *m*-pyr), 150.4 (s, CN), 163.7 [q, *ipso*, $^1J(^{13}C-^{11}B)$ 49.3 Hz]. *Ips*o-C of pyridyl moiety was not observed. MS-FAB, *m/z* 999 ($M^+ - 2BPh_4$). Anal. Calcd for $C_{92}H_{80}N_8P_4B_2Pt$ (1638.3): C, 67.45; N, 6.84; H, 4.92; found: C, 67.69; N, 6.83; H, 4.96 %.

4.4.4 Preparation of $[Pd(d2pyrpe)_2]Cl_2$ (**2f**)

This compound was prepared in a similar manner to the platinum analogue (**2e**). 1,2-bis-(di-2-pyridylphosphino)ethane (d2pyrpe) (0.54 g, 1.342 mmol) was added to a stirred solution of Na_2PdCl_4 (0.20 g, 0.680 mmol) in THF. A pale yellow solid was formed after 1 hr of stirring. After stirring vigorously for 12hrs, the yellow solution was filtered and off white residue was dried *in vacuo*.

Yield (crude): 430 mg (60 %). $^{31}P\{^1H\}$ NMR (DMSO, δ , ppm): 64.0 and $^370.4$.

³ This chemical shift indicates the presence of the *mono*-chelated compound, $[PdCl_2(d2pyrpe)]$.

4.4.5 Preparation of $[Pd(d2pyrpe)_2][PF_6]_2$ (3f)

This compound was prepared as previously described for complexes containing PF_6^- . NH_4PF_6 (0.07 g, 0.429 mmol) was reacted with a crude sample $[Pd(d2pyrpe)_2]Cl_2$ (0.22 g, ~0.224 mmol) in acetone to yield a white solid.

Yield: 100 mg (37%). $^{31}P\{^1H\}$ NMR (DMSO, δ , ppm): 64.0 (s), -143.3 (spt, $^1J_{PF} = 711$ Hz, PF_6^-). ^{13}C NMR (DMSO): δ 25.8 (s, bridging CH_2), 126.5 (m, *p*-Ph), 132.1 (d, *o*-Ph), 137.2 (m, *m*-Ph), 151.0 (m, CN). *Ips*o-C not observed. MS-FAB, *m/z* 910 ($M^+ - 2PF_6^-$). Anal. Calcd for $C_{44}H_{40}N_8P_6F_{12}Pd$ (1201.1): C, 44.00; N, 9.33; H, 3.36; found: C, 44.26; N, 9.32; H, 3.31 %.

4.5 Preparation of 3-pyridyl phosphine complexes

4.5.1 Preparation of $[PtCl_2(d3pyrpe)_2]$ (1g)

1,2-bis-(di-3-pyridylphosphino)ethane (d3pyrpe) (0.24 g, 0.602 mmol) was added to a stirred solution of Na_2PtCl_4 (0.25 g, 0.653 mmol) in THF. A yellow precipitate formed immediately. After stirring for 12 hours at room temperature, filtration was carried out and the yellow residue was dried *in vacuo*.

Yield (crude): 320 mg (82%). $^{31}P\{^1H\}$ NMR (DMSO, δ , ppm): 37.8 ($^1J_{PtP} = 3583$ Hz).

4.5.2 Preparation of $[Pt(d3pyrpe)_2]Cl_2$ (2g)

This compound was prepared by modification of a literature method (Jones *et al.*, 2005). $PtCl_2$ (0.10 g, 0.38 mmol) in CH_3CN (15 ml) was refluxed for 2h to give a yellow solution. The ligand, d3pyrpe (0.30 g, 0.746 mmol) was added to the hot solution to give a yellow precipitate.

Yield: 450 mg (56 %). $^{31}P\{^1H\}$ NMR (DMSO, δ , ppm): 41.4 ($^1J_{PtP} = 2352$ Hz).

4.5.3 Preparation of [Pt(d3pyrpe)₂][PF₆]₂ (3g)

Preparation of this compound was similar to the one described for **3e**. NH₄PF₆ (0.12 g, 0.736 mmol) was added to a stirred solution of [Pt(d3pyrpe)₂]Cl₂ (0.40 g, ~0.374 mmol) in acetone. The white compound contained traces of the unreacted ligand and hence it was triturated with THF to yield a pale yellow solid.

Yield: 130 mg (45 %). ³¹P{¹H} NMR (DMSO, δ, ppm): δ 42.3 (¹J_{PtP} = 2332 Hz), -143 (spt, ¹J_{PF} = 711 Hz, PF₆⁻). Anal. Calcd for [Pt(d3pyrpe)₂][PF₆]₂·4DMF (C₅₆H₆₈N₁₂O₄P₆F₁₂Pt); C, 42.51; N, 10.62; H, 4.33; found: C, 42.46; N, 10.46; H, 4.24 %.

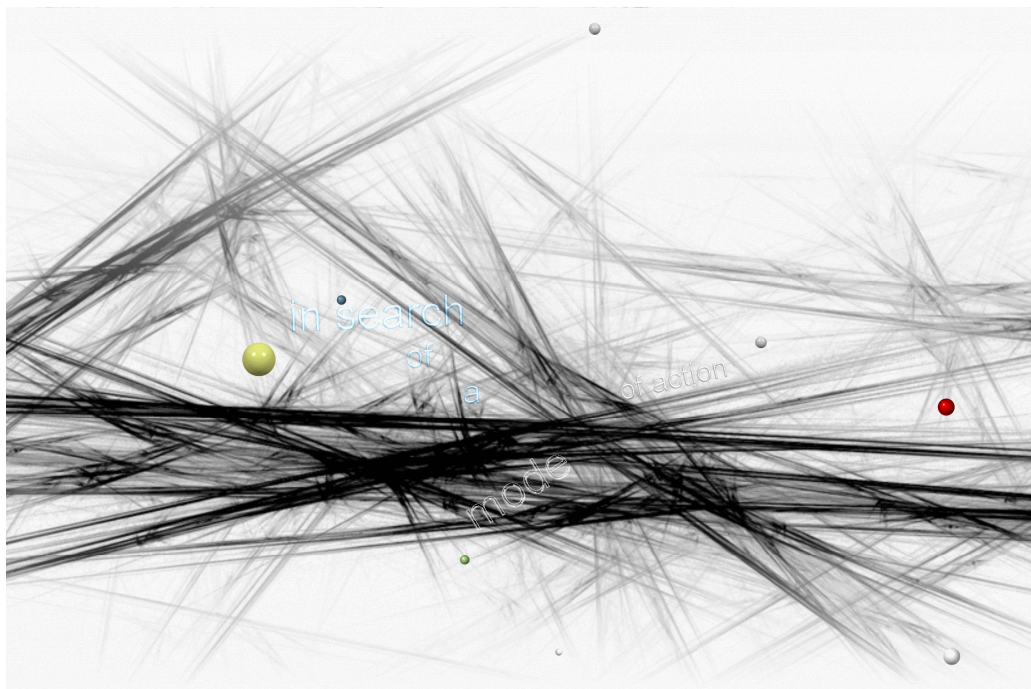
4.5.4 Preparation of [Pt(d3pyrpe)₂][BPh₄]₂ (4g)

AgO₃SCF₃ (0.23 g, 0.898 mmol) was added to a stirred solution of [PtCl₂(d3pyrpe)] (0.30 g, 0.449 mmol) in CH₂Cl₂ (15 ml). The ligand was sparingly soluble in DCM and a pale yellow precipitate was formed after 30 mins of stirring. After 1 h of stirring, the formed AgCl was filtered off. Additional d3pyrpe (0.10 g, 0.251 mmol) was added to the remaining solution. The pale yellow solution changed to light brown in colour on addition of the ligand and this mixture was stirred for 12 hrs at room temperature. NaBPh₄ (0.11 g, 0.309 mmol) was added to the clear yellow solution of impure [Pt(d3pyrpe)₂][CF₃SO₃]₂ (0.20 g, ~0.154 mmol) in CH₂Cl₂. After stirring for 20 minutes, the clear yellow solution became turbid. The mixture was stirred for 12 hrs to yield a clear deep yellow solution and yellow oil. The solvent was removed *in vacuo* to give a mustard coloured compound. This compound was purified from CH₂Cl₂ at -5°C.

Yield: 100 mg (40 %). ³¹P{¹H} NMR (DMSO, δ, ppm): 42.0 (¹J_{PtP} = 2332 Hz). ¹³C NMR (DMSO): δ 30.1 (s, bridging CH₂), 121.4 (s, BPh), 124.3 (s, BPh), 125.2 (s, BPh), 135.5 (s, *p*-pyr), 140.6 (s, *o*-pyr), 153.1 (s, *m*-pyr), 153.8 (s, CN), 163.3 [q, *ipso*, ¹J(¹³C-¹¹B) 49.4 Hz]. *Ipso*-C of pyridyl moiety was not observed. MS-FAB: m/z 999 (M⁺-2BPh₄). Anal. Calcd for [Pt(d3pyrpe)₂][BPh₄]₂·2CH₂Cl₂ (C₉₄H₈₄N₈P₄B₂Cl₄Pt, 1808.17): C, 62.44; N, 6.20; H, 4.68; found: C, 62.54; N, 6.27; H, 5.35 %.

Chapter V

Stability, Lipophilicity and Cytotoxicity



5.1 Stability

Stability requires a working definition tailored to the environmental characteristics important for assessing survival rates (Poole and Poole, 2003). Serum albumin, the most abundant protein in the blood stream (accounting for 60% of total plasma protein), is a major circulatory protein of known structure (Liu *et al.*, 2006). The diversity of chemical functions presented at the surface of the protein has multiple lipophilic binding sites, which may combine with hydrophobic substances like drugs especially neutral and negatively charged lipophilic compounds. Protein-binding plays an important role in pharmacokinetics and pharmacodynamics of the drug, because it affects both the activity of the drug and their disposition.

An important aspect has been to consider the stability of complexes under biologically relevant conditions (Berners-Price *et al.*, 1988). In general for metal complexes, there are likely to be a number of competing ligand exchange reactions that may lead to the breakdown of the complex in the external medium before it enters the cell. An active complex may not be that administered or tested *in vitro*; it may be transformed by ligand substitution and/or redox reactions before it reaches the target site (Berners-Price and Sadler, 1996). The distribution in such media is often impossible to calculate with any degree of certainty because not only are the appropriate thermodynamic and kinetic constants unknown, but the media are complex heterogeneous mixtures of lipid components and aqueous solutions (Bell *et al.*, 1987).

Auranofin (1-thio- β -D-glucopyranose-2,3,4,6-tetraacetato-S) (triethylphosphine) gold(I) is active against intraperitoneally (ip) implanted P388 leukaemia mice (but only when administered ip) and it is inactive in other tumour models (Berners-Price *et al.*, 1990). This restricted range of activity may be related to facile ligand-exchange reactions which auranofin can undergo. In plasma and in cells, the tetraacetyl- β -D-thioglucose is readily displaced by other thiolate ligands, and the phosphine ligand can be released and undergo oxidation to the oxide. In contrast, *bis*-chelated Au(I) phosphine complexes related to $[\text{Au}(\text{dppe})_2]^+$ are active against a spectrum of tumour models in mice (Berners-Price and Sadler, 1996). This

difference is likely to be related to the lower reactivity of the tetrahedral complexes, which can undergo ligand exchange reactions only by the chelate ring opening.

The ligand of $[\text{Au}(\text{dppe})_2]\text{Cl}$, dppe, was shown to have *in vitro* cytotoxic properties in tumour cells and it was suggested that the toxic response was a consequence of the delivery of dppe to the appropriate biological target (Smith *et al.*, 1989). Additionally, this free diphosphine exhibits good anti-tumour activity in a similar range of animal models, but its potency is more than 25-fold lower than the gold complex (Berners-Price and Sadler, 1987b). Unfortunately, this phosphine is easily susceptible to air oxidation (Khokhar *et al.*, 1990). Replacement of the phenyl substituents by ethyls reduced both the cytotoxic potency and activity against P388 leukaemia (Berners-Price *et al.*, 1990). The compound $\text{Et}_2\text{P}(\text{CH}_2)_2\text{PEt}_2$ (depe) exhibits no anti-tumour activity and is relatively non-toxic to mice. This can be rationalised by the ease with which it (depe) undergoes oxidation in aqueous media in comparison with phenyl-substituted diphosphines, which in turn is related to the difference in autoxidation pathways for alkyls and aryl phosphines.

5.2 Nuclear Magnetic Resonance Spectroscopy (NMR)

NMR spectroscopy is a powerful method for investigating the speciation of metal complexes in solution and to a lesser extent in the solid state (Berners-Price and Sadler, 1996). Spin- $\frac{1}{2}$ nuclei offer the most potential for the study of metallodrugs. ^1H NMR spectroscopy will continue to be the most widely used for investigating ligand behaviour and ^{31}P (100% abundance) with high sensitivity is invaluable for studies of metal phosphine drugs. ^{31}P NMR has shown that $[\text{Au}(\text{dppe})_2]^+$ (unlike auranofin) remains essentially intact in human plasma and does not react significantly with glutathione or albumin. The results obtained suggest that the complex could be transported in plasma and transferred intact through membranes.

Recent ^{31}P NMR studies of tetrahedral bisphosphine Au(I) complexes with pyridyl substituents (R and R' are 2-pyridyl, 4-pyridyl) have also shown that these are

stable for at least 30 h when incubated in blood plasma at 37 °C (Berners-Price and Sadler, 1996). They are also kinetically stable and undergo slow exchange in the presence of a sodium salt of β -D-thioglucose. However, it must be noted that the concentrations of the complex employed in the studies are more than 100 times those of physiological relevance (Berners-Price and Sadler, 1987b). This was necessary on account of the relative insensitivity of NMR techniques.

5.3 Evaluation of stability of the test compounds by ^{31}P NMR spectroscopy.

In biological assays, DMSO, ethanol or H_2O are the solvents most commonly used to dissolve compounds and cell culture medium (supplemented with 10% foetal calf serum) is used to dilute the stock solution. *In vitro* assays involve incubation of cells with the compounds for a varied period of time (hours to days). The aim of carrying out these tests was to determine the stability of the test compounds before carrying out any biological work. ^{31}P NMR spectra of all the compounds contained one phosphorus peak and hence appearance of other (new) peaks was used to track any chemical changes.

5.4 Materials and methods

5.4.1 Reagents and compounds

- Analytical grade dimethylsulphoxide (DMSO)-Acros Organics-Belgium
- Deuterated DMSO- d_6 —Sigma Aldrich (Germany)
- Cell culture medium (EMEM supplemented with 10% foetal calf serum)
- Impure sample of $[\text{Pt}(\text{d}2\text{pyrpe})_2]\text{Cl}_2$
- Test compounds (7) i.e, $[\text{Pt}(\text{dppe})_2][\text{PF}_6]_2$ (**Pg 1**), $[\text{Pd}(\text{dppe})_2][\text{PF}_6]_2$ (**Pg 3**), $[\text{Pd}(\text{dppen})_2][\text{PF}_6]_2$ (**Pg 4a**), $[\text{Pt}(\text{d}2\text{pyrpe})_2][\text{PF}_6]_2$ (**Pg 5**), $[\text{Pt}(\text{d}3\text{pyrpe})_2][\text{PF}_6]_2$ (**Pg 6**), $[\text{Pd}(\text{d}2\text{pyrpe})_2][\text{PF}_6]_2$ (**Pg 8**) and $[\text{Au}(\text{dppe})_2]\text{Cl}$

5.4.2 General experimental procedure

Small amounts (~6 mg) of the test compounds were dissolved in DMSO, DMSO- d_6 and/or cell culture medium (EMEM). Immediate analysis with a NMR Bruker 300 spectrophotometer (121.5 MHz) was carried out. The samples were analysed at 0 h, 24 h and 7 days with incubation at 37°C between analyses.

5.5 Results

The first complex to be tested was an impure sample of $[Pt(d2pyrpe)_2]Cl_2$. Purification of this compound was unsuccessful due to decomposition and this precluded the synthesis of additional compounds with Cl^- as counterion. The crude sample which was a mixture of $[PtCl_2(d2pyrpe)]$ and $[Pt(d2pyrpe)_2]Cl_2$ (Fig 5.1) was treated as described in the general procedure.

Figure 5.1 shows the structures of the compounds in the impure sample while **Table 5.1** shows the ^{31}P chemical shifts changes.

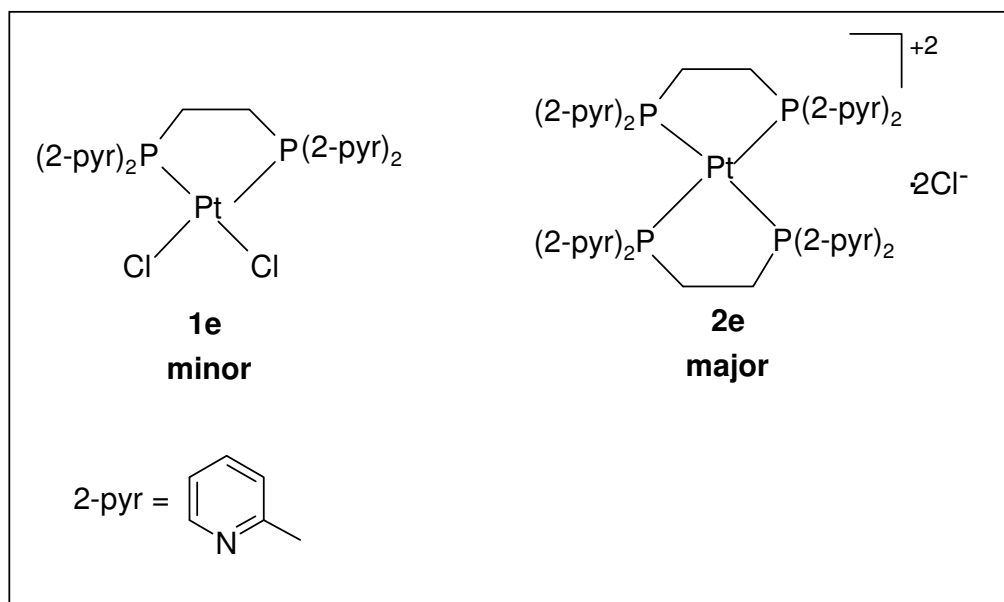


Figure 5.1: Mixture of $[PtCl_2(d2pyrpe)]$ (**1e**) and $[Pt(d2pyrpe)_2]Cl_2$ (**2e**)

Table 5.1: $^{31}\text{P}\{^1\text{H}\}$ NMR chemical shift changes of the mixture containing compound **1e** and **2e**

	DMSO	EMEM
0h	*55.1	55.1
	#47.6	47.6
24h	47.6	47.6
7 days	47.6	55.1**
		47.6**

*Major compound, $[\text{Pt}(\text{d}2\text{pyrpe})_2]\text{Cl}_2$

Minor compound, $[\text{PtCl}_2(\text{d}2\text{pyrpe})]$

** Equal intensity

Figures 5.2-5.4 depict the changes that occurred as seen from actual NMR spectra (DMSO) and 5.5-5.7 (EMEM).

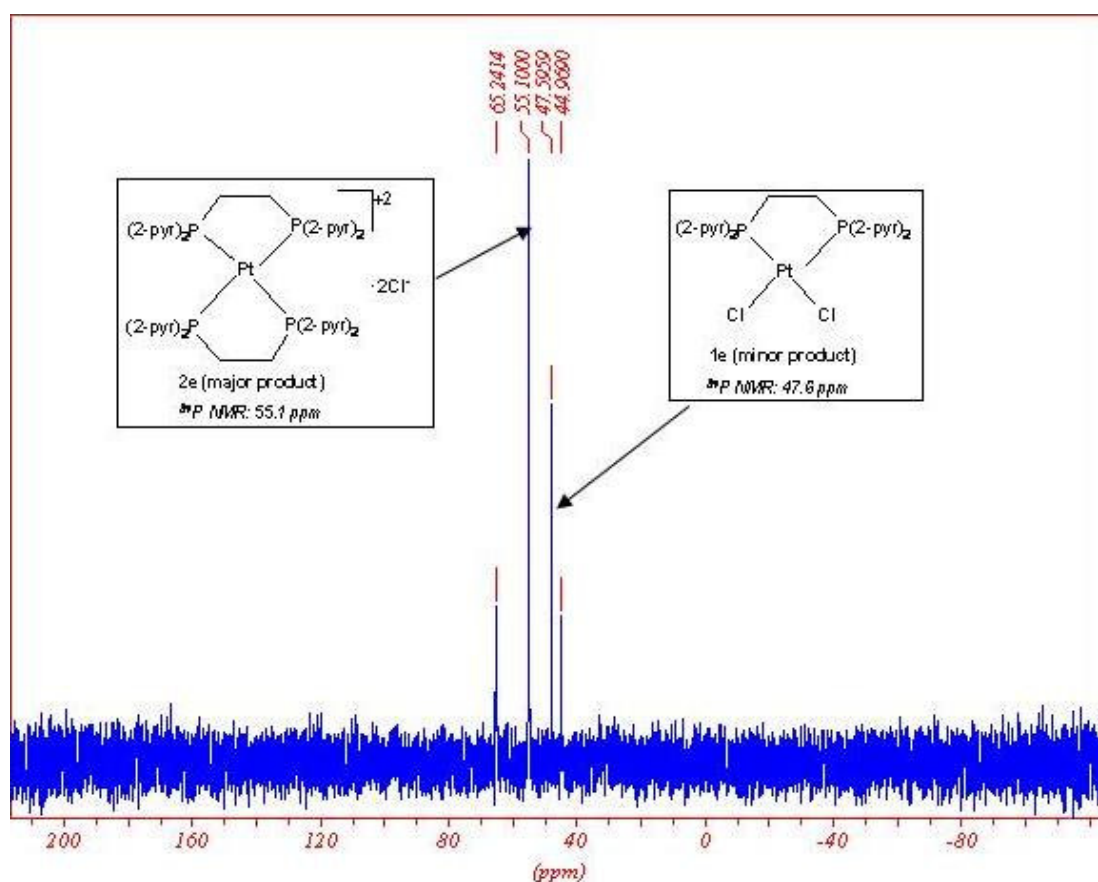


Fig 5.2: $^{31}\text{P}\{^1\text{H}\}$ NMR spectrum of the mixture at 0h in DMSO

The desired compound $[\text{Pt}(\text{d}2\text{pyrpe})_2]\text{Cl}_2$ (**2e**) was not stable (*Table 5.1 and Figures 5.2-5.4*). At the beginning of the experiment, **2e** was the major complex in the mixture but it was replaced by the *mono*-chelated species, $[\text{PtCl}_2(\text{d}2\text{pyrpe})]$ (**1c**) after 24h incubation in DMSO (*Fig 5.3*). These analyses demonstrated that purification of the compound was hindered by instability.

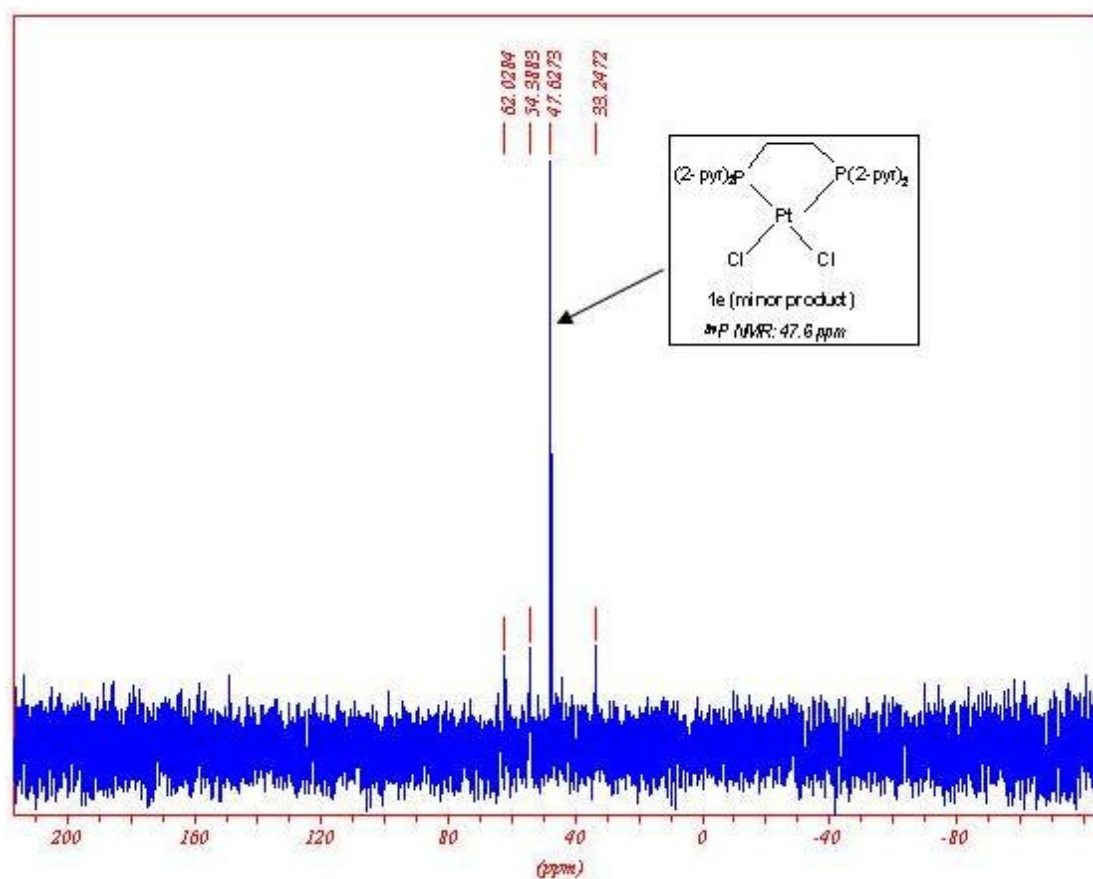


Fig 5.3: $^{31}\text{P}\{^1\text{H}\}$ NMR spectrum of the mixture after 24 h in DMSO

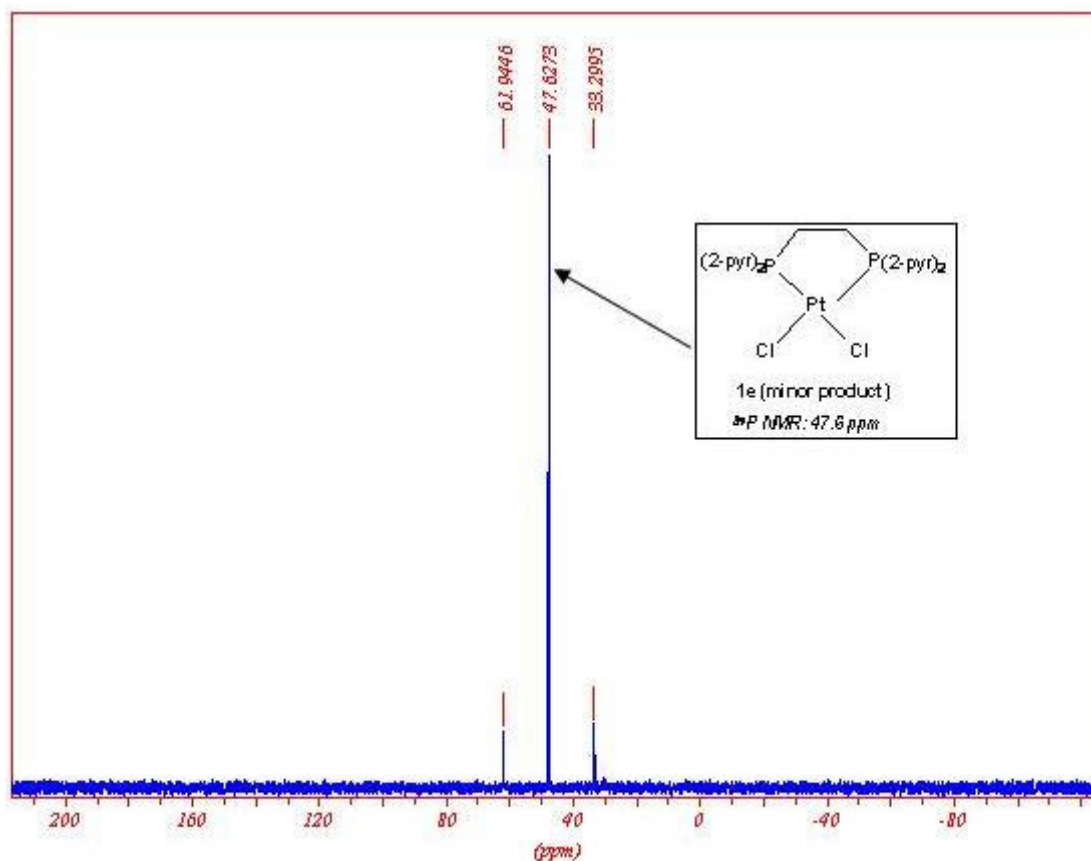


Fig 5.4: $^{31}\text{P}\{^1\text{H}\}$ NMR spectrum of the mixture after 7 days in DMSO

The sample in DMSO exhibited different behaviour from that dissolved in cell culture medium (*Table 5.1* and *Figures 5.5-5.7*). In DMSO, the mixture was converted to the *mono*-chelated complex **1e** and remained the same up to day 7. In contrast, the *mono*-chelated species (**1e**) (*Fig 5.6*) was converted back to the *bis*-chelated complex (**2e**) by day 7 (*Fig 5.7*). This last spectrum shows the two compounds existing in equal amounts at the end of the study.

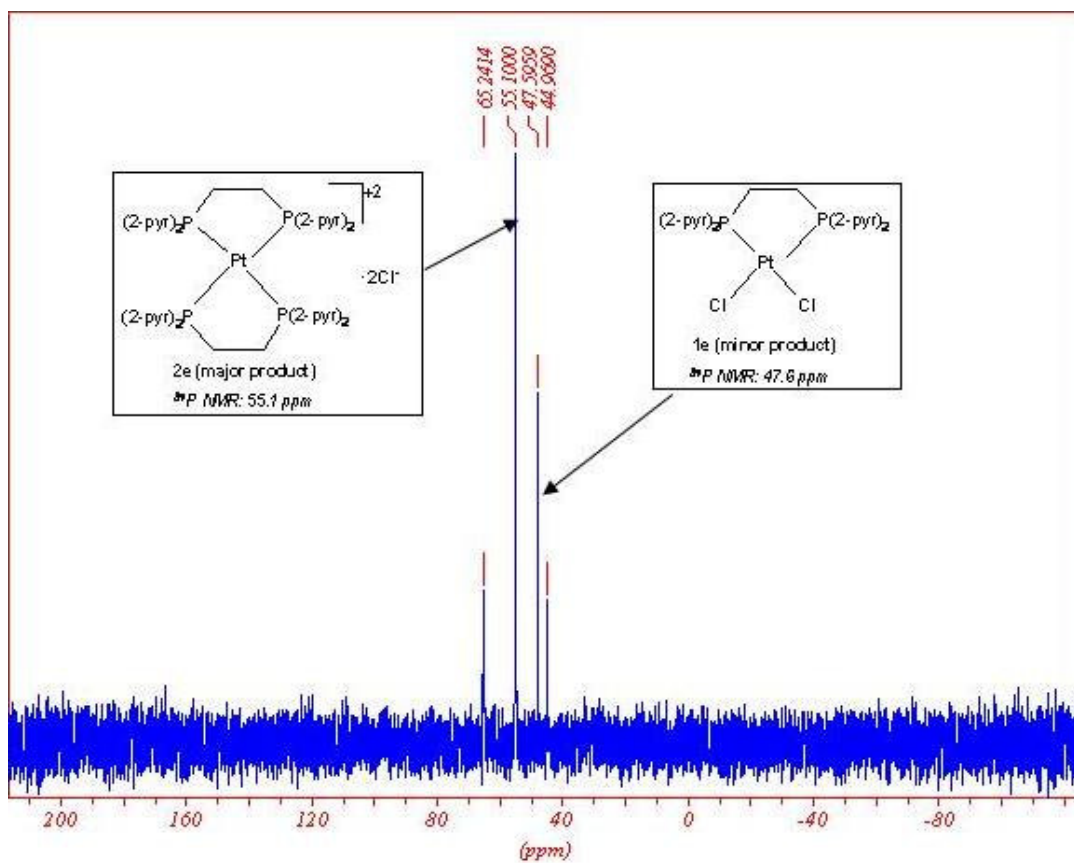


Fig 5.5: $^{31}\text{P}\{^1\text{H}\}$ NMR spectrum of the mixture at 0 h in EMEM

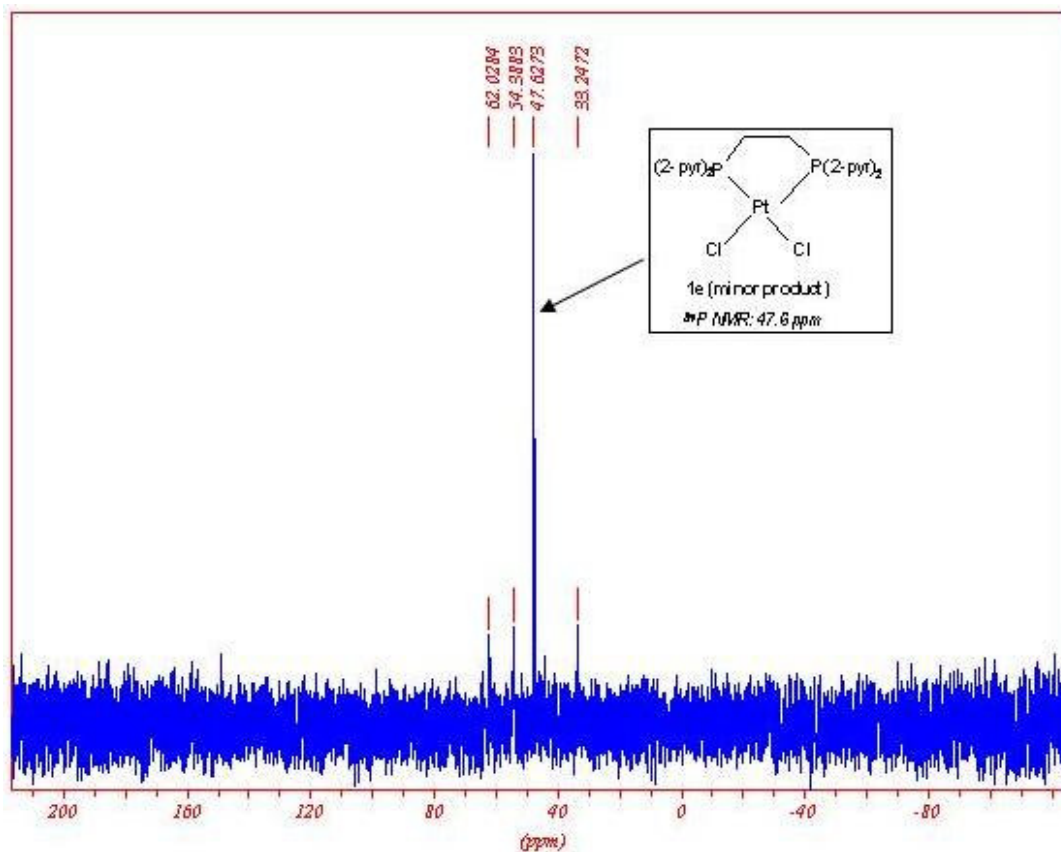


Fig 5.6: $^{31}\text{P}\{^1\text{H}\}$ NMR spectrum of the mixture after 24 h in EMEM

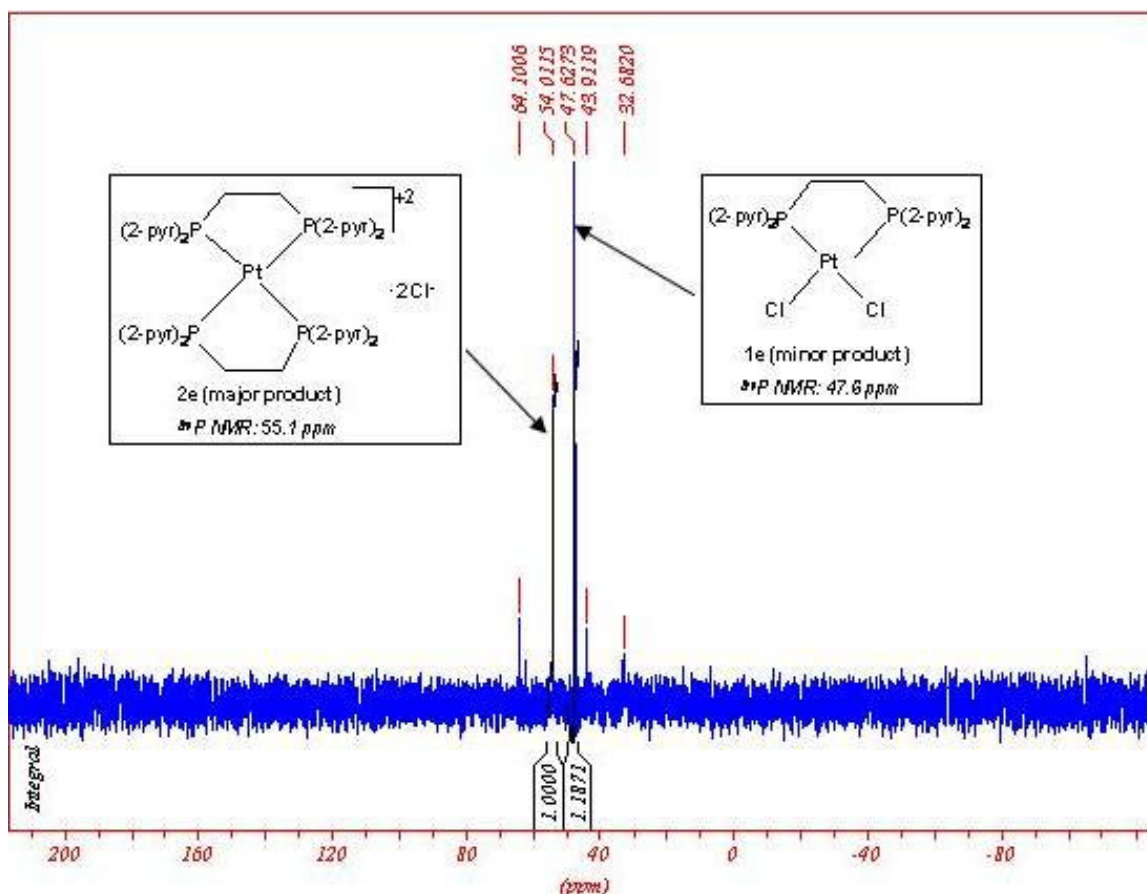


Fig 5.7: $^{31}\text{P}\{^1\text{H}\}$ NMR spectrum of the mixture after 7 days in EMEM

These stability tests validated the fact that the compounds with Cl^- as the counterion were labile and hence unsuitable for any biological work. Failure in purifying the compounds was also clarified by these tests. Replacement of the chlorides with BPh_4^- and/or PF_6^- led to stable and pure complexes. One of the complexes, $[\text{Pt}(\text{d}2\text{pyrpe})_2][\text{BPh}_4]_2$ precipitated out in the presence of cell culture media and showed no toxicity against cells. This precluded the synthesis of similar compounds as possible candidates for anti-cancer application.

The compounds discussed in Chapters 3 and 4 were investigated for stability as described above. The results from ^{31}P NMR spectroscopy for the seven (7) compounds are tabulated below (Table 5.2).

Table 5.2: $^{31}\text{P}\{^1\text{H}\}$ NMR chemical shifts (ppm) of test compounds in DMSO and/or EMEM

Compound	Chemical shift (0 h)		Chemical shift (24 h)		Chemical shift (7 days)	
	DMSO	EMEM	DMSO	EMEM	DMSO	EMEM
Pg 1	49.4	49.3	49.4	49.6	49.4	No peak
Pg 3	58.1	58.0	58.1	58.1	58.1	36.8
Pg 4a	65.1	67.4	65.1	68.4 20.9	65.1	20.9
Pg 5	55.8	55.8	55.8	54.8	55.8	54.9 33.2
Pg 6	42.0	42.0	42.0	41.6 37.8	42.0	41.5 36.6 31.2
Pg 8	64.0	62.9	64.0	29.5	64.0	29.5
[Au(dppe)₂]⁺	22.5	No peak	22.5	No peak	22.5	No peak

All the compounds were soluble in DMSO and no precipitation occurred throughout the experiment. In contrast, precipitation (negligible) of the test compounds occurred in the presence of cell culture medium (EMEM). Table 5.2 shows that the compounds dissolved in DMSO were stable throughout the experiment as the chemical shifts remained the same. The EMEM fraction exhibited large chemical shift changes during the course of the experiment (0h-7 days).

The platinum complexes (**Pg 5** and **Pg 6**) contained extra peaks at the end of the experiment but the original peaks were still present. In contrast, new peaks completely replaced the original peaks in the palladium complexes (**Pg 3**, **Pg 4a** and **Pg 8**). The new peaks (range of 20.9-36.8 ppm) can be attributed to oxidation products of the phosphine ligands in cell culture media. Autoxidation studies carried out on the ligand, dppe, showed that 65% of the ligand had oxidised ($^{31}\text{P} = 32.8$ ppm) after standing in CDCl_3 (deuterated chloroform) for 5 days (Berners-Price *et al.*, 1987a). Diphosphine dioxide with ^{31}P NMR chemical shifts of 31.2

and 38.5 (in methanol and dimethylacetamide, respectively) were observed. *cis*-dppen was the most stable diphosphine studied, no appreciable oxidation was observed after 2 days in CDCl_3 , DMA or methanol.

The ^{31}P NMR signal for $[\text{Au}(\text{dppe})_2]\text{Cl}$ in our studies could not be observed due to broadening of the peak. This could be as a result of a number of factors: for example, an exchange process with another species for which the ^{31}P resonance is too broad or too low in intensity to be resolved (Berners-Price and Sadler, 1987b). Studies of the above compound in plasma concluded that broadening could arise from an inhomogeneous distribution of the complex (within the plasma), chemical shift anisotropy, or a relative (on the NMR time scale) immobilisation of the complex through binding interactions. These could involve ion-pairing between the $[\text{Au}(\text{dppe})_2]^+$ cation and negatively charged plasma components, or hydrophobic interactions involving the phenyl rings and lipophilic components of the plasma. In studies where cisplatin was incubated with Dulbecco's cell culture medium, the singlet for the S-methyl of L-methionine in the medium disappears and a new peak characteristic of Pt-bound L-Met appears (Berners-Price and Sadler, 1996).

5.6 Lipophilicity

Lipophilicity expressed as a ratio of octanol solubility to aqueous solubility appears in some form in almost every analysis of physico-chemical properties related to absorption (Lipinski *et al.*, 1997). If a third substance is added to a system of two immiscible liquids in equilibrium, the added component will distribute itself between the two liquid phases until the ratio of its concentrations in each phase attains a certain value: the distribution constant or partition coefficient (Berthod and Carda-Broch, 2004). Chemists and pharmacologists began to take an interest in partition coefficients at the turn of the 20th century (Albert, 1979). Their stimulus was the positive correlation that Overton and Meyer (1899) had demonstrated between the bio-depressant (e.g. hypnotic) action of many chemically unrelated substances, and their preference for the lipid layer when partitioned between olive oil and water.

Combinatorial chemistry is able to produce large numbers of new compounds that could be potential drugs (Berthod and Carda-Broch, 2004). A drug has to cross four barriers associated with absorption, distribution, metabolism and excretion referred to ADME interface. The core properties required to estimate absorption, distribution, and transport in biological systems are solubility, stability, and acid-base character (Poole and Poole, 2003). These properties are used directly or through structure-activity relationships to help design active compounds and determine toxicity and membrane permeation. The 1-octanol-water partition coefficient ($\log P$) is widely used in quantitative structure-activity relationships/quantitative structure-property relationship (QSAR/QSPR) approaches (Molnár *et al.*, 2004).

5.6.1 Relationship between lipophilicity and activity

Octanol/water partitioning has been shown to correlate with serum protein binding and is also suited for modelling lipophilic interactions with membranes that have high amounts of proteins incorporated (Hartmann and Schmitt, 2004). Lipophilicity can be an important determinant of activity because passive uptake across the lipid bilayer making up the cell membrane is facilitated by higher lipophilicity (Hambley, 1997). The biodistribution, protein binding, and metabolism of drugs may be altered by their lipophilicity (Poole and Poole, 2003). It is generally held that lipophilic compounds are preferred targets for metabolism, often leading to high clearance rates and frequently, lipophilicity correlates positively with a high protein binding. Changes in drug lipophilicity appear to alter host toxicity associated with non-specific binding and renal drug elimination (McKeage *et al.*, 2000). Compounds that can be delivered at high doses are expected to prove more active because of the dependence of activity on tumour drug concentration *in vitro* and *in vivo* models.

One of the most reliable methods in medicinal chemistry to improve *in vitro* activity is to incorporate properly positioned lipophilic groups (Lipinski *et al.*, 1997). The hydrophilic character of metal ions can be changed by conjugation with organic compounds (Zimmermann *et al.*, 2003). This process is often found in nature to enhance or impede the transfers of metals through the cell membrane. The use of

aromatic cations (also known as lipophilic cations) as anti-cancer agents has had a long history (McKeage *et al.*, 2000). Strongly positively charged terephthalanilide derivatives were developed for clinical trials over 30 years ago, but were abandoned because of toxicity. Bisquaternary derivatives of the above compound were synthesised in an approach to controlling drug lipophilicity and many showed excellent activity against the transplantable L1210 leukaemia in mice.

5.7 Aim of the experiment

The experiment described below aimed at determining lipophilicity (Log *P*) of each compound and correlating it to cytotoxicity and selectivity.

5.8 Materials and methods

5.8.1 Reagents and compounds

- Analytical grade *n*-octanol (Sigma-Aldrich, Germany)
- Distilled water
- Test compounds (7) i.e, [Pt(dppe)₂][PF₆]₂ (**Pg 1**), [Pd(dppe)₂][PF₆]₂ (**Pg 3**), [Pd(dppen)₂][PF₆]₂ (**Pg 4a**), [Pt(d2pyrpe)₂][PF₆]₂ (**Pg 5**), [Pt(d3pyrpe)₂][PF₆]₂ (**Pg 6**), [Pd(d2pyrpe)₂][PF₆]₂ (**Pg 8**) and [Au(dppe)₂]Cl

5.8.2 General procedure for determination of lipophilicity

A volume of water-saturated octanol and a volume of octanol-saturated water were prepared by shaking equal volumes of octanol and water for 15 min and then allowing the layers to separate overnight in a separating funnel (Bowen, 1999). The two fractions were collected separately being careful not to allow cross contamination of one solvent layer onto the other. Hereafter, the octanol will refer to distilled water-saturated octanol and water will refer to as octanol-saturated distilled water. 60 μM octanol stock solutions of the complexes were prepared followed by preparation of 40 μM and 20 μM solutions by further dilution with octanol, so that the final volumes were 5 ml.

Each of these solutions was analysed separately by U.V-visible spectroscopy to give an absorbance maxima at a wavelength *ca* 251 and 298 nm. This absorbance corresponded to the C_i value (initial concentration) for each solution. 5 ml of water was added to each of these solutions to make up a final volume of 10 ml. Each of the solutions was shaken vigorously and then independently transferred to separating funnels. Separation of the aqueous extract from the octanol took place after the two phases settled over periods between 30 min to 15 hours. Analysis of this extract by UV-visible spectroscopy gave absorbance maxima at a wavelength identified from the C_i determination. This absorbance corresponded to C_w (concentration in water) value for each solution. C_i - C_w established the concentration of each complex remaining in the octanol layer, C_o . Partition coefficient ($\log P$) defined as the logarithmic ratio of compound concentrations in the organic and aqueous phases ($\log C_o/C_w$) (McKeage *et al.*, 2000) was then calculated.

5.8.3 Statistical analysis

The experiment was performed three times and results (Fig 5.8) are an average of triplicate values (\pm SEM).

5.9 Results and discussion

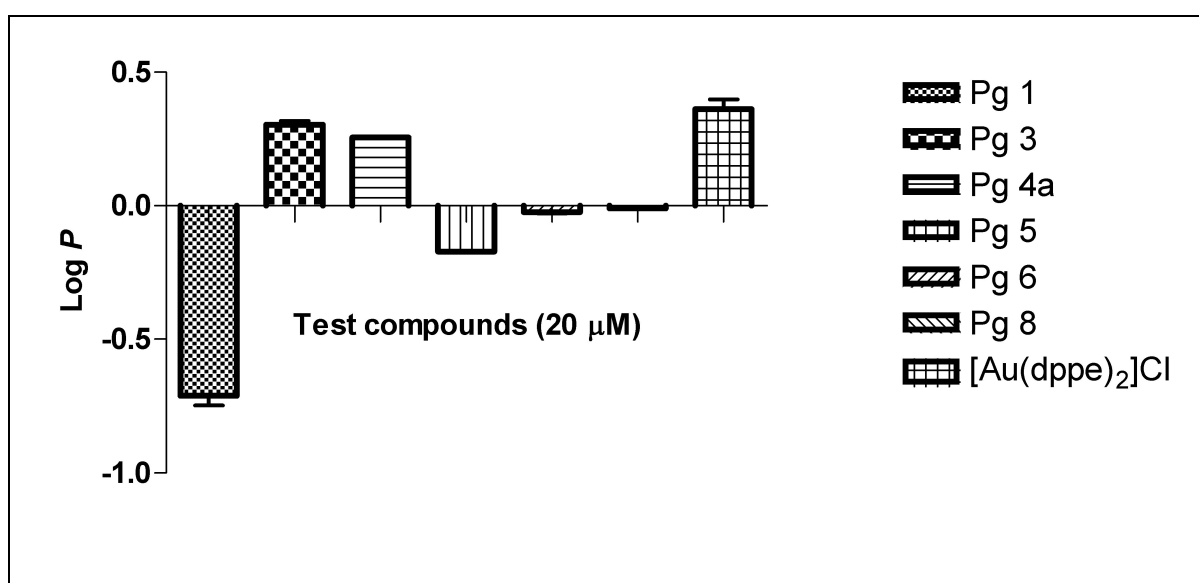


Fig 5.8: Log P values of the test compounds at 20 μ M. Positive values indicate more lipophilic character while negative values point towards less lipophilic character.

With the exception of **Pg 1**, all the complexes with phenyl groups, **Pg 3**, **Pg 4a** and $[\text{Au}(\text{dppe})_2]\text{Cl}$ showed lipophilic character (positive values). $[\text{Au}(\text{dppe})_2]\text{Cl}$ showed the greatest lipophilic character ($\log P = 0.362$) followed by **Pg 3a** ($\log P = 0.303$) and **Pg 4a** ($\log P = 0.256$). As expected, complexes with pyridyl groups (**Pg 5**, **Pg 6**, **Pg 8**) had negative $\log P$ values, indicating less lipophilic character (more hydrophilicity). The platinum pyridyl complexes **Pg 5** and **Pg 6** (which differ by the position of the N in the pyridyl ring) showed hydrophilic character with the former being more hydrophilic ($\text{Log } P = -0.172$) than the latter ($\text{Log } P = -0.024$). The degree of hydrophilicity depends critically on the presence of the pyridyl ligand and on the position of the N atom (McKeage *et al.*, 2000).

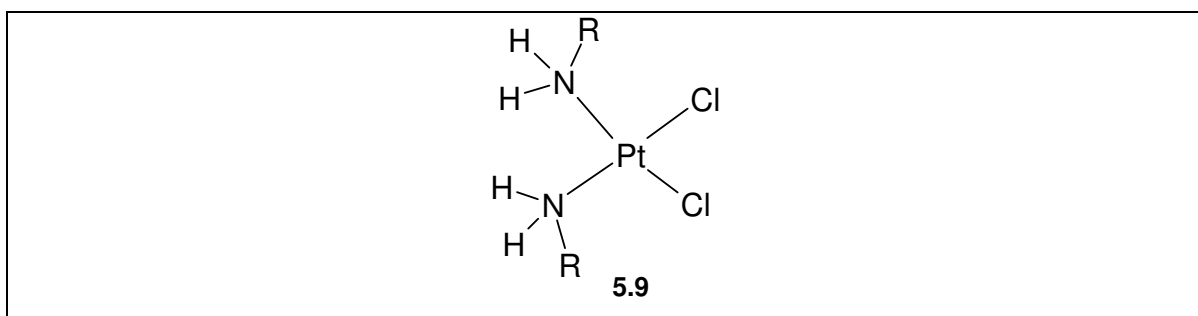
Practical considerations are important in the determination of octanol-water partition coefficients using the above procedure (Poole and Poole, 2003).

- Complete separation of the layers is important as any droplets of octanol in the aqueous phase may contain large amounts of sample;
- Pre-saturation of the two phases is required;
- The sample concentration must be less than the critical micelle concentration;
- Measurements need to be carried out at concentrations below the aqueous solubility limit and;
- Lipophilic basic compounds may adsorb onto surface of the apparatus.

The unexpected results from **Pg 1** ($\log P = -0.710$) may have been as a result of an interface that formed between octanol and water. There is a possibility that some of the precipitated compound was collected into the water phase during separation. At $60 \mu\text{M}$, it had a $\log P$ value of 0.222 which indicated that a larger portion of the compound partitioned into the octanol phase at higher concentration. This trend was seen in the standard, $[\text{Au}(\text{dppe})_2]\text{Cl}$ which had a $\log P$ value of 1.036 at $60 \mu\text{M}$ vs 0.362 at $20 \mu\text{M}$. Future developments will probably include less dependence on $\text{Log } P$ as a single descriptor for property estimations in favour of a suite of models tailored to individual distribution and transport properties based on the solvation parameter model (Poole and Poole, 2003).

5.10 Cytotoxicity

Understanding both the thermodynamics and kinetics of metal speciation is crucial to the advancement of inorganic molecular pharmacology (Berners-Price and Sadler, 1996) and the establishment of structure-activity relationships is an important part of the drug design process. One of the biggest challenges lies in the control of the toxicities of metal compounds and hence understanding the species which are responsible. The roles played by the intact metal complex itself and either the metal or its ligands separately must be considered. In a series of Pt(II) and Pt(IV) complexes with *cis* chloro and *cis* substituted amine ligands, the role of solubility and lipophilicity was considered in relation to toxicity (Hambley, 1997). For complex 5.9, it emerged that equal solubility in water and lipids correlated with minimum toxicity and maximum therapeutic index but maximum activity was observed with maximum solubility.



The ongoing challenge of this work has been to find a molecule with suitable pharmacological properties-high solubility, high stability, low toxicity and favourable pharmacokinetics-for use in humans (Don and Hogg, 2004).

[Au(d2pyrpe)₂] was shown to be toxic to B16 melanoma while its analogue [Au(d4pyrpe)₂]Cl was inactive (Berners-Price *et al.*, 1990). Additional experiments on human blood confirmed that the 2-pyridyl complex readily partitioned between plasma and red cells while the 4-pyridyl complex was retained in the blood plasma fraction (Berners-Price and Sadler, 1996).

5.11 Determination of cytotoxicity

Cytotoxicity assays were performed on cell cultures to evaluate the level of sensitivity of cancer cells and normal healthy cells to the experimental compounds. The aim of this assay was to correlate cytotoxicity to structure (metal or ligand) as well as lipophilicity. Additionally, it was used to select the most potent and selective compound(s) for further biological assays.

5.12 Materials and methods

5.12.1 Reagents and compounds

- Supplemented cell culture medium – Cell culture medium with 10% foetal calf serum (FCS).
- Phosphate buffered saline (PBS).
- DMSO (Sigma-Aldrich, Germany)
- MTT [3-(4,5-dimethylthiazol-2-yl)-2,5-diphenyl tetrazolium bromide] (Sigma Diagnostics Inc)
- Phytohaemagglutinin (PHA)
- Test compounds (7) - dissolved in DMSO (20 mM) and diluted in cell culture medium.

5.12.2 Cell lines and culture

Various human and murine cancer cell lines (sources are indicated in parentheses) were grown as monolayer cultures at 37 °C in 5% CO₂ in appropriate tissue culture medium (indicated in parentheses) supplemented with 10% v/v heat-inactivated serum (FCS) and 1% penicillin-streptomycin.

The following cancerous cell lines were used:

- HeLa- human adenocarcinoma of the cervix (ATCC) (EMEM)
- A2780- human ovarian cancer (EACC) (RPMI)
- A2780-cis- human ovarian cancer-cisplatin resistant (EACC) (RPMI)
- MCF-7- human breast cancer (ATCC) (DMEM)

- CoLo 320 DM- human colon cancer (ATCC) (RPMI)
- DU 145- human prostate cancer (ATCC) (RPMI)
- Jurkat- human T-cell line (NRBM) (RPMI)
- Novikoff- rat hepatocellular cancer (DKFZ) (RPMI)
- B16- mouse melanoma (ATCC) (RPMI)

Normal cells included:

- Human lymphocytes (resting and PHA stimulated)- fresh venous blood was obtained from healthy volunteers followed by isolation of lymphocytes (Anderson *et al.*, 1993).
- Chicken embryo fibroblasts- cells were isolated from chicken embryos (Freshney, 2005).
- Porcine hepatocytes- obtained from the Bio-artificial liver project under the supervision of Dr S. van der Merwe, Department of Internal Medicine, University of Pretoria (Fruhauf *et al.*, 2004).

5.12.3 Sample preparation

All the complexes were dissolved in DMSO to give a stock concentration of 20 mM (stored at -70 °C). Immediately before the cell experiments, the stock solution was diluted in appropriate growth medium (containing 10% FCS) to give final DMSO concentrations not exceeding 0.5% and drug concentrations of 0.003-100 µM.

5.13 General procedure

The assays were performed using a metabolic assay based on the reactivity of MTT [3-(4,5-dimethylthiazol-2-yl)-2,5-diphenyl tetrazolium bromide] (Mosmann, 1983; Meyer *et al.*, 2005). MTT is a pale yellow substance that is metabolised to dark blue formazan crystals by metabolically active cells. The amount of formazan produced is directly proportional to the amount of cells over a wide range.

80 µl of medium (60 µl in the case of the lymphocytes earmarked to be stimulated) was dispensed into each well of a 96 well tissue culture plate (micro-titer plate).

100 μ l of cell suspension (2×10^4 – 2×10^6 cells/ml/well depending on the cell type) was added and then allowed to incubate for 1 hour at 37°C in an atmosphere of 5% CO₂. 20 μ l of the experimental drug (eight varying concentrations) was added in triplicate to the wells. However, control wells received 20 μ l of growth medium instead of the experimental drug. Lymphocytes earmarked to be stimulated received 20 μ l PHA 5 minutes after the addition of the drug.

After the incubation period (3 and 7 days for lymphocytes and cancerous cells respectively), 20 μ l MTT (5 mg/ml) was added to each well and cultures were incubated for 4 hours. Cells were then centrifuged for 10 min at 2000 rpm (800 g) (Beckman TJ 6 centrifuge) and the supernatant removed without disturbing the pellet. The cells were washed with 150 μ l PBS (per well) and centrifuged for 10 min at 2000 rpm (800 g) (Beckman TJ 6 centrifuge). The supernatant was removed and plates were left to dry in the dark. 100 μ l DMSO was added to each well to solubilise the formazan crystals and the plates were shaken for 2-4 hours. Culture plates were read on a plate reader using a wavelength of 570 nm and a reference wavelength of 630 nm.

5.14 Statistical analysis

Percentage survival (percentage of the relevant untreated control systems) was calculated and this value was used to determine the IC₅₀ value (IC₅₀ = the concentration (μ M) of the experimental compound inducing a 50% decrease in cell growth).

5.15 Results and discussion

Table 5.3: IC₅₀ values (μM) and S.E.M (±) of 7 compounds on various cancer cell lines as well as normal cells. The values are presented as a mean of three experiments carried out in triplicate.

	Pg 1	Pg 3	Pg 4a	Pg 5	Pg 6	Pg 8	[Au(dppe) ₂]Cl
Hela	> 50	4.985 ± 0.367	5.467 ± 0.505	> 50	> 50	0.638 ± 0.054	0.288 ± 0.009
A2780	> 50	0.707 ± 0.053	0.147 ± 0.015	6.119 ± 0.283	17.501 ± 2.909	0.974 ± 0.203	0.011
A2780-cis	> 50	> 50	5.054 ± 0.703	> 50	> 50	2.029 ± 0.273	0.494 ± 0.043
MCF-7	> 50	18.087 ± 3.059	2.873 ± 0.235	> 50	> 50	2.520 ± 0.219	0.585 ± 0.010
Jurkat	> 50	3.598 ± 0.569	1.445 ± 0.130	37.704 ± 1.808	> 50	0.711 ± 0.005	0.131 ± 0.012
CoLo	> 50	13.257 ± 0.224	5.341 ± 0.374	13.803 ± 1.225	19.590 ± 1.172	1.723 ± 0.021	0.914 ± 0.028
DU145	1.350 ± 0.315	0.253 ± 0.024	0.299 ± 0.001	2.485 ± 0.087	9.380 ± 0.448	0.541 ± 0.046	0.007 ± 0.002
Resting lymphocytes	> 100	> 100	> 100	> 100	> 100	> 100	0.903 ± 0.041
Stimulated lymphocytes	> 100	> 100	> 100	> 100	> 100	> 100	0.182 ± 0.032

In general, the platinum complexes were less toxic than the palladium ones with **Pg 1** being the least toxic compound followed by **Pg 6** and **Pg 5** (*Table 5.3*). **Pg 8** was the most toxic of the palladium complexes followed by **Pg 4a** and **Pg 3**. With regard to all the novel complexes, prostate cancer (DU-145) was the most sensitive cell line (IC₅₀ values of 0.253-9.380 μM) while ovarian cancer-cisplatin resistant cell line (A2780-cis) was the most resistant (IC₅₀ values of 2.029-> 50 μM). Human ovarian cancer cell line- cisplatin sensitive (A2780) was sensitive to all the palladium complexes with IC₅₀ values of 0.617 μM (**Pg 3**), 0.136 μM (**Pg 4a**) and 0.974 μM (**Pg 8**). Overall, **Pg 8** was the most toxic (over the whole range of cells) of the novel compounds followed by **Pg 4a** which showed comparative activity against Jurkat and MCF-7 cell lines.

[Au(dppe)₂]Cl was more toxic than the novel compounds (*Table 5.3*). However, it exhibited non-selectivity as it was also toxic to both resting (IC₅₀ = 0.903 μM) and

stimulated lymphocytes ($IC_{50} = 0.182 \mu\text{M}$) while the experimental compounds were not toxic even at a concentration of $100 \mu\text{M}$.

Table 5.4: Cytotoxicity data of test compounds tabulated in order of increasing lipophilicity

Compound and Log P	Pg 5 -0.172	Pg 6 -0.024	Pg 8 -0.009	Pg 4a 0.256	Pg 3 0.303	[Au(dppe) ₂]Cl 0.362
Hela	> 50	> 50	0.638 ± 0.054	5.467 ± 0.505	4.985 ± 0.367	0.288 ± 0.009
A2780	6.119 ± 0.283	17.501 ± 2.909	0.974 ± 0.203	0.147 ± 0.015	0.707 ± 0.053	0.011
A2780-cis	> 50	> 50	2.029 ± 0.273	5.054 ± 0.703	> 50	0.494 ± 0.043
MCF-7	> 50	> 50	2.520 ± 0.219	2.873 ± 0.235	18.087 ± 3.059	0.585 ± 0.010
Jurkat	37.704 ± 1.808	> 50	0.711 ± 0.005	1.445 ± 0.130	3.598 ± 0.569	0.131 ± 0.012
CoLo	13.803 ± 1.225	19.590 ± 1.172	1.723 ± 0.021	5.341 ± 0.374	13.257 ± 0.224	0.914 ± 0.028
DU145	2.485 ± 0.087	9.380 ± 0.448	0.541 ± 0.046	0.299 ± 0.001	0.253 ± 0.024	0.007 ± 0.002
Resting lymphocytes	> 100	> 100	> 100	> 100	> 100	0.903 ± 0.041
Stimulated lymphocytes	> 100	> 100	> 100	> 100	> 100	0.182 ± 0.032

Non-specific toxicity is expected to correlate with a compound's propensity to accumulate in cell membranes and therefore, its lipophilicity (Poole and Poole, 2003). [Au(dppe)₂]Cl was shown (*Fig 5.8*) to be the most lipophilic compound ($\log P = 0.362$) of the experimental compounds and as expected, the most toxic (*Table 5.4*). Research has shown that there is a relationship between octanol-water partition coefficient and cytotoxic potency against human ovarian tumour cells (Berners-Price *et al.*, 1999a). There is a general increase in potency with increase in lipophilicity.

In the results presented in *Table 5.4*, one has to consider the role of different metals in interpretation of the data. The more hydrophilic compounds (**Pg 5** and **Pg 6**) were far less toxic than the lipophilic ones (**Pg 3** and **Pg 4a**). **Pg 8**, with intermediate lipophilicity was the most toxic of the novel compounds and hence

expected to show high selectivity. Studies have shown that the 2-pyridyl complexes of Ag(I) and Au(I) were cytotoxic to human ovarian cancer (JAM, CI-80-13S), cervical tumour (HeLa) and melanoma (MM96) cell lines (Bowen, 1999).

Pg 4a, **Pg 8** and $[\text{Au}(\text{dppe})_2]\text{Cl}$ were tested on murine cancer cell lines as well as on normal cells (*Table 5.5*).

Table 5.5: IC_{50} values (μM) of **Pg 4a**, **Pg 8** and the standard $[\text{Au}(\text{dppe})_2]\text{Cl}$ on murine cancer cell lines as well normal cells. The values are presented as a mean of three experiments carried out in triplicate.

	Pg 4a	Pg 8	$[\text{Au}(\text{dppe})_2]\text{Cl}$
B16	0.872 ± 0.028	0.983 ± 0.035	0.0148 ± 0.0001
Novikoff	6.917 ± 0.394	0.654 ± 0.011	0.073 ± 0.002
Porcine hepatocytes	31.080 ± 5.320	1.755 ± 0.234	0.165 ± 0.026
Chicken embryo fibroblasts	2.379 ± 0.405	0.812 ± 0.037	0.220 ± 0.024

As seen previously (*Table 5.3*), $[\text{Au}(\text{dppe})_2]\text{Cl}$ showed high potency and non-selectivity. **Pg 4a** was the most selective with IC_{50} values of 31.08 and 2.379 μM in porcine hepatocytes and chicken embryo fibroblasts, respectively. **Pg 8** gave comparable IC_{50} values in all the cells with the lowest being 0.654 μM (Novikoff) and the highest being 1.755 μM (porcine hepatocytes).

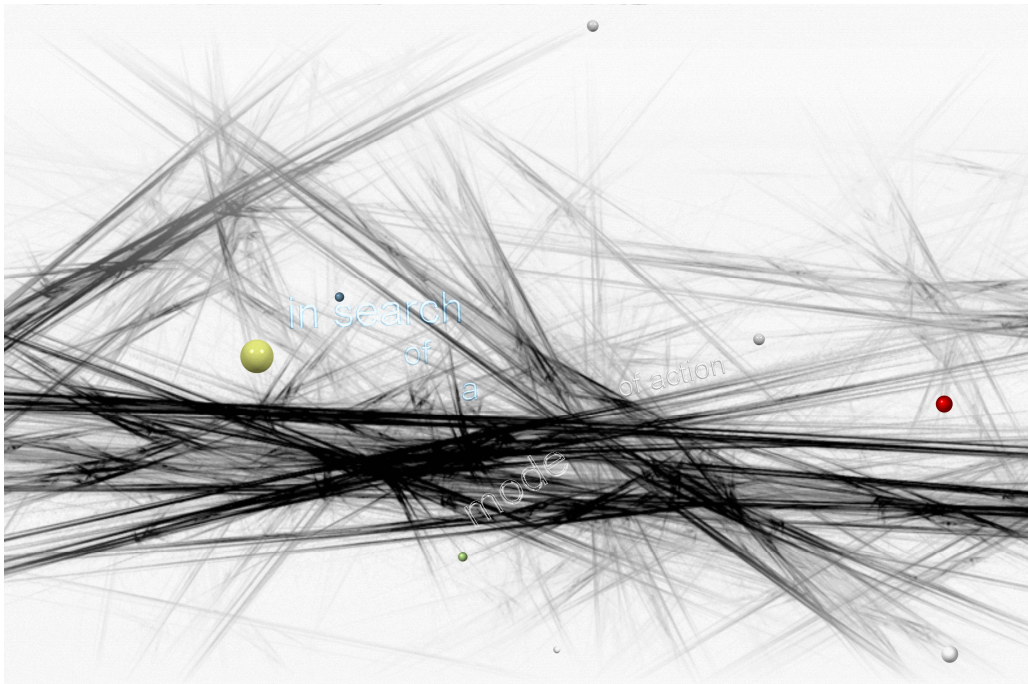
$[\text{Ag}(\text{dppe})_2]\text{NO}_3$ were highly cytotoxic to B16 melanoma cells *in vitro* with an IC_{50} value of 4 μM (2 h exposure) while $[\text{Au}(\text{dppe})_2]\text{Cl}$ had a value of 4.5 μM (Berners-Price *et al.*, 1988). Activity was retained when Au(I) was substituted by Ag(I) and Cu(I) as they possessed similar kinetic lability of the M-P bonds (Berners-Price and Sadler, 1996). In the current study, comparative compounds $[\text{Pt}(\text{dppe})_2][\text{PF}_6]_2$ (**Pg 1**) and $[\text{Pd}(\text{dppe})_2][\text{PF}_6]_2$ (**Pg 3**) displayed different anti-tumour behaviour. While the platinum complex was only active in prostate cancer cell line, the palladium analogue showed activity in all the cancer cell lines except A2780-cis. The high thermodynamic stability and high kinetic lability make palladium(II)

chelates more suitable for interacting with cancer cells and destroying them (Ali *et al.*, 2002).

[Pd(d2pyrpe)₂][PF₆]₂ (**Pg 8**) was selected for further tests in an effort to elucidate its mechanism of action. It was selected due the fact that it showed greater toxicity to more cancer lines than the rest of the experimental compounds. [Au(dppe)₂]Cl was included in these investigations as a standard. Jurkat cells were used for the remainder of the assays as they could be compared to lymphocytes.

Chapter VI

Analysis of mitochondrial function



6.1 The Mitochondria

During the period 1900-1930, most cytologists recognised the mitochondrion as a well-defined and ubiquitous organelle, although at that time there was no agreement about its function (Modica-Napolitano and Singh, 2002). The identification of mitochondria as centres of energy metabolism came at the heels of refinements in cell fractionation techniques during the late 1940s, which allowed the successful separation of relatively pure, functionally intact mitochondria from other cellular components in liver cell homogenates. Mitochondria are involved in many of the normal processes occurring in living cells such as ATP synthesis, oxidative phosphorylation, calcium uptake and release, production of NADPH, pH control, synthesis of DNA, the tricarboxylic acid cycle and β -oxidation pathway (McKeage *et al.*, 2002).

In mitochondria, NADH and $FADH_2$, reducing equivalents derived from the degradation of food substrates donate electrons to oxygen, the final electron acceptor, and the energy released during this process is used to pump protons from the mitochondrial matrix to the intermembrane space (Schrauwen *et al.*, 2006) (*Fig 6.1*). As a result, an electrochemical gradient is created across the inner mitochondrial membrane. The exported protons flow back into the mitochondrial matrix through the F_0F_1 -ATPase and the energy generated is used to synthesise ATP from ADP and inorganic phosphate (Pi).

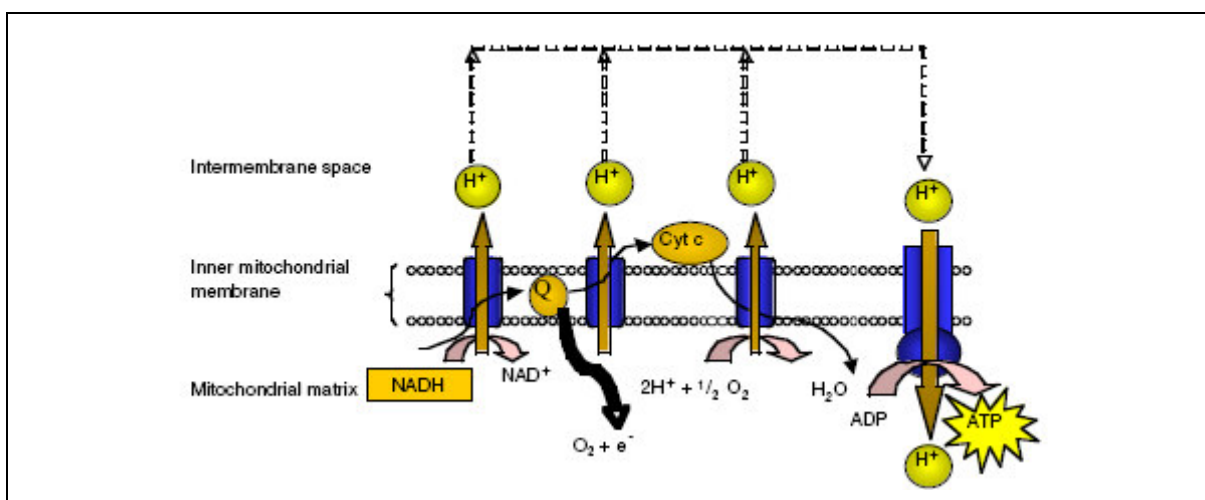


Fig 6.1: The electron transport chain (Schrauwen *et al.*, 2006).

The mitochondrial membrane potential, in situ, $\Delta\Psi_m$, is a sensitive indicator for the energetic state of the mitochondria and the cell, and can be used to assess the activity of the mitochondrial proton pumps, electrogenic transport systems, and the activation of the mitochondrial permeability transition (Rottenberg and Wu, 1998).

6.2 Mitochondria and cancer

Otto Warburg proposed in 1930 that respiratory deficiency might result in differentiation of cells and hence neoplastic transformation. Early studies of differences between the mitochondria of normal cells and those of cancer cells focused on the respiratory deficiencies common to rapidly growing cancer cells (Modica-Napolitano and Singh, 2002). Mitochondrial alterations have been implicated in a wide variety of acute and chronic human conditions, including cancer, intoxication, neuro-degenerative diseases, and aging (Horbinski and Chu, 2005). While precise contribution of mitochondria to carcinogenesis remains unclear, it has been reported that mitochondrial DNA (mtDNA) mutations, ranging from a single base mutation to a large deletion, were detected in a variety of tumours (Dias and Bailly, 2005). The analysis of the complete mitochondrial genome of 10 colorectal cancer cell-lines has shown that seven displayed mtDNA point-mutations that were not detected in normal tissue from which the tumour is derived (somatic mutation). To date, no particular mtDNA mutations have been correlated to a specific cancer.

6.3 Mitochondria as cancer drug targets

Mitochondria play a key role in the regulation of apoptosis and recent findings suggest that many apoptotic pathways converge at a single event- mitochondrial membrane permeabilisation (Barnard *et al.*, 2003). Targeting mitochondria has the potential to overcome the two overriding problems in cancer chemotherapy- the common occurrence of drug-resistant tumour cells and the lack of selectivity of cancer drugs in differentiating between tumour cells and normal tissues (Barnard *et al.*, 2004).

Compounds that specifically target cancer cell mitochondria must have a function that is based on differences in the bioenergetic or protein composition of the transformed cells (Don and Hogg, 2004). It is well established that transformed cells take up glucose more rapidly than normal counterparts and derive a larger proportion of their energy through aerobic glycolysis. Significantly, carcinoma cells have elevated plasma and mitochondrial membrane potentials relative to normal cells, leading to a more rapid accumulation of lipophilic cations, which are concentrated within mitochondria in response to the negative mitochondrial membrane potential (Barnard *et al.*, 2004).

Lonidamine is an anti-cancer agent that has been used in combination chemotherapy and has undergone clinical trials for the treatment of tumours that are refractory to conventional chemotherapy (Don and Hogg, 2004). Evidence indicates that it inhibits aerobic glucose utilisation, a mechanism that is probably mediated through a direct inhibition of mitochondrial-associated hexokinase. Increased expression and activity of hexokinase, which is associated with the outer mitochondrial membrane, is a feature of cancer cells that enables them to maintain high rates of glucose use. A good summary of drugs that target mitochondrial functions to control tumour growth has recently appeared in the literature (Dias and Bailly, 2005).

6.3.1 Lipophilic cations as potential chemotherapeutic agents

A variety of lipophilic cations with delocalised charges accumulate in the mitochondria of carcinoma-derived cells more rapidly than in most untransformed cells (Rideout *et al.*, 1989). These compounds concentrate in mitochondria due to their lipophilic-cationic character and exhibit preferential cytotoxicity to carcinoma cells with hyperpolarised membranes (Summerhayes *et al.*, 1982; Davis *et al.*, 1985; Nadakavukaren *et al.*, 1985; Chen, 1988). A study aimed at determining the mechanism of action of cationic phosphonium salts against carcinomas, with particular emphasis on the effects of tetraphenyl phosphonium chloride (TPP) on FaDu human hypopharyngeal squamous carcinoma cells was carried out (Rideout *et al.*, 1994). The abnormally high mitochondrial membrane potential in FaDu cells

caused preferential concentration of TPP in mitochondria, leading in turn to mitochondrial membrane damage.

Several structurally diverse lipophilic cations have demonstrated strong activity by concentrating in mitochondria, for example, rhodamin 123 (Johnson *et al.*, 1980), dequalinium (Weiss *et al.*, 1987), pyronine Y (Darzynkiewicz *et al.*, 1986), ditercalinium (Roques *et al.*, 1979), AA-1 (Sun *et al.*, 1994) and MKT-077 (Koya *et al.*, 1996), the latter having advanced to Phase I clinical trial. It has been shown that the mitochondria of carcinoma cells derived from kidney, ovary, pancreas, lung, adrenal cortex, skin, breast, prostate, cervix, vulva, colon, liver and testis accumulated Rh123 (*Fig 6.2*) to a greater extent and with a longer retention time than normal cells derived from bladder, breast, kidney, oesophagus, skin and lung (Don and Hogg, 2004).

Dequalinium chloride (DEQ) (*Fig 6.2*) has been shown to prolong the life span of mice implanted with bladder carcinoma >190%, which was significantly greater than other anti-cancer drugs that were tested (i.e., cisplatin, cytosine arabinoside, methotrexate and cyclophosphamide) (Berlin *et al.*, 1998). DEQ was shown to induce a delayed inhibition of cell growth in cultured human carcinoma cells as well as cause a selective loss of mitochondria DNA (mtDNA).

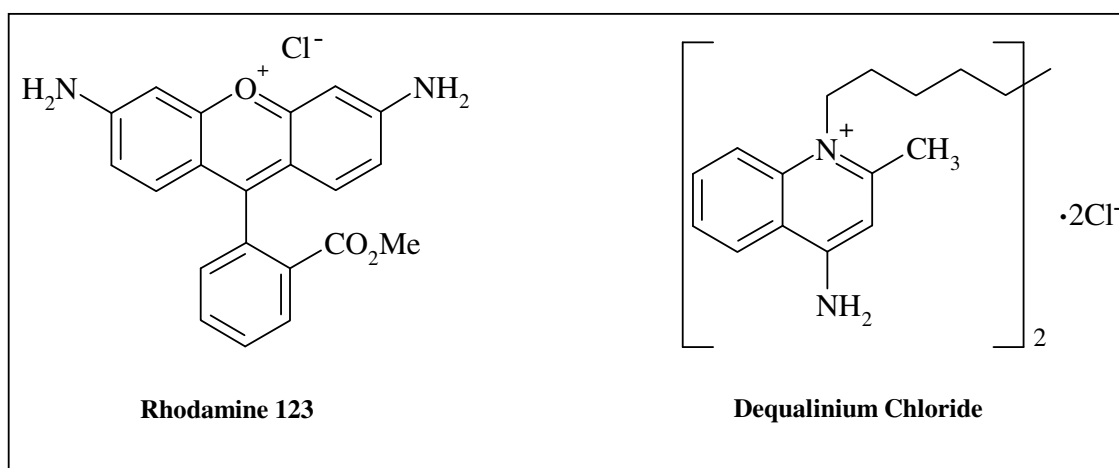


Fig 6.2: Some examples of lipophilic cations that have been shown to concentrate in mitochondria.

After screening more than 1000 lipophilic cations, Chen and co-workers found that the monovalent lipophilic cation, 2,6-bis-(4-amino-phenyl)-4-[4-

(dimethylamino)phenyl]thiopyrylium chloride (AA1) (Fig 6.3), displayed remarkable anti-carcinoma activity both *in vitro* and *in vivo* (Sun *et al.*, 1994). Compared with previously reported anti-carcinoma lipophilic cations such as rhodamine 123 and dequalinium chloride, AA1 appeared to display a more effective anti-carcinoma activity *in vivo*.

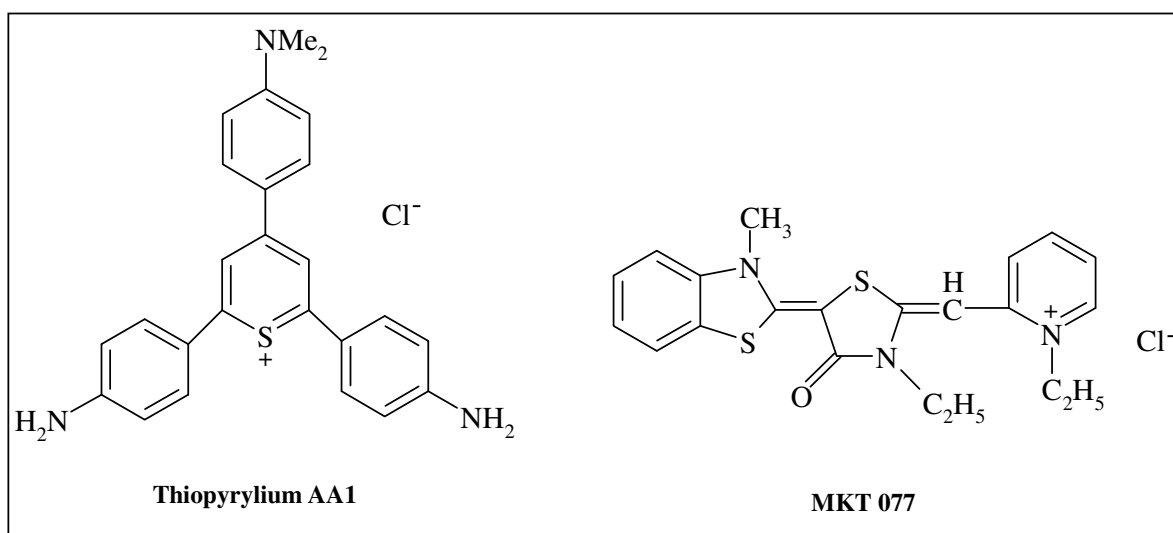


Fig 6.3: Some examples of lipophilic cations that have been shown to concentrate in mitochondria.

Rhodacyanine MKT-077 (Fig 6.3) accumulates in tumour cell mitochondria leading to ultrastructural changes, loss of mitochondrial DNA, generalised perturbation of mitochondrial membrane and non-specific damage to membrane enzymes (Sun *et al.*, 1994). It has been shown to possess significant activity against human renal carcinoma, prostate carcinoma, and melanoma tumours implanted in nude mice (Berlin *et al.*, 1998). Since many normal cells are reliant on oxygen consumption and oxidative phosphorylation for ATP production and tumours are primarily reliant on glycolysis for production of ATP, anti-mitochondrial agents that target oxidative phosphorylation pathways are likely to be limited in their therapeutic application by host toxicity and poor anti-tumour selectivity (McKeage *et al.*, 2002).

Interestingly, one research group manipulated membrane potentials in order to determine the uptake of TPP on FaDu (Rideout *et al.*, 1994). They found that depolarisation of the plasma membrane caused a 4-fold decrease in uptake of TPP and depolarisation of both plasma and mitochondrial membranes caused a 16.3-fold decrease in uptake. It is of further interest to note that, although

increased membrane potential is necessary to achieve selective cytotoxicity by delocalised lipophilic cations, it is not sufficient on its own (Modica-Napolitano and Singh, 2002). If this were the case, then cardiac muscle cells, which have been shown to exhibit high mitochondrial membrane potential would be susceptible to the cytotoxic effects of these compounds (i.e. MKT077 or dequalinium). Conversely, myelotoxicity is less of a problem with these compounds than conventional chemotherapeutics, because bone marrow cells have a low $\Delta\Psi_m$ (Don and Hogg, 2004).

6.4 Analysis of mitochondrial membrane potential

6.4.1 Fluorescent probes

Probes include those which exhibit optical and fluorescence activity after accumulation into energised systems (Cossarizza and Salvioli, 1997). Examples are 3,3'-diehexiloxadicyanin iodide [DiOC₆ (3)], nonylacridine orange (NAO), safranin O and rhodamine-123 (Rh 123), radiolabelled probes, (i.e., [³H]methyltriphenyl-phosphonium) and unlabelled probes used with specific electrodes [i.e., tetraphenyl-phosphonium ion (TPP⁺)]. These probes allow the analysis of changes in mitochondrial membrane potential (rhodamine 123) or modifications of mitochondrial mass (nonyl acridine orange) (Cossarizza *et al.*, 1993). However, the results these probes can put in evidence are expressed as decreases or increases in fluorescence intensity, so that variations of membrane potential are usually expressed as decreases or increases in this fluorescent intensity. For example, while rhodamine 123 is highly specific for living cells, it does not possess the ability to differentiate between mitochondria of low and high membrane potential (Gravance *et al.*, 1999).

While fluorescent labelling of cells provides important information regarding the functional status of the cell, the true utility of fluorescent markers is the ability to assess these staining patterns using flow cytometry (Gravance *et al.*, 1999). Flow cytometry (FCM) allows the characterisation and analysis of several cell parameters and functions, such as lymphocyte phenotype cell cycle, apoptosis, among others (Cossarizza *et al.*, 1993). A consistent advantage of FCM techniques is the possibility to analyse thousands of living cells in a few seconds.

The lipophilic cationic compound 5,5',6,6'-tetrachloro 1,1',3,3'-tetra ethylbenzimidazolyl carbocyanine iodide (JC-1) possesses the unique ability to differentially label mitochondria with high and low membrane potential (Gravance *et al.*, 2001). JC-1 is more advantageous over rhodamines and other carbocyanines capable of entering selectively into mitochondria, since it changes reversibly its colour from green to orange as membrane potentials increase (over values of about 80-100 mV) (Cossarizza and Salvioli, 1997). This property is due to the reversible formation of JC-1 aggregates upon membrane polarisation that causes shifts in emitted light from 530 nm (*i.e.*, emission of JC-1 monomeric form) to 590 nm (*i.e.*, emission of J-aggregate) when excited at 490 nm; the colour of the dye changes reversibly from green to greenish orange as the mitochondrial membrane becomes more polarised.

Both colours can be detected using the filters commonly mounted in all flow cytometers, so that green emission can be analysed in fluorescence channel 1 (FL1) and greenish orange emission in channel 2 (FL2) (Cossarizza and Salvioli, 1997). The main advantage of using JC-1 is that it can be both qualitative, considering the shift from green to orange fluorescence emission, and quantitative, considering the pure fluorescence intensity, which can be detected in both FL1 and FL2 channels. This cytofluorimetric method (Salvioli *et al.*, 1997):

- allows the identification of populations with different mitochondria content;
- has already been utilised for studying behaviour of these organelles in a variety of conditions, including apoptosis;
- has been further validated by analysing $\Delta\psi$ at the level of single mitochondria

6.5 Objective of this experiment

The intention of the experiments described below was to determine whether the observed cytotoxicity (*Chapter 5*) was due to loss of mitochondrial membrane potential to either resting lymphocytes or Jurkat cells. Jurkat cells were selected for these experiments as they could be compared to lymphocytes (normal cells).

The expected outcome was that these cationic compounds would selectively accumulate in the mitochondria of Jurkat cells rather than in lymphocytes. Depolarisation of the membrane potential would then lead to a decrease in J-aggregates (orange fluorescence) and an increase in j-monomers (green fluorescence).

The procedure used to analyse mitochondrial membrane potential changes was adapted from the literature (Cossarizza and Salvioli, 1997). Valinomycin, a classical K⁺ ionophore that dissipates the membrane potential but not the pH gradient, was used to reduce the orange fluorescence emission of JC-1 (Cossarizza *et al.*, 1993).

6.6 Materials and methods

6.6.1 Reagents

- Cell culture medium (RPMI + 10% FCS).
- Phosphate buffered saline (PBS).
- JC-1 (Sigma-Aldrich).
- Valinomycin (Sigma-Aldrich).
- ⁴Pg **8** (0.711 μM and 1.422 μM) and [Au(dppe)₂]Cl (0.131 μM and 0.262 μM) –Jurkat.
- **Pg 8** (100 μM and 200 μM) and [Au(dppe)₂]Cl (0.903 μM and 1.806 μM)-lymphocytes.

6.6.2. Cell cultures

Human T-cell line (Jurkat) was cultured in RPMI 1640 supplemented with 10% v/v heat-inactivated FCS and 1% penicillin-streptomycin. Cells were maintained in a humidified atmosphere of 5% carbon dioxide at 37 °C.

⁴ The concentrations used here represent the IC₅₀ values (and double) that were obtained in cytotoxicity assays (Chapter 5).

6.6.3. Flow cytometric analysis of mitochondrial membrane potential changes

Cells (Jurkat = 3×10^5 or lymphocytes = 2×10^6 cells/ml) were treated with $[\text{Au}(\text{dppe})_2]\text{Cl}$ and **Pg 8** for 24 h [10 mins with 10 μM valinomycin]. After incubation, all the untreated and treated cells were decanted from the flasks into centrifuge tubes and centrifuged for 5 min at 500 g. The cell pellets were suspended in 1 ml of complete RPMI followed by addition of 100 μl of 1.5 $\mu\text{g}/\text{ml}$ JC-1. The suspension was mixed well and samples kept in the dark for 15-20 minutes. At the end of incubation period, the cells were washed twice while centrifuging at 500 g (5 min) with double volume of cold PBS. The pellet was then re-suspended in 1 ml of PBS (10% FCS).

Analyses were performed using a flow cytometer (Beckman Cytomics FC 500) equipped with a single 488 nm argon laser. The instrument was programmed to calculate the ratio of FL2:FL1, which would signify either hyperpolarisation or depolarisation of the mitochondrial membrane. An increase in the ratio would indicate hyperpolarisation (less j-monomers and more j-aggregates) while a decrease would signify depolarisation due to reduction of orange fluorescence (more j-monomers and less j-aggregates).

6.6.4. Statistical methods

Statistical analyses were performed by One Way Analysis of Variance (ANOVA) followed by Dunnett's Multiple Comparison Test to determine the treatments that were significantly different from the fresh, viable cells. The averages (\pm SEM) for each treatment represent at least six independent experiments. However, Student's t-test was performed for section 6.7.2. The treatment that was significantly different from the untreated cells is denoted with an asterisk (*) and $P < 0.05$ was considered significant.

6.7 Results and discussion

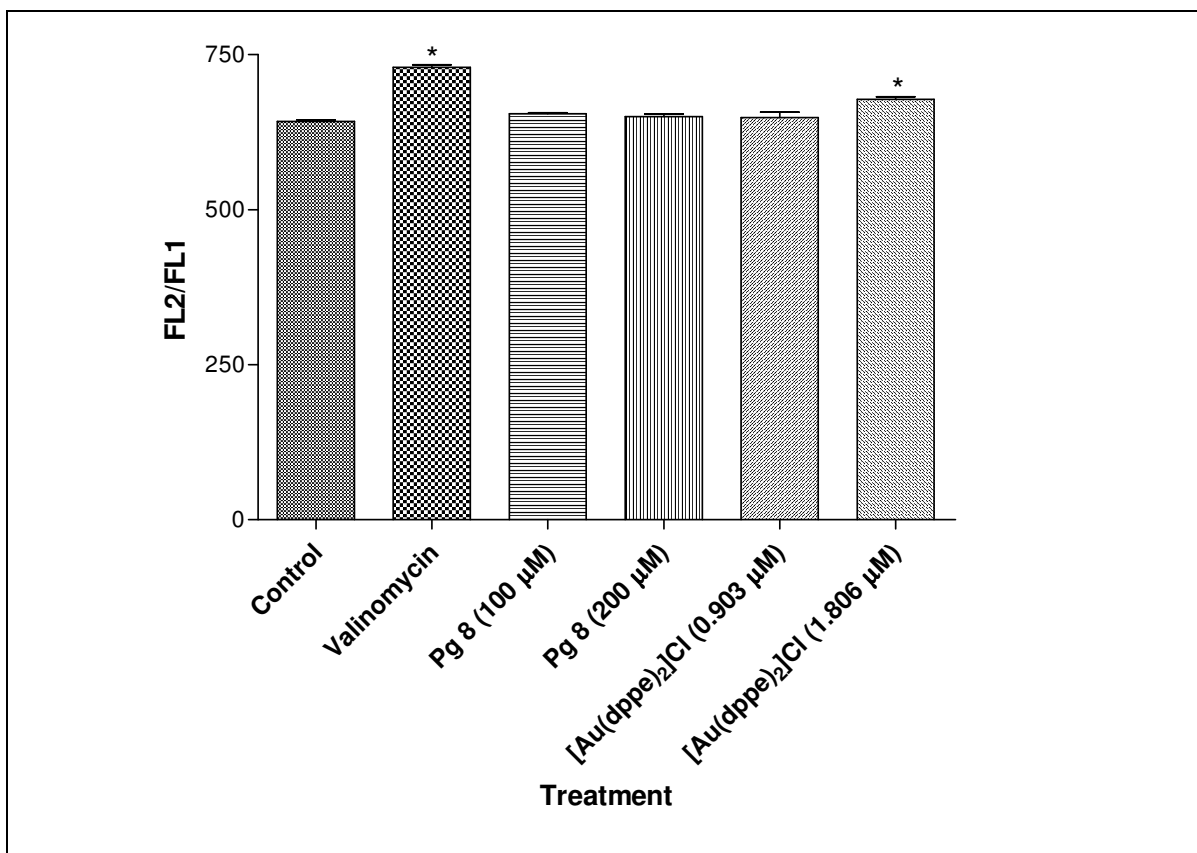


Fig 6.4: Ratio of J-aggregates (FL2): J-monomers (FL1) in resting lymphocytes after treatment (24 h) with valinomycin (10 µM), **Pg 8** (100 µM and 200 µM) and **[Au(dppe)₂]Cl** (0.903 µM and 1.806 µM). The cells were stained with JC-1 for 30 mins and analysed by flow cytometry. The data shown here is an average of at least 6 independent experiments.

Exposure of valinomycin (10 µM) and **[Au(dppe)₂]Cl** (1.806 µM) to resting lymphocytes led to an increase in ratio between the j-monomers and j-aggregates (ratio of FL2:FL1 increased) (*Fig. 6.4*). This indicated that polarisation of the membrane potential had taken place as the amount of JC-1 aggregates were found to be significantly higher ($P < 0.01$) than those found in untreated cells. Cells treated with **Pg 8** (100 and 200 µM) and **[Au(dppe)₂]Cl** (0.903 µM) did not induce any loss of mitochondrial membrane potential.

Hyperpolarisation of the mitochondria of lymphocytes has been described by authors and it seems to represent a pre-requisite for rapid mitochondrial-mediated apoptotic cell death that eventually leads to the loss of mitochondrial membrane potential (Giovannini *et al.*, 2002). These hyperpolarisation effects can result from

different actions, such as increased mitochondrial mass and number per cell or an increase in matrix volume, the latter leading to swelling and rupture of the outer membrane, followed by a decrease in $\Delta\Psi_m$. Another research group has shown that methyl protodioscin, a furostanol bisglycoside with anti-tumour properties induced hyperpolarisation in mitochondria of human chronic myelogenous leukaemia K562 cells, with the loss of mitochondrial membrane permeabilisation as a secondary response (Liu *et al.*, 2005).

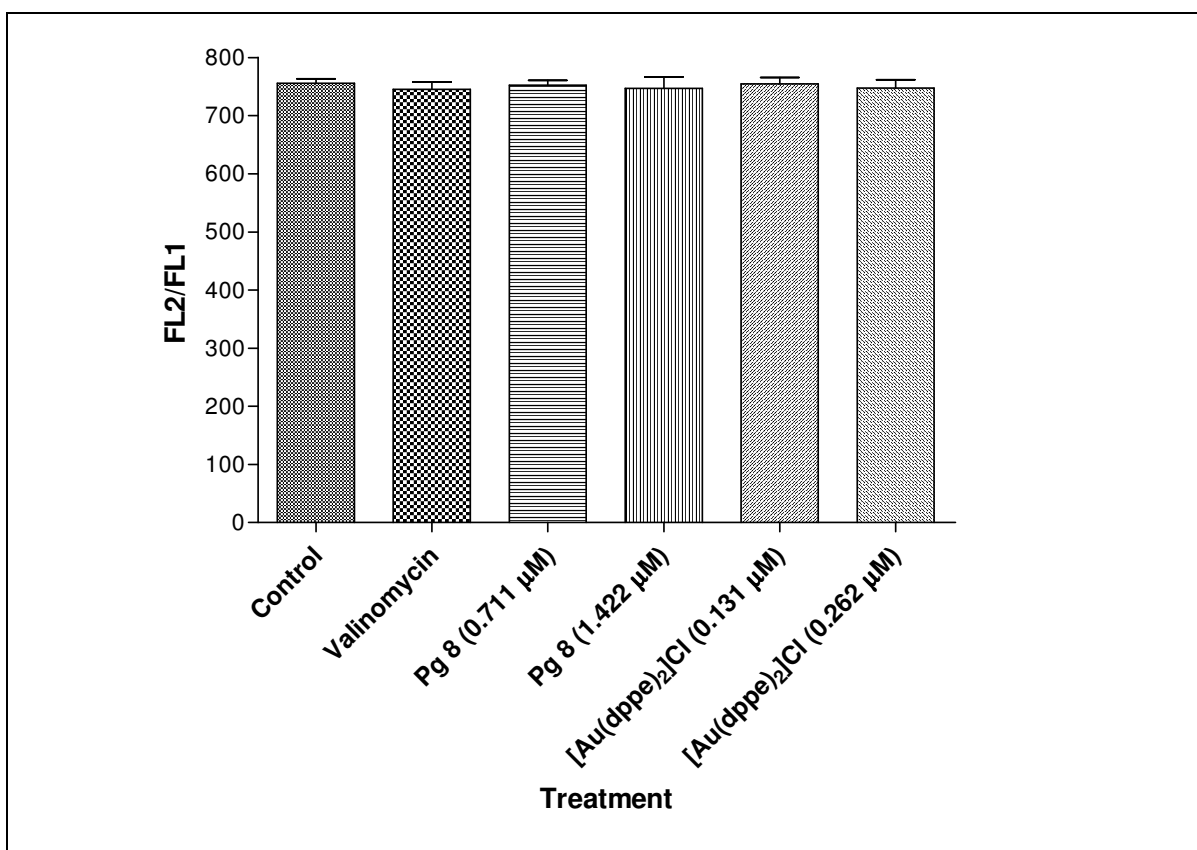


Fig 6.5: Ratio of J-aggregates (FL2): J-monomers (FL1) in Jurkat cells after treatment with valinomycin (10 µM), **Pg 8** (0.711 µM and 1.422 µM) and **[Au(dppe)₂]Cl** (0.131 µM and 0.262 µM). The cells were stained with JC-1 for 30 mins and analysed by flow cytometry. The data shown here is an average of at least 6 independent experiments.

No changes in membrane potential of Jurkat cells occurred when exposed to the test compounds (*Fig 6.5*). The expectation was that the compounds would accumulate in the mitochondria of cancerous cells faster and induce depolarisation of the mitochondrial membrane. It is worth noting that untreated Jurkat cells (Mean FL2:FL1 ratio = 756) were more polarised ($P < 0.0001$) than untreated resting lymphocytes (Mean FL2:FL1 ratio = 642).

From the above results, it is clear that the experimental compounds did not depolarise the mitochondrial membrane of Jurkat cells at low concentrations as well as after 24 hours. Hence, two further experiments were designed to determine whether longer incubation times or higher drug concentrations would lead to changes in membrane potentials.

6.7.1 Determination of mitochondrial membrane potential changes of cells exposed to higher drug concentrations

To determine whether $[\text{Au}(\text{dppe})_2]\text{Cl}$ induced cytotoxicity was related to changes in the mitochondria, studies of induced toxicity and biochemical alterations in intact rat hepatocytes were carried out (McKeage *et al.*, 2002). Within 30 min of exposure, $[\text{Au}(\text{dppe})_2]\text{Cl}$ (5-20 μM) had been taken up by isolated hepatocytes and distributed to mitochondria. Within the same period of time, isolated rat hepatocytes formed blebs on the plasma membrane, lost ATP, showed increased oxygen consumption and developed morphological changes in mitochondria as detected by electron microscopy. It also induced rapid dissipation of the inner mitochondrial membrane potential, efflux of calcium, increased mitochondrial respiration, mitochondrial swelling and increased permeability of the inner membrane to cations and protons.

This assay aimed at determining whether the experimental compounds induced a loss of mitochondrial membrane potential at higher concentrations (10 and 15 μM).

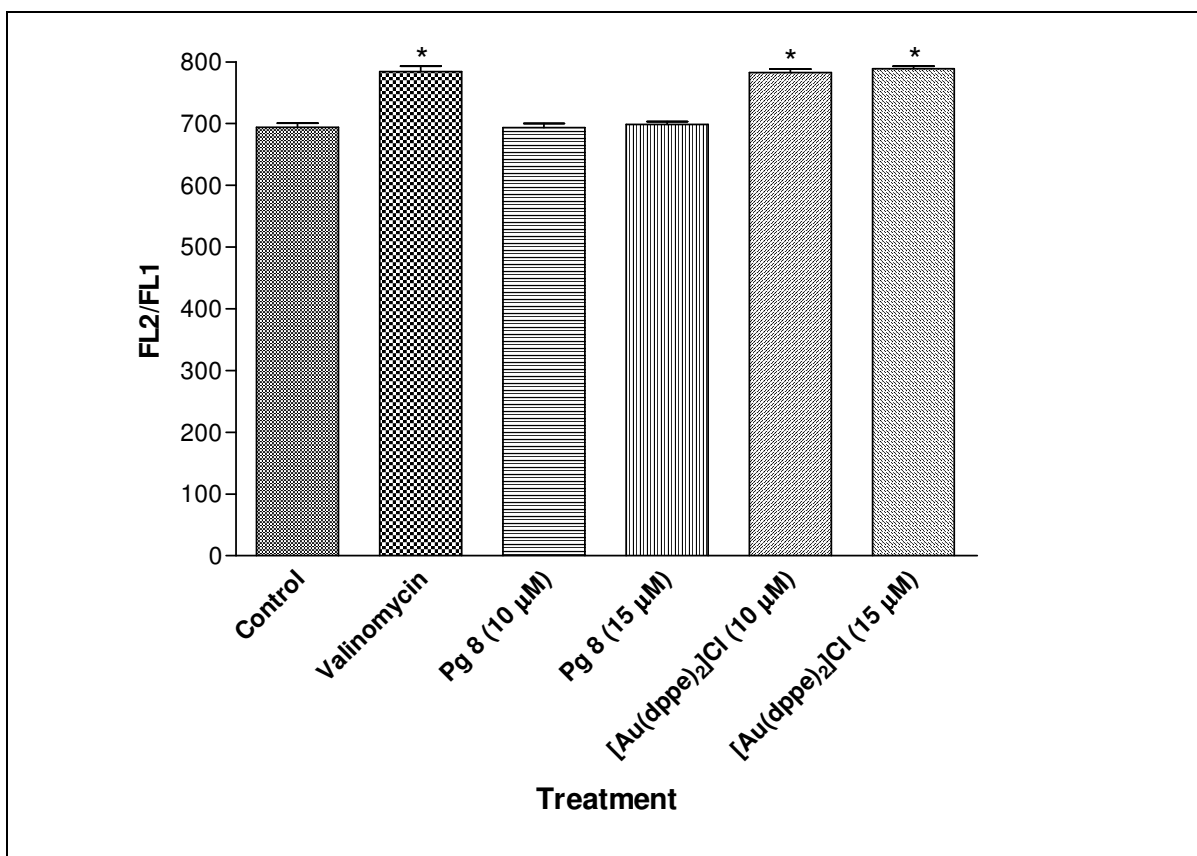


Fig 6.6: Ratio of J-aggregates (FL2): J-monomers (FL1) in Jurkat cells after treatment with valinomycin (10 µM), **Pg 8** (10 µM and 15 µM) and **[Au(dppe)₂]Cl** (10 µM and 15 µM). The cells were stained with JC-1 for 30 mins and analysed by flow cytometry. The data shown here is an average of at least 3 independent experiments.

Pg 8 (10 and 15 µM) did not decrease nor increase membrane potentials of Jurkat cells (*Fig 6.6*). There was a significant increase ($P < 0.0001$) in FL2/FL1 ratio of cells that were treated with valinomycin and **[Au(dppe)₂]Cl**. These results also show that **[Au(dppe)₂]Cl** caused changes in the mitochondrial membrane potential of Jurkat cells at concentrations that were much higher (~75 times) than that required to cause death to the cells. Studies carried out with **[Au(dppe)₂]Cl** on isolated heart or hepatocyte mitochondria showed that the rate and degree of drug-induced dissipation of the electrochemical potential difference was concentration dependent (Hoke *et al.*, 1989). At a concentration of 15 and 20 µM **[Au(dppe)₂]Cl**, the dissipation of the electrochemical gradient was not complete. However, exposure of the mitochondria to 30 or 60-µM drug resulted in a complete dissipation of electrochemical gradient.

6.7.2 Determination of mitochondrial membrane potential changes of cells exposed to Pg 8 for 7 days

This experiment involved the incubation of Jurkat cells with **Pg 8** (0.711 μM) for 7 days. The mitochondrial membrane potential changes were monitored every 24 hours to determine the time required for the test compound to induce changes in the mitochondria. It has been shown that the lipophilic cation Rh123 requires at least 6 days to exhibit significant activity against some carcinoma cells (Rideout *et al.*, 1994). It was also shown that TPP caused damage to the mitochondrial inner membrane of FaDu cells under conditions that inhibit cell proliferation by 50% (0.45 μM , 6 day exposure).

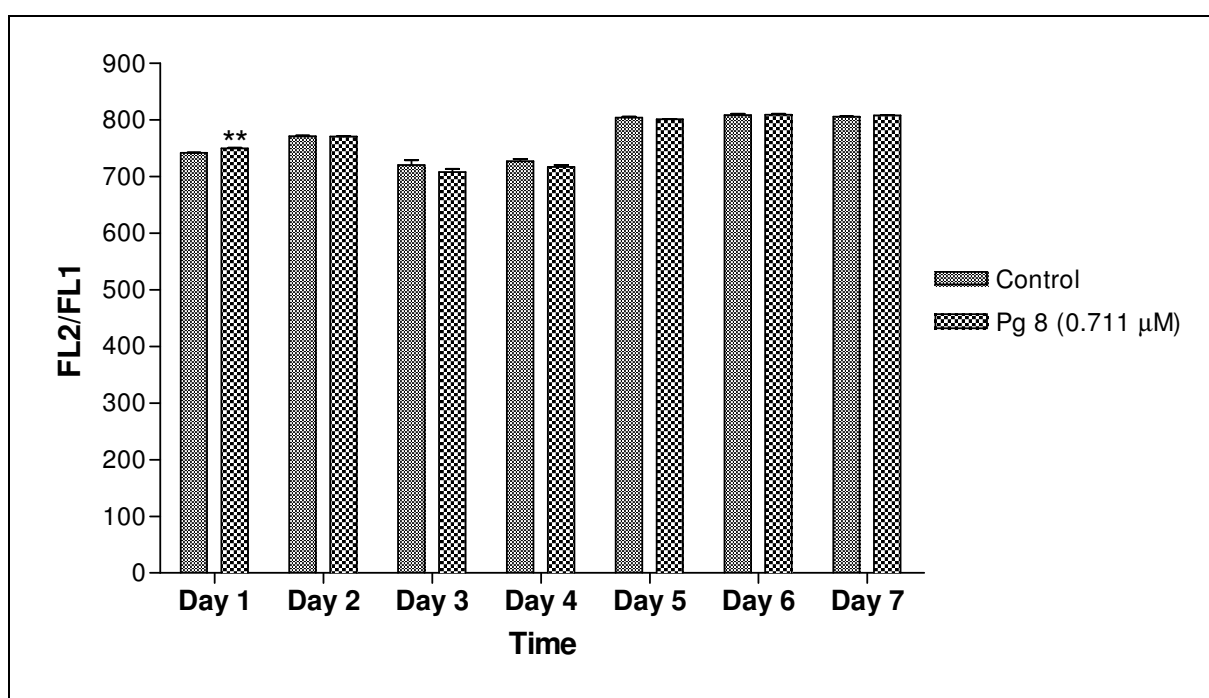


Fig 6.7: Ratio of J-aggregates (FL2): J-monomers (FL1) in Jurkat cells after treatment (7 days) with **Pg 8** (0.711 μM). The cells were incubated in cell culture flasks and samples were analysed by flow cytometry every 24 h. The data shown here is an average of at least 3 independent experiments carried out in triplicate.

The ratio of j-aggregates vs j-monomers on day 1 was higher ($P < 0.05$) in Jurkat cells treated with **Pg 8** (0.711 μM) than in untreated cells (*Fig 6.7*). No differences in membrane potentials were noted for the remainder of the study.

6.8 Plasma membrane Potential

The plasma membrane is a lipid bilayer that accommodates a significant number of proteins with diverse structures and tasks necessary for the proper function of the cells (Vámosi *et al.*, 2006). A primary function of the plasma membrane is the maintenance of a potential difference by its ability to barricade the free passage of ions across the membrane (Mann and Cidlowski, 2001). Normally, most cells maintain an electrical potential across the plasma membrane of -60 mV to -70 mV that renders the inside of the membrane more negative than the outside. In living cells, mitochondria are surrounded by the plasma membrane whose membrane potential has been shown to have a pre-concentrating effect on the accumulation of lipophilic cations by mitochondria (Smiley *et al.*, 1991).

Plasma membrane potential (E_m) contributes to the driving force of ions like Ca^{2+} across the plasma membrane and is therefore essential for different signal transduction pathways and the regulation of uptake and excretion of the metabolites (Nolte *et al.*, 2004). The intact plasma membrane integrity includes preservation of its basal function, like a barrier for ions and macromolecular structures, and active transport pumps (Vermes *et al.*, 2000). Apoptosis is characterised by maintenance of an intact plasma membrane during a significant part of its time course.

Until recently, the role of plasma membrane potential in apoptosis has been largely ignored; however, studies have suggested that the plasma membrane potential may be compromised during apoptosis of lymphocytes (Mann and Cidlowski, 2001). For example, in Jurkat cells, three different stimuli that differ in their mode of action, anti-Fas antibody, A23187, and thapsigargin, all induced a loss in plasma membrane potential associated with apoptosis. In lymphocyte-apoptosis, actively induced plasma membrane depolarisation has been previously investigated as the maintenance of the E_m is of vital importance for cells (Nolte *et al.*, 2004).

Dexamethasone has been shown to increase DiBAC₄(3) fluorescence in primary isolated thymocytes (Mann and Cidlowski, 2001). This is consistent with the fact that it increases the percentage of cells undergoing apoptosis and percentage of cells with a depolarised plasma membrane. In the same study, when HeLa cells were treated with 100 nm dexamethasone for 6 h, there was no observable difference in DiBAC₄(3) fluorescence between control and treated cells. These results indicated that the ability of glucocorticoids to induce a loss of plasma membrane potential correlates with their ability to induce apoptosis.

6.9 Analysis of plasma membrane changes by flow cytometry

In order to stain mitochondria, any probe has to enter into the cell and reach the organelles (Salvioli *et al.*, 1997). Its cytoplasmic accumulation is a crucial event, because a critical intracellular concentration is required to obtain an adequate fluorescence signal. Bis-(1,3-dibarbituric acid)trimethine (DiBAC₄), is an ionic probe whose distribution across the cell membrane depends on membrane potential (Radosevic *et al.*, 1993). Upon depolarisation, when the inside of the cell becomes more positively charged, more dye enters the cell resulting in an increase in cellular fluorescence. Upon hyperpolarisation, the dye is extruded from the cell resulting in a decrease in fluorescence. The analyses described below investigated whether plasma membrane potential changes occurred when Jurkat cells were treated with the test compounds. The procedure was modified from published methods (Mann and Cidlowski, 2001, Radosevic *et al.*, 1993).

6.10 Materials and methods

6.10.1 Reagents

- Supplemented cell culture medium (RPMI).
- Phosphate buffered saline (PBS).
- DiBAC₄(3) (Sigma-Aldrich)- Stock solution was prepared from ethanol
- Propidium Iodide (PI) (Sigma-Aldrich)
- Dexamethasone (Sigma-Aldrich)

- ⁵Pg 8 (0.711 μM and 1.422 μM) and [Au(dppe)₂]Cl (0.131 μM and 0.262 μM) –Jurkat
- Pg 8 (100 μM and 200 μM) and [Au(dppe)₂]Cl (0.903 μM and 1.806 μM)-lymphocytes

6.10.2 Cell cultures

Human T-cell lines (Jurkat) were cultured in RPMI 1640 supplemented with 10% v/v heat-inactivated FCS and 1% penicillin-streptomycin. Cells were maintained in a humidified atmosphere of 5% carbon dioxide at 37 °C.

6.10.3 Flow cytometric analysis of plasma membrane potential changes

1.8 ml of cell suspension (Jurkat 3×10^5 and lymphocytes 2×10^6 cells/ml) was incubated with 0.2 ml of test compounds for 24 hrs at 37°C, 5% CO₂. Dexamethasone (100 nm, 6 hours incubation) was used as a positive control. After incubation period, cells were centrifuged at 500 g for 5 min followed by re-suspension of the pellet in 2 ml of cold complete medium. Centrifugation was carried out and the pellet re-suspended in 900 μl of cold complete medium. 100 μl of DiBAC₄(3) (150 nm) was added to each tube. The cell suspension was incubated for 30 min at 37 °C, 5% CO₂.

To exclude cells that had lost membrane integrity, 100 μl of propidium iodide (final concentration of 10 μg/ml) was added to each tube and analysis was carried out immediately using flow cytometer (Beckman Coulter FC 500). Propidium iodide fluorescence was measured on FL-3 (650 nm) to exclude non-viable cells. To determine membrane potential, the DIBAC₄(3) fluorescence of 15,000 viable cells was measured on FL-1 (excitation at 488 nm, emission at 530 nm). The percentage of cells with increased DIBAC₄(3) fluorescence was determined by gating on the fresh, viable population of cells.

⁵ The concentrations used here represent the IC₅₀ values (and double) that were obtained in cytotoxicity assays (Chapter 5).

6.10.4. Statistical methods

Statistical analyses were performed by One Way Analysis of Variance (ANOVA) followed by Dunnett's Multiple Comparison Test to determine the treatments that were significantly different from the fresh, viable cells. The averages \pm SEM for each treatment represent at least six independent experiments. However, Student's t-test was performed for the 7-day study. The treatment that was significantly different from the untreated cells is denoted with an asterisk (*) and $P < 0.05$ was considered significant.

6.11 Results and discussion

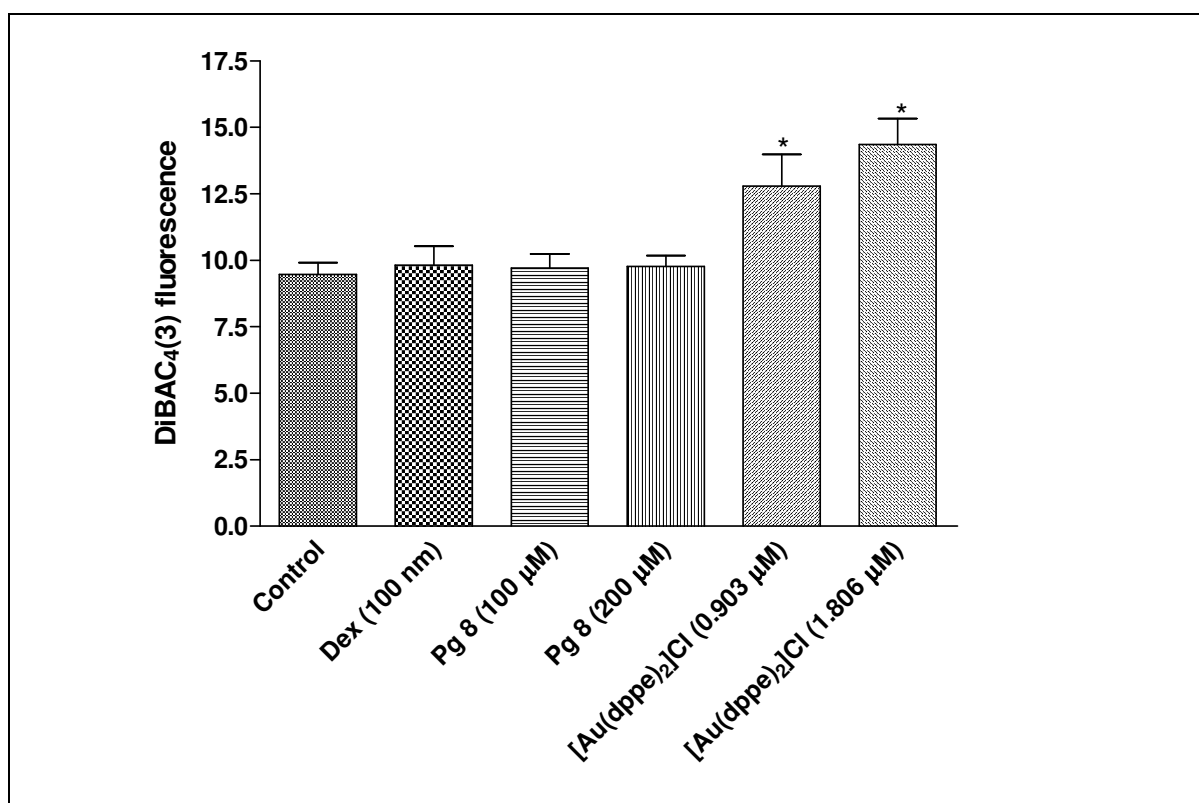


Fig 6.8: Fluorescent intensity of untreated and treated resting lymphocytes. The cells were exposed to the experimental compounds for 24 h followed by incubation with DiBAC₄(3) for 30 min and analysed by flow cytometry. The data shown here is an average of at least 6 independent experiments.

Treatment of lymphocytes with dexamethasone and **Pg 8** (100 and 200 µM) did not show any increase in DiBAC₄(3) fluorescence (*Fig 6.8*). The inability of **Pg 8** to depolarise the plasma membrane potential of lymphocytes is in agreement with

its lack of toxicity even at 100 μM (*Chapter 5*). However, lymphocytes treated with $[\text{Au}(\text{dppe})_2]\text{Cl}$ (0.131 and 0.262 μM) showed a significant increase ($P < 0.05$ and $P < 0.01$, respectively) in $\text{DiBAC}_4(3)$ fluorescence. This indicates a decrease in plasma membrane potential as a result of depolarisation. These results are in agreement with the high toxicity of $[\text{Au}(\text{dppe})_2]\text{Cl}$ ($\text{IC}_{50} = 0.131 \mu\text{M}$) to resting lymphocytes (*Chapter 5*) and changes observed in mitochondrial membrane potential. In lymphocytes, plasma membrane depolarisation plays a central role in lymphocyte activation (Mann and Cidlowski, 2001). Activation of the T-cells by antigen-dependent or antigen-independent stimuli results in plasma membrane depolarisation, turnover of polyphosphoinositides, and an increase in free intracellular calcium.

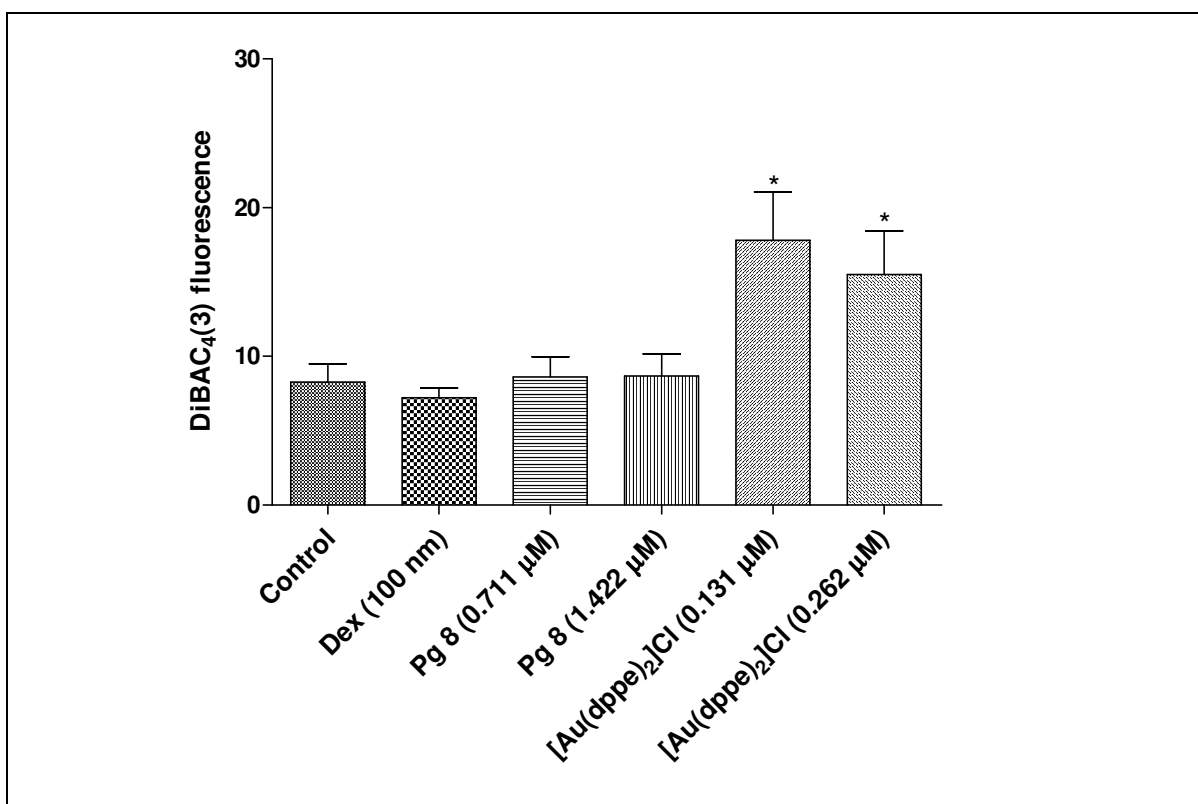


Fig 6.9: Fluorescent intensity of untreated and treated Jurkat cells. The cells were exposed to the experimental compounds for 24 h followed by incubation with $\text{DiBAC}_4(3)$ for 30 min and analysed by flow cytometry. The data shown here is an average of at least 6 independent experiments.

Pg 8 and dexamethasone did not induce any plasma membrane potential changes in Jurkat cells (*Fig 6.9*). $[\text{Au}(\text{dppe})_2]\text{Cl}$ (0.131 and 0.262 μM) caused a significant increase ($P < 0.01$ and $P < 0.05$, respectively) in $\text{DiBAC}_4(3)$ fluorescence. This is in contrast to the results obtained in the determination of mitochondrial membrane

potential changes where no differences were noted between the untreated and treated Jurkat cells.

As previously done in the determination of mitochondrial membrane potential changes, Jurkat cells were exposed to higher drug concentrations (10 and 15 μM).

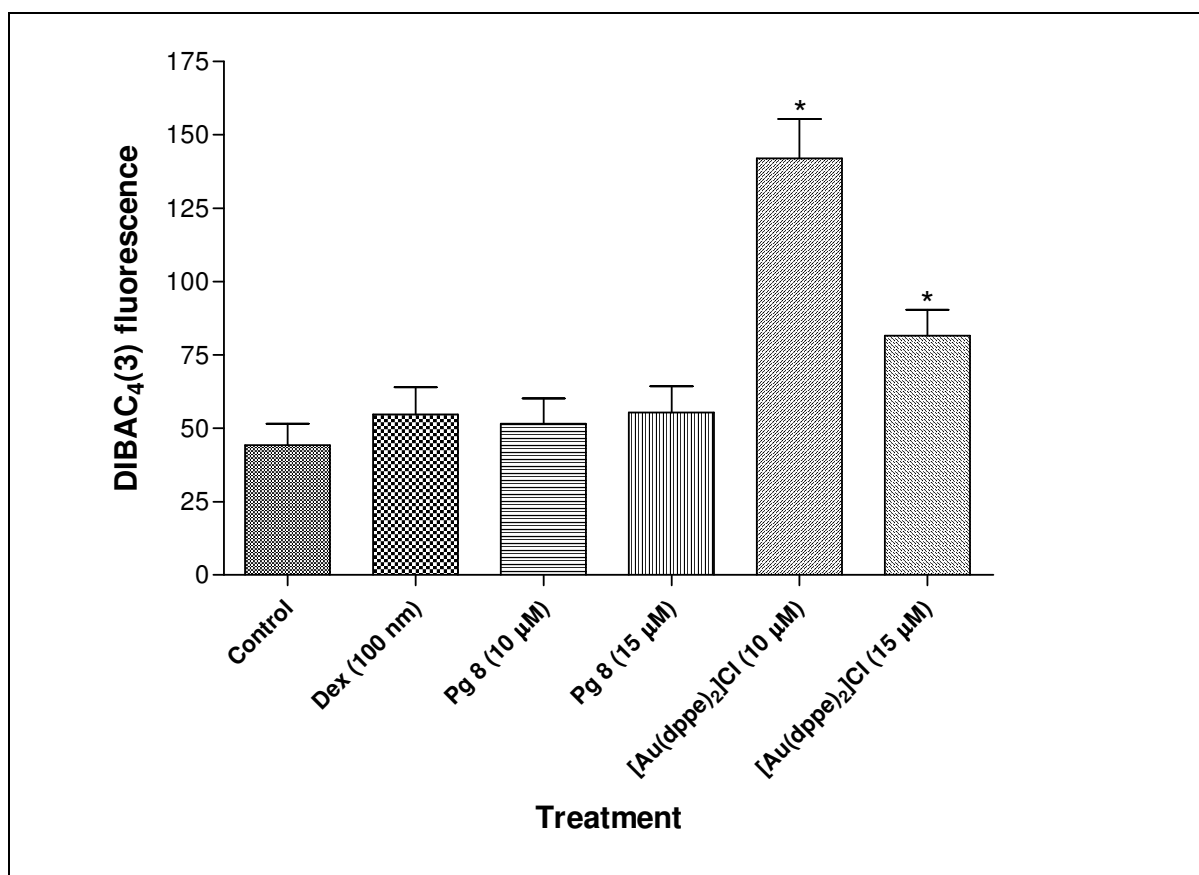


Fig 6.10: Fluorescent intensity of untreated and treated Jurkat cells. The cells were exposed to the experimental compounds (10 and 15 μM) for 24 h followed by incubation with DIBAC₄(3) for 30 min and analysed by flow cytometry. The data shown here is an average of at least 6 independent experiments.

Jurkat cells that were treated with [Au(dppe)₂]Cl (10 and 15 μM) showed a significant increase ($P < 0.01$ and $P < 0.05$, respectively) in DiBAC₄(3) fluorescence (Fig. 6.10). As observed previously, cells treated with Dexamethasone and **Pg 8** caused no loss in plasma membrane potential as the amount of DiBAC₄(3) fluorescence was not significantly higher than that found in the untreated cells.

To establish whether there was any relationship between cytotoxicity of **Pg 8** and plasma membrane potential changes, a time-course experiment was carried out. Jurkat cells were exposed to **Pg 8** (0.711 μM) for 7 days and DiBAC₄(3) fluorescence intensities were monitored every 24 hours.

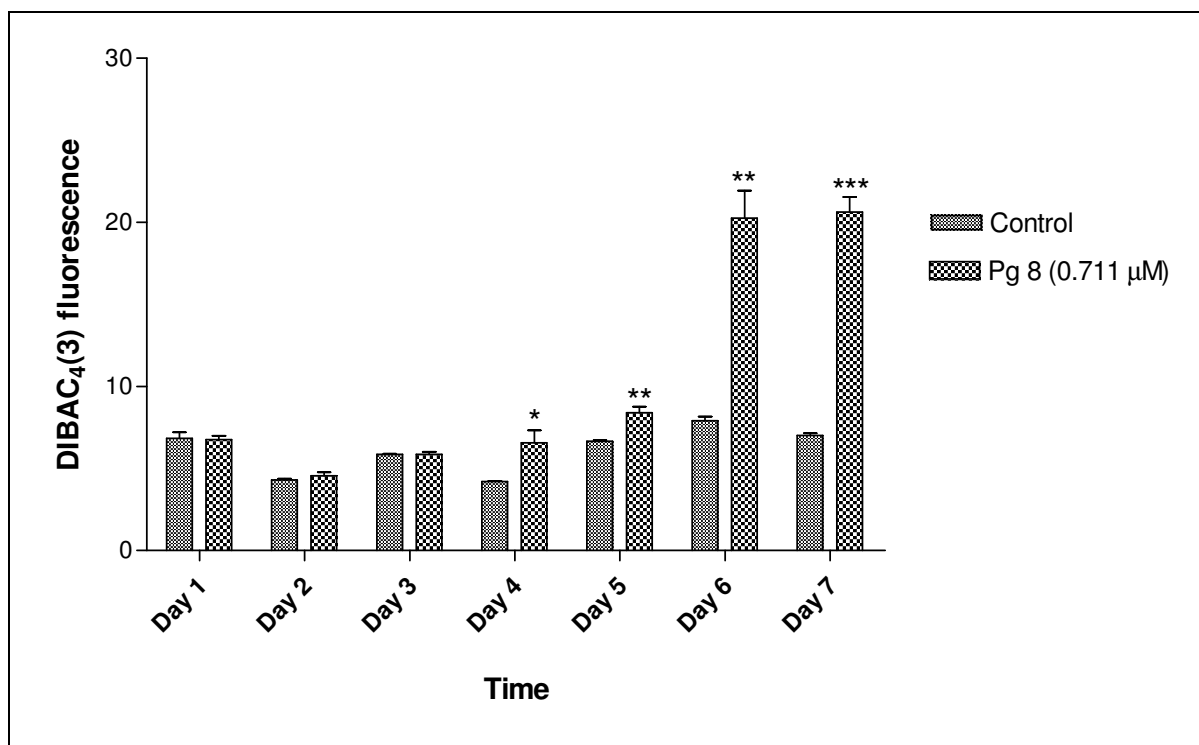


Fig 6.11: Fluorescent intensity of jurkat cells treated with Pg 8 (0.711 μM) for 7 days. The cells were harvested every 24 h, incubated with DiBAC₄(3) for 30 min and analysed by flow cytometry. The experiment was carried out in triplicate.

There was a significant increase ($P < 0.05$) in DiBAC₄(3) fluorescence in cells treated with **Pg 8** from day 4 (Fig.6.11). This depolarisation of the plasma membrane continued to increase up to day 7 of the experiment. This study showed that **Pg 8** (IC₅₀) depolarised plasma membrane potentials in a time-dependent manner. This is in contrast to the results obtained on mitochondrial membrane potential (Fig 6.7).

6.11.1: Relationship between plasma membrane changes and chemical changes of Pg 8 over a 7 day period

A study was carried out in order to establish a relationship between chemical changes of **Pg 8** and depolarisation of plasma membrane potential over a 7 day period. The stability test was carried out as previously discussed in **Chapter 5** (5.4.2). Small amounts of **Pg 8** were dissolved in DMSO, DMSO-d₆ and cell culture medium (EMEM). Two samples were prepared with one containing EMEM with FCS and the other without. The use of cell culture medium with or without FCS was to observe if there were any chemical changes differences between the two samples as a result of presence of thiols in the serum. It has been proposed that the cellular association of auranofin involves ligand exchange with membrane-localised thiols and Et₃PAuCl reacted with whole blood gives P-Au-S species (Berners-Price *et al.*, 1987b).

Both samples were soluble in DMSO (yellow solutions) and no precipitation was observed on addition of EMEM. The two samples were analysed immediately by ³¹P NMR and every 24 h for six consecutive days (7 days in total) with incubation at 37 °C between each analysis. Chemical shift changes (ppm) (*Table 6.1*) as well as physical changes were noted. After 24 hours incubation, both solutions changed from yellow to reddish-brown and small amounts of precipitated solids were observed. More precipitation took place on day 2 and day 3. While the sample in EMEM containing 10 % FCS continued to precipitate throughout the duration of the experiment, the one in medium without FCS remained the same from day 3.

Table 6.1. Chemical shift changes (ppm) of $[Pd(d2pyrpe)_2]PF_6)_2$ (**Pg 8**) as monitored by ^{31}P NMR spectroscopy every 24 h for 7 days. Samples were dissolved in DMSO, d_6 -DMSO and EMEM with or without Foetal calf serum (FCS). The ratio of the original chemical shift (68.2 ppm) and the new peak (37.6 ppm) is shown in parentheses.

	EMEM without FCS		EMEM with 10% FCS	
	Major peak	Minor peak	Major peak	Minor peak
0hr	67.1 (3)	38.5 (1)	68.2	
Day 1	67.2 (1)	38.4 (3)	67.4 (2)	37.5 (1)
Day 2	38.4		67.4 (2)	37.6 (1)
Day 3	38.4		67.4 (2)	37.6 (1)
Day 4	38.6		67.4 (1.5)	37.6 (1)
Day 5	38.4		37.8 (1)	67.4 (0.8)
Day 6	38.5		37.8 (1)	67.3 (0.7)
Day 7	38.5		37.8 (1)	67.3 (1)

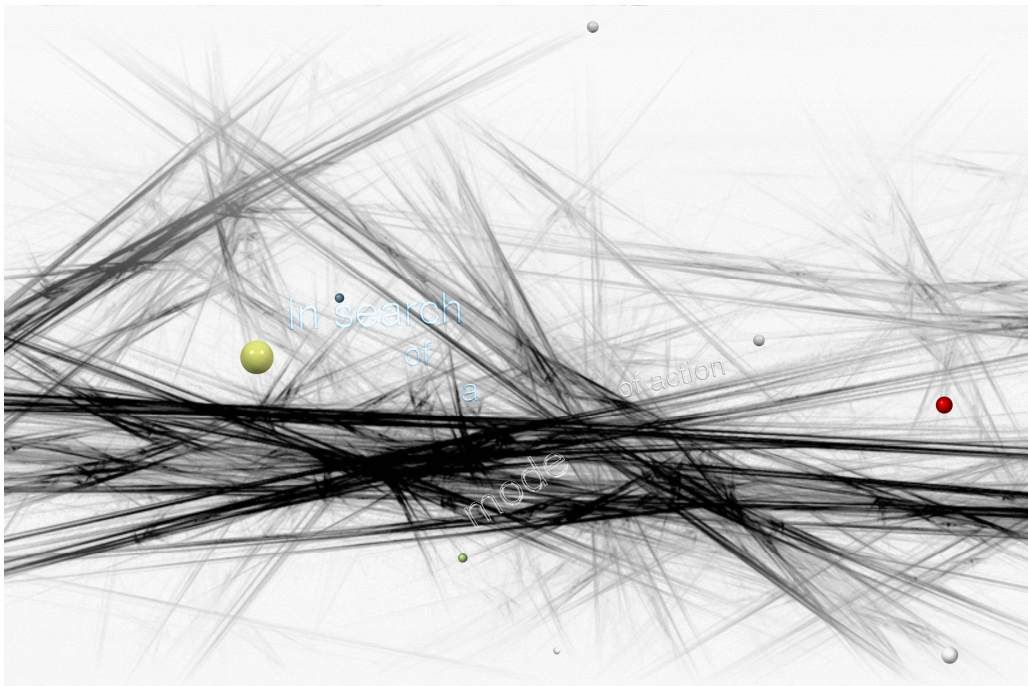
Results show that a new phosphorus peak (38.5 ppm) appeared immediately in the sample with EMEM without FCS (*Table 6.1*). The peak of the new species replaced the signal of the original compound (67.2 ppm) by the third day. In contrast, the peak at 37.5 ppm appeared after 24 h in the sample dissolved in EMEM (+10% FCS). From day 1 to day 3, the amount of the original compound was twice the amount of the new species (as indicated by the ratio). On day four, the ratios were reversed and the new species was 1.5 times more than the original compound. The two species reached equilibrium by the seventh day. The major difference was that while the original compound in EMEM (without FCS) was completely replaced by a new species, the one in medium (+10% FCS) seemed to equilibrate with the new species.

The chemical changes observed on day 4 can be correlated with increase in DIBAC₄(3) fluorescence in Jurkat cells treated with **Pg 8**. (*Fig.6.11*). The amount of the new species continued to increase (with subsequent reduction of the amount of the original compound) from day 4 and depolarisation of the plasma membrane continued to increase from day 4 to day 7. It is not clear whether the new species with a chemical shift of 37.6 ppm caused the loss in plasma membrane changes or the presence of both species (67.4 and 37.6 ppm). The

chemical shift 37.6 ppm may be attributed to diphosphine dioxide formed from oxidation of the ligand (d2pyrpe). The ligand in $[\text{Au}(\text{dppe})_2]\text{Cl}$ (dppe) was shown to form diphosphine dioxide with ^{31}P NMR shift of 38.5 ppm (in methanol) (Berners-Price *et al.*, 1987a). However, the biological properties of some products, e.g. the phosphinites and secondary phosphine oxides, are unknown.

Chapter VII

Apoptosis



7.1 Introduction

Programmed cell death (PCD), of which apoptosis is the most common morphological expression, is described as an orchestrated collapse of the cell (Ludovico *et al.*, 2002). This process plays an important role in the normal development of the cell and homeostasis of multicellular organisms. Apoptosis serves many critical functions, such as cell deletion during embryonic development, balancing cell numbers in continuously renewing tissues, hormone-dependent involution in the adult, immune system development, selective immune cell deletion, and many other physiologic processes (Allen *et al.*, 1997). Continuous signalling by growth factors, hormones, cytokines, cell-cell contacts and cell-matrix interactions are necessary for cells to refrain from undergoing apoptosis, keeping them alive (Vermes *et al.*, 2000). Cells that are most sensitive for survival signals stay alive and those that cannot compete with their more avid sister cells undergo apoptosis due to relative shortness of survival factors.

7.1.1 Apoptosis vs necrosis

In the middle of the last century, the concept of apoptosis emerged with its unique and dynamic morphological features that are distinguishable from senescence or necrosis, such as cell shrinkage, plasma membrane blebbing, chromatin condensation, nuclear membrane breakdown, and formation of small vesicles from the cell surface known as apoptotic bodies (Jiang and Wang, 2004). After apoptosis, phagocytes rapidly engulf the apoptotic bodies, and thus a potential inflammatory response is avoided. If apoptotic cells are not phagocytosed, they may develop secondary necrosis and cells undergoing post-apoptotic necrosis have been reported to reduce capacity to promote inflammation compared with primary necrotic cells (Magner and Tomasi, 2005).

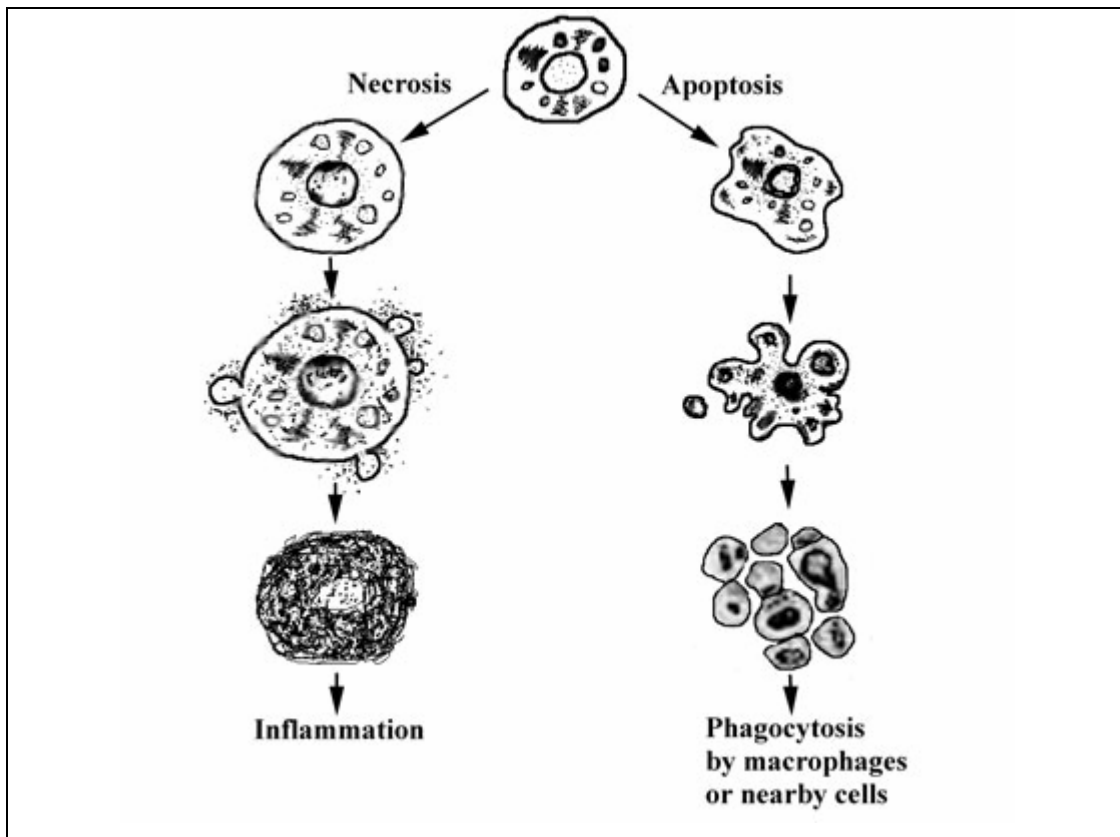


Fig. 7.1: Diagrammatic representation of the differences between apoptosis and necrosis.

Necrosis occurs only in response to a pathologic form of cellular injury and generally affects large groups of cells, characteristically causing an inflammatory response on tissue level (Allen *et al.*, 1997). ATP depletion is a critical precursor to the morphological changes occurring in the necrotic cell. Lethal levels of different toxicants may trigger either apoptotic or necrotic cell death, depending on the cell type and severity of the injury (Orrenius, 2004).

At least two major apoptotic pathways have been described in mammalian cells (Ludovico *et al.*, 2002). One requiring the participation of mitochondria, called “intrinsic pathway,” and another in which the mitochondria are bypassed and caspases are activated directly, called “extrinsic pathway”.

7.1.2 Apoptosis and mitochondria

Apoptosis induced by extracellular cues and internal insults such as DNA damage is mainly dependent on mitochondria, with the perturbation of inner membrane as an early event (Liu *et al.*, 2005). Mitochondrial membrane permeabilisation

(MMP), regulated by the mitochondrial permeability transition pore (MPT- a voltage dependent, cyclosporine A (CsA) sensitive, high conductance inner membrane channel), is widely accepted as being central to the process of mitochondrially induced apoptosis (Barnard *et al.*, 2004). Extensive evidence indicates that during apoptosis, the outer mitochondrial membrane (OMM) becomes permeable to intermembrane space proteins, including cytochrome *c* (Orrenius, 2004). Once released, cytochrome *c* promotes the activation of pro-caspase-9 directly within the apoptosome complex.

Four major arguments suggest the involvement of mitochondria in apoptosis (Susin *et al.*, 1998):

- Kinetic studies indicate that mitochondria undergo major changes in membrane integrity before classical signs of apoptosis manifest.
- Cell-free systems demonstrate that mitochondrial products are rate limiting for the activation of caspases and endonucleases in cell extracts.
- Pharmacological data indicate that certain drugs that stabilise mitochondrial membranes can prevent apoptosis.
- Extensive analysis of the proto-oncogene product Bcl-2 and its homologs has revealed that they act on mitochondria to regulate apoptosis.

Ever since the discovery that the Bcl-2 protein resides in mitochondrial membranes, the world of mitochondrial physiology and apoptosis has been inextricably linked (Reed *et al.*, 1998). The Bcl-2 family consists of both cell death promoters and cell death preventers. Mammalian species appear to contain at least 14 members, including the anti-apoptotic proteins Bcl-2, Bcl-XL, Mcl-1, A1/Bfl-1, and Bcl-W, and the pro-apoptotic members Bax, Bcl-XS, Bak, Bad, Bik, Bim, Bid, Hrk and Bok. Members of the Bcl-2 family proteins modulate permeabilisation of the OMM (Orrenius, 2004). Bcl-2 and Bcl-XL inhibit protein release whereas Bax and Bak stimulate this release. However, the precise mechanisms whereby mitochondrial proteins cross the OMM during apoptosis, and how Bcl-2 family proteins regulate this process are less certain.

The process of cell death is gene-regulated and elicits degradation of intracellular components and changes of plasma membrane (PM) structure (van Engeland *et al.*, 1996). These alterations of cellular constitution probably serve the purpose of elimination by phagocytosis before the dying cell provokes an inflammatory response. The mechanisms of the breakdown of plasma membrane potential (E_m) and the regulation of ion channels during apoptosis are under debate (Nolte *et al.*, 2004). These processes located at the plasma membrane are of great importance due to their key role in the regulation of apoptotic volume decrease (AVD), a feature that distinguishes apoptosis from necrosis. To date, breakdown in E_m has been described for a few apoptosis inducing agents like inducing Fas-antibodies, Ca^{2+} - ionophores, thapsigargin and dexamethasone.

7.1.3. “Extrinsic pathway”

Apoptosis was recognised as death by orchestrated sequence of countless cuts by hydrolytic enzymes, which degrade macromolecular structures like DNA and cytoskeleton, which underlie the observed apoptotic morphology (Vermes *et al.*, 2000). Members of a family of cysteine proteases play a directing role in this hydrolytic eruption. These proteases called caspases, appear to be the major players involved in the morphological process described in apoptosis, namely the ordered disassembly of the cell. All caspases are present constitutively in precursor forms (30-50 kDa) that must be proteolytically cleaved in order to be activated (Orrenius, 2004). An active caspase can subsequently activate additional pro-caspases, like itself, and/or different pro-caspases.

The caspases implicated in apoptosis can be divided into two functional subgroups based on their known or hypothetical roles in the process: initiator caspase (caspase-2, -8, -9 and -10) and effector caspases (caspase-3, -6 and -7) (Wang *et al.*, 2005). The functions of caspases can be summarised as to:

- arrest the cell cycle and inactivate DNA repair;
- inactivate the inhibitor of apoptosis (XIAP); and
- dismantle the cellular cytoskeleton.

In particular, caspase-9-driven apoptotic machinery seems to mainly involve mitochondrial-associated caspase cascade, while caspase-8-mediated apoptosis appears to be of importance in the receptor-mediated, i.e. Fas-mediated, cell death (Giovannini *et al.*, 2002).

Two proteins have been known to trigger apoptosis when released from mitochondria into the cytosol: cytochrome *c* and apoptosis inducing factor (AIF), a putative protease of 50 kDa (Reed *et al.*, 1998). Cytochrome *c* activates caspases through its effects on a protein called Apaf-1 (apoptosis protease activating factor). Upon binding cytochrome *c*, Apaf-1 binds pro-caspase-9, which eventually results in its proteolytic activation. AIF appears to directly activate certain members of the caspase family, resulting in proteolytic processing of their proproteins and production of the mature enzymes.

7.2 Apoptosis and cancer

Aberrations in cell death signalling (in membrane or cytoplasmic receptors; or alterations in genes that govern apoptosis) are involved in the pathogenesis of congenital malformations and many acquired diseases (Vermes *et al.*, 2000). Numerous pathologically induced conditions such as Alzheimer's, autoimmune disease, cancer, and AIDS, often show varying levels of apoptosis, with greatest significance lying in whether deregulation of apoptosis is a primary event in the pathology and subsequent clinical sequelae (Allen *et al.*, 1997). Defective apoptosis facilitates metastasis, because the cells can ignore restraining signals from neighbours and survive detachment from the extracellular matrix (Ray *et al.*, 2006).

Rapid growth of neoplasias appears to be closely associated with an impairment of the tumour cells to enter apoptosis (van Engeland *et al.*, 1996). Several genes involved in the apoptotic process have been found to be mutated or to be dysregulated at the transcriptional level. For instance, the p53 gene, which is thought to induce apoptosis, is frequently mutated in many tumour types. In contrast, over-expression of the bcl-2 gene, which is believed to protect cells from

apoptosis, is frequently observed in various malignancies. It is over-expressed in the majority of patients with low-grade non-Hodgkin's lymphoma and ~ 50% of high grade cases (Don and Hogg, 2004).

7.3 Apoptosis and chemotherapy

Mitochondria are believed to play a fundamental role in the regulation of programmed cell death and consequently in diseases characterised by abnormal apoptotic responses such as cancer (Barnard *et al.*, 2004). Consequently, there is considerable interest in targeting the mitochondrial cell death pathway in the development of new chemotherapeutic agents (*Fig 7.2*). Early results of clinical trials suggest the feasibility of targeting mitochondrial-based apoptosis regulatory pathways in human cancer therapy without limiting toxicity or significant effects on oxidative phosphorylation pathways (McKeage *et al.*, 2002). Augmerosen (G3139), an antisense 18-base phosphorothioate oligonucleotide complementary to the first 16 codons of Bcl-2 mRNA, hybridises to the target mRNA causing decreases in mRNA and protein levels of Bcl-2 on the membrane of the mitochondria. In clinical trials, augmerosen induced decreased Bcl-2 protein in tumour samples; biologically relevant plasma concentrations and clinical anti-tumour responses. These early experiences provide some support for the principle of targeting mitochondria with therapeutic agents to produce selective toxicity and clinically relevant anti-tumour responses.

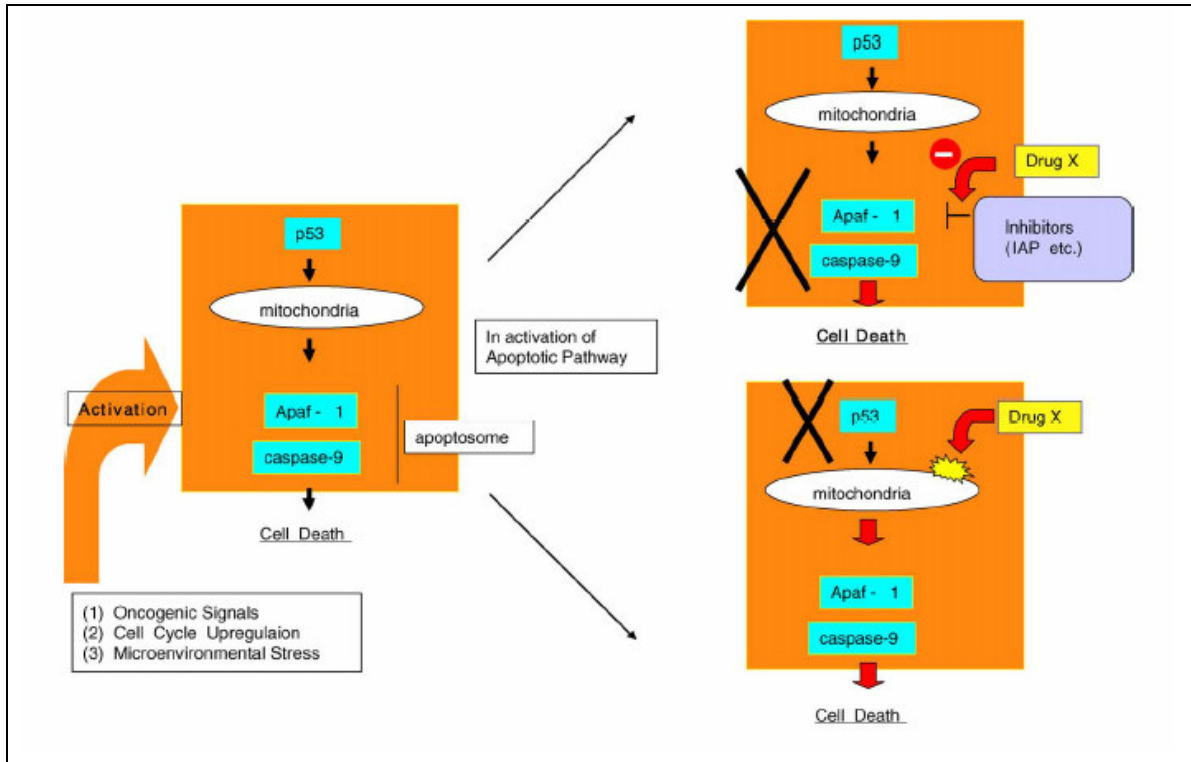


Fig. 7.2: Alteration of the apoptosis pathway in cancer cells and the strategy to induce selective death (Mashima and Tsuruo, 2005).

Induction of apoptosis by targeting specific molecules or pathways is not always straightforward. p53 has long been considered a prime target for therapeutic intervention (Yu, 2006). The role of p53 in apoptosis is complex, as it is able to *promote* and to *suppress* apoptosis. Clinically, the effect of p53 mutations on the sensitivity of tumours to the induction of a chemotherapeutic response has been disputed and so far p53 has failed to demonstrate a definite role in predicting treatment response. Conflicting results have been observed in various cancers. For example, p53 status appears to positively correlate to cisplatin response in ovarian cancer, but it did not seem to play a role in response to chemotherapy in small cell lung cancer (SCLC) patients.

Different cancer cells are likely to have different resistance mechanisms (Makin and Dive, 2001). For example, MCF-7 breast cancer cells are deficient in caspase 3, which renders them insensitive to apoptosis induced by many conventional chemotherapeutic agents. Reconstitution of caspase 3 renders these cells sensitive to etoposide and doxorubicin. Such an approach is, however, unlikely to be helpful in cells that are not deficient in caspase 3. Important emerging

questions are the pattern of alterations in the apoptotic pathway in particular tumours (cell) and the best strategy to exploit them and induce selective tumour cell death (Mashima and Tsuruo, 2005).

7.4 Detection of apoptosis by flow cytometry

In the early stages of apoptosis, changes occur at the cell surface, which until now have remained difficult to recognise (Vermes *et al.*, 1995). One of these plasma membrane alterations is the translocation of phosphatidylserine (PS) from the inner side of the plasma membrane to the outer layer, by which PS becomes exposed at the external surface of the cell. Annexin V is a Ca^{2+} dependent phospholipid-binding protein with high affinity for PS. Hence, this protein can be used as a sensitive probe for PS exposure upon the cell membrane. Translocation of PS to the external cell surface is not unique to apoptosis, but occurs also during cell necrosis. The difference between these two forms of cell death is that during the initial stages of apoptosis the cell membrane remains intact, while at the very moment that necrosis occurs the cell membrane loses its integrity and becomes leaky.

Functional analyses of apoptotic preparations are complicated by the presence of varying proportions of necrotic cells (Magner and Tomasi, 2005). Relying on differences in permeability of plasma membrane of live, dead and apoptotic cells to DNA dyes like propidium iodide (PI), ethidium bromide (EB) and Hoechst-33342 (HO33342), one can discriminate vital, apoptotic and necrotic cells (Vermes *et al.*, 2000). PI is not excluded by necrotic cells and after entering the cell, it intercalates with DNA causing red fluorescence of the necrotic nucleus. Apoptotic cells, which still have an intact membrane exclude PI and are not stained.

Viability tests can also be performed with 7-amino-actinomycin D (7-AAD) which penetrates cell membranes of dying or dead cells and intercalates into double-stranded nucleic acids, especially to guanine cytosine (GC)-rich regions (Huth *et al.*, 2006). 7-AAD can be excited by 488 nm argon laser and emits in the far red range of the spectrum ($\lambda_{\text{em}_{\text{max}}}$: 655 nm) (Derby *et al.*, 2001). Its spectral

emission can be effectively separated from the emissions of phycoerythrin (PE) ($\lambda_{em_{max}}$: 578 nm). Measurements of annexin V binding, executed simultaneously with the 7-AAD uptake test, provides an excellent way to detect apoptotic cells and to discriminate between different stages of apoptosis at the single cell level. Annexin V assay has been used to measure apoptosis of cell types that occur naturally in suspension (van Engeland *et al.*, 1996). Monitoring apoptosis-related PS exposure by tissue-bound or adherent cell types in cultures faces the problem of PS exposure by sample handling for flow cytometry analysis.

The current study aimed at investigating whether cytotoxicity (*Chapter 5*) was due to induction of apoptosis and/or necrosis by $[Au(dppe)_2]Cl$ and **Pg 8** on Jurkat cells. Annexin V binding assay was carried out and cells were evaluated for apoptosis by flow cytometry. Camptothecin (1 μM), a topoisomerase I inhibitor that efficiently induces apoptosis in Jurkat cells (Sané *et al.*, 2004) was used as a positive control. The procedure was modified from the literature (Allen *et al.*, 1997).

7.5 Materials and methods

7.5.1 Reagents

- RPMI and Foetal Calf Serum.
- Phosphate buffered saline (PBS).
- Binding buffer (238 mg Hepes, 876 mg NaCl, 37.3 mg KCl, 26.5 mg $CaCl_2$, 9.5 mg $MgCl_2$ in de-ionised water, at pH 7.4)
- Annexin V- FITC (BD Biosciences Pharmingen)
- Propidium Iodide (PI) (Sigma-Aldrich)
- Camptothecin (1 μM) (Sigma-Aldrich)
- **Pg 8** (0.711 and 1.422 μM)
- $[Au(dppe)_2]Cl$ (0.131 and 0.262 μM)

7.5.2 Cell lines and culture

The human Jurkat cell line was cultured in RPMI 1640 supplemented with 10% v/v heat-inactivated FCS and 1% penicillin-streptomycin. Cells were maintained in a humidified atmosphere of 5% carbon dioxide at 37 °C.

7.5.3 Flow cytometric analysis of apoptosis

Cells (1×10^5 cells/ml) were treated with $[\text{Au}(\text{dppe})_2]\text{Cl}$ and **Pg 8** for 18, 24 and 48 h in cell culture flasks. After an incubation period, cells were decanted from flasks and centrifuged for 5 min at 200 g. The cell pellet was washed with PBS (1% FCS) and resuspended in 1 ml binding buffer. 100 μl of cell suspension was transferred to flow cytometer tubes. 5 μl of Annexin V-FITC and 10 μl propidium iodide were added to some tubes (unstained samples were also prepared). The cell suspensions were mixed gently and incubated for 15 min in the dark at room temperature (25 °C). 400 μl of binding buffer was then added to each tube and analysis was carried out within an hour with a flow cytometer (Beckman Coulter FC 500).

7.5.4 Statistical methods

All assays were performed at least three times and results are presented as \pm S.E.M. The statistical evaluation of the results was performed by two way ANOVA followed by Bonferroni's Multiple Comparison Test. Significance was established at $P < 0.05$. The treatment that was significantly different from the fresh, viable cells is denoted with an asterisk (*).

7.6 Results and discussion

Fig 7.3 shows the percentages of cells undergoing various stages of apoptosis and are an average of three separate experiments (\pm S.E.M). Figure 7.4 shows actual histograms of treated and untreated cells undergoing apoptosis (48 h).

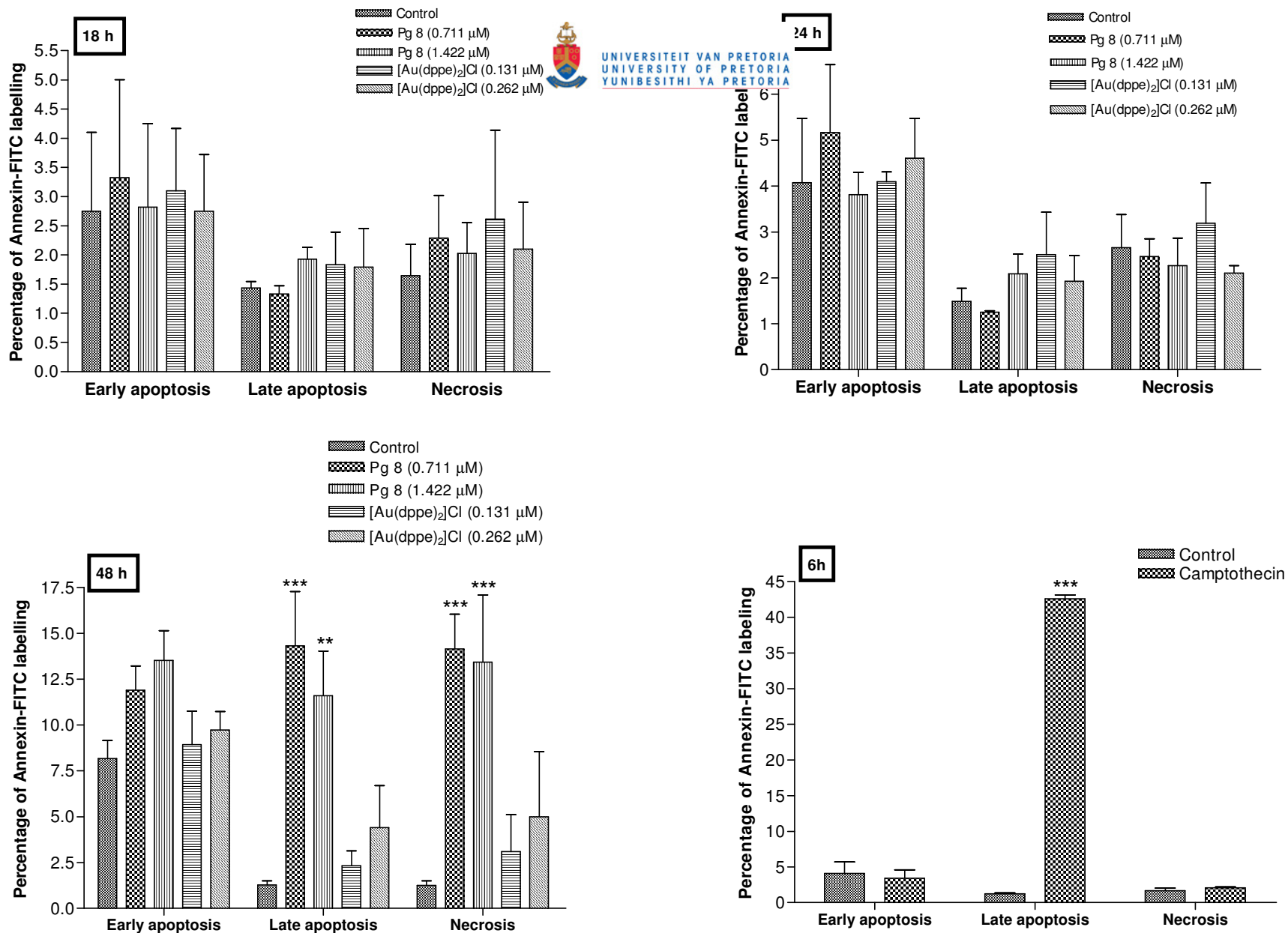


Fig. 7.3: Percentage of Jurkat cells undergoing apoptosis and necrosis after treatment with experimental compounds for 18, 24 and 48 h. The cells treated with camptothecin were incubated for 6h. The data is presented as a mean of three experiments (\pm S.E.M).

After incubation of Jurkat cells with the compounds for 18 and 24 h, no significant differences were noted between the untreated and the treated groups as between 85 and 90% of cells were viable. However, after exposure of the cells for 48 h, significant differences were observed. Untreated cells had an average of 85% of cells in a viable state and only 8% at the early apoptotic stage. $[\text{Au}(\text{dppe})_2]\text{Cl}$ (0.131 and 0.262 μM) induced apoptosis in 12% of the cells (9% in early apoptosis and 3% in the stage of late apoptosis) while 77% of the cells were still viable. In contrast, **Pg 8** (0.711 and 1.422 μM) significantly induced apoptosis in 25% of the cells while 14% of cells had undergone necrosis. Only 50% of the cells were viable in this group. Unlike **Pg 8** and $[\text{Au}(\text{dppe})_2]\text{Cl}$, camptothecin (1 μM) induced apoptosis in Jurkat cells within a short time. After incubation for 6h, about 40% of the cells were in the late apoptotic stage. Viable cells were just over 50% while only 2% of the cells were necrotic. DNA topoisomerase I and II inhibitors induce apoptosis in various cell lines and this is due to DNA-protein complex formation stabilised by DNA topoisomerase I inhibitors that ultimately signal the onset of apoptosis (Sané *et al.*, 2004).

The two compounds behaved differently as observed from the histograms (Fig 7.4). $[\text{Au}(\text{dppe})_2]\text{Cl}$ treated group had more viable cells (77%) and very few in the necrotic stage (~4 %) while **Pg 8** had a lower percentage of viable cells (50%) and most notably a much higher percentage of them in the necrotic stage (14%). This difference is significant as cytotoxicity assays showed that the former drug was more toxic ($\text{IC}_{50} = 0.131 \mu\text{M}$) while **Pg 8** was at least 5 times less toxic ($\text{IC}_{50} = 0.711 \mu\text{M}$) to Jurkat cells. The mode of cell killing differs as $[\text{Au}(\text{dppe})_2]\text{Cl}$ mainly induced apoptosis while **Pg 8** seemed to induce both apoptosis and necrosis. While the former compound was toxic to lymphocytes ($\text{IC}_{50} = 0.903 \mu\text{M}$), **Pg 8** was not cytotoxic even at 100 μM . This selectivity for cancer cells by the latter compound may be due to this difference in induction of cell death (necrosis vs. apoptosis). However, it is not clear which factors play a role in triggering an apoptotic or necrotic pathway in the different cells (lymphocytes vs. jurkat cells).

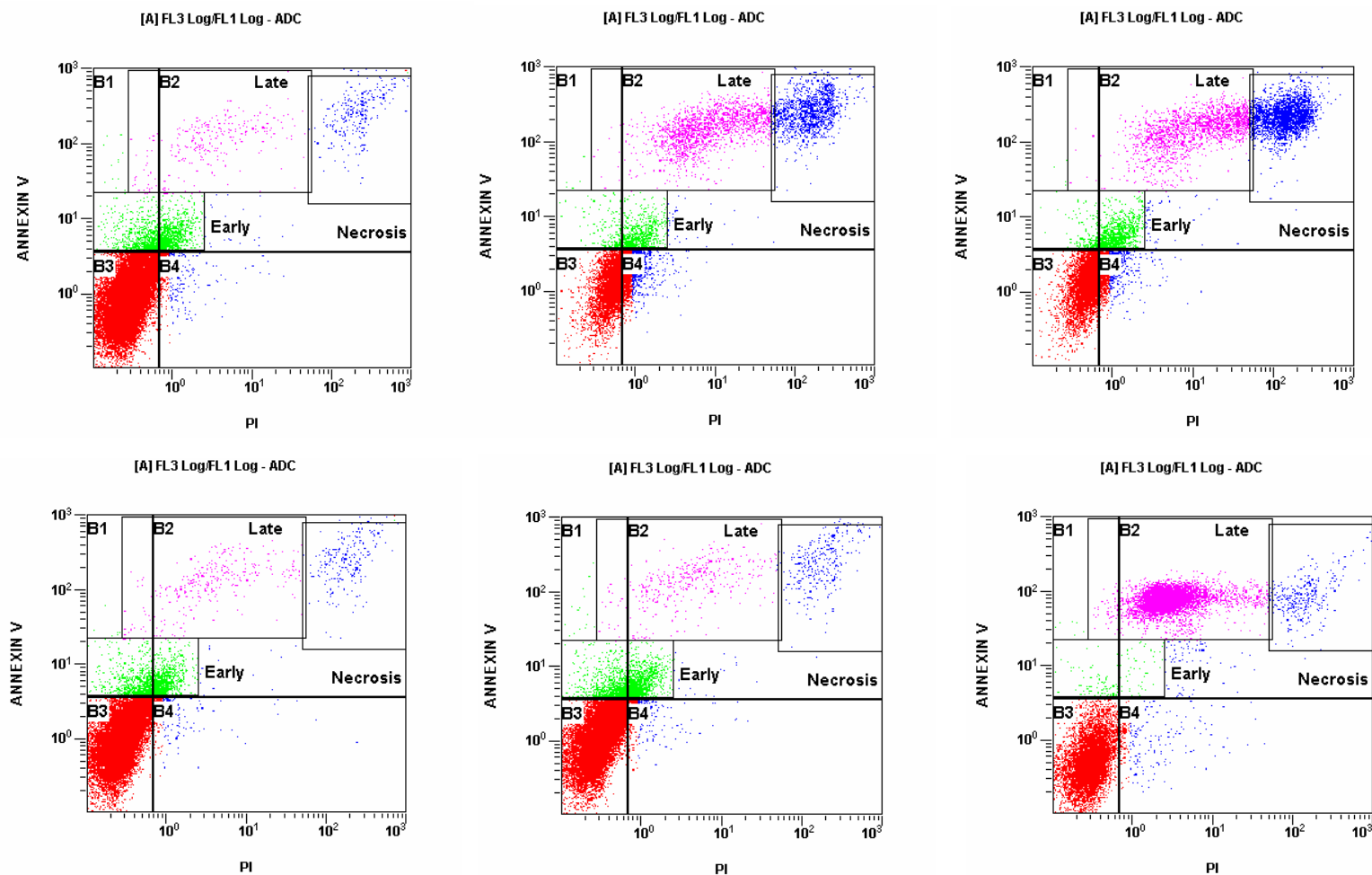


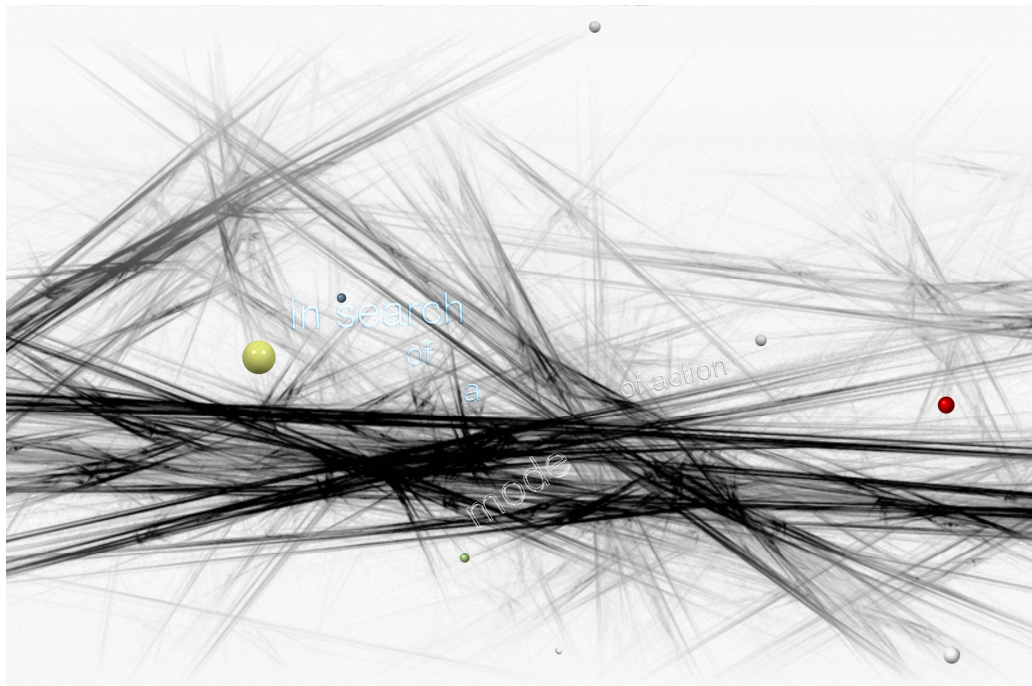
Fig. 7.4: Contour diagram of FITC-Annexin V/PI flow cytometry of Jurkat cells cultured for 48 h with and without experimental compounds. One representative experiment is shown. The top three diagrams (left to right) represent untreated, **Pg 8** (0.711 μM) and **Pg 8** (1.422 μM) while the bottom three diagrams (left to right) represent $\{[\text{Au}(\text{dppe})_2]\text{Cl}\}$ (0.131 μM) and 0.262 μM and camptothecin (1 μM).

Chemotherapeutic drugs induce damage at a number of different loci, and it is the balance between the pro-apoptotic signals engendered by this damage and survival signals that determines the cellular fate (Makin and Dive, 2001). Various paradigms integrating cytotoxic chemicals and cell death are evolving as pathways become better characterised (Orrenius, 2004). Lethal levels of different toxicants may trigger either apoptotic or necrotic cell death, depending of the cell type and severity of the injury. Further, effectuation of the apoptotic death program requires maintenance of a sufficient intracellular energy level and of a redox state compatible with caspase activation. Thus, ATP depletion or severe oxidative stress may re-direct otherwise apoptotic cell death to necrosis.

A substantial body of recent experimental data suggests that targeting cancer-specific alterations of the apoptotic pathway is an effective strategy to elicit tumour regression *in vivo* (Mashima and Tsuruo, 2005). Further elucidation of the molecular mechanisms of apoptosis in tumour cells and the molecular classification of tumour cells is required to identify an individual strategy to induce selective death to each tumour.

Chapter VIII

The cell cycle



8.1 Introduction

Cell cycle is arguably the most fundamental process that occurs in eukaryotic cells and is quite literally a matter of life and death (Thomas and Goodyer, 2003). The stages vary greatly in duration among cell types, but typical time spans are as follows (Hernandez and Rathinavelu, 2006):

- *S* phase: 10 to 20 hours. This is the synthesis phase, where DNA replication occurs.
- *M* phase: 0.5 to 1 hour. This phase is where mitosis occurs; mitosis is the actual cell division where the two DNA copies separate.
- *G*₁ and *G*₂ phases: The duration of the *G*₂ phase is in the same range of 2 to 10 hours. These are gaps that occur between mitosis and synthesis, which prepare the cell for the next phase.
- *G*₀ phase: A sub-phase of *G*₁ in which the cells are resting, i.e., they are not preparing to divide.

The DNA content of cell nuclei varies through the cell cycle in a predictable fashion- cells in *G*₂ or *M* have twice the DNA content of cells in *G*₁, and cells undergoing DNA synthesis in *S* phase have an intermediate amount of DNA (Thomas and Goodyer, 2003).

8.1.1 Cell cycle regulation

The progression of the cell cycle is tightly regulated by defined temporal and spatial expression, localisation and destruction of several cell cycle regulators, which exhibit highly dynamic behaviour during the cell cycle (Thomas and Goodyer, 2003). It is firmly established that a family of protein kinases, termed cyclin-dependent kinases (CDKs), controls the transitions between successive phases of the cell cycle in all eukaryotic cells (Nigg, 1995). CDKs are serine/threonine protein kinases that are activated at specific points of the cell cycle (Schafer, 1998). Sequential formation, activation and subsequent inactivation of cyclins and CDKs are critical for the control of the cell cycle (Kurita-Ochiai *et al.*, 2006). In addition, CDK inhibitors (CKIs) can play a key role in

controlling cell cycle progression by negatively regulating CDK activities at specific times in the cycle.

Table 8.1. Cyclin-CDK complexes are activated at specific points of the cell cycle. CAK, CDK activating kinase (Vermeulen *et al.*, 2003).

CDK		Cyclin	Cell cycle phase activity
CDK4		Cyclin D1, D2, D3	G ₁ phase
CDK6		Cyclin D1, D2, D3	G ₁ phase
CDK2		Cyclin E	G ₁ /S phase transition
CDK2		Cyclin A	S phase
CDK1	(cdc2)	Cyclin A	G ₂ /M phase transition
CDK1	(cdc2)	Cyclin B	Mitosis
CDK7		Cyclin H	CAK, all cell cycle phases

There are two classes of mammalian CDKI known to date (Park *et al.*, 2002). One group is the CIP/KIP family, including p21, p27 and p57 having broad specificity. The other is the INK4 family, including p15, p16, p18 and p19, which target the CDK4 and CDK6 (*Fig. 8.1*).

In normal human cells, the diverse checkpoints represent fail-safe mechanisms whose key role is to avoid the accumulation of genetic errors during cell division (Bartek *et al.*, 1999). Among the best-known checkpoints are G₁ arrest mediated by p53/p21 axis in response to DNA damage, checkpoints that monitor the quality of DNA replication and the occurrence of DNA damage during the S-phase, and the status of spindle assembly in mitosis. Although some DNA damage checkpoint cascades respond to DNA damage in quiescent cells, most operate only in proliferating cells, with the nature of the response dependent on variables such as cell type and differentiation, extent of DNA damage, and the position of the cell in the cell cycle (Scott *et al.*, 2004). Thus normal cells that have not passed the G₁ restriction point will arrest in G₁, S-phase cells will undergo a delay in S and may undergo a subsequent G₂ arrest, and those cells already in G₂ will be prevented from entering M-phase until repair of potentially lethal damage is complete.

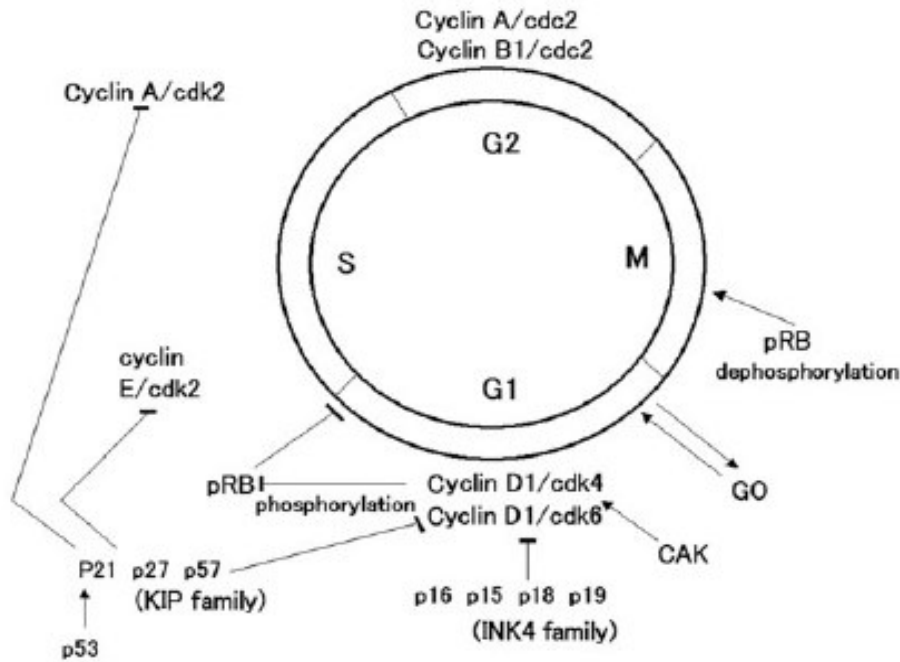


Fig. 8.1: Scheme of cell cycle regulation. CAK, cdk-activating kinase; cdk, cyclin-dependent kinase; INK4, inhibitor of cdk4; KIP, kinase inhibitor protein; pRB, retinoblastoma protein (Dobashi, 2005).

8.2 Cell cycle and carcinogenesis

The cell cycle is an ubiquitous, complex process involved in the growth and proliferation of cells, organismal development, regulation of DNA damage repair, tissue hyperplasia as a response to injury, and diseases such as cancer (Schafer, 1998). Cancer is increasingly viewed as a cell cycle disease (Bartek *et al.*, 1999). This view reflects the evidence accumulated that the vast majority of, and quite likely all tumours have suffered one or more defects that derail the cell cycle machinery. The process of tumourigenesis leads to multiple genetic changes that alter the regulation of signalling pathways, such as those involved in cell cycle and mitotic spindle checkpoints, DNA repair, and apoptosis that lead to further molecular abnormalities and increased cell proliferation (Scott *et al.*, 2004).

Most, if not all, human cancers show a deregulated control of G₁ phase progression, a period when cells decide whether to start proliferating or to stay quiescent (Golias *et al.*, 2004). In the normal cell, oncoproteins carry a signal from

the cell surface to the nucleus with the end result being transcription and initiation of the cell cycle (Schafer, 1998). In transformed cells these signal transduction pathways are always “turned on” or their inhibitory pathways are “turned off” (*Table 8.2*).

Table 8.2. Cell cycle regulators in neoplasia

Oncoprotein/ Tumour suppressor	Normal cell cycle function	Oncogenic alteration
p53	Promotes G ₁ arrest after DNA damage	Mutation
pRb	Restriction point regulator	Deletion
Mdm-2	Overrides p53 transcriptional activity	Gene amplification or enhanced mRNA translation
P16	Inactivates G ₁ cyclin-cdk complexes	Deletion
Cyclin D1	Initiates cell cycle	Gene amplification
Cdc25A, cdc25B	Activates G ₁ /S cdk	Overexpression

In terms of molecular pathogenesis of cancer, cell cycle defects can either represent the initial, predisposing event, or contribute to tumour progression (Bartek *et al.*, 1999). The tumour suppressor gene p53 codes for a transcription factor which regulates oncogene expression, gene transcription, and DNA synthesis and repair systems, as well as apoptosis (Ahn *et al.*, 2002). As a transcription factor, the p53 protein binds to a specific sequence on the promoter region and then activates the transcription of cellular genes. In normal cells, DNA damage induces p53 expression, leading to cell cycle arrest in the G₁ phase and apoptosis, as well as inhibition of DNA replication. However, normal function of p53 is missing in immortalised cells. It has been reported that, except for cervical cancers, most (50%) cancer development results from p53 gene mutation.

8.3 Cell cycle and chemotherapy

The prediction of tumour behaviour and response to treatment has led to interest in the assessment of the proliferative potential of tumours (Golias *et al.*, 2004). Understanding the molecular details of the cell cycle regulation and checkpoint abnormalities in cancer, and manipulation of these control mechanisms offers

insight into potential therapeutic strategies. Anti-cancer agents may alter one or more regulatory events in the cell cycle resulting in blockade of cell cycle progression, thereby reducing the growth and proliferation of the cancer cells (Adhami *et al.*, 2004). For example, the function of p53 in sentencing inappropriately growing cells to death has implications for cancer development and chemotherapy (Collins *et al.*, 1997). Murine tumours with functional p53 respond to chemotherapy by promoting their own demise, but those lacking p53 typically do not.

Initially, some anti-cancer agents were investigated for their abilities to inhibit cell cycle transitions and suppress hyperproliferation by either down-regulating cyclin/cdk expression or up-regulating the CKI (Dobashi, 2005). Now, however, much attention is being paid to their potential for inducing apoptosis. The up-to-date rational drug development in cancer therapy appears to concentrate on the discovery of effective pharmaceutical reagents that can intervene diverse signaling pathways (Liu *et al.*, 2005). The regulatory system that controls normal cell proliferation and cell death stays balanced through orchestrated cascades of multiple interacting signalling routes. When this rhythmic scheme is perturbed by biochemical agents, it often results in the breakdown of cell cycle machinery, subsequently entering into apoptosis.

The most potent anti-cancer drugs act by damaging DNA; their effect is greatest during the S phase (Hernandez and Rathinavelu, 2006). Other anti-cancer drugs, such as Taxol™ block the formation of the mitotic spindle in the M phase. For anti-cancer drugs to be effective, a high percentage of tumour cells must be undergoing division (S and M phases). Anti-folates such as methotrexate, trimetrexate and CB3717 (N¹⁰-propargyl-5,8-dideazafolic acid) tend to cause accumulation of cells in S phase or at the G₁/S interphase (Skelton *et al.*, 1999). Agents which disrupt formation of the mitotic spindle, such as the *Vinca* alkaloids, arrest cells in G₂/M, phase.

Replication process is directly disrupted with DNA-damaging agents such as cisplatin, mitomycins, bleomycins, etoposide and irinotecan (a camptothecin derivative) (Owa *et al.*, 2001). Camptothecin (CPT) is a DNA topoisomerase I

inhibitor that blocks the DNA religation of topoisomerase I cleavage complexes (Zhou *et al.*, 2002). During DNA replication, the collision between topoisomerase I cleavage complexes and DNA replication forks generates double-strand breaks. Therefore, CPT is most potent during DNA replication and arrest of cells in G₂ phase results in DNA damage. CPT derivatives are used clinically to treat many types of solid tumours, including colorectal and ovarian carcinomas, but not all cancer cell lines are equally sensitive to it.

8.4 Determination of the effect of Pg 8 and [Au(dppe)₂]Cl on cell cycle of Jurkat cells

It has been shown (**Chapter 7**) that **Pg 8** and [Au(dppe)₂]Cl caused Jurkat cells to undergo apoptosis after exposure for 48 h. The aim of this experiment was to determine if cell death was as a result of cell cycle arrest by these compounds. The procedure was modified from the literature (Scott *et al.*, 2004). Cell cycle analysis was performed by flow cytometric evaluation of DNA content.

8.5 Materials and methods

8.5.1 Reagents

- RPMI and foetal calf serum
- RNase (Sigma-Aldrich)
- Propidium Iodide (PI) (Sigma-Aldrich)
- Phosphate buffered saline (PBS)
- Ethanol (100%) (Sigma-Aldrich)
- **Pg 8** (0.711 and 1.422 µM)
- [Au(dppe)₂]Cl (0.131 and 0.262 µM)

8.5.2 Cell lines and culture

Human T-cell lines (Jurkat) were cultured in RPMI 1640 supplemented with 10% v/v heat-inactivated FCS and 1% penicillin-streptomycin. Cells were incubated with the experimental compounds for 18, 24 and 48 hours at 37 °C and 5% carbon dioxide.

8.5.3. Flow cytometric analysis of cell cycle progression

Cells (1×10^5 cells/ml) were treated with $[\text{Au}(\text{dppe})_2]\text{Cl}$ and **Pg 8** for 18, 24 and 48h in cell culture flasks. After the incubation period, they were decanted from flasks and centrifuged for 5 min at 200 g. The cell pellet was re-suspended in 500 μl PBS and chilled on ice. The cold cell suspension was then added rapidly to flow cytometer tubes containing 500 μl of ice cold ethanol. Mixing was carried out by forcing air bubbles through the suspension and then kept on ice for 15 minutes. The cells were then centrifuged for 3 minutes at 300 g followed by suspension of the cell pellet in 125 μl of RNase (2mg/ml 1.12% w/v sodium citrate). After incubation for 15 minutes at 37 °C in a water bath, 125 μl of PI was added to each tube and mixed well. Samples were allowed to stand for 30 minutes at room temperature before analysis by flow cytometry (Beckman Coulter FC 500). DNA histograms were collected and estimation of the percentages of cells in G_1 , S and G_2/M was performed with a computer software program (Multicycle, Phoenix Flow systems, San Diego, CA).

8.5.4 Statistical methods

All assays were performed at least five times and all data are presented as \pm S.E.M. Differences in the cell cycle profiles (G_0/G_1 , S and G_2/M phases) of untreated and treated cells were also compared by ANOVA (2-way) followed by Bonferroni's Multiple Comparison Test (*Fig. 8.7*). Significance was established at $P < 0.05$. The treatment that was significantly different from the fresh, viable cells is denoted with an asterisk (*).

8.6 Results and discussion

Representative histograms and graphs showing changes in the cell cycle profiles (G_0/G_1 , S and G_2/M phases) after 18, 24 and 48 h with or without exposure to the experimental compounds are shown below (Fig 8.2-8.6).

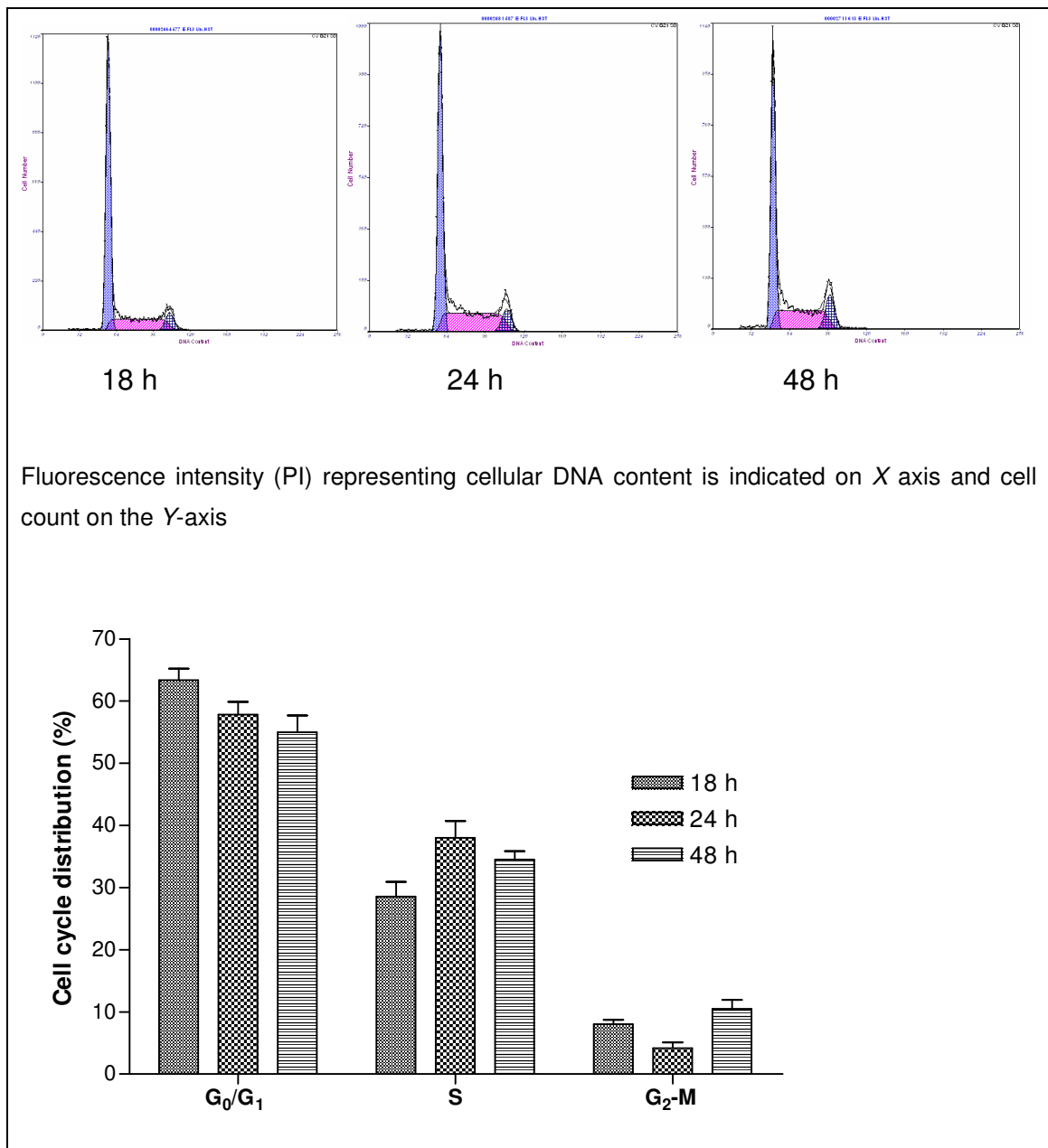


Fig. 8.2: Cell cycle progression of untreated Jurkat cells. Cells were incubated for 18, 24 and 48 hours without the experimental compounds. Cell cycle analysis was performed using flow cytometric evaluation of DNA content.

At 24 h, there was a decrease in the number of cells in G₁ phase (from 63 to 58%), which was complimented by a slight increase in the number of cells in the S-phase (from 29 to 38 %) (*Fig. 8.2*). At 48 h, there was a decrease in the S-phase (from 38 % to 35 %) and a marked increase in the G₂ phase (from 4 to 11%). The observed changes in the cell cycle progression of untreated cells were used to determine if any changes had occurred in the treated samples (*Fig. 8.3-8.6*).

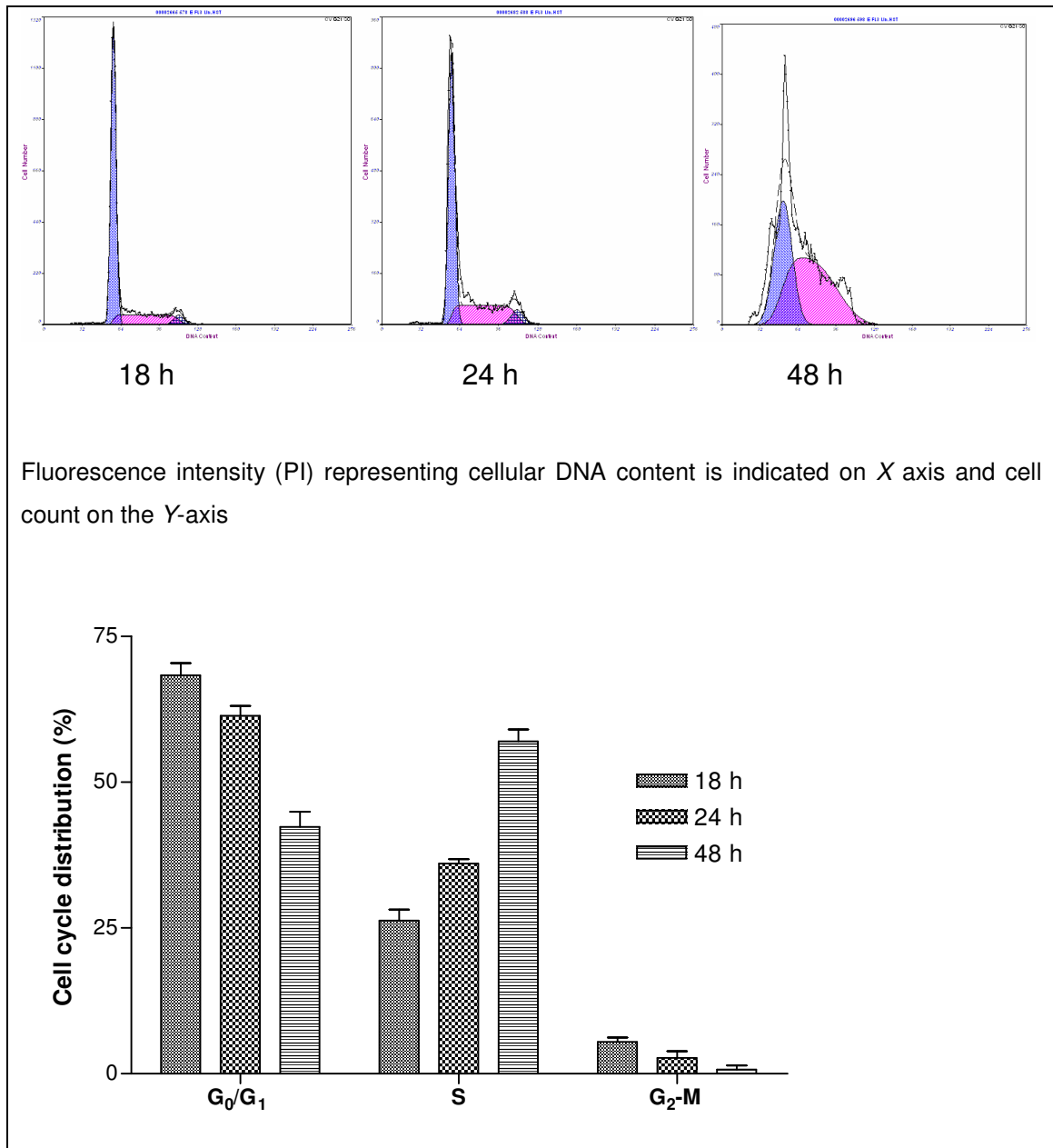


Fig. 8.3: Effect of 0.711 μM of **Pg 8** on the cell cycle progression of Jurkat cells after 18, 24 and 48 h treatment.

Cells exposed to 0.711 μM of **Pg 8** for 18 and 24 h did not exhibit any differences in cell cycle progression (*Fig. 8.3*). After 48 h, the number of cells in G_1 was significantly reduced (from 61 to 47%) with the subsequent accumulation of cells in S-phase (from 36 to 57%). Due to this blockade of the S-phase, G_2 phase contained virtually no cells (1%).

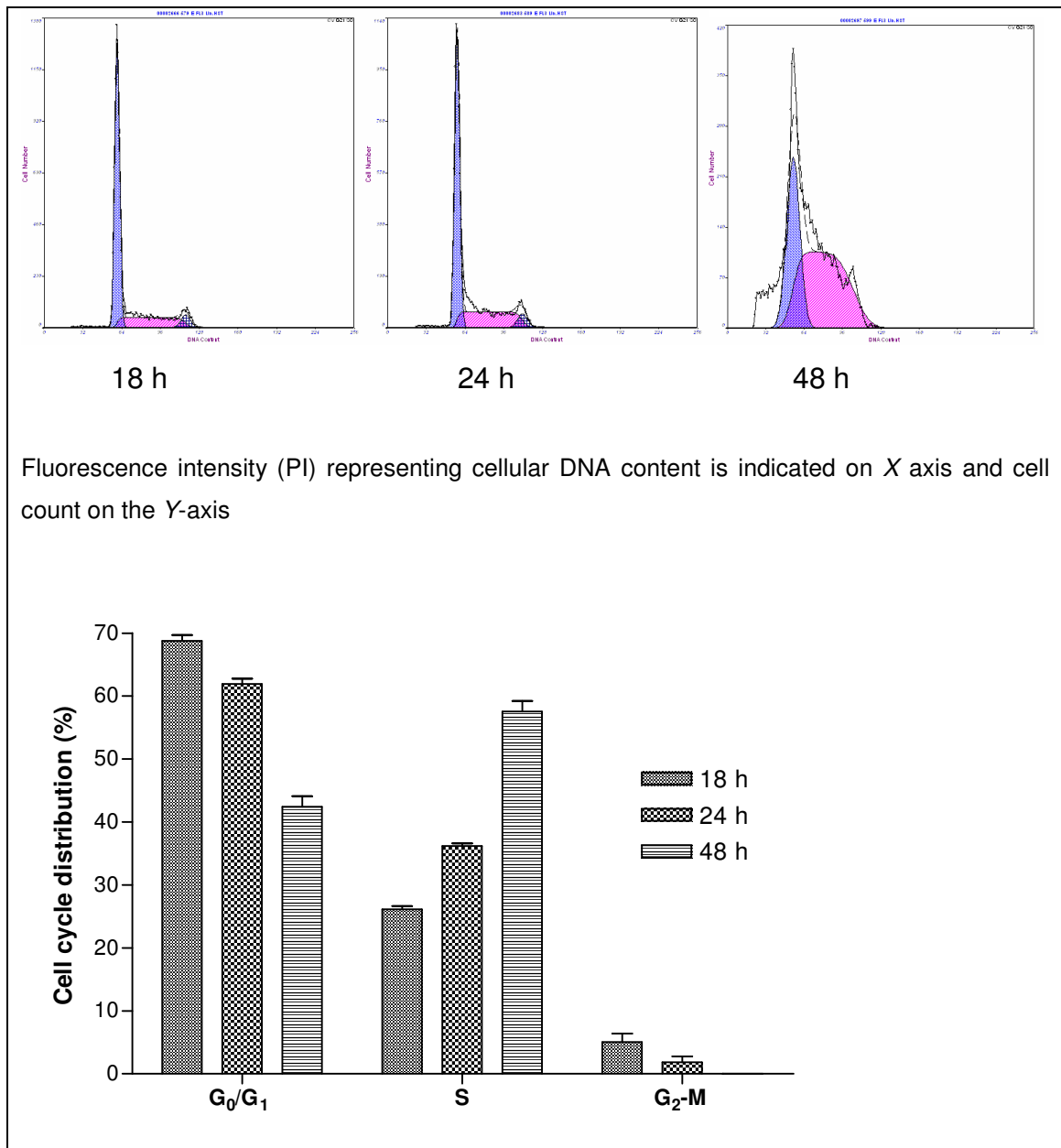


Fig. 8.4: Effect of 1.422 μM of **Pg 8** on the cell cycle progression of Jurkat cells after 18, 24 and 48 h treatment.

Cells exposed to 1.422 μM of **Pg 8** (*Fig. 8.4*) showed the same behaviour as the ones exposed to half the concentration (*Fig. 8.3*). After 48 h, the number of cells

in G₁ was significantly reduced (from 62 to 47 %) with the subsequent accumulation of cells in S-phase (from 36 to 58%). There were no cells in the G₂ phase.

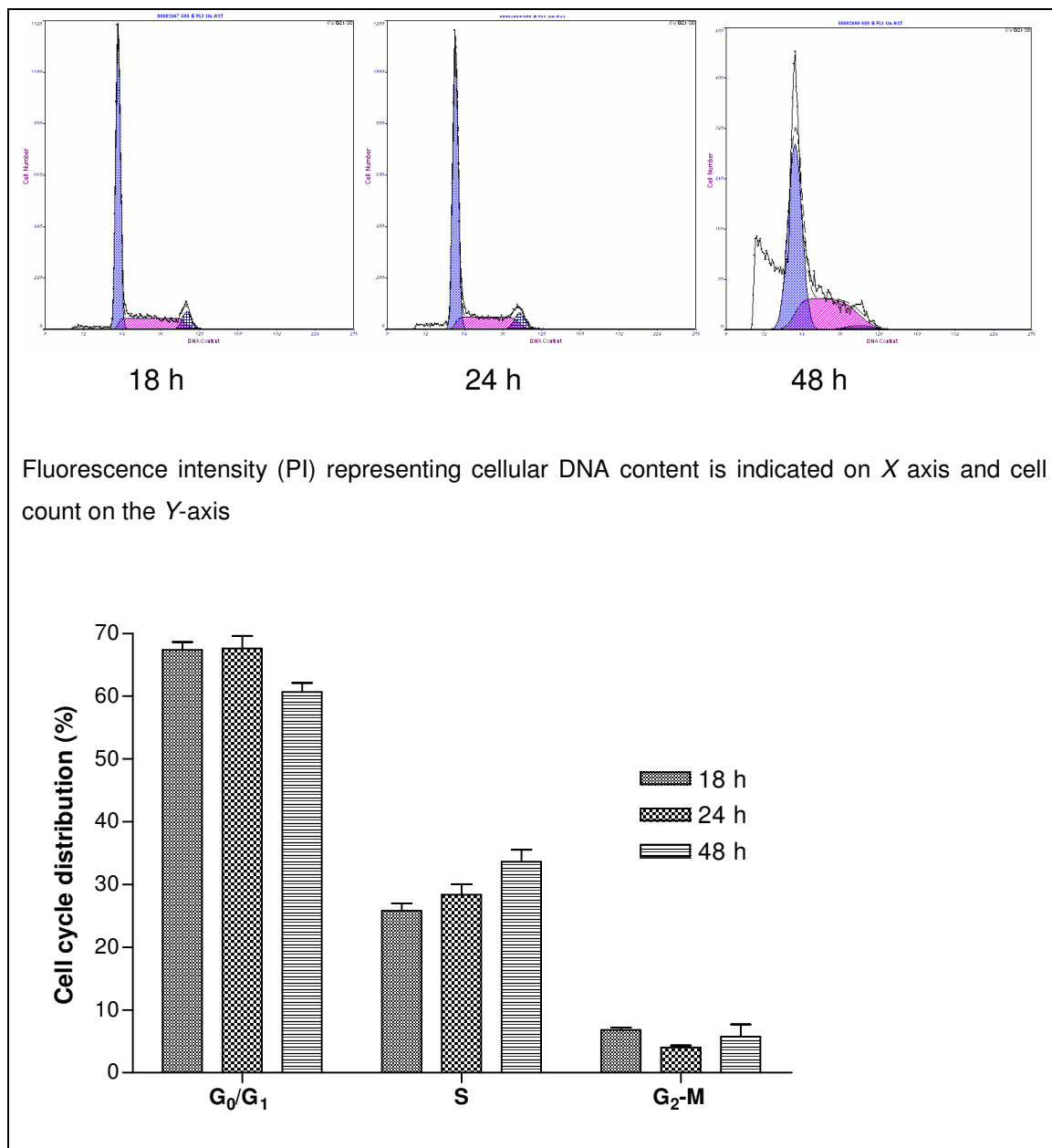


Fig. 8.5: Effect of 0.131 μM of $[\text{Au}(\text{dppe})_2]\text{Cl}$ on the cell cycle progression of Jurkat cells after 18, 24 and 48 h treatment..

After exposure of Jurkat cells to $[\text{Au}(\text{dppe})_2]\text{Cl}$ (0.131 μM) for 18 h and 24 h, no significant changes to progression of cell cycle were observed (*Fig. 8.5*). However, significant changes were observed after 48h. The number of cells in G₁

decreased from 68 to 61 % while there was an increase in S-phase (from 28 to 34%). The number of cells in G₂ phase increased insignificantly (from 4 to 5%).

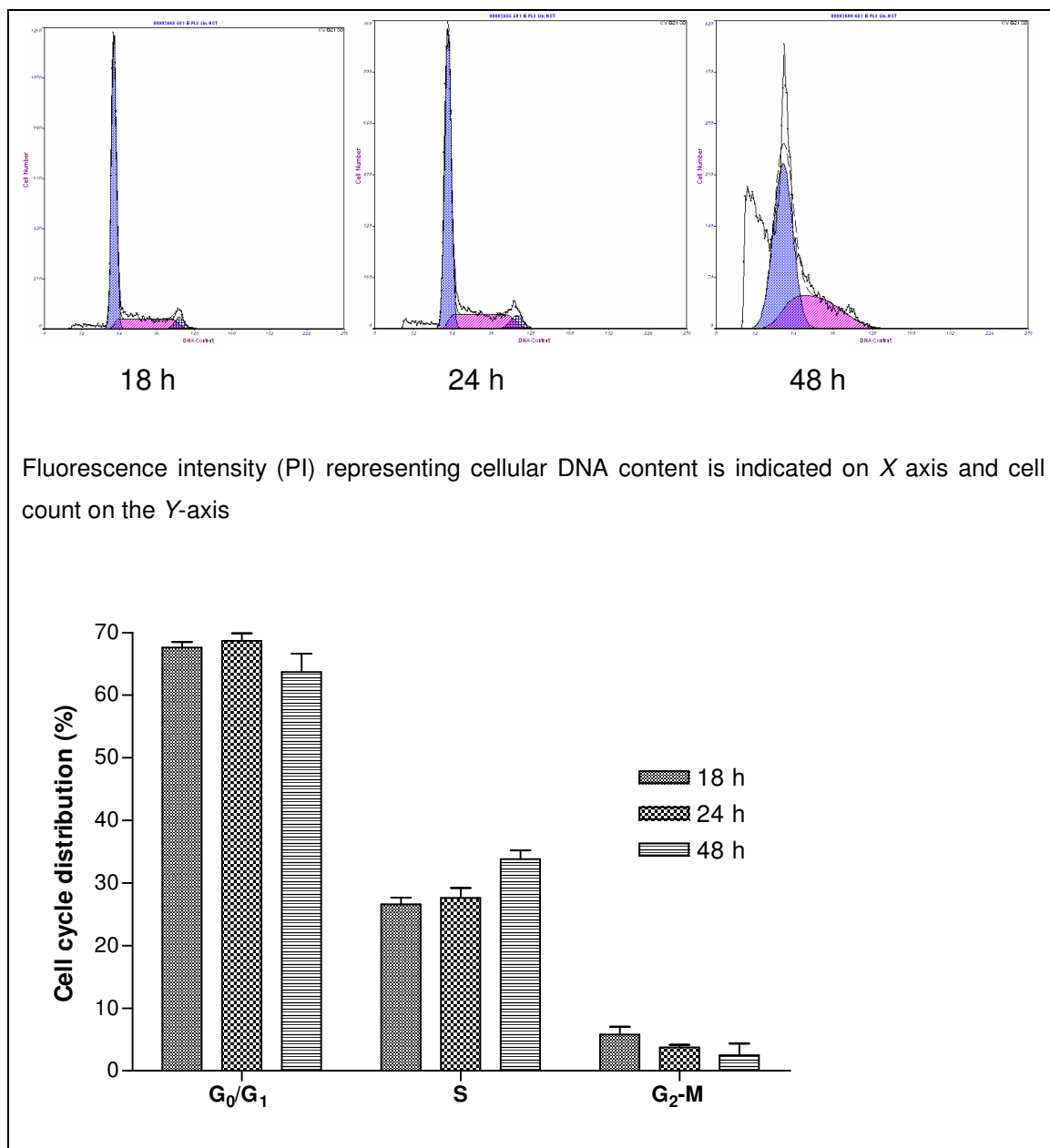


Fig. 8.6: Effect of 0.262 μM of $[\text{Au}(\text{dppe})_2]\text{Cl}$ on the cell cycle progression of Jurkat cells after 18, 24 and 48 h treatment..

Cells exposed to 0.262 μM of $[\text{Au}(\text{dppe})_2]\text{Cl}$ showed the same pattern as those exposed to half the concentration (*Fig. 8.6*). At 48 h, the number of cells in G₁ decreased from 69 to 64 % while S-phase increased from 28 to 34%. G₂ phase showed an insignificant decrease (from 4 to 3%).

The DNA histogram yields the relative number of cells in G_1/G_0 , S, and G_2/M phases of the cell cycle (Ormerod, 2002). Although some information about cell cycle progression can be deduced by following changes in the cell cycle phases with time, it gives static information. For example, although it is possible to estimate the percentage of cells in S phase, the measurement does not directly tell whether those cells are still moving through the S phase. A very distinct connection has been forged between the cell cycle clock apparatus and apoptosis (Lundberg and Weinberg, 1999). The paclitaxel-induced apoptosis of human breast cancer cells has been found to depend upon the induction of the cdc2 kinase at the G_2/M phase transition of the cell cycle.

Comparison of untreated and treated cells at different time intervals showed significant changes (*Fig. 8.7*). At 18 h, cells treated with **Pg 8** (0.711 and 1.422 μM) showed an increase of cells ($P < 0.05$) in the G_0/G_1 phase but there was no complimentary decrease in the number of cells in either the S or G_2 phase. After 24 h, only cells treated with $[\text{Au}(\text{dppe})_2]\text{Cl}$ (0.130 and 0.262 μM) showed any changes in cell cycle progression. There was a significant increase ($P < 0.01$) in the number of cells in the G_0/G_1 phase with a concomitant decrease in the number of cells in the S-phase. After 48 h, the treated cells showed significant differences in the cell cycle sequence. Cells treated with $[\text{Au}(\text{dppe})_2]\text{Cl}$ (0.262 μM) had significantly larger number ($P < 0.05$) of cells in G_0/G_1 phase than the untreated cells. However, this difference was not as large as that observed at 24 h. It is probable that $[\text{Au}(\text{dppe})_2]\text{Cl}$ induced apoptosis was not necessarily as a result of cell cycle arrest.

In contrast, cell cycle progression at 48 h was greatly perturbed by **Pg 8**. The number of cells in G_1 phase was reduced by 15% while those in the S-phase increased by 22% at both concentrations ($P < 0.01$). There were no cells detected in the G_2 phase due to this blockade in the S-phase. Taken together, these results indicate that **Pg 8** inhibited cellular proliferation of Jurkat cells via an S-phase arrest of the cell cycle following exposure for 48 h.

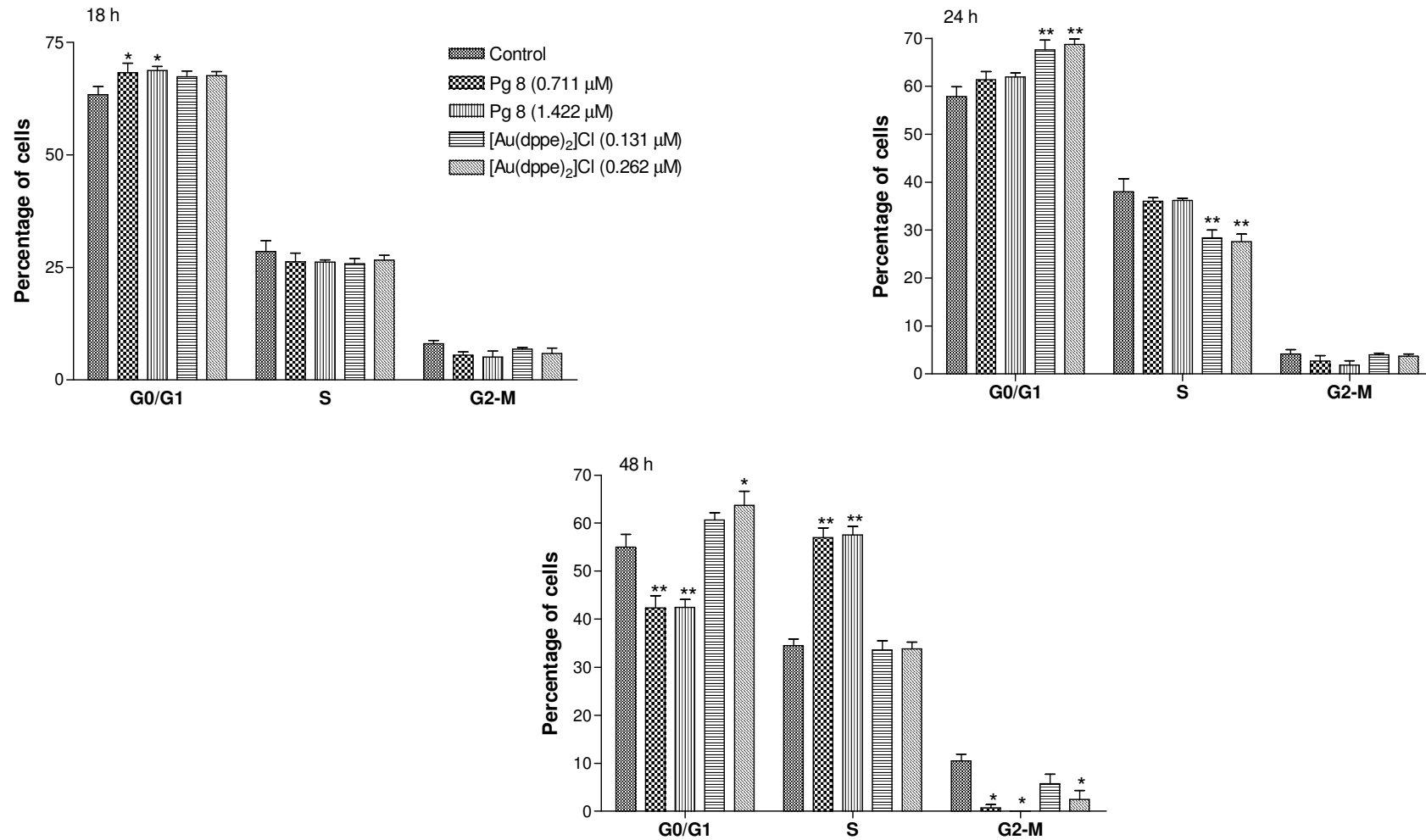
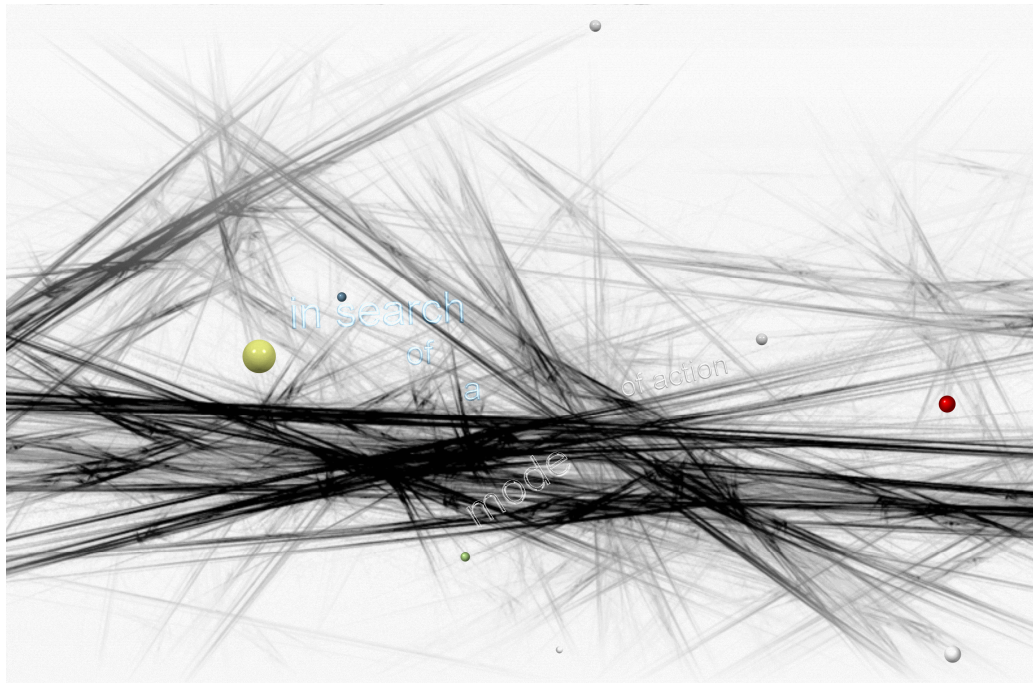


Fig. 8.7: Comparison of cell cycle progression of untreated Jurkat cells and those treated with **Pg 8** (0.711 and 1.422 M) and [Au(dppe)₂]Cl (0.131 and 0.262 μM) after 18, 24 and 48 h. Differences in G₀/G₁, S and G₂/M phases of untreated and treated cells were compared by 2-way ANOVA. Significance was established at $P < 0.05$.

Chapter IX

Uptake studies



9.1 Introduction

The main cause of treatment failure and death of cancer patients is metastases—the formation of secondary tumours in organs distant from the original cancer (Zeevaart *et al.*, 2004). The effect of some anti-tumour agents is related to the extent of their penetration, accumulation and retention within tumour cells (Tsuruo *et al.*, 1982). The acquired resistance of tumour cells in some agents, a crucial problem in cancer chemotherapy, is related to intracellular drug accumulation and retention. Although therapeutic efficiency of the drug will also depend upon drug retention in the tumour and the ability of the molecules to cross cellular membranes, inefficient drug transfer from plasma to tissue can be a major impediment in achieving effective tumour chemotherapy (Artemov *et al.*, 2001).

One of the major, present-day uses of radiolabelled compounds in metabolic studies is in pre-clinical drug development (Billington *et al.*, 1992). The metabolism of the candidate-radiolabelled drug is studied from three standpoints: a) excretion studies b) tissue distribution and, c) formation of metabolites. Experiments on $[\text{Au}(\text{dppe})_2]\text{Cl}$ in human plasma indicated that it was transferred relatively rapidly from plasma to red cells with an approximate half-life of 3 h at 25 °C (Berners-Price and Sadler, 1987b). After 18 h, 60% of the initial amount of $[\text{Au}(\text{dppe})_2]\text{Cl}$ remained in the plasma. The 2-pyridyl and 4-pyridyl analogs of $[\text{Au}(\text{dppe})_2]\text{Cl}$ were evaluated previously for anti-tumour activity in mice bearing i.p. P388 leukaemia; whereas the 2-pyridyl complex had comparable activity to $[\text{Au}(\text{dppe})_2]\text{Cl}$, the 4-pyridyl analog was inactive (Berners-Price *et al.*, 1999a). These differences may be related, at least in part, to differences in their uptake into cells as a consequence of their different hydrophilic character.

The assays discussed in this chapter aimed at determining the uptake and bio-distribution of the experimental compounds (^{103}Pd labelled $[\text{Pd}(\text{d}2\text{pyrpe})_2][\text{PF}_6]_2$ and ^{198}Au labelled $[\text{Au}(\text{dppe})_2]\text{Cl}$). These complexes provided a tool to follow the uptake into cells on an *in vitro* scale and the bio-distribution on an *in vivo* scale⁶.

⁶ The radioactivity was not expected to contribute to toxicity as much higher levels of radiation are required for that.

The test compounds were kindly synthesised at South African Nuclear Energy Corporation Ltd (NECSA) by Judith Wagener.

9.2 Preparation of ^{103}Pd labelled $[\text{Pd}(\text{d2pyrpe})_2][\text{PF}_6]_2$

9.2.1 Irradiation of Na_2PdCl_4

Na_2PdCl_4 (94 mg, 0.32 mmol) was irradiated for 3.5 days. According to Origen™ calculations, the combined dose rates for ^{103}Pd and ^{109}Pd was equal to 13 mCi for 100 mg Na_2PdCl_4 after 3.5 days irradiation at a thermal neutron flux of 1.79×10^{14} n.cm⁻².s⁻¹ in the hydraulic position, BE-1 or BW-1 in SAFARI-1.

9.2.2. Preparation of $[\text{Pd}(\text{d2pyrpe})_2]\text{Cl}_2$

An activity of 1.77 mCi was read on the Capintec (Pd-103 calibration factor = 562 X 10) (extrapolated value from Origen™ S calculation 2.59 mCi). The activated Na_2PdCl_4 (84.6 mg, 0.288 mmol) was transferred to a vial (activity of 1.488 mCi Pd-103). A total volume of ± 7 ml THF was added to the palladium salt. The ligand (d2pyrpe) (262.09 mg, 0.64 mmol) was weighed (under argon) and added as a solid to the stirred solution of Na_2PdCl_4 . The mixture was stirred for 12 hrs at room temperature to yield a yellow-green precipitate. The excess THF was extracted with a syringe and the yellow precipitate dried *in vacuo*. Crude Yield: 216.09 mg (76.4%).

9.2.3 Preparation of $[\text{Pd}(\text{d2pyrpe})_2][\text{PF}_6]_2$

NH_4PF_6 (68.66 mg, 0.418 mmol) was added to a stirred solution (8 ml of acetone) of $[\text{Pd}(\text{d2pyrpe})_2]\text{Cl}_2$ (205.29 mg, 0.209 mmol). After stirring for 45 min, the yellow-green suspension turned grey in colour. A syringe was packed with Celite 545 (Kieselgur) (a Teflon frit was placed at the bottom and top of the celite). The filter medium was washed with 5 ml acetone and additional 2 X 5 ml fractions. The reaction mixture was filtered through the celite column. The celite was washed with 2 X 2ml acetone. Slight pressure was introduced with the syringe plunger and the combined fractions of the clear pale yellow filtrate were reduced to ~2 ml with an aspirator.

Ether (4 ml) was added to the filtrate and a white/cream precipitate was formed. The precipitate was washed twice with ether (1 ml) and the excess solvent was extracted with a syringe. The product was then dried *in vacuo* for 30 min. Activity on the Celite column was high relative to the acetone filtrate containing the product and this may have been contributed by Cl-36 of NH_4Cl that had formed and was retained. According to a similar procedure using non-irradiated Na_2PdCl_4 , 60% yield was obtained and therefore it was assumed that $170 \mu\text{Ci} = 60\%$ product (150 mg). The final specific activity was $1.133 \mu\text{Ci}/\text{mg}$.

9.3 Preparation of ^{198}Au labelled $[\text{Au}(\text{dppe})_2]\text{Cl}$

All manipulations were carried out under an inert atmosphere (argon).

9.3.1 Irradiation of Au-metal

The radioactive experiment was carried out with activated Au (41.9 mg) and non-irradiated Au (30.5 mg) for the synthesis ClAuTHT (the precursor for $[\text{Au}(\text{dppe})_2]\text{Cl}$). Gold was activated for 10 min in the hydraulic B-position.

9.3.2 Preparation of $\text{HAuCl}_4 \cdot 4\text{H}_2\text{O}$

$680 \mu\text{l}$ HCl/HNO_3 (3:1) was added to a vial containing activated gold (41.9 mg) and non-irradiated gold (30.5 mg, 0.368 mmol). 18.15 mCi was read on the Capintec (Au-198 calibration factor = 149). The vial was placed inside a lead pot on a hotplate (45°C) while stirring and covered with a test tube (serving as a watch glass) to minimise evaporation of the acid. This dissolution step took approximately 2 h. The aqua regia was evaporated by increasing the temperature to 50°C while blowing argon into the vial (60-90 min). The yellow residue was washed with HCl ($650 \mu\text{l}$) followed by H_2O ($650 \mu\text{l}$) and dried at 50°C after each addition. The products' activity was 19.2 mCi and a yield of 100% was assumed.

9.3.3 Preparation of CIAuTHT

HAuCl₄.4H₂O was dissolved in 900 µl EtOH/H₂O (5:1) and the insoluble particles were removed by filtration through a Millex GP 0.22 µm filter. The filter was rinsed 3 times with additional EtOH/H₂O. The combined filtrate was evaporated to ±1000 µl and the activity of HAuCl₄.4H₂O was 16.7mCi.

The vial was sealed and an argon needle was inserted followed by a vent-needle. THT (600 µl) was added dropwise to HAuCl₄.4H₂O. The mixture was stirred for 15 min followed by extraction of the solution with a syringe. The remaining white precipitate was washed twice with ethanol (500µl) and extracted as described above. The precipitate was dried under vacuum and dissolved in a minimum volume of chloroform (calculated as 12.3 mg/ml CHCl₃).

9.3.4 Preparation of [¹⁹⁸Au(dppe)₂]Cl

2.93 µl of CIAuTHT/CHCl₃ (3.6 mg; 0.011 mmol) was evaporated and dppe (8.84 mg, 0.022 mmol) in THF (1 ml) was added to it. The reaction mixture was stirred for 15 min (a precipitate formed after stirring for 7 min). The white precipitate was then dried *in vacuo*.

9.4 Uptake of [¹⁰³Pd(d2pyrpe)₂][PF₆]₂ and [¹⁹⁸Au(dppe)₂]Cl by Jurkat cells

The procedure for the determination of the uptake and distribution of [¹⁰³Pd(d2pyrpe)₂][PF₆]₂ and [¹⁹⁸Au(dppe)₂]Cl in Jurkat cells was modified from the literature (Tsuruo *et al.*, 1982).

9.5 Materials and methods

9.5.1 Reagents

- RPMI and foetal calf serum
- Phosphate buffered saline (PBS)
- ¹⁰³Pd labelled [Pd(d2pyrpe)₂][PF₆]₂ (**Pg 8**)- 5 and 10 µM in DMSO
- ¹⁹⁸Au labelled [Au(dppe)₂]Cl- 5 and 10 µM in DMSO

9.5.2 Cell lines and culture

Human T-cell lines (Jurkat) were cultured in RPMI 1640 supplemented with 10% v/v heat-inactivated FCS and 1% penicillin-streptomycin. The cell culture was maintained at 37 °C and 5% CO₂.

9.5.3 Experimental procedure

200 µl of radiolabelled [Pd(d2pyrpe)₂][PF₆]₂ and [Au(dppe)₂]Cl (both at a concentration of 5 and 10 µM) were added to test tubes containing a suspension (1,800 µl) of Jurkat cells (5 x 10⁶ cells/ml). The mixture was incubated while mixing at 37 °C (+ 5% CO₂) for 1 hr. After incubation, the cells were centrifuged at 800 g (2000 rpm TJ 6) for 10 min. The supernatant was poured into new, clean, marked 5 ml test tubes (kept separately). The pellet was resuspended in PBS (3 ml) and centrifuged as before. The PBS was poured into new, clean, marked 5 ml test tubes and kept separately. The tubes were counted separately using 1261 multigamma manual gamma counter (LKB Wallac).

9.5.4 Statistical methods

Cells from eight different cell culture flasks were used for these assays. The activity that was obtained from the experiments was determined from counts per minute (CPM). Hence this represented the amount of compound distributed either in the supernatant or cell. Statistics was carried out on Graphpad™ and One Way Analysis of Variance (ANOVA) followed by Bonferroni's Multiple Comparison Test to determine significance between the two experimental compounds in the cells and/or supernatant. *P* < 0.001 was considered significant.

9.6 Results and discussion

The distribution of the radiolabelled compounds in Jurkat cells after 1 h is presented in Fig 9.1.

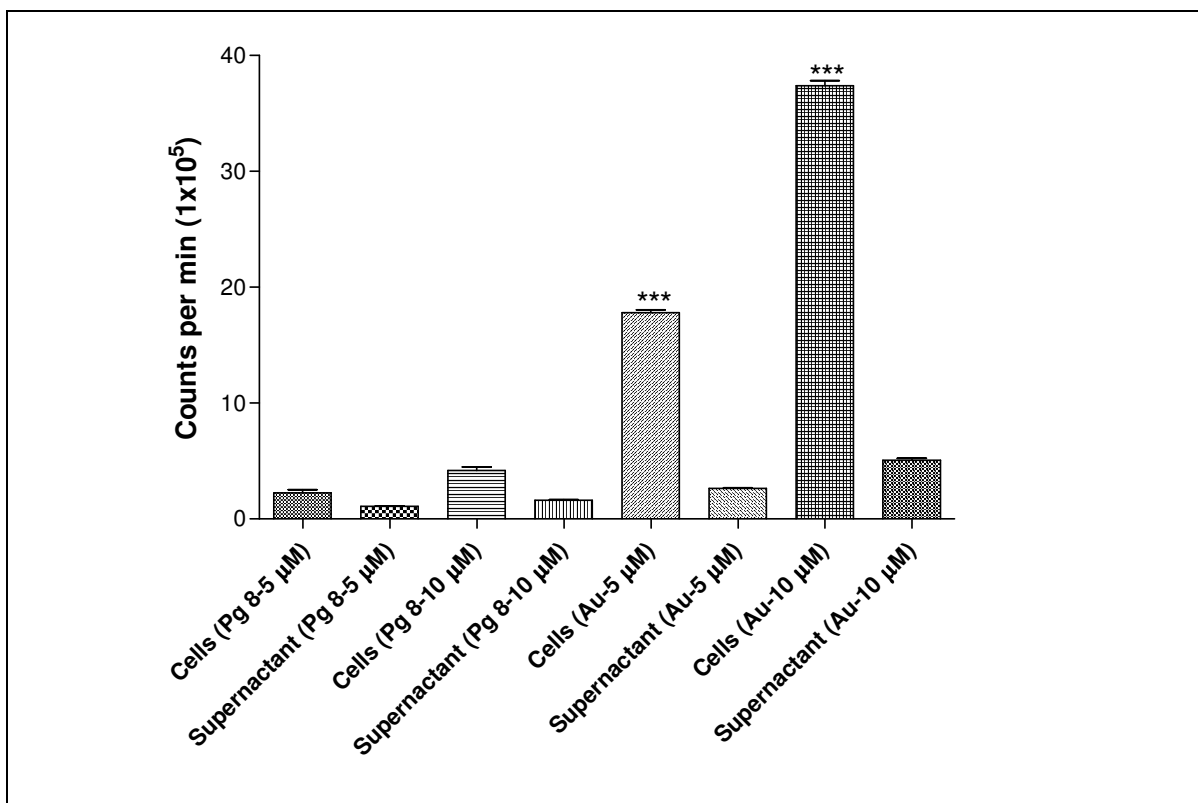


Fig. 9.1: Comparison of distribution of $[^{198}\text{Au}(\text{dppe})_2]\text{Cl}$ (5 and 10 μM) and $[^{103}\text{Pd}(\text{d2pyrpe})_2][\text{PF}_6]_2$ (5 and 10 μM) in Jurkat cells after exposure for 1 h. The results shown here were obtained from an average of 8 different cell populations and the values are means \pm SEM.

In general, there was a significant difference ($P < 0.001$) between the amounts of compound taken up into the cells when compared to the amount left in the supernactant for both complexes. After incubation for 1h, $[^{198}\text{Au}(\text{dppe})_2]\text{Cl}$ (5 and 10 μM) was taken up into the cells at significantly larger amounts ($P < 0.001$) than $[^{103}\text{Pd}(\text{d2pyrpe})_2][\text{PF}_6]_2$ (5 and 10 μM). This large difference in uptake may be as a consequence of lipophilicity. The former compound was found to be more lipophilic ($\log P = 0.362$) than the former ($\log P = -0.093$) and hence able to pass through the lipid layers of cells more rapidly.

In both compounds, the higher concentration (10 μM) was found to accumulate in larger amounts ($P < 0.001$) than the lower concentration (5 μM). Uptake studies of [^{14}C][Au(dppe) $_2$]Cl by isolated rat hepatocytes showed that rapid maximal uptake took place within 30 min (Smith *et al.*, 1989). The amount of radiolabelled drug associated with hepatocytes was also concentration-dependent. The authors proposed that the mechanism by which [Au(dppe) $_2$]Cl gained access to the intracellular compartments was most likely linked to its lipid solubility. In other experiments, NMR studies showed that nearly half of the [Au(dppe) $_2$]Cl added to plasma was transferred into cells (Berners-Price and Sadler, 1987b). Experiments on red cell ghosts confirmed that the complex can bind intact in the membrane.

9.7 Biodistribution of [$^{103}\text{Pd}(\text{d}2\text{pyrpe})_2$][PF $_6$] $_2$ and [$^{198}\text{Au}(\text{dppe})_2$]Cl in rats

This study was carried out by Judith Wagener and Dr Jan-Rihn Zeevaart (NECSA) at the University of Pretoria Biomedical Research Centre (UPBRC). Animal experimentation was done according to the National Code for the Handling and Use of Animals in Research, Education, Diagnosis and Testing of Drugs and Related Substances in South Africa. Ethical approval by the AUCC (Animal Use and Care Committee) was obtained (Protocol No. H1206) and the study was done according to the rules and regulations laid down by the International Controlling Body for Radioisotope Studies.

9.7.1 Formulations

- [$^{103}\text{Pd}(\text{d}2\text{pyrpe})_2$][PF $_6$] $_2$ (75 mg) was dissolved in DMSO (140 μl), ethanol (800 μl) and H $_2$ O (3200 μl). The filtered 4000 μl fraction had an activity of 3 μCi . An injection volume of 450 μl and an activity of 0.3 μCi was used (7.5×10^{-4} $\mu\text{Ci}/\mu\text{l}$).
- [$^{198}\text{Au}(\text{dppe})_2$]Cl (11.43 mg) was dissolved in ethanol (1200 μl) and H $_2$ O (7200 μl) and 3 ml of the solution was filtered (Millex GP 0.22 μm). An injection volume of 500 μl and an activity of 25 μCi were used (5.0×10^{-2} $\mu\text{Ci}/\mu\text{l}$).

9.7.2 Experimental animals

Adult male Sprague Dawley rats (six rats per compound) were used to follow the biodistribution on a gamma camera. The animals were kept in separate cages and fed a balanced diet and water *ad libitum*.

9.7.3 Experimental design

On the day of the experiment, the animals were anaesthetised by an intraperitoneal (i.p.) injection of 6 % sodium pentobarbitone solution at a dose of 1 ml/kg. A 24 G jelco was inserted into the tail vein of the animals to administer the radiolabelled compounds. The rats were each injected with an extremely low, non-toxic dosage of radio labelled compound (^{198}Au labelled $[\text{Au}(\text{dppe})_2]\text{Cl}$ and ^{103}Pd labelled $[\text{Pd}(\text{d2pyrpe})_2][\text{PF}_6]_2$). Animals were screened from time to time to monitor the realisation of steady state bio-distribution.

Two animals per group were scanned in parallel with an Elscint Gamma Camera at the Diagnostic Imaging unit at UPBRC in order to obtain the radionuclide imaging. Two minute static studies were performed every half an hour up to 6 hours. Isoflurane was used to immobilize the animals for the 2 minute static studies. The animals were sacrificed using an isoflurane overdose after a six hour period. The organs were separated and counted in a well type counter at NECSA [Canberra Model uniSPEC Universal MCA (Multichannel Analyzer) system with Canberra 3" x 3" NaI(TL) well detector]. From the organ counts as well as the reference activity in a syringe, the %ID/g (Injected Dose/gram) was calculated.

9.7.4 Statistical methods

Statistics was carried out on Graphpad™ and One Way Analysis of Variance (ANOVA) followed by Bonferroni's Multiple Comparison Test to determine significance between the two experimental compounds in the organs. $P < 0.001$ was considered significant.

9.8 Results and discussion

In interpreting the *in vivo* results, it must be kept in mind that only the distribution of the radio-nuclide entity of the complex is observed; which is not necessarily the same as the radio-nuclide-ligand complex that has been administered, due to possibilities of *in vivo* transchelators (Zeevaart *et al.*, 2001). The biodistribution at 6 h (expressed as percentage of injected dose per gram of organ) of the radiolabelled compounds is presented in Fig 9.2.

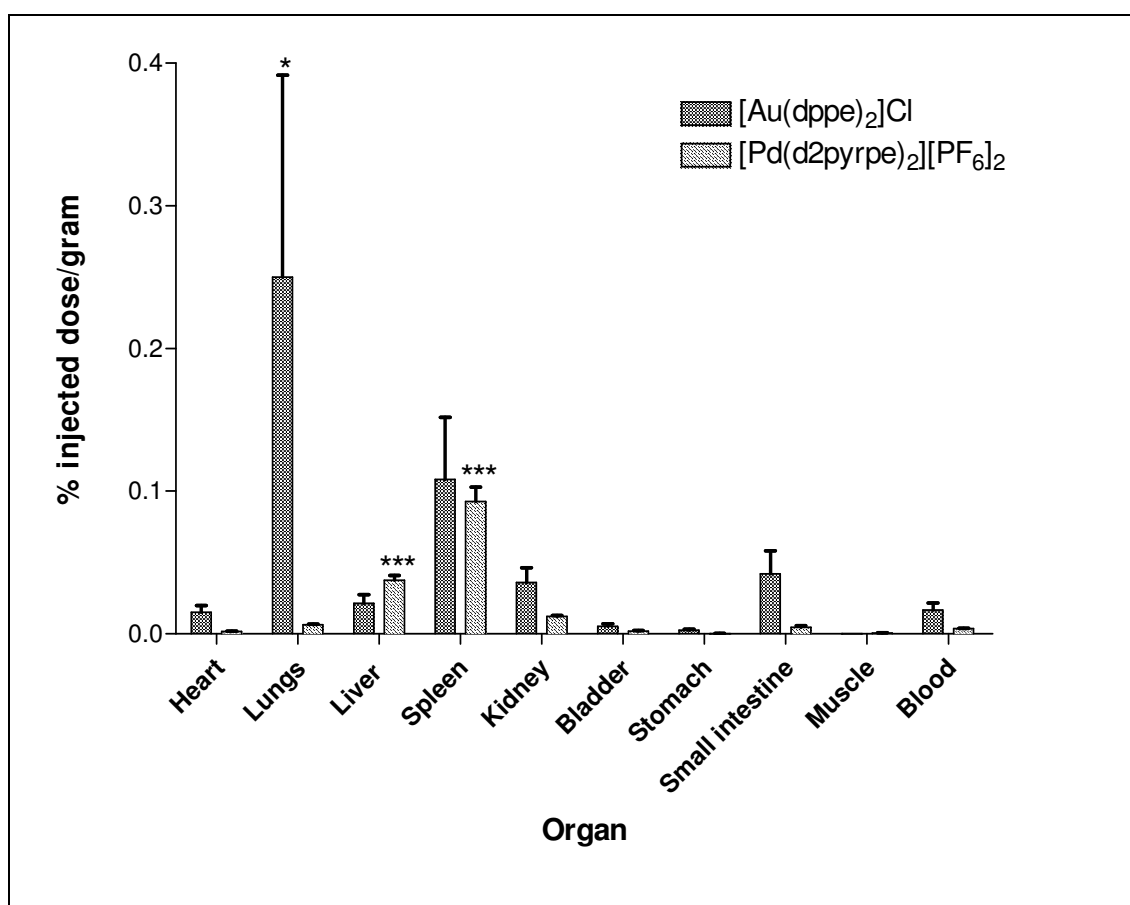


Fig. 9.2: Biodistribution of selected organs of adult male Sprague Dawley rats as expressed as a percentage of injected dose per gram of [¹⁹⁸Au(dppe)₂]Cl and [¹⁰³Pd(d2pyrpe)₂][PF₆]₂ at 6 h. Illustrated values are means ±S.E.M.

The biodistribution showed predominantly high reticulo-endothelial uptake for the two compounds. In terms of the total uptake it was found that [¹⁹⁸Au(dppe)₂]Cl which is more lipophilic was taken more efficiently in organs than [¹⁰³Pd(d2pyrpe)₂][PF₆]₂ which is less lipophilic. These findings correlate to the

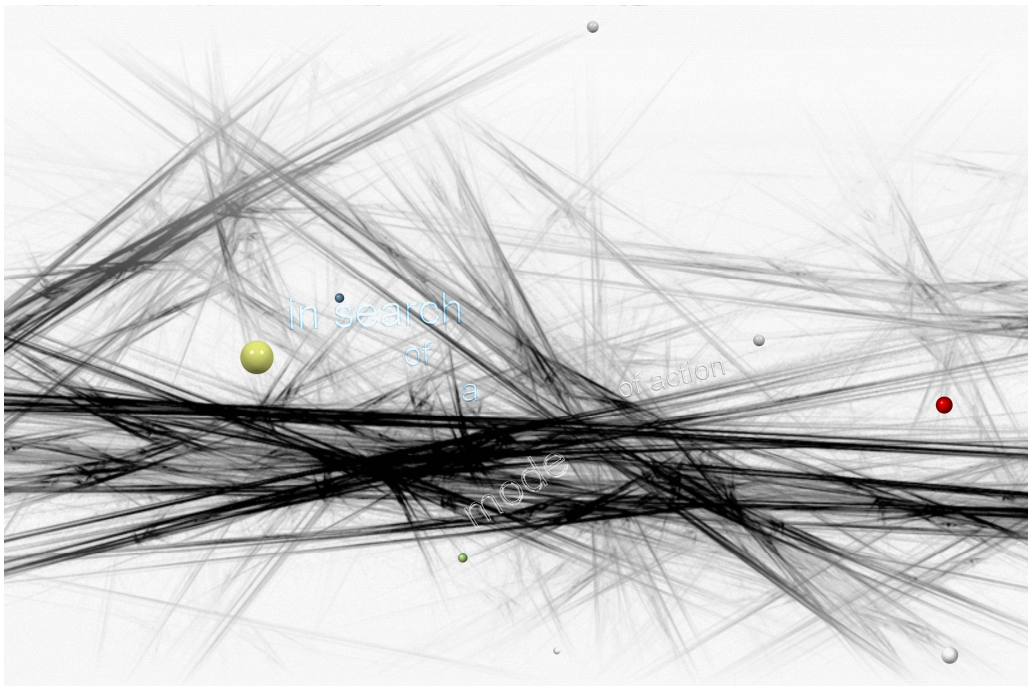
results obtained from *in vitro* uptake studies carried out on Jurkat cells (Section 9.6).

$[^{198}\text{Au}(\text{dppe})_2]\text{Cl}$ accumulated significantly ($P < 0.05$) in the lungs followed by the spleen, small intestine and liver, while $[^{103}\text{Pd}(\text{d2pyrpe})_2][\text{PF}_6]_2$ was mostly taken up in the spleen followed by the liver. The amount of $[^{103}\text{Pd}(\text{d2pyrpe})_2][\text{PF}_6]_2$ that accumulated in the spleen and liver was significantly higher ($P < 0.001$) than that found in the rest of the organs. The liver organ mainly traps neutral and positively charged molecules (Zeevaart *et al.*, 2004).

In comparing the biodistribution of the two compounds in similar organs, it was found that the amounts taken up were not significantly different apart from that observed in the lungs. The amount of $[^{198}\text{Au}(\text{dppe})_2]\text{Cl}$ accumulated in the lungs was much higher than that of $[^{103}\text{Pd}(\text{d2pyrpe})_2][\text{PF}_6]_2$ ($P < 0.001$). In summary, while the gold compound seemed to accumulate in most organs, most of the palladium compound appears to have been excreted. $[^{103}\text{Pd}(\text{d2pyrpe})_2][\text{PF}_6]_2$ showed similar behaviour to that of hydrophilic drugs, which are expected to have limited bio-distribution (as compared to lipophilic drugs). This might imply a more selective tumour uptake since it does not show a tendency to accumulate in the body.

Chapter X

Acute toxicity studies



10.1 Introduction

In the process of drug discovery, selected active substances are further differentiated according to their toxicity (Popiolkiewicz *et al.*, 2005). It is desired to find not only the most active, but also the least toxic substances as well. Toxicity studies on animals, which must be conducted before planning any clinical trial, constitute an important part of the whole drug discovery process. Acute toxicity studies are conducted in animals to ascertain the total adverse biological effects caused during a finite period of time following administration of a single, frequently large dose of an agent (or several doses repeated over a short interval of time) (Ecobichon, 1997).

The definition of hepatotoxicity is based on biological parameters (elevation of alkaline phosphatase enzyme (ALT, AST and GGT) or on clinical abnormalities (hepatitis, jaundice) (Ozcanli *et al.*, 2006). The degree of damage to the tissue or whole body, respectively, can be assessed by specific tests of enzymes (Conková *et al.*, 2005). In clinical diagnostics, determination of transaminases is of great importance. In the rat, ALT is chiefly a liver specific enzyme while AST has a ubiquitous tissue distribution (Elovaara *et al.*, 2007). Increased plasma levels of ALT are therefore attributed to liver damage but those of AST may imply damage to organs other than the liver. The absence of any notable increases in plasma ALP and GGT indicate that there are no marked changes involving the biliary system. A lot of medications may induce a clinical or biological hepatic toxicity and they need to be carefully supervised (Ozcanli *et al.*, 2006).

The influence of the route of administration of $[\text{Au}(\text{dppe})_2]\text{Cl}$ on its activity against i.p. P388 leukaemia was investigated (Berners-Price *et al.*, 1986). The complex was less toxic when given i.v., s.c. or p.o. but was inactive in this tumour system by these three routes of administration. Preliminary toxicological studies on $[\text{Au}(\text{dppe})_2]\text{Cl}$ revealed some local toxicity after sub-cutaneous administration, and pulmonary toxicity after intravenous injection (Berners-Price and Sadler, 1987b). It is possible that these effects could be related to the apparent disruption of lipoprotein structures which was observed *in vitro*. The maximum tolerated dose

of the ligand (dppe) was found to be 50 $\mu\text{mol/kg}$ and it was shown to be active in these tumour models also (Berners-Price *et al.*, 1987c).

In a preclinical evaluation of its toxicity, $[\text{Au}(\text{dppe})_2]\text{Cl}$ produced toxicity in the liver, heart and lung in male beagle dogs (Smith *et al.*, 1989). After a single *i.v* administration of the compound (272 mg/m^2), serum aspartate aminotransferase, alanine aminotransferase and alkaline phosphatase activities were elevated markedly within 48 hr. Histopathologic evaluation revealed multiple, focal areas of necrosis distributed throughout all zones of the liver. Additionally, $[\text{Au}(\text{dppe})_2]\text{Cl}$, an effective chemotherapeutic agent in animal models of neoplasia was cardiotoxic to rabbits (Hoke *et al.*, 1989). This resulted in scattered zones of subendocardial and myocardial cellular necrosis and mineralization, along with areas of contraction band necrosis. Non-specific binding to proteins or other macromolecules might explain the high host toxicity associated with very lipophilic cations such as $[\text{Au}(\text{dppe})_2]\text{Cl}$ (McKeage *et al.*, 2000).

10.2 Motivation for the study

In vitro results of $[\text{Au}(\text{dppe})_2]\text{Cl}$ and $[\text{Pd}(\text{d}2\text{pyrpe})_2][\text{PF}_6]_2$ (**Pg 8**) showed that the latter exhibited more selectivity than the former. The expected outcome was that the toxicity of the novel compound $[\text{Pd}(\text{d}2\text{pyrpe})_2][\text{PF}_6]_2$ (**Pg 8**) would be lower than that of $[\text{Au}(\text{dppe})_2]\text{Cl}$ (i.e., higher maximum tolerated dose).

10.3 Aim

This study was carried out in order to establish the maximum tolerated dose (MTD) of $[\text{Pd}(\text{d}2\text{pyrpe})_2][\text{PF}_6]_2$ (**Pg 8**) in mice.

10.4 Materials and Methods:

Ethical approval by the AUCC (Animal Use and Care Committee) was obtained (Protocol No. H1706). The study was conducted at the University of Pretoria

Biomedical Research Centre (UPBRC) from 24-29 August, 2006 and 22-27 September 2006.

10.4.1 Animals

Inbred female Balb/C mice of 6-8 weeks were used and housed individually in standard mouse cages in rooms with controlled environmental conditions. The animals were fed normal pellets (EPOL) and water *ad libitum*.

10.4.2 Sample size, dosage and route of administration

The study was carried out in two phases with 4 groups of 6 mice each being used per phase (total of 48 mice). The maximum tolerated dose of $[\text{Au}(\text{dppe})_2]\text{Cl}$ was $3.0 \mu\text{mol/kg/day}$ for 5 days (Berners-Price *et al.*, 1990) and hence this concentration was used as a guideline. The weight of the mice was determined to adapt the dosages according to their body weight. The novel compound $[\text{Pd}(\text{d2pyrpe})_2][\text{PF}_6]_2$ (**Pg 8**) and $[\text{Au}(\text{dppe})_2]\text{Cl}$ (standard) were dissolved in analytical quality ethanol, with subsequent addition of water to make up a final dose volume of 0.5 ml and a concentration of ~5% ethanol. The dosages were prepared immediately prior to each i.p administration. $[\text{Au}(\text{dppe})_2]\text{Cl}$ was soluble in ethanol while **Pg 8** ($15 \mu\text{mol/kg}$) was sparingly soluble. Solubility was achieved by sonication for 15 minutes. However both compounds precipitated out slightly and were mixed prior to injection.

A summary of the number of animals and dosages used in both phase 1 and phase 2 is shown below (*Table 1 and 2*)

Table10.1: Summary of dosages used in Phase 1 of the acute toxicity study carried out on Balb/c mice

	Control group	Dose 1	Dose 2
[Au(dppe)₂]⁺	Ethanol-water solution 0.5 ml daily from day 1 to 5 administered to 6 mice (5% ethanol)	3.0 µmol/kg daily from day 1 to 5 administered to 6 mice (5% ethanol)	
Pg 8		3.0 µmol/kg daily from day 1 to 5 administered to 6 mice (5% ethanol)	6.0 µmol/kg daily from day 1 to 5 administered to 6 mice (5% ethanol)

Table 10.2: Summary of dosages used in Phase 2 of the acute toxicity study carried out on Balb/c mice

	Control group	Dose 1	Dose 2
[Au(dppe)₂]⁺	Ethanol-water solution 0.5 ml daily from day 1 to 5 administered to 6 mice (5% ethanol)	6.0 µmol/kg daily from day 1 to 5 administered to 6 mice (5% ethanol)	
Pg 8		12.0 µmol/kg daily from day 1 to 5 administered to 6 mice (5% ethanol)	15.0 µmol/kg daily from day 1 to 5 administered to 6 mice (5% ethanol)

10.4.3 Duration of study

The total duration of the study was 10 days and each group of mice was injected i.p. every day for 5 days. For Phase 1, the ethanol-water solution and the first and second dosages of 3 $\mu\text{mol/kg}$ and 6 $\mu\text{mol/kg}$ were administered each day from day 1 to 5. Phase 2 followed whereby the ethanol-water solution and the third and fourth dosages of 6 mol $\{[\text{Au}(\text{dppe})_2]\text{Cl}\}$ and 12 $\mu\text{mol/kg}$ and 15 $\mu\text{mol/kg}$ (**Pg 8**) were administered every day from day 1 to 5. At the end of the study, the mice were weighed followed by anaesthetisation via isoflurane inhalation. Maximum blood was drawn via cardiac puncture while they were at the surgical plane of anaesthesia. Finally, the animals were further exposed to isoflurane until death occurred. Mice in Phase 2 category were dissected and major organs (liver, heart and kidneys) were weighed.

10.4.4 Evaluation of pain and distress

Body weights were recorded immediately prior to dosing (on day 1) so that an objective monitoring of weight could be done, indicating food intake, which is a good measure of animal well-being. The animals were also monitored for pain and stress (behavioural changes) immediately after the injection.

10.4.5 Chemical analysis

A whole blood profile was carried out on all the blood samples by the Department of Clinical Pathology at the Faculty of Veterinary Science (University of Pretoria). Standard liver enzymes (AST and GGT) were also analysed as well as levels of serum creatinine. Toxicity was to be established if adverse effects were observed on the experimental animals or if there was elevation of liver enzymes.

10.4.6 Statistical Analysis

Statistical analysis on levels of AST, GGT and creatinine was done on Graphpad™ by One Way Analysis of Variance (ANOVA) followed by Bonferroni's Multiple Comparison Test. Significance was indicated if $P < 0.05$.

10.5 Results and discussion

Acute toxicities of $[\text{Au}(\text{dppe})_2]\text{Cl}$ and **Pg 8** were investigated in mice after i.p administration for 5 days. On the second day of the study (in both phases), mice injected with the former compound emitted squeaking sounds upon injection. This sign of discomfort was not observed for the remainder of the study.

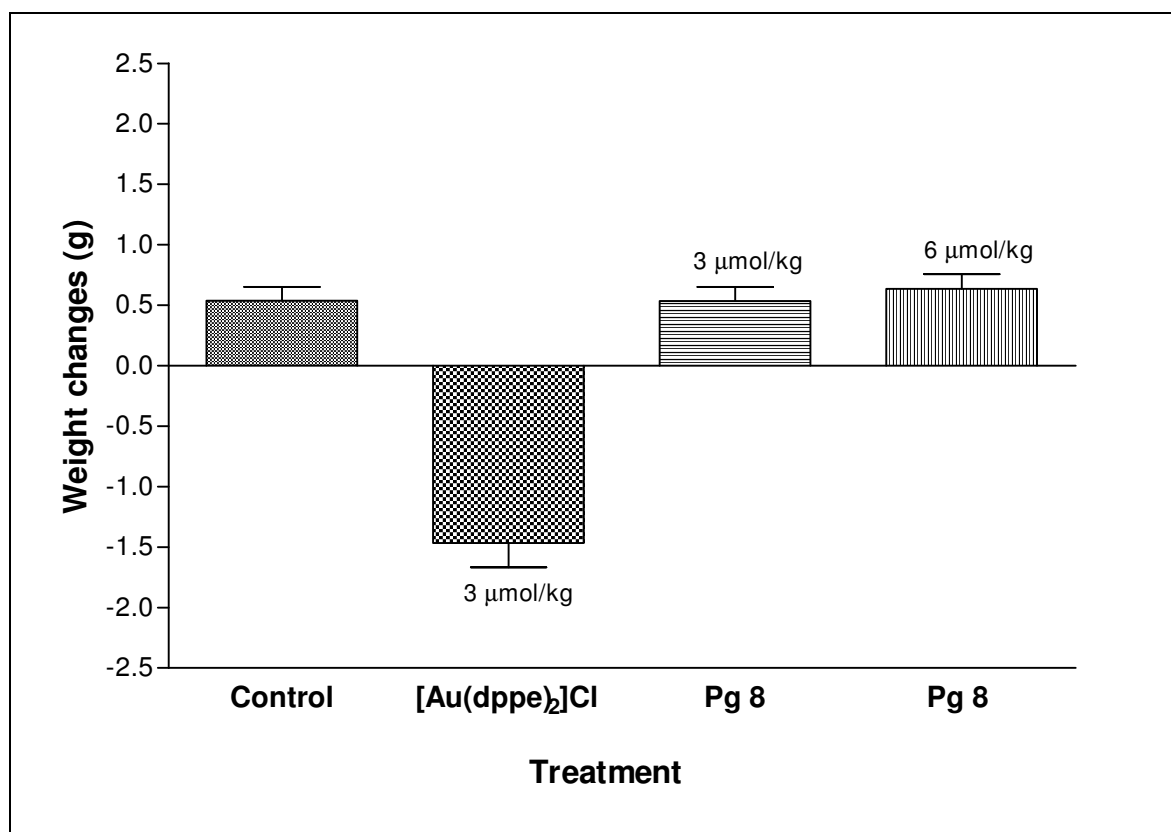


Fig.10.1: Mean body weight changes of control mice and mice treated with $[\text{Au}(\text{dppe})_2]\text{Cl}$ (3 $\mu\text{mol}/\text{kg}$) and **Pg 8** (3 and 6 $\mu\text{mol}/\text{kg}$) in Phase 1 study.

In Phase 1, the average weight change in the control and **Pg 8** (3 and 6 $\mu\text{mol}/\text{kg}$) groups were comparable (2.6, 2.63 and 3.1 %) (*Fig. 10.1*). However, the animals

in the $[\text{Au}(\text{dppe})_2]\text{Cl}$ ($3 \mu\text{mol/kg}$) group lost an average of 7.6 % of their total body weight.

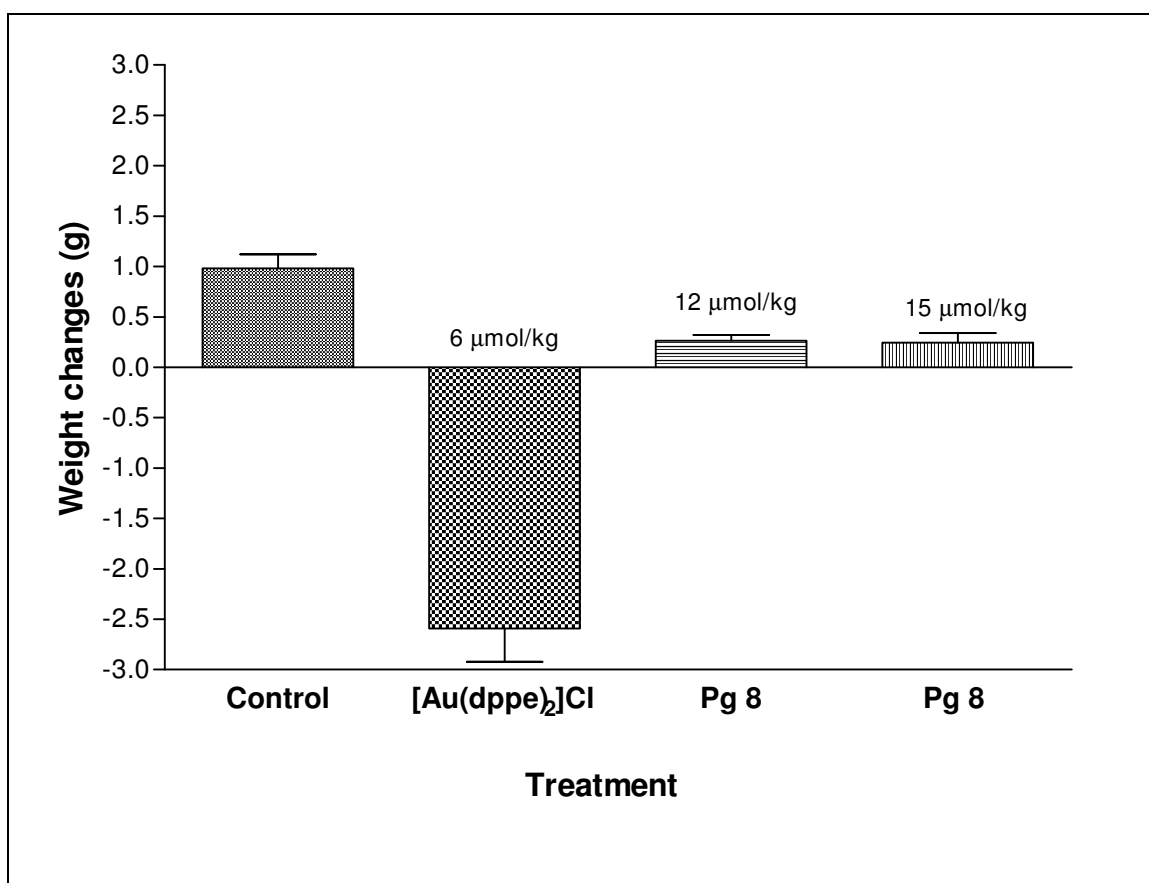


Fig.10.2 Mean body weight changes of control mice and mice treated with $[\text{Au}(\text{dppe})_2]\text{Cl}$ ($6 \mu\text{mol/kg}$) and **Pg 8** (12 and $15 \mu\text{mol/kg}$) in Phase 2 study.

In Phase 2, the mice in $[\text{Au}(\text{dppe})_2]\text{Cl}$ ($6 \mu\text{mol/kg}$) group lost an average of 12.4% when injected with the compound for five days (*Fig 10.2*). The mice treated with **Pg 8** (12 and $15 \mu\text{mol/kg}$) did not show a reduction in body weight but exhibited reduced weight gain. They gained an average of 1% of their total body weight which was less than that observed in the untreated mice (4.7 %).

After completion of Phase 2, the major organs were surgically removed and weighed. The results are tabulated below (*Table 10.3*).

Table 10.3: Mean organ weight and organ/body weight ratio of control mice and mice treated with $[\text{Au}(\text{dppe})_2]\text{Cl}$ ($6 \mu\text{mol/kg}$) and **Pg 8** (12 and $15 \mu\text{mol/kg}$) in Phase 2 study

Group	Body weight (g)	Heart (g)		Liver (g)		Kidneys (g)	
		g	%	g	%	g	%
Control	22.02	0.116	0.53	1.217	5.53	0.149	0.68
$[\text{Au}(\text{dppe})_2]\text{Cl}$ ($6 \mu\text{mol/kg}$)	18.52	0.104	0.56	1.194	6.45	0.142	0.77
Pg 8 ($12 \mu\text{mol/kg}$)	22.38	0.120	0.54	1.321	5.90	0.153	0.68
Pg 8 ($15 \mu\text{mol/kg}$)	21.12	0.112	0.53	1.217	5.76	0.144	0.68

No significant gross pathologic differences were observed between the control and treated groups. The average heart and kidney weights did not differ significantly among all the groups but the mean liver weights of the mice exposed to $[\text{Au}(\text{dppe})_2]\text{Cl}$ were greater (by ~1%) than the rest (*Table 10.3*). However, this could be as a result of reduced body weight.

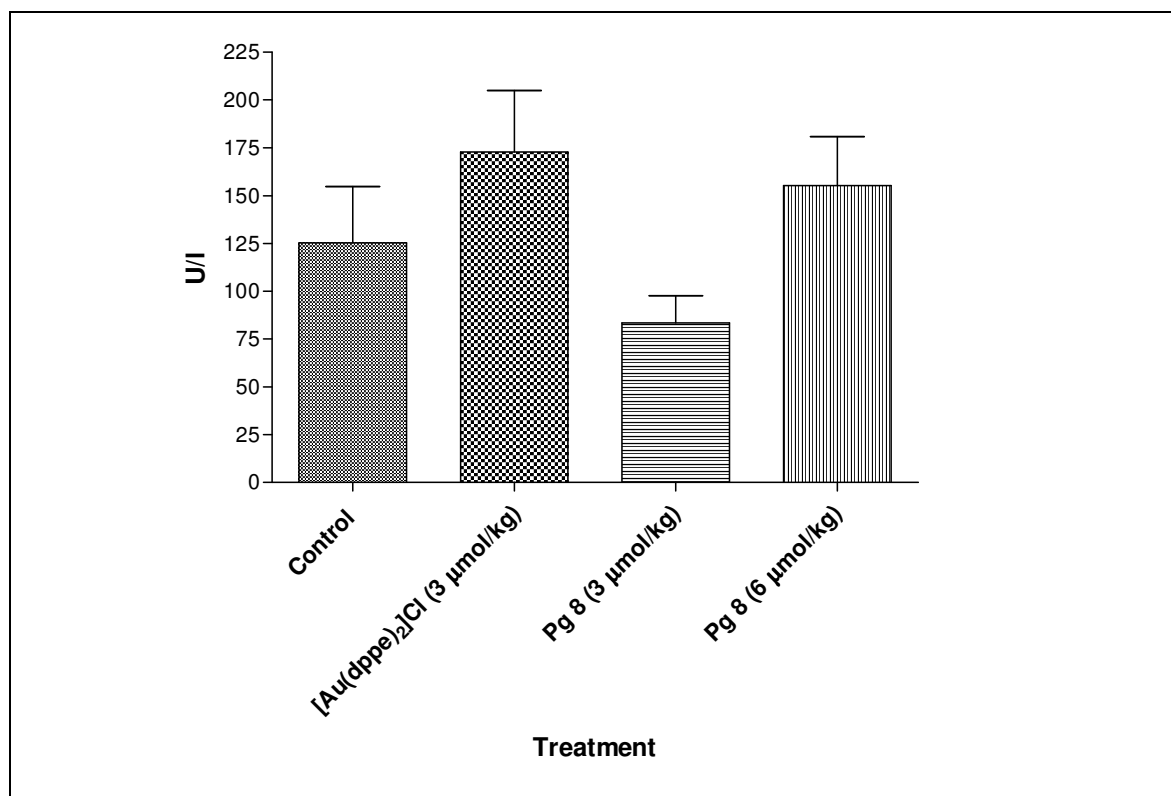


Fig. 10.3: AST levels of untreated mice and mice treated with $[\text{Au}(\text{dppe})_2]\text{Cl}$ ($3 \mu\text{mol/kg}$) and **Pg 8** (3 and $6 \mu\text{mol/kg}$) in Phase 1 study.

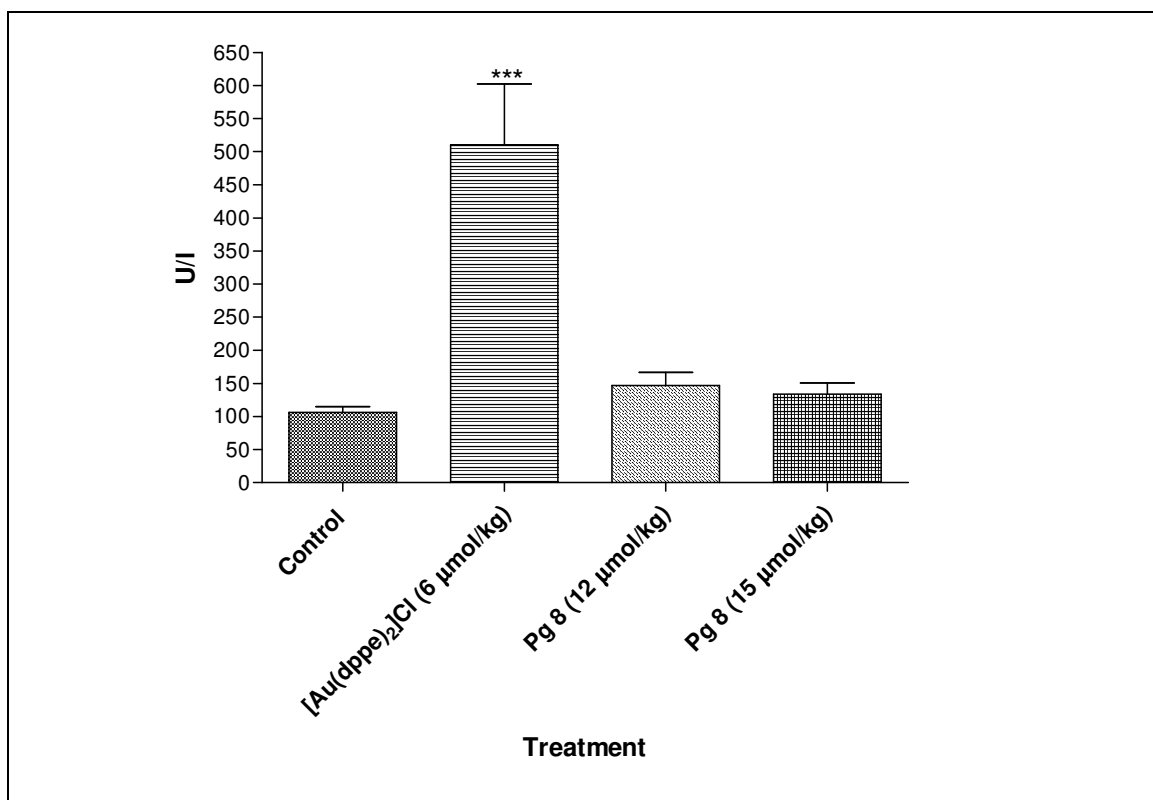


Fig. 10.4: AST levels of untreated mice and mice treated with [Au(dppe)₂]Cl (6 µmol/kg) and **Pg 8** (12 and 15 µmol/kg) in Phase 2 study.

Analysis of liver enzyme AST, showed that there were no significant differences in their levels in all the groups (untreated and treated) in Phase 1 (*Fig. 10.3*). However, in Phase 2, the mice treated with [Au(dppe)₂]Cl (6 µmol/kg) had significantly elevated levels of AST ($P < 0.001$). These levels of AST were significantly higher than those found in the untreated and **Pg 8** (12 and 15 µmol/kg) treated mice (*Fig. 10.4*).

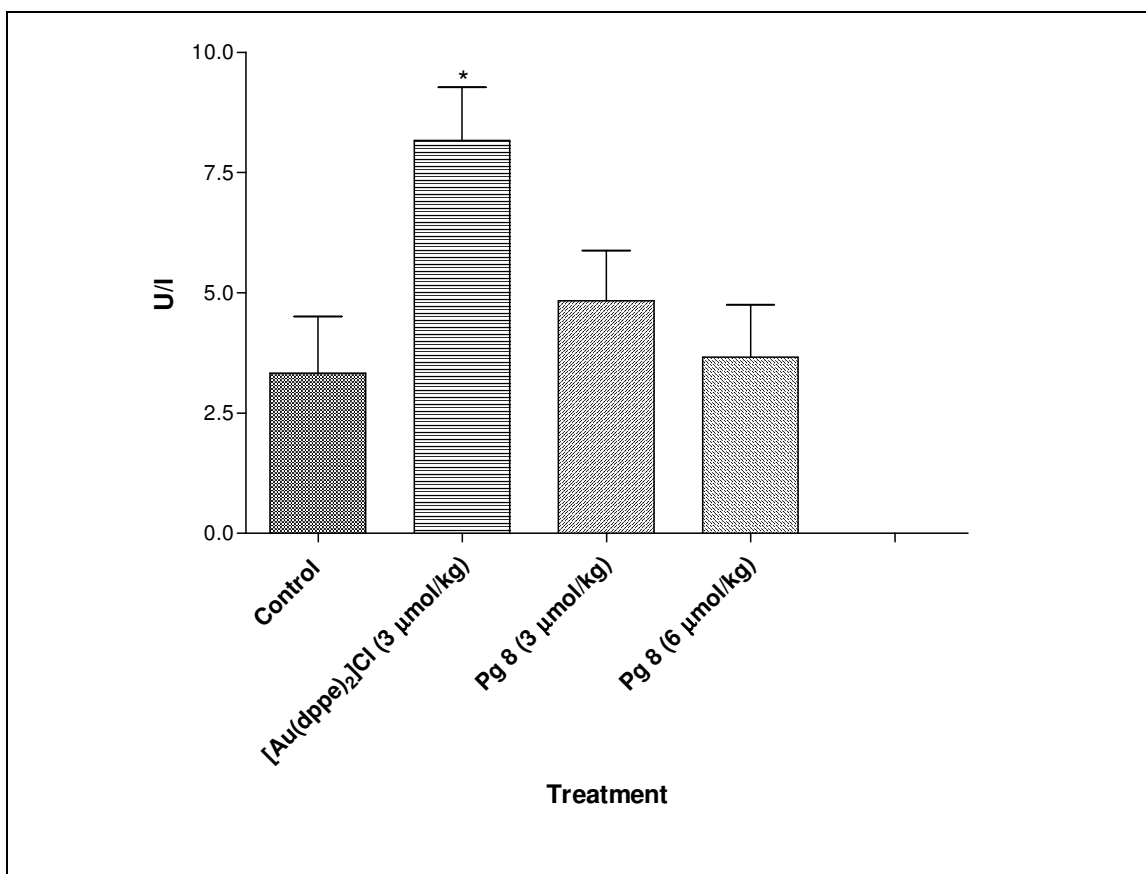


Fig. 10.5: GGT levels of untreated mice and mice treated with [Au(dppe)₂]Cl (3 µmol/kg) and **Pg 8** (3 and 6 µmol/kg) in Phase 1 study.

GGT levels (*Fig.10.5*) were also slightly elevated ($P < 0.05$) in the group treated with [Au(dppe)₂]Cl (3 µmol/kg) when compared to the untreated mice. However, the levels did not differ significantly with the mice treated with **Pg 8** (12 and 15 µmol/kg)

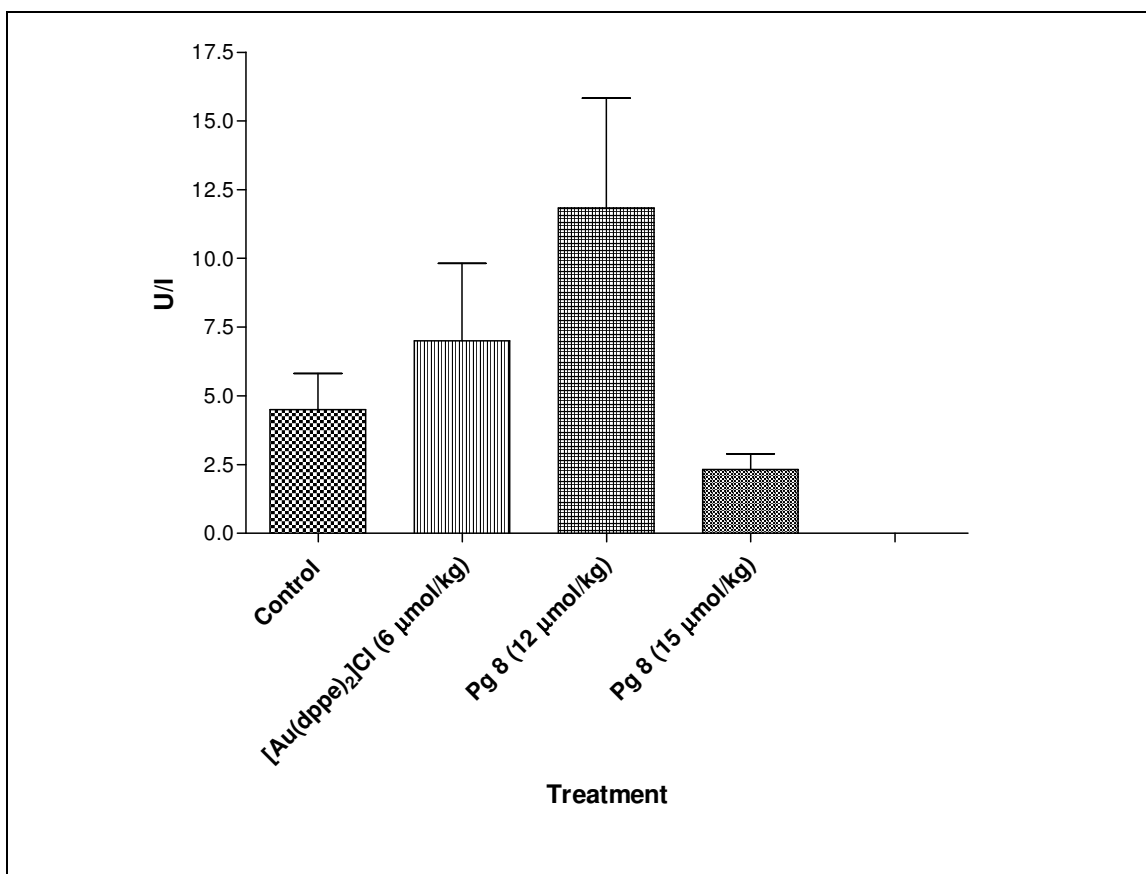


Fig. 10.6: GGT levels of untreated mice and mice treated with [Au(dppe)₂]Cl (6 µmol/kg) and **Pg 8** (12 and 15 µmol/kg) in Phase 2 study.

In Phase 2 of the study, GGT levels did not show significant differences in all the groups (untreated and treated). Notably, the mice treated with 12 µmol/kg of **Pg 8** exhibited higher levels of GGT than the highest dose (15 µmol/kg). However, this difference was not significant.

Creatinine levels in all the groups did not vary (*Figs. 10.7 and 10.8*)⁷. This was an indication of lack of toxicity to the kidneys.

⁷ Creatinine levels are expressed in mmol/l and not U/l as AST and GGT.

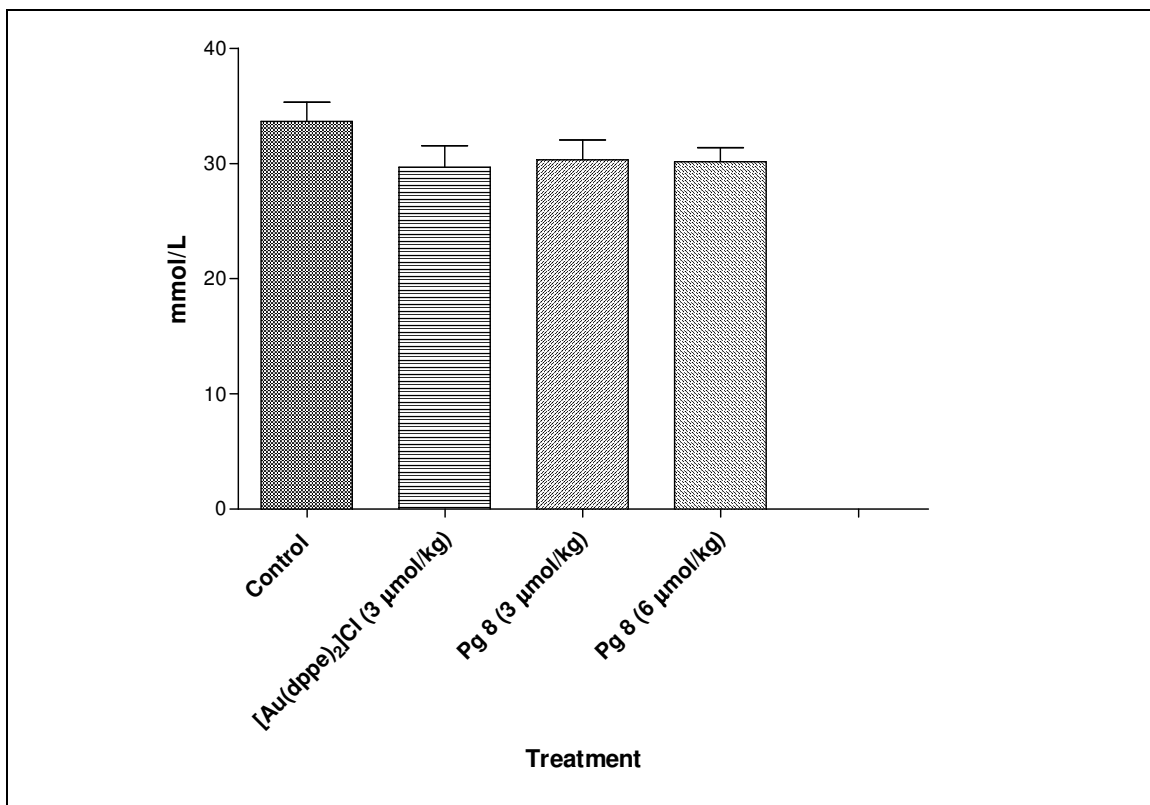


Fig. 10.7: Creatinine levels of untreated mice and mice treated with [Au(dppe)₂]Cl (3 μmol/kg) and **Pg 8** (3 and 6 μmol/kg) in Phase 1 study.

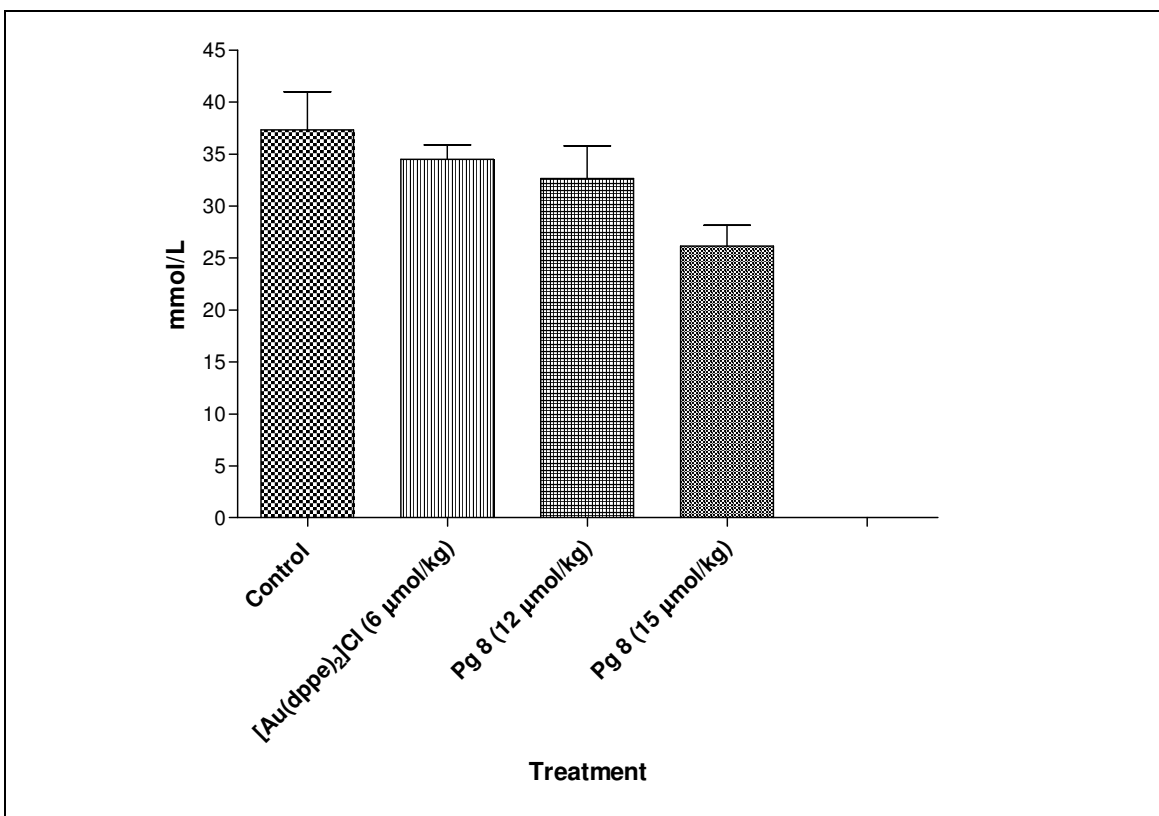


Fig. 10.8: Creatinine levels of untreated mice and mice treated with [Au(dppe)₂]Cl (6 μmol/kg) and **Pg 8** (12 and 15 μmol/kg) in Phase 2 study.

No significant differences in full blood counts were observed as haematological parameters between the untreated and treated groups did not vary. Overall, the mice treated with $[\text{Au}(\text{dppe})_2]\text{Cl}$ lost a greater amount of body weight than those treated with **Pg 8** at all concentrations. However, at higher concentrations (12 and 15 $\mu\text{mol}/\text{kg}$), the amount of weight gained over a period of 5 days was reduced in the latter compound. This observation was a sign that these elevated dosages caused discomfort to the animals. Subsequently, this could have led to reduced food intake. Analyses of the liver enzymes (AST and GGT) showed that $[\text{Au}(\text{dppe})_2]\text{Cl}$ caused toxicity to the mice and this was contrary to the results obtained from the mice treated with **Pg 8**. Creatinine levels did not vary in all the experimental animals (untreated and treated).

Chapter XI

Conclusions

In the search for novel anti-cancer agents with mitochondrial mode of action, palladium and platinum derivatives of the known lipophilic cation $[\text{Au}(\text{dppe})_2]\text{Cl}$ were prepared. This compound was shown to non-selectively target the mitochondria of all cells and research was stopped at pre-clinical phase due to severe host toxicity. To avoid similar problems, the ligand was varied in order to alter lipophilicity. Lipophilicity has been shown to play a role in determining toxicity as well as selectivity for cancer cells. The effect of changing the metal in analogous compounds was also investigated with special focus on reactivity, solubility, stability and biological activity. Cationic palladium and platinum phosphine complexes that were stable enough to undergo biological assays on cancer cells were synthesised.

Initially, dicationic complexes with Cl^- as a counterion were synthesised. The first compounds were complexed to 1,2-bis-(diphenylphosphino)ethane (dppe) and 1,2-bis-(diphenylphosphino)ethene (*cis*-dppen). The preparation of the 2, 3 and 4-pyridyl complexes proved more problematic than the phenyl ones. The reaction of the 1,2-bis-(di-2-pyridylphosphino)ethane with Pt or Pd led to production of both the *mono*-, $[\text{MCl}_2(\text{d2pyrpe})]$ and *bis*-chelated, $[\text{M}(\text{d2pyrpe})_2]\text{Cl}_2$ complexes irrespective of stoichiometry used. Separation of the mixtures by various methods proved futile as decomposition occurred.

This instability was attributed to the lability of the Cl and it was confirmed by stability tests carried out by ^{31}P NMR spectroscopy (**Chapter 5**). This necessitated a complete overhaul of the project as stability of a potential drug is of utmost importance if it is to retain its cytotoxic properties until it reaches the target (tumour cell). A pure product is also crucial as impurities would contribute to inaccurate results in biological studies. It was proposed that replacement of the counterion (Cl^-) with other counterions would be a suitable approach in ensuring stability. The first complex, $\text{Pt}(\text{d2pyrpe})_2[\text{BPh}_4]_2$ proved to be stable and was successfully purified (as shown by X-ray crystallography). However, it precipitated out in the presence of cell culture medium and was non-toxic ($\text{IC}_{50} > 50$) to cervical cancer cells (HeLa). The other alternative, PF_6^- was proposed and the obtained compounds were purified without decomposition taking place.

The differences in reactivity between dppe and *cis*-dppen led to formulation of different synthetic routes. The final procedure for dppe complexes, $[\text{Pt}(\text{dppe})_2][\text{PF}_6]_2$ and $[\text{Pd}(\text{dppe})_2][\text{PF}_6]_2$, involved replacement of the chloride counter ion with PF_6 (crystal structure of latter compound was obtained). In the case of $[\text{Pt}(\textit{cis}\text{-dppen})_2][\text{PF}_6]_2$ and $[\text{Pd}(\textit{cis}\text{-dppen})_2][\text{PF}_6]_2$, chloride abstraction was in contrast carried out first before addition of the second dppen moiety. $[\text{Pt}(\textit{cis}\text{-dppen})_2][\text{PF}_6]_2$ was obtained in extremely low yields (19%) and this precluded its investigations in biological assays. Both dppe and *cis*-dppen metal complexes were extremely insoluble in various solvents and hence characterised mainly by ^{31}P NMR spectroscopy. The chemical shift differences between the *mono*- and *bis*-chelate compounds were used to monitor the reactions.

As mentioned earlier, preparation of the pyridyl complexes was very challenging. The preparation of the 2-pyridyl complexes for both metals was the simplest in this category. In the preparation of 3-pyridyl complexes, a 1:1 ratio (Na_2MCl_4 :d3pyrpe) produced only *mono*-chelated complexes and addition of a second equivalent of ligand did not lead to the formation of the *bis*-chelated complexes. Substitution of the coordinated Cl in $[\text{MCl}_2(\text{d3pyrpe})]$ with triflate was carried out but separation of the products was difficult. The mixtures were also insoluble in most solvents and hence identification was not possible by NMR spectroscopy. This route was also time consuming, laborious and led to great losses. It was not pursued further.

In the case of the palladium complexes, $[\text{PdCl}_2(\text{NCMe})_2]$ was used instead of $\text{Na}_2[\text{PdCl}_4]$ but this gave more or less the same results. The synthesis of $[\text{Pd}(\text{d3pyrpe})_2]\text{Cl}_2$ was quite problematic as the final product contained two phosphorus signals in ^{31}P NMR signifying the presence of two non-equivalent phosphorus atoms. Deduction of the structure was not possible from MS-FAB nor NMR but X-ray crystallography showed co-crystallisation of both *mono*- and *bis*-chelated chloride complexes, $[\text{PdCl}_2(\text{d3pyrpe})]$ and $[\text{Pd}(\text{d3pyrpe})_2]\text{Cl}_2$. While the preparation of $[\text{Pd}(\text{d2pyrpe})_2][\text{PF}_6]_2$ (**Pg 8**) from a crude mixture of $[\text{PdCl}_2(\text{d2pyrpe})]$ and $[\text{Pd}(\text{d2pyrpe})_2]\text{Cl}_2$ led to a pure product (as shown by X-ray crystallography), similar attempts in metathesis failed in the case of the 3-pyridyl analogue. Similarly, the preparation of $[\text{Pt}(\text{d3pyrpe})_2][\text{PF}_6]_2$ was distinctly different from the synthesis of the 2-pyridyl analogue.

Preparation of the 4-pyridyl complexes proved even more challenging than the 2 or 3-pyridyl ones. Decomposition products were obtained in most cases and in other cases, the reaction did not proceed to completion. Similar to $[\text{Pt}(\text{cis-dppen})_2][\text{PF}_6]_2$ complex, the yield of the 4-pyridyl complex was so extremely low that satisfactory analyses could not be carried out. However, ^{31}P NMR studies showed that $[\text{Pt}(\text{d4pyrpe})_2]\text{Cl}_2$ and $[\text{PdCl}_2(\text{d4pyrpe})]$ had been successfully obtained. In broad terms, identification of the intermediates and the final complexes was not straightforward by NMR spectroscopy. The ^1H NMR spectra were almost identical while the phosphorus chemical shift changes were very marginal in some cases. In general, the platinum complexes were obtained in lower yields than the palladium ones.

The trend observed in cytotoxicity assays carried out on cancerous cells indicated that palladium complexes were more toxic than the platinum ones. $[\text{Au}(\text{dppe})_2]\text{Cl}$, which was the most lipophilic compound, exhibited the highest toxicity and non-selectivity. All the novel compounds were non-toxic to both resting and stimulated lymphocytes. From cytotoxicity assays (**Chapter 5**), one novel compound, **Pg 8** was selected as the lead compound as it exhibited the highest activity against a range of cancer cell lines. The hypothesis was that this toxicity was as a result of depolarisation of the mitochondrial membrane. Investigations to define its mode of action with special reference to the mitochondria led to various experiments. The mitochondria was selected as the target organelle because its analogue $[\text{Au}(\text{dppe})_2]\text{Cl}$ has been shown to act specifically on the mitochondria.

Analysis of mitochondrial membrane potential changes concluded that **Pg 8** did not depolarise the mitochondrial membrane of Jurkat cells even at high concentrations (10 and 15 μM) and neither after prolonged exposure (7 days). Similarly, this compound did not cause any changes in the plasma membrane potential when exposed to Jurkat cells for 24 h (10 and 15 μM). In contrast, exposure of **Pg 8** (0.711 and 1.422 μM) to Jurkat cells for 7 days showed that loss of plasma membrane potential began to take place from day 4. This observation seemed to be related to chemical changes that occurred as analysed by ^{31}P NMR spectroscopy.

In the quest to define the mode of action, induction of apoptosis by this compound was investigated. It was shown to induce apoptosis as well as necrosis to Jurkat cells after incubation for 48 h. Further investigations showed that **Pg 8** disrupted cell cycle progression of Jurkat cells after 48 h. There was a significant increase in number of cells in the S-phase signifying blockade in this phase. This disruption of cell cycle sequence may have led the cell to undergo apoptosis and necrosis followed by death. Studies with radiolabelled $[\text{Au}(\text{dppe})_2]\text{Cl}$ and **Pg 8** on Jurkat cells showed that both complexes accumulated in the cells although the former compound accumulated in larger amounts. Biodistribution studies in Wistar rats showed that the gold compound seemed to accumulate in most organs, while most of the the palladium compound seemed to have been excreted.

This accumulation of the $[\text{Au}(\text{dppe})_2]\text{Cl}$ in major organs may be the reason why it causes *in vivo* toxicity. Injection of the compound for 5 days caused Balb/c mice to lose a considerable amount of body weight at MTD ($3\ \mu\text{M}$) and $6\ \mu\text{M}$. This sign of toxicity was expected as this compound was toxic to normal cells such as lymphocytes, chicken embryo fibroblasts and hepatocytes. In contrast, animals treated with **Pg 8** did not lose any body weight even at $15\ \mu\text{M}$. However, at this concentration, their weight gain was reduced when compared to the control group. Measurement of biochemical parameters revealed that AST, GGT and creatinine levels were not significantly elevated in mice treated with **Pg 8**. Groups treated with $[\text{Au}(\text{dppe})_2]\text{Cl}$, showed marked elevation of AST and GGT levels.

The platinum complexes analysed in this study were less active on cancer cells than the palladium ones. This research has demonstrated that a balance between kinetic and thermodynamic properties of some palladium complexes may lead to development of compounds that show selective toxicity to cancer cells. This study has proven the hypothesis that varying the metal and lipophilicity may lead to modification of selectivity and cytotoxic properties of anti-neoplastic drugs containing Platinum Group Metals. In conclusion, **Pg 8** has the potential to be developed as an anti-cancer drug based on its role in cell cycle arrest and apoptosis as well as its lack of *in vivo* toxicity.

References

Abou-Jawde R, Choueiri T, Alemany C, Mekhail T (2003). An overview of targeted treatments in cancer, *Clin. Ther.* **25**: 2121-2137

Abu-Surrah A, Al Allaf TAK, Klinga M, Ahlgren M (2003). Chiral palladium(II) and platinum(II) complexes of diaminocyclohexane: X-ray structures of (1R,2R)-(-)-1,2-diaminocyclohexane dihydrochloride and its corresponding oxalato platinum(II) complex, *Polyhedron* **22**: 1529-1534

Adhami VM, Aziz MH, Reagan-Shaw SR, Nihal M, Mukhtar H, Ahmad N (2004). Sanguinarine causes cell cycle blockade and apoptosis of human prostate carcinoma cells via modulation of cyclin kinase inhibitor-cyclin-cyclin-dependent kinase machinery, *Mol. Cancer Ther.* **3**: 933-940

Ahn WS, Han YJ, Bae SM, kim T-H, Rho MS, Lee JM, Namkoong SE, Park YS, Kim CK, Sin J-I (2002). Differential suppression of human cervical cancer cell growth by adenovirus delivery of p53 *in vitro*: Arrest phase of cell cycle is dependent on cell line, *Jpn. J. Cancer Res.* **93**: 1012-1019

Ahrland S (1983). Factors influencing the affinities between metal ions and donor atoms in ligands of biological interest, *Inorg. Chim. Acta.* **79**: 94-96

Akdi K, Vilaplana R, Kamah S, Navarro J, Salas J, Gonzalez-Vilchez F (2002). Study of the biological effects and DNA damage exerted by a new dipalladium-Hmtpo complex on human cancer cells, *J. Inorg. Biochem.* **90**: 51-60

Albert A (1979). Differences in distribution: the first principle of selectivity., in *Selective toxicity: the physico-chemical basis of therapy*, Chapman and Hall, London p 51-95

Ali MA, Mirza AH, Butcher RJ, Tarafder MTH, Keat TB, Ali AM (2002). Biological activity of palladium(II) and platinum(II) complexes of the acetone Schiff bases of S-methyl- and S-benzylidithiocarbamate and the X-ray crystal structure of the

[Pd(asme)₂] (asme = anionic form of the acetone Schiff base of S-methyldithiocarbamate) complex, *J. Inorg. Biochem.* **92**: 141-148

Allen RT, Hunter WJ, Agrawal DK (1997). Morphological and biochemical characterization and analysis of apoptosis, *J. Pharmacol. Toxicol. Meth.* **37**: 215-228

Alverdi V, Giovagnini L, Marzano C, Seraglia R, Bettio F, Sitran S, Graziani R, Fregona D (2004). Characterisation studies and cytotoxicity assays of Pt(II) and Pd(II) dithiocarbamate complexes by means of FT-IR, NMR spectroscopy and mass spectrometry, *J. Inorg. Biochem.* **98**: 1117-1128

Amin OH, Al-Hayaly LJ, Al-Jibori SA, Al-allaf TAK (2004). Heterobimetallic complexes of palladium(II) and platinum(II) bridged by the ligand 5-phenyl-1,3,4-oxadiazole-2-thione, *Polyhedron* **23**: 2013-2020

Anderson R, Smit MJ, Van Rensburg CEJ (1993). Lysophospholipid-mediated inhibition of Na⁺, K⁺-adenosine triphosphatase is a possible mechanism of immunosuppressive activity of cyclosporine A, *Mol. Pharmacol.* **44**: 605-619

Artemov D, Solaiyappan M, Bhujwalla ZM (2001). Magnetic resonance pharmacoangiography to detect and predict chemotherapy delivery to solid tumours, *Cancer Res.* **61**: 3039-3044

Baird IR, Smith MB, James BR (1995). Nickel(II) and nickel(0) complexes containing 2-pyridylphosphines ligands, including water-soluble species, *Inorg. Chim. Acta.* **235**: 291-297

Balcarová Z, Kašpárková J, Žáková A, Nováková O, Sivo M, Natile G, Brabec V (1998). DNA interactions of a novel platinum drug, *cis*-[PtCl(NH₃)₂(N7-Acyclovir)]⁺, *Mol. Pharmacol.* **53**: 846-855

Banditelli G, Bandini AL, Bonati F, Minghetti G (1982). A series of pyrazole adducts and pyrazolato derivatives of platinum(II) containing various chelating phosphines as ligands: characterisation, ¹H and ³¹P{¹H} NMR spectra, *Inorg. Chim. Acta.* **60**: 93-98

Barnard P, Baker M, Berners-Price S, Day D (2004). Mitochondrial permeability transition induced by dinuclear gold(I)-carbene complexes: potential new antimitochondrial antitumour agents, *J.Inorg.Biochem.* **98**: 1642-1647

Barnard P, Baker M, Skelton B, White A, Berners-Price S (2003). Synthesis and biological activities of some new gold(I)-carbene complexes: potential antimitochondrial antitumour agents. *J.Inorg.Biochem.* **96**, 99

Bartek J, Lukas J, Bartkova J (1999). Perspective; Defects in cell cycle control and cancer, *J. Pathol.* **187**: 95-99

Bell CF (1977). Properties of ligands and chelate rings, in *Principles and applications of metal chelation*, ed. Atkins PW, Holker JSE, and Holliday AK, Oxford University Press, p 9-29

Bell J, Norman R, Sadler P (1987). Coordination chemistry in biological media: reactions of antitumor Pt(II) and Au(III) complexes with cell culture media, *J. Inorg. Biochem.* **31**: 241-246

Berlin KRS, Ammini CV, Rowe TC (1998). Dequalinium induces a selective depletion of mitochondrial DNA from HeLa human cervical carcinoma cells, *Expt. Cell Res.* **245**: 137-145

Berners-Price SJ, Bowen RJ, Galettis P, Healy PC, McKeage MJ (1999a). Structural and solution chemistry of gold(I) and silver(I) complexes of bidentate pyridyl phosphines: selective antitumour agents, *Coord. Chem. Revs.* **185-186**: 823-836

Berners-Price SJ, Bowen RJ, Hambley TW, Healy PC (1999b). NMR and structural studies of gold(I) chloride adducts with bidentate 2-, 3- and 4-pyridyl phosphines, *J. Chem. Soc., Dalton Trans.* 1337-1346

Berners-Price SJ, Bowen RJ, Harvey PJ, Healy PC, Koutsantonis GA (1998). Silver(I) nitrate adducts with bidentate 2-, 3- and 4-pyridyl phosphines. Solution ^{31}P and [^{31}P - ^{109}Ag] NMR studies of 1:2 complexes and crystal structure of dimeric $[\{\text{Ag}(\text{d}2\text{pyrpe})(\mu\text{-d}2\text{pyrpe})\}_2][\text{NO}_3]_2 \cdot 2\text{CH}_2\text{Cl}_2$, *J. Chem. Soc., Dalton Trans.* 1743-1750

Berners-Price SJ, Colquhoun LA, Healy PC, Byriel KA, Hanna JV (1992). Copper(I) and gold(I) complexes with *cis*-bis(diphenylphosphino)ethylene. Crystal structures and ^{31}P cross-polarization magic angle spinning nuclear magnetic resonance studies, *J. Chem.Soc., Dalton Trans.*, 3357-3363

Berners-Price SJ, Johnson RK, Giovenella AJ, Faucette LF, Mirabelli CK, Sadler PJ (1988). Anti-microbial and anti-cancer activity of tetrahedral, chelated, diphosphine silver(I) complex: comparison with copper and gold, *J. Inorg. Biochem.* **33**: 285-295

Berners-Price SJ, Norman R, Sadler PJ (1987a). The autoxidation and proton dissociation constants of tertiary diphosphines: relevance of biological activity, *J. Inorg. Biochem.* **31**: 197-209

Berners-Price SJ, Sadler PJ (1986). Gold(I) complexes with bidentate tertiary phosphine ligands: Formation of annular vs. tetrahedral chelated complexes, *Inorg. Chem.* **25**: 3822-3827

Berners-Price SJ, Girard GR, Hill DT, Sutton BM, Jarrett PS, Faucette LF, Johnson RK, Mirabelli CK, Sadler PJ (1990). Cytotoxicity and antitumour activity of some tetrahedral bis(diphosphino)gold(I) chelates, *J. Med. Chem.* **33**: 1386-1392

Berners-Price SJ, Jarret PS, Sadler PJ (1987b). ^{31}P NMR studies of $[\text{Au}_2(\mu\text{-dppe})]^{2+}$ antitumour complexes. Conversion into $[\text{Au}(\text{dppe})_2]^+$ induced by thiols and blood plasma, *Inorg. Chem* **26**: 3074-3077

Berners-Price SJ, Sadler PJ (1987a). Phosphines in medicine, *Chem. Br.* 541-544

Berners-Price S, Johnson R, Mirabelli C, Faucette L, McCabe F, Sadler P (1987c). Copper(I) complexes with bidentate tertiary phosphine ligands: solution chemistry and anti-tumour activity, *Inorg. Chem.* **26**: 3383-3387

Berners-Price S, Mirabelli C, Johnson R, Mattern M, McCabe F, Faucette L, Sung C, Mong S, Sadler P, Croke S (1986). *In vivo* antitumor activity and *in vitro* cytotoxic properties of bis[1,2-bis(diphenylphosphino)ethane]gold(I) chloride, *Cancer Res.* **46**: 5486-5493

Berners-Price S, Sadler P (1987b). Interaction of the antitumor Au(I) complex $[\text{Au}(\text{Ph}_2\text{P}(\text{CH}_2)_2\text{PPh}_2)_2]\text{Cl}$ with human blood plasma, red cells, and lipoproteins: ^{31}P and ^1H NMR studies, *J. Inorg. Biochem.* **31**: 267-281

Berners-Price S, Sadler P (1996). Coordination chemistry of metallodrugs: insights into biological speciation from NMR spectroscopy, *Coord. Chem. Revs* **151**: 1-40

Berthod A, Carda-Broch S (2004). Determination of liquid-liquid partition coefficients by separation methods, *J. Chromatogr.A* **1037**: 3-14

Bianchini C, Meli A, Oberhauser W (2003). Taking too many precautions in making a catalyst is never a loss of time: A lesson we learned at our own expense, *Organometallics* **22**: 4281-4285

Billington D, Jayson GG, Maltby PJ (1992). *Radioisotopes: Introduction to biotechniques*, BIOS Scientific Publishers Limited

Bowen RJ (1999). Hydrophilic bidentate phosphines and their group 11 complexes: potential antitumour agents, *Ph.D Thesis*

Bowen R, Garner A, Berners-Price S, Jenkins I, Sue R (1998). Convenient synthetic routes to bidentate and monodentate 2-, 3- and 4-pyridyl phosphines: potentially useful ligands for water-soluble complex catalysts, *J. Organomet. Chem.* **554**: 181-184

Broxterman HJ, Lankelma J, Hoekman K (2003). Resistance to cytotoxic and anti-angiogenic anticancer agents: similarities and differences, *Drug Resist. Updates* **6**: 111-127

Bruker. SAINT+. [6.02] (1999a). Madison, Winsconsin, USA, Bruker AXS Inc. *Computer Program*

Bruker. SHELXTL. [5.1] (1999b). Madison, Winsconsin, USA, Bruker AXS Inc. *Computer Program*

Budzelaar PHM, Frijns JHG, Orpen AG (1990). Synthesis and coordination chemistry of a new class of binucleating ligands: pyridyl-substituted diphosphines, *Organometallics* **9**: 1222-1227

Butler I, Licence P, Coles S, Hursthouse M (2000). The synthesis and characterisation of bis(phenylpyridylphosphino)ethane, *J. Organomet. Chem.* **598**: 103-107

Canovese L, Visentin F, Uguagliati P, Bianca FD, Fontana A, Crociani B (1996). Organometallic nucleophiles. A mechanistic study of halide displacement at saturated carbon by 2- and 4-pyridyl complexes of palladium(II) and platinum(II), *J. Organomet. Chem.* **525**: 43-48

Chen L (1988). Mitochondrial membrane potentials in living cells, *Annu. Rev. Cell. Biol.* **4**: 155-181

Chow K, Levason W, McAuliffe C (1974). Bidentate group VB chelates, Part VII. Some palladium(II) complexes with diphosphine, phosphine-arsine, and diarsine ligands, including some thiocyanate derivatives, *Inorg. Chim. Acta.* **15**: 79-83

Collins K, Jacks T, Pavletich NP (1997). The cell cycle and cancer, *Proc. Natl. Acad. Sci. U.S.A* **94**: 2776-2778

Conková E, Laciaková A, Pástorová B, Seidel H, Kováč G (2005). The effect of zearalenone on some enzymatic parameters in rabbits, *Toxicol. Lett.* **121**: 145-149

Cossarizza A, Bacarani-Contri M, Kalashnikova G, Franceschi C (1993). A new method for the cytofluorimetric analysis of mitochondrial membrane potential using the J-aggregate forming lipophilic cation 5,5',6,6'-tetrachloro-1,1',3,3'-tetraethylbenzimidazolcarbocyanine iodide (JC-1), *Biochem. Biophys. Res. Comm.* **197**: 40-45

Cossarizza A, Salvioli S (1997). Analysis of mitochondrial membrane potential with the sensitive fluorescent probe JC-1. The Purdue Cytometry CD-ROM **4**. Purdue University Cytometry Laboratories, West Lafayette, IN 1997, ISBN 1-890473-03-.

Crabtree RH (2005). NHC ligands versus cyclopentadienyls and phosphines as spectator ligands in organometallic catalysis, *J. Organomet. Chem.* **690**: 5451-5457

Daghriri H, Huq F, Beale P (2004). Studies on activities, cell up take and DNA binding of four multinuclear complexes of the form: [trans-PtCl(NH₃)₂ 2μ-trans-Pd(NH₃)₂-(H₂N(CH₂)_nNH₂)₂]Cl₄ (n = 4-7, *J. Inorg. Biochem* **98**: 1722-1733

Darzynkiewicz Z, Kapuscinski J, Carter S, Schmid F, Melamed M (1986). Cytostatic and cytotoxicity properties of pyronin Y: relation to mitochondrial localization of the dye and its interaction with RNA, *Cancer Res.* **46**: 5760-5766

Davies WC, Mann FG (1944). The stereochemistry of organic derivatives of phosphorus. Part I. The synthesis of acidic and basic dissymmetric tertiary phosphines. The optical resolution of phenyl-*p*-(carboxymethoxy)phenyl-*n*-butylphosphine sulphide, *J. Chem. Soc.* 276-283

Davis S, Weiss M, Wong J, Lampidis T, Chen L (1985). Mitochondrial and plasma membrane potentials cause unusual accumulation and retention of rhodamine 123 by human breast adenocarcinoma-derived MCF-7 cells, *J. Biol. Chem.* **260**: 13844-13850

Derby E, Reddy V, Kopp W, Nelson E, Baseler M, Sayers T, Malyguine A (2001). Three-color flow cytometric assay for the study of the mechanisms of cell-mediated cytotoxicity, *Immunol. Lett.* **78**: 35-39

Desoize B, Madoulet C (2002). Particular aspects of platinum compounds used at present in cancer treatment, *Crit. Rev. Oncol. Hematol.* **42**: 317-325

Devic T, Batail P, Fourmigué M, Avarvari N (2004). Unexpected reactivity of PdCl₂ and PtCl₂ complexes of the unsaturated diphosphine *o*-Me₂TTF(PPh₂)₂ toward chloride abstraction with thallium triflate, *Inorg. Chem* **43**: 3136-3141

Dias N, Bailly C (2005). Drugs targeting mitochondrial functions to control tumour cell growth, *Biochem. Pharmacol.* **70**: 1-12

Dobashi Y (2005). Cell cycle regulation and its aberrations in human lung carcinoma, *Path. Inter.* **55**: 95-105

Don AS, Hogg PJ (2004). Mitochondria as cancer drug targets, *TRENDS in Molecular Medicine* **10**: 372-378

Durran SE, Smith MB, Dale SH, Coles SJ, Hursthouse MB, Light ME (2006). New pyridyl modified phosphines: Synthesis and late transition-metal coordination studies, *Inorg. Chim. Acta.* **359**: 2980-2988

Ecobichon DJ (1997). Acute toxicity studies, CRC press, New York p 43

Effendy, Hanna JV, Marchetti F, Martini D, Pettinari C, Pettinari R, Skelton BW, White AH (2004). Synthesis and spectroscopic characterisation (IR, ^1H and ^{31}P NMR, electrospray ionisation mass) of mono-, di-, tetra- and poly-meric complexes of silver(I) with diphosphine ligands: X-ray crystal structures of $\text{AgNO}_2:(\text{Ph}_2\text{PCH}_2\text{PPh}_2)$ (1:1)₂, $\text{AgNO}_2:(\text{Ph}_2\text{P}(\text{CH}_2)_3\text{PPh}_2)$ (1:1)₂, $\text{AgNO}_2:(\text{Ph}_2\text{PCH}=\text{CHPPh}_2)$ (2:1)₂ and $\text{AgNO}_2:\{p\text{-tolyl}\}_2\text{P}(\text{C}_{10}\text{H}_6)_2\text{P}(p\text{-tolyl})_2\}$ (1:1). *Inorg. Chim. Acta.* **357**, 1523-1537.

Elovaara E, Stockmann-Juvala H, Mikkola J, Gelboin HV (2007). Interactive effects of methyl tertiary-butyl ether (MTBE) and tertiary-amyl methyl ether (TAME), ethanol and some drugs: Triglyceridemia, liver toxicity and induction of CYP (2E1, 2B1) and phase II enzymes in female Wistar rats, *Environ. Toxicol. Pharmacol.* **23**: 64-72

Engelhardt LM, Patrick JM, Raston CL, Twiss P, White AH (1984). Crystal structures of bis[(ethane-1,2-diyl)-bis(diphenylphosphine)]-palladium(II) and -platinum(II) dichloride dichloromethane and dichloro[(ethane-1,2-diyl)bis(diphenylphosphine)]platinum(II) dichloromethane., *Aust. J. Chem.* **37**: 2193-2200

Espinet P, Soulantica K (1999). Phosphine-pyridyl and related ligands in synthesis and catalysis, *Coord. Chem. Revs.* **193-195**: 499-556

Espinosa E, Zamora P, Feliu J, Baron GM (2003). Classification of anticancer drugs--a new system based on therapeutic targets, *Cancer Treat. Rev.* **29**: 515-523

Ferguson G, Lough AJ, McAlees AJ, McCrindle R (1993). Bis[1,2-bis(diphenylphosphino)ethane]platinum(II) iodide bis(deuteriochloroform)solvate, *Acta. Cryst.* **C49**: 573-576

Fredericks EJ, Gindling MJ, Kroll LC, Storhoff BN (1994). Phosphine-nitrile ligands: the molecular structure of *cis*-2-diphenylphosphino-1-cyanocyclopentane and studies of the donor/acceptor properties of this and related ligands, *J. Organomet. Chem.* **465**: 289-296

Freshney RI (2005). Primary culture, in *Culture of animals: a manual of basic technique*, Wiley, New York p 175-197

Fruhauf NR, Oldhafer KJ, Holtje M, Kaiser GM, Fruhauf JH, Stavrou GA, Bader A, Broelsch CE (2004). A bioartificial liver support system using primary hepatocytes: a preclinical study in a new porcine hepatectomy model, *Surgery* **136**: 47-56

Galanski M, Yasemi A, Jakupec M, Keyserlingk N, Keppler B (2005). Synthesis, cytotoxicity, and structure-activity relationships of new oxaliplatin derivatives, *Monatshefte für Chemie* **136**: 693-700

Gambaro JJ, Hohman WH, Meek DW (1989). Synthesis and characterisation of trigonal-bipyramidal rhodium(I) complexes of tris(2-(diphenylphosphino)ethyl)phosphine and determination of a spectroscopic trans-influence series by $^{31}\text{P}\{^1\text{H}\}$ NMR spectroscopy, *Inorg. Chem.* **28**: 4154-4159

Garrou PE. Δ_R ring contributions to ^{31}P NMR parameters of transition-metal-phosphorus chelate complexes. *Chem.Rev.* **81**, 229-266. 1981.

Giovannini C, Matarrese P, Scazzocchio B, Sanchez M, Masella R, Malorni W (2002). Mitochondria hyperpolarization is an early event in oxidized low-density lipoprotein-induced apoptosis in Caco-2 intestinal cells, *FEBS Letters* **523**: 200-206

- Golias CH, Charalabopoulos A, Charalabopoulos K (2004). Cell proliferation and cell cycle control: a mini review, *Int. J. Clin. Pract.* **58**: 1134-1141
- Gravance CG, Garner DL, Baumber J, Ball BA (1999). Assessment of equine sperm mitochondrial function using JC-1. *Theriogenology*, 1691-1703.
- Gravance CG, Garner DL, Miller MG, Berger T (2001). Fluorescent probes and flow cytometry to assess rat sperm integrity and mitochondrial function, *Reprod. Toxicol.* **15**: 5-10
- Grella G, Cabras M, Murineddu G, Pau A, Pinna G (2003). Synthesis and cytotoxicity of substituted 2-benzyl-naphth[2,3-d]imidazoles, *Eur. J. Pharm. Sci.* **20**: 267-272
- Gupta N, Price PM, Aboagye EO (2002). PET for *in vivo* pharmacokinetic and pharmacodynamic measurements, *Eur. J. Cancer* **38**: 2094-2107
- Hambley T (1997). The influence of structure on the activity and toxicity of Pt anti-cancer drugs, *Coord. Chem. Revs.* **166**: 181-223
- Hartmann T, Schmitt J (2004). Lipophilicity- beyond octanol/water: a short comparison of modern technologies, *Drug. Discov. Today* **1**: 431-439
- Hernandez MA, Rathinavelu A (2006). Chemical approaches to the treatment of cancer in *basic pharmacology: Understanding drug actions and reactions*. CRC Press, p 77-90
- Hoke GD, Macia RA, Meunier PC, Bugelski PJ, Mirabelli CK, Rush GF, Matthews WD (1989). *In vivo* and *in vitro* cardiotoxicity of a gold-containing antineoplastic drug candidate in the rabbit, *Toxicol. Appl. Pharmacol.* **100**: 293-306
- Hope EG, Levason W, Powell NA (1986). Coordination chemistry of higher oxidation states. Platinum -195 NMR studies of platinum(II) and platinum (IV) complexes of the bi- and multi-dentate phosphorus, arsenic and sulphur ligands, *Inorg. Chim. Acta.* **115**: 187-192
- Horbinski C, Chu CT (2005). Kinase signalling cascades in the mitochondrion: a matter of life or death, *Free Radic. Biol. Med.* **38**: 2-11

Huq F, Daghriri H, Yu JQ, Tayyem H, Beale P, Zhang M (2004). Synthesis, characterisation, activities, cell uptake and DNA binding of [trans-PtCl(NH₃)₂ [μ]-(H₂N(CH₂)₆NH₂) trans-PdCl(NH₃)₂](NO₃)Cl, *Eur. J. Med. Chem.* **39**: 947-958

Huth US, Schubert R, Peschka-Suss R (2006). Investigating the uptake and intracellular fate of pH-sensitive liposomes by flow cytometry and spectral bio-imaging, *J. Controlled Release* **110**: 490-504

Jakupec MA, Galanski M, Keppler BK (2003). Tumour-inhibiting platinum complexes-state of the art and future perspectives, *Revs. Physiol. Biochem. Pharmacol.* **146**: 1-54

Jeffrey JC, Rauchfuss TB (1979). Metal complexes of hemilabile ligands. Reactivity and structure of dichlorobis(*o*-(diphenylphosphino)anisole)ruthenium(II), *Inorg. Chem.* **18**: 2658-2666

Jiang X, Wang X (2004). Cytochrome c-mediated apoptosis, *Annu. Rev. Biochem.* **73**: 87-106

Johnson L, Walsh M, Chen L (1980). Localization of mitochondria in living cells with rhodamine 123, *Proc. Natl. Acad. Sci. U.S.A* **77**: 990-994

Jones ND, Meessen P, Losehand U, Patrick BO, James BR (2005). Platinum(II) and Palladium(II) Complexes of Bisphosphine Ligands Bearing *o*-*N,N* Dimethylanilinyll substituents; a Hint of Catalytic Olefin Hydration, *Inorg. Chem.* **44**: 3290-3298

Jones N, MacFarlane K, Smith M, Schutte R, Rettig SJ, James B (1999). Coordination Chemistry of the 2-Pyridyldiphosphine Ligands, (py)₂P(CH(CH₂)₃CH)P(py)₂ and (py)₂P(CH₂)₂P(py)₂ (py) 2-Pyridyl), with Platinum(II) and Ruthenium(II). Ruthenium-Catalyzed Hydrogenation of Imines, *Inorg. Chem.* **38**: 3956-3966

Khokhar AR, Xu Q, Siddik ZH (1990). Synthesis, characterization, and antitumor activity of 1,2-bis(diphenylphosphino) ethane platinum(II) and palladium(II) complexes, *J. Inorg. Biochem.* **39**: 117-123

- Kim JY, Lee YA, Park KM, Chae HK, Jung OS (2002). Molecular strands and related properties of silver(I) triflate with 3,3' - oxybispyridine vs 3,3' - thiobispyridine, *Bull. Korean Chem. Soc.* **23**: 1106-1110
- Koukourakis MI, Danielidis V (2005). Preventing radiation induced xerostomia, *Cancer Treat. Rev.* **31**: 546-554
- Koya K, Li Y, Wang H, Ukai T, Tatsuta N, Kawakami M, Chen LB (1996). MKT-077, a novel rhodacyanine dye in clinical trials, exhibits anticarcinoma activity in preclinical studies based on selective mitochondrial accumulation, *Cancer Res.* **56**: 538-543
- Kuduk-Jaworska J, Puszko A, Kubiak M, Pelczynska M (2004). Synthesis, structural, physico-chemical and biological properties of new palladium(II) complexes with 2,6-dimethyl-4-nitropyridine, *J. Inorg. Biochem.* **98**: 1447-1456
- Kurita-Ochiai T, Hashizume T, Yonezawa H, Ochiai K, Yamamoto M (2006). Characterisation of the effects of butyric acid on cell proliferation, cell cycle distribution and apoptosis, *FEMS Immunol. Med. Microbiol.* **47**: 67-74
- Kweekel DM, Gelderblom H, Guchelaar H-J (2005). Pharmacology of oxaliplatin and the use of pharmacogenomics to individualize therapy, *Cancer Treat. Rev.* **31**: 90-105
- Landis-Piwowar KR, Milacic V, Chen D, Yang H, Zhao Y, Chan TH, Yan B, Dou QP (2006). The proteasome as a potential target for novel anticancer drugs and chemosensitizers, *Drug Resist. Updates* **9**: 263-273
- Lassahn P-G, Lozan V, Wu B, Weller AS, Janiak C (2003). Dihalogeno(diphosphane)metal(II) complexes (metal = Co, Ni, Pd) as pre-catalysts for the vinyl/addition polymerisation of norbornene-elucidation of the activation process with $B(C_6F_5)_3/AlEt_3$ of $Ag[closo-1-CB_{11}H_{12}]$ and evidence for the in situ formation of "naked" Pd^{2+} as a highly active species, *Dalton Trans.* 4437-4450
- Liles D. Structure of 3e (2006). *Personal Communication*

Lipinski CA (2000). Drug-like properties and the causes of poor solubility and poor permeability, *J. Pharmacol. Toxicol.Meth.* **44**: 235-249

Lipinski CA, Lombardo F, Dominy BW, Feeney PJ (1997). Experimental and computational approaches to estimate solubility and permeability in drug discovery and development settings, *Adv. Drug Deliv. Rev.* **23**: 3-25

Liu M-J, Yue PY-K, Wang Z, Wong RN-S (2005). Methyl protodioscin induces G₂/M arrest and apoptosis in K562 cells with the hyperpolarisation of mitochondria, *Cancer Lett.* **224**: 229-241

Liu X, Song D, Zhang Q, Tian Y, Liu Z, Zhang H (2006). Characterisation of drug-binding levels to serum albumin using a wavelength modulation surface plasmon resonance sensor, *Sens. Actuators B* **117**: 188-195

Lobana TS, Verma R, Hundal G, Castineiras A (2000). Metal-heterocyclic thione interactions. Heterocyclic 2-thiolates of platinum(II) and palladium(II): the crystal structures of first examples of *cis*- [M(η^1 -S-pyridine-2-thiolato)₂ (L-L)] {M = Pt, Pd, L-L = 1,2-bis(diphenylphosphino)ethane; M = Pt, L-L = 1,2-bis(diphenylphosphino)ethene } complexes, *Polyhedron* **19**: 899-906

Ludovico P, Rodrigues F, Almeida A, Silva MT, Barrientos A, Corte-Real M (2002), Cytochrome c release and mitochondrial involvement in programmed cell death induced by acetic acid in *saccharomyces cerevisiae*, *Mol.Biol.Cell* **13**: 2598-2606

Lundberg AS, Weinberg RA (1999). Control of the cell cycle and apoptosis, *Eur. J. Cancer* **35**: 1886-1894

Magner WJ, Tomasi TB (2005). Apoptotic and necrotic cells induced by different agents vary in their expression of MHC and costimulatory genes, *Mol. Immunol.* **42**: 1033-1042

Makin G, Dive C (2001). Apoptosis and cancer chemotherapy, *TRENDS Cell Biol.* **11**: S22-S26

- Mann CL, Cidlowski JA (2001). Glucocorticoids regulate plasma membrane potential during rat thymocyte apoptosis in vivo and in vitro, *Endocrinology* **142**: 421-429
- Marson A, van Oort AB, Mul WP (2002). In situ preparation of palladium diphosphane catalysts, *Eur. J. Inorg. Chem.* 3028-3031
- Mashima T, Tsuruo T (2005). Defects of the apoptotic pathway as therapeutic target against cancer, *Drug Resist. Updates* **8**: 339-343
- McIntyre P (2007). Rising tide of cancer poses global challenge. Cancer World: www.uicc.org
- McKeage M, Berners-Price S, Galettis P, Bowen R, Brouwer W, Ding L, Zhuang L, Baguley BC (2000). Role of lipophilicity in determining cellular uptake and anti-tumour activity of gold phosphine complexes, *Cancer Chemother. Pharmacol.* **46**: 343-350
- McKeage M, Maharaj L, Berners-Price S (2002). Mechanisms of cytotoxicity and antitumor activity of gold(I) phosphine complexes: the possible role of mitochondria, *Coord. Chem. Revs.* **232**: 127-135
- Meyer R, Brink S, van Rensburg CEJ, Joone GK, Gorls H, Lotz S (2005). Synthesis, characterization and antitumor properties of titanocene derivatives with thiophene containing ligands, *J. Organomet. Chem.* **690**: 117-125
- Miedaner A, DuBois DL, Curtis CJ (1993). Generation of Metal Formyl Complexes Using Nickel and Platinum Hydrides as Reducing Agents. *Organometallics* **12**, 299-303.
- Minahan DMA, Hill WE, McAuliffe CA (1984). An investigation of the chelate effect: the binding of bidentate phosphine and arsine chelates in square-planar transition metal complexes, *Coord. Chem. Revs.* **55**: 31-54
- Mingos DMP (1998). Transition elements (d block), lanthanides, and actinides (f block elements), in *Essential Trends in Inorganic Chemistry*, Oxford University Press, Inc., New York, p 273-388

- Modica-Napolitano JS, Singh KV (2002). Mitochondria as targets for detection and treatment of cancer, *Expert Revs. Mol. Med.* 1-19
- Mohlala MS, Guzei IA, Darkwa J, Mapolie SF (2005). Pyridine linker pyrazolyl palladium complexes: Synthesis, characterization and ethylene polymerization activity, *J. Mol. Catal. A: Chem.* **241**: 93-100
- Mollinedo F, Gajate C (2006). Fas/CD95 death receptor and lipid rafts: New targets for apoptosis-directed cancer therapy, *Drug Resist. Updates* **9**: 51-73
- Molnár L, Keserü GM, Papp A, Gulyás Z, Darvas F (2004), A neural network based prediction of octanol-water partition coefficients using atomic5 fragmental descriptors., *Bioorg. Med. Chem. Lett.* **14**: 851-853
- Morris KT, Song TJ, Fong Y (2006). Recent advancements in diagnosis and treatment of metastatic colorectal cancer to the liver, *Surg. Oncol.* **15**: 129-134
- Mosmann T (1983). Rapid colorimetric assay for cellular growth and survival: Application to proliferation and cytotoxicity assays, *J. Immunol. Methods* **65**: 55-63
- Moura EM, Dickman MH, Siebald HGL, Gama GJ (1999). Synthesis, characterisation and structure determination of $\{[\text{CpRu}(\text{Cl})]_2 (\eta^2, \mu_2\text{-dppe})_2\}$ complexes ($X = \text{Cl}, \text{N}_3$; $\text{dppe} = \text{Ph}_2\text{PCH}_2\text{CH}_2\text{PPh}_2$), *Polyhedron* **18**: 2899-2906
- Nadakavukaren KK, Nadakavukaren JJ, Chen LB (1985), Increased rhodamine 123 uptake by carcinoma cells, *Cancer Res.* **45**: 6093-6099
- Newkome GR (1993). Pyridylphosphines, *Chem.Rev.* **93**: 2067-2089
- Nigg EA (1995). Cyclin-dependent protein kinases: key regulators of the eukaryotic cell cycle, *Bioassays* **17**: 471-480
- Nolte F, Friedrich O, Rojewski M, Fink RHA, Schrezenmeier H, Körper S (2004). Depolarisation of the plasma membrane in the arsenic trioxide (As_2O_3)- and anti-CD95-induced apoptosis in myeloid cells, *FEBS Letters* **578**: 85-89
- Nygren P, Larsson R (2003). Overview of the clinical efficacy of investigational anticancer drugs, *J. Intern. Med.* **253**: 46-75

Oberhauser W, Bachmann C, Bruggeller P (1995). Palladium (II) and platinum (II) complexes of cis-1,2-bis(diphenylphosphino)ethene: completely planar structures due to p bonding in the case of platinum (II), *Inorg. Chim. Acta.* **238**: 35-43

Oberhauser W, Bachmann C, Stampfl T, Bruggeller P (1997a). Binuclear palladium(II), platinum(II) and platinum(IV) complexes containing 1,2-bis(diphenylphosphino)acetylene: different orientations of the diphosphine-bridges due to metal-phosphorus d[pi]-d[pi] back bonding, *Inorg. Chim. Acta.* **256**: 223-234

Oberhauser W, Bachmann C, Stampfl T, Haid R, Bruggeller P (1997b). Structural differences in nickel(II) and palladium(II) complexes containing cis-1,2-bis(diphenylphosphino)ethene or 1,2-bis(diphenylphosphino)ethane, *Polyhedron* **16**: 2827-2835

Oberhauser W, Bachmann C, Stampfl T, Haid R, Langes C, Rieder A, Bruggeller P (1998). Nickel(II), palladium(II), platinum(II) and platinum(IV) complexes of cis-1,2-bis(diphenylphosphino) ethene and nitrogen-containing heterocycles or sulfur ligands, *Inorg. Chim. Acta.* **274**: 143-154

Ormerod MG (2002). Investigating the relationship between the cell cycle and apoptosis using flow cytometry, *J. Immunol. Meth.* **265**: 73-80

Orrenius S (2004). Mitochondrial regulation of apoptotic cell death, *Toxicol. Lett.* **149**: 19-23

Owa T, Yoshino H, Yoshimatsu K, Nagasu T (2001), Cell cycle regulation in G1 phase: A promising target for the development of new chemotherapeutic anticancer agents, *Curr. Med. Chem.* **8**: 1487-1503

Ozcanli T, Erdogan A, Ozdemir S, Onen B, Ozmen M, Doksat K, Sonsuz A (2006). Severe liver enzyme elevations after three years of Olanzapine treatment: A case report and review of Olanzapine associated hepatotoxicity, *Prog. Neuro-psychopharm. Biol. Psych.* **30**: 1163-1166

Park WH, Seol JG, Kim ES, Kang WK, Im YH, Jung CW, Kim BK, Lee YY (2002). Monensin-mediated growth inhibition in human lymphoma cells through cell cycle arrest and apoptosis, *Brit. J. Haematol.* **119**: 400-407

- Poole SK, Poole CF (2003). Separation methods for estimating octanol-water partition coefficients., *J. Chromatogr. B* **797**: 3-19
- Popiolkiewicz, Polkowski K, Skierski JS, Mazurek AP (2005). In vitro toxicity evaluation in the development of new anticancer drugs-genistein glycosides, *Cancer Lett.* **229**: 67-75
- Radosevic K, Tom C, van Graft M, de Grooth BG, Greve J (1993). A flow cytometric study of the membrane potential of natural killer and K562 cells during the cytotoxic process, *J. Immunol. Meth.* **161**: 119-128
- Ray RS, Rana B, Swami B, Venu V, Chatterjee M (2006). Vanadium mediated apoptosis and cell cycle arrest in MCF-7 cell line, *Chem. Biol. Interact.* **163**: 239-247
- Reed JC, Jurgensmeier JM, Matsuyama S (1998). Bcl-2 family proteins and mitochondria, *Biochim. Biophys. Acta.* **1366**: 127-137
- Reedijk J (2003). New clues for platinum antitumour chemistry: Kinetically controlled metal binding to DNA, *Proc. Natl. Acad. Sci. USA* **100**: 3611-3616
- Rideout DC, Bustamante A, Patel J (1994). Mechanism of inhibition of FaDu hypopharyngeal carcinoma cell growth by tetraphenylphosphonium chloride, *Int. J. Cancer* **57**: 247-253
- Rideout D, Calogeropoulou T, Jaworski J, Dagnino R, McCarthy M (1989). Phosphonium salts exhibiting selective anti-carcinoma activity *in vitro*, *Anti-Cancer Drug Design* **4**: 265-280
- Ronconi L, Sadler PJ (2007). Using coordination chemistry to design new medicines, *Coord. Chem. Revs.* **251**: 1633-1648
- Roodt A, Otto S, Steyl G (2003). Structure and solution behaviour of rhodium(I) Vaska-type complexes for correlation of steric and electronic properties of tertiary phosphines ligands., *Coord. Chem. Revs.* **245**: 121-137

Roques B, Pelaprat D, le Guen I, Porcher G, Gosse C, le Pecq J (1979). DNA bifunctional intercalators: Antileukemic activity of new pyridocarbazole dimers, *Biochem. Pharmacol.* **28**: 1811-1815

Rottenberg H, Wu S (1998). Quantitative assay by flow cytometry of the mitochondrial membrane potential in intact cells, *Biochim. Biophys. Acta.* **1404**: 393-404

Sadler P. Metal complexes in medicine: Design and mechanism of action. *J. Inorg. Biochem.* **67**[1-4], 4. 1997.

Salvioli S, Ardizzoni A, Franceschi C, Cossarizza A (1997). JC-1, but not DiOC₆ (3) or rhodamine 123, is a reliable fluorescent probe to assess ψ changes in intact cells: implications for studies on mitochondria functionality during apoptosis, *FEBS Lett.* **411**: 77-82

Sanchez RI, Mesia-Vela S, Kauffman FC (2001). Challenges of cancer drug design: A drug metabolism perspective, *Curr. Cancer Drug Tar.* **1**: 1-32

Sané A-T, Cantin AM, Paquette B, Wagner JR (2004). Ascorbate modulation of H₂O₂ and camptothecin-induced cell death in Jurkat cells, *Cancer Chemoth. Pharm.* **54**: 315-321

Schafer KA (1998). The Cell Cycle: A Review, *Vet. Pathol.* **35**: 461-478

Schrauwen P, Hoeks J, Hesselink MKC (2006). Putative function and physiological relevance of the mitochondrial uncoupling protein-3: Involvement in fatty acid metabolism?, *Prog. Lipid. Res.* **45**: 17-41

Schurig J, Meinema H, Timmer K, Long B, Casazza A (1989). Antitumor activity of bis[bis(diphenylphosphino)alkane and alkene] group VII metal complexes, *Prog. Clin. Biochem. Med.* **10**: 205-216

Scott SL, Gumerlock PH, Beckett L, Li Y, Goldberg Z (2004). Survival and cell cycle kinetics of human prostate cancer cell lines after single- and multifraction exposures to ionisation radiation, *Int. J. Radiation Oncology Biol. Phys.* **59**: 219-227

Screnci D, McKeage M (1999). Platinum neurotoxicity: clinical profiles, experimental models and neuroprotective approaches, *J. Inorg. Biochem.* **77**: 105-110

Selikoff I (2005). Global action against cancer. www.uicc.org .

Sheldrick GM. SADABS. [2004/1]. 1996. Germany, University of Göttingen. Computer Program

Shiu M-H (2003). A surgeon's look at the treatment of cancer, *Ann.Coll.Surg.H.K* **7**: B7-B17

Skelton LA, Ormerod MG, Titley J, Kimbell R, Brunton LA, Jackman AL (1999). A novel class of lipophilic quinazoline-based folic acid analogues: cytotoxic agents with a folate-independent locus, *Brit. J. Cancer* **79**: 1692-1701

Smiley ST, Reers M, Mottola-Hartshorn C, Lin M, Chen A, Smith TW, Steele GD, Chen LB (1991). Intracellular heterogeneity in mitochondrial membrane potentials revealed by a j-aggregate-forming lipophilic cation JC-1, *Proc. Natl. Acad. Sci. USA* **88**: 3671-3675

Smith P, Hoke G, Alberts D, Bugelski P, Lupo P, Mirabelli C, Rush G (1989). Mechanism of toxicity of an experimental bidentate phosphine gold complexed antineoplastic agent in isolated rat hepatocytes, *J. Pharmacol. Exp. Ther.* **249**: 944-950

Song Y, Vittal J, Srinivasan N, Chan S, Leung P (1999). Synthesis and anti-cancer activities of a pair of enantiomeric gold(I) complexes containing sulfanyl-substituted P-stereogenic phosphines, *Tetrahedron-Asymmetr.* **10**: 1433-1436

Spek AL (2003). Xray, *J.Appl.Cryst.* **36**: 7-13

Stockland RA, Levine AM, Giovine MT, Guzei IA, Cannistra JC (2004). Reductive elimination from metal phosphonate complexes: Circumvention of competing protonolysis reactions., *Organometallics* **23**: 647-656

Summerhayes I, Lampidis T, Bernal S, Nadakavukaren J, Nadakavukaren K, Shepherd E, Chen L (1982). Unusual retention of rhodamine 123 by mitochondria in muscle and carcinoma cells, *Proc. Natl. Acad. Sci. U.S.A* **79**: 5296

Sun X, Wong JR, Song K, Hu J, Garlid KD, Chen LB (1994). AA1, a newly synthesized monovalent lipophilic cation, expresses potent *in vivo* antitumor activity, *Cancer Res.* **54**: 1465-1471

Susin SA, Zamzami N, Kroemer G (1998). Mitochondria as regulators of apoptosis: doubt no more, *Biochim. Biophys. Acta.* **1366**: 151-165

Suyama K, Shapiro I, Guttman M, Hazan RB (2002). A signaling pathway leading to metastasis is controlled by N-cadherin and the FGF receptor, *Cancer Cell* **2**: 301-314

Tanase T, Kawahara K, Ukaji H, Kobayashi K, Yamazaki H, Yamamoto Y (1993). Electrochemical preparation and characterisation of binuclear palladium(I) complexes containing aromatic isocyanide and chelating diphosphine ligands, *Inorg. Chem.* **32**: 3682-3688

The National Cancer Registry (2003). Cancer statistics 1997.

Thirupathi N, Amoroso D, Bell A, Protasiewicz JD (2005). Synthesis and reactivity of cationic palladium phosphine carboxylate complexes, *Organometallics* **24**: 4099-4102

Thomas N, Goodyer ID (2003). Stealth sensors: real-time monitoring of the cell cycle, *TARGETS* **2**: 26-33

Tiekink E (2002). Gold derivatives for the treatment of cancer, *Crit. Rev. Oncol. Hemat.* **42**: 225-248

Tiekink E (2003). Gold derivatives for the treatment of cancer. 2003. World Gold Council.

Tolman CA (1977). Steric effects of phosphorus ligands in organometallic chemistry and homogenous catalysis, *Chem. Rev.* **77**: 313-348

Trécourt F, Breton G, Bonnet V, Mongin F, Marsais F, Quéguiner G (2000). New syntheses of substituted pyridines via bromine-magnesium exchange, *Tetrahedron* **56**: 1349-1360

Tsuruo T, Lida H, Tsukagoshi S, Sakurai Y (1982). Increased accumulation of vincristine and adriamycin in drug-resistant P388 tumor cells following incubation with calcium antagonists and calmodulin inhibitors, *Cancer Res.* **42**: 4730-4733

Uhlig E, Maaser M (1966). Komplexchemisches Verhalten von funktionellen Derivaten des 2-äthyl-pyridins. VI. Das -(Bis-phenyl-phosphino)-äthyl-pyridin-(2), *Z. Anorg. Allg. Chem.* **344**: 205-213

Vámosi G, Bodnár A, Damjanovich S, Nagy P, Varga Z, Damjanovich L (2006). The role of supramolecular protein complexes and membrane potential in transmembrane signalling processes of lymphocytes, *Immunol. Lett.* **104**: 53-58

van Engeland M, Ramaekers F, Schutte B, Reutelingsperger C (1996). A novel assay to measure loss of plasma membrane asymmetry during apoptosis of adherent cells in culture, *Cytometry* **24**: 131-139

Vermes I, Haanen C, Reutelingsperger C (2000). Flow cytometry of apoptotic cell death, *J. Immunol. Meth.* **243**: 167-190

Vermes I, Haanen C, Steffens-Nakken H, Reutellingsperger C (1995). A novel assay for apoptosis flow cytometric detection of phosphatidylserine expression on early apoptotic cells using fluorescein labelled Annexin V, *J. Immunol. Meth.* **184**: 39-51

Vermeulen K, van Bockstaele DR, Berneman ZN (2003). The cell cycle: a review of regulation, deregulation and therapeutic targets in cancer, *Cell Prolif.* **36**: 131-149

Vink SR, van Blitterswijk WJ, Schellens JHM, Verheij M (2007). Rationale and clinical application of alkylphospholipid analogues in combination with radiotherapy, *Cancer Treat. Rev.* **33**: 191-202

- Vogler A, Kunkely H (2002). Excited state properties of transition metal phosphine complexes., *Coord. Chem. Revs.* **230**: 243-251
- Wang RB, Kuo CL, Lien LL, Lien EJ (2003). Structure-activity relationship: analyses of p-glycoprotein substrates and inhibitors, *J. Clin. Pharm. Ther.* **28**: 203-228
- Wang Z-B, Liu Y-Q, Cui Y-F (2005). Pathways to caspase activation, *Cell Biol. Int.* **29**: 489-496
- Weiss J, Wong J, Chul S, Bleday R, Salem R, Steele G, Chen LB (1987). Dequalinium, a topical antimicrobial agent, displays anticarcinoma activity based on selective mitochondrial accumulation, *Proc. Natl. Acad. Sci. U.S.A* **84**: 5444-5448
- Westland A (1965). Five co-ordinate Palladium (II) and Platinum (II), *J. Chem. Soc.* 3060-3067
- Workman P (2001). New drug targets for genomic cancer therapy: successes, limitations, opportunities and future challenges, *Curr. Cancer Drug Tar.* **1**: 33-47
- World Health Organisation (2003). Global cancer rates could increase by 50% to 15 million by 2020. www.who.int .
- World Health Organisation (2005). www.who.int.
- Xie Y, James BR (1991). Synthesis and chemistry of 2-pyridyl(phosphine) complexes of Pt(0), *J. Organomet. Chem.* **417**: 277-288
- Yu Q (2006). Restoring p53-mediated apoptosis in cancer cells: New opportunities for cancer therapy, *Drug Resist. Updates* **9**: 19-25
- Zeevaart JR, Jansen DR, Filomena BM, Abrunhosa A, Gomes C, Metello L, Kolar ZI, Krijger GC, Louw WKA, Dormehl IC (2004). Comparison of the predicted in vivo behaviour of the Sn(II)-APDDMP complex and the results as studied in a rodent model, *J. Inorg. Biochem.* **98**: 1521-1530

Zeevaart J, Jarvis N, Louw W, Jackson G (2001). Metal-ion speciation in blood plasma incorporating the tetraphosphonate, N,N-dimethylenephosphonate-1-hydroxy-4-aminopropylidenediphosphonate (APDDMP), in therapeutic radiopharmaceuticals, *J. Inorg. Biochem.* **83**: 57-65

Zhang ZZ, Cheng H (1996). Chemistry of 2-(diphenylphosphino)pyridine, *Coord. Chem. Revs.* **147**: 1-39

Zhou Y, Gwadry FG, Reinhold WC, Miller LD, Smith LH, Scherf U, Liu ET, Kohn KW, Pommier Y, Weinstein JN (2002). Transcriptional regulation of mitotic genes by camptothecin-induced DNA damage: Microarray analysis of dose- and time-dependent effects, *Cancer Res.* **62**: 1688-1695

Zhuravel CD, Glueck DS (1999). Synthesis and structure of dinuclear diphosphine-bridged palladium(II) complexes, *Organometallics* **18**: 4673-4676

Zimmermann S, Menzel CM, Stüben D, Taraschewski H, Sures B (2003). Lipid solubility of the platinum group metals Pt, Pd and Rh in dependence on the presence of complexing agents, *Environ. Pollut.* **124**: 1-5